ADVANCES IN TREATMENT OF RECURRENT AND METASTATIC NASAL-CRANIAL BASE TUMORS

EDITED BY: Yumin Wang, Weihong Jiang, Xiaobiao Zhang and Li Lan

PUBLISHED IN: Frontiers in Oncology and Frontiers in Surgery

frontiers Research Topics

ISSN 1664-8714
ISBN 978-2-88976-071-8
DOI 10.3389/978-2-88976-071-8

About Frontiers

Frontiers is more than just an open-access publisher of scholarly articles: it is a pioneering approach to the world of academia, radically improving the way scholarly research is managed. The grand vision of Frontiers is a world where all people have an equal opportunity to seek, share and generate knowledge. Frontiers provides immediate and permanent online open access to all its publications, but this alone is not enough to realize our grand goals.

Frontiers Journal Series

The Frontiers Journal Series is a multi-tier and interdisciplinary set of open-access, online journals, promising a paradigm shift from the current review, selection and dissemination processes in academic publishing. All Frontiers journals are driven by researchers for researchers; therefore, they constitute a service to the scholarly community. At the same time, the Frontiers Journal Series operates on a revolutionary invention, the tiered publishing system, initially addressing specific communities of scholars, and gradually climbing up to broader public understanding, thus serving the interests of the lay society, too.

Dedication to Quality

Each Frontiers article is a landmark of the highest quality, thanks to genuinely collaborative interactions between authors and review editors, who include some of the world's best academicians. Research must be certified by peers before entering a stream of knowledge that may eventually reach the public - and shape society; therefore, Frontiers only applies the most rigorous and unbiased reviews.
Frontiers revolutionizes research publishing by freely delivering the most outstanding research, evaluated with no bias from both the academic and social point of view. By applying the most advanced information technologies, Frontiers is catapulting scholarly publishing into a new generation.

What are Frontiers Research Topics?

Frontiers Research Topics are very popular trademarks of the Frontiers Journals Series: they are collections of at least ten articles, all centered on a particular subject. With their unique mix of varied contributions from Original Research to Review Articles, Frontiers Research Topics unify the most influential researchers, the latest key findings and historical advances in a hot research area! Find out more on how to host your own Frontiers Research Topic or contribute to one as an author by contacting the Frontiers Editorial Office: frontiersin.org/about/contact

ADVANCES IN TREATMENT OF RECURRENT AND METASTATIC NASAL-CRANIAL BASE TUMORS

Topic Editors:
Yumin Wang, Central South University, China
Weihong Jiang, Central South University, China
Xiaobiao Zhang, Fudan University, China
Li Lan, Massachusetts General Hospital Cancer Center, United States

Citation: Wang, Y., Jiang, W., Zhang, X., Lan, L., eds. (2022). Advances in Treatment of Recurrent and Metastatic Nasal-Cranial Base Tumors.
Lausanne: Frontiers Media SA. doi: 10.3389/978-2-88976-071-8

Table of Contents

frontiers in Oncology

ORIGINAL RESEARCH
published: 22 July 2021
doi: 10.3389/fonc.2021.716729

Clinical Outcomes of Salvage Endoscopic Nasopharyngectomy for Patients With Advanced Recurrent Nasopharyngeal Carcinoma

Wanpeng Li[†], *Huankang Zhang*[†], *Hanyu Lu*, *Huan Wang*, *Yurong Gu*, *Houyong Li*, *Xicai Sun*[*], *Hongmeng Yu*[*] and *Dehui Wang*[*]

Department of Otolaryngology-Head and Neck Surgery, Affiliated Eye Ear Nose and Throat Hospital, Fudan University, Shanghai, China

OPEN ACCESS

Edited by:
Weihong Jiang,
Central South University, China

Reviewed by:
Peter H. Hwang,
Stanford University, United States
Zhenlin Wang,
Capital Medical University, China

***Correspondence:**
Xicai Sun
laryngeal@163.com
Hongmeng Yu
hongmengyush@163.com
Dehui Wang
wangdehuient@sina.com

[†]*These authors have contributed equally to this work*

Specialty section:
This article was submitted to Surgical Oncology, a section of the journal Frontiers in Oncology

Received: 29 May 2021
Accepted: 09 July 2021
Published: 22 July 2021

Citation:
Li W, Zhang H, Lu H, Wang H, Gu Y, Li H, Sun X, Yu H and Wang D (2021) Clinical Outcomes of Salvage Endoscopic Nasopharyngectomy for Patients With Advanced Recurrent Nasopharyngeal Carcinoma. Front. Oncol. 11:716729. doi: 10.3389/fonc.2021.716729

Background: Salvage endoscopic nasopharyngectomy has better survival prognosis and fewer complications in the management of early stage rNPC, compared to re-irradiation. However, the treatment modality of advanced recurrent nasopharyngeal carcinoma (rNPC) remains controversial. Thus, the purpose of this study was to investigate the demographics, clinical outcomes, and prognostic factors associated with salvage endoscopic nasopharyngectomy in advanced rNPC.

Methods: This study conducted a retrospective analysis of advanced rNPC patients who underwent salvage surgery betweenm January 2014 and December 2019. The overall survival (OS) and progression-free survival (PFS) were analyzed. Univariable and multivariable analyses of OS and PFS were performed using the Cox regression model. The predicted values of the parameters were determined by means of the receiver operating characteristic (ROC) curve analysis.

Results: Among the 120 patients included, there were 75 patients with rT3 stage and 45 patients with rT4 stage. With the median follow-up time of 18 months,the 3 -year OS and PFS were 55.2% and 29.4%, respectively. Multivariate analyses showed that the rNPC patients with older age, low BMI (Body Mass Index), rT4 stage, tumor necrosis, and tumor invasion into the ICA was predictive of worse OS, whereas low BMI and rT4 stage were associated with worse PFS. In addition, the rT stage was identified as a better predictor of OS (area under the ROC curve: 0.669; *P*=0.003) than the other clinical features.

Conclusions: Salvage treatment using endoscopic nasopharyngectomy appears to be an effective treatment in the management of patients with advanced rNPC. In addition, case matching studies and prospective studies with larger clinical samples are required to further evaluate the efficacy of endoscopic surgery compared with re-irradiation in advanced rNPC.

Keywords: recurrent nasopharyngeal carcinoma, endoscopic, nasopharyngectomy, survival, prognostic factors

INTRODUCTION

Nasopharyngeal carcinoma (NPC), an epithelial malignant tumor originating from the mucosal lining of the nasopharynx, is endemic in Southern China and Southeast Asia (1). As a result of the advancements in the field of intensity-modulated radiotherapy (IMRT) in the management of patients with NPC, local recurrence remains one of the most important modes of treatment failure. Overall, 10% to 15% of the patients who undergo definitive radiotherapy will display local recurrence after undergoing treatment (2). Re-irradiation with IMRT for the management of recurrent nasopharyngeal carcinoma (rNPC) is often accompanied by serious complications, such as radiation necrosis of the bone, multiple cranial nerve dysfunction, and brain necrosis, which damages the quality of life of the patients and even leads to death (3). Moreover, Yu et al. reported that treatment with re-irradiation for the management of rNPC could only improve the survival rates in the patients with rT1-2 disease, whereas no significant changes were observed in the patients with rT3-4 disease (4).

Several recent studies have investigated the employment of salvage endoscopic nasopharyngectomy in the management of rNPC, in view of the fact that it might have better survival prognosis and fewer complications, compared to re-irradiation (5, 6). Liu et al. reported that endoscopic surgery significantly improved the overall survival (OS), compared to IMRT, in the patients with early stage rNPC (tumors confined to the nasopharyngeal cavity, the postnaris or nasal septum, the superficial parapharyngeal space, or the base of the sphenoid sinus) (7). Furthermore, a previous study by the authors on patients with rNPC showed that the site-specific and sinonasal-related quality of life were maintained after endoscopic nasopharyngectomy, compared to the preoperative quality of life. Endoscopic surgery appears to be a valuable therapeutic option in the management of patients with rNPC (8).

In scenarios involving advanced rNPC (rT3 and rT4 stages), endoscopic surgery is a challenging endeavor, owing to the frequent invasion into the internal carotid artery (ICA), skull base, orbit, infratemporal fossa, dura mater, cranial nerves, etc. Previous literature reports on the subject are few and involved small sample sizes. Consequently, the survival prognosis and the independent prognostic factors remain controversial (9, 10). The current study retrospectively collected the data pertaining to 120 patients with advanced rNPC who underwent endoscopic nasopharyngectomy during the time period from January 2014 to December 2019. To the best of our knowledge, the present study involves the highest number of reported cases of endoscopic surgery for the management of advanced rNPC. The present study focused on the demographics, clinical outcomes, and prognostic factors pertaining to these patients with rNPC.

METHODS

Study Population

The present study performed a retrospective chart review of 120 patients who were diagnosed with advanced rNPC and underwent endoscopic nasopharyngectomy for the management of the same at the Department of Otorhinolaryngology of the Affiliated Eye, Ear, Nose, and Throat Hospital at Fudan University during the time period from January 2014 to December 2019. The patients with T1 and T2 rNPC, and missing data pertaining to important variables were excluded from the study. The reasons for the missing data pertaining to important variables included incomplete preoperative clinical data and inability to contact the patient (e.g., phone number was no longer valid). In addition, there are also some cases without surgically resectable for patients with advanced rNPC: (1) The tumors extensively invaded the intracranial structure, especially the important blood vessels and nerves; (2) The tumors invaded the intracranial structure with obvious radiation brain edema after previous radiotherapy; (3) distant metastasis; (4) unresectable neck lymph node metastasis. The tumor margin to the ICA of less than 0.5 cm was considered as tumor invasion into the ICA (7). The current study was approved by the Institutional Review Board of the Affiliated Eye, Ear, Nose, and Throat Hospital at Fudan University.

Salvage Endoscopic Nasopharyngectomy

The decision to perform salvage endoscopic nasopharyngectomy was based on the location and extent of the tumor, taking into account the patient preferences and consultations with the radiation oncologists and surgeons. In case of the lesions involving the sphenoid sinus, bilateral sphenoidal sinuses were opened, and the septum was removed. The posterior end of the nasal septum was removed, and the base of the sphenoid sinus was ground off to outline the sphenoid sinus and nasopharynx. In order to remove the tumors invading the base of the middle cranial fossa and infratemporal fossa, a modified Caldwell-Luc approach through the anterior wall of the ipsilateral maxillary sinus into the infratemporal fossa and the base of the middle cranial fossa was often required to create a better surgical space and to complete the surgical procedure. The external pterygoid plate was abraded, and the foramen ovale and the main trunk of the mandibular nerve were exposed backwards. Bleeding from the pterygoid venous plexus was arrested by packing with quick yarn. The lingual and inferior alveolar nerves on the posteromedial side of the external pterygoid muscle were located, and the middle meningeal artery and sphenoid spine were exposed posteriorly.

The skull base bone can be divided into cancellous substance and cortex. When the tumor invades the cancellous bone of skull base, sometimes it is not easy to distinguish from the inflammatory granulation tissue after radiation. Pathological biopsy can be taken during the operation to determine whether there is tumor invasion, so as to ensure the negative margin. When the tumor invades the cortex of the skull base, surgeons can judge the extent of tumor invasion by endoscopic visual field and grind the invaded bone to the normal boundary by drill.

In cases with tumor invasion into the internal carotid artery (ICA), some patients underwent balloon occlusion test (BOT) of the ICA prior to the surgical procedure. If BOT was negative, ICA occlusion could be performed immediately, and the lesion could be removed during surgery (**Figure 1**). The parapharyngeal, petrosal, foramen, and clival segments of the ICA were exposed, and the related ICA was resected, in accordance with the extent of invasion. If BOT was positive, bypass surgery between the external carotid artery and middle cerebral artery was performed prior to the tumor resection. Subsequently, the rNPC resection was performed after two weeks. In order to prevent postoperative complications, such as wound infection caused by the extensive exposure of the skull base, nasal free mucosal flap, septal pedicled mucosal flap, or temporal muscle flap were used to repair the skull base defect (**Figure 2**).

Clinical Data

The current study retrieved the following clinical data pertaining to the patients: the demographic and clinical features such as the age, sex, history of smoking, alcohol consumption, diabetes, hypertension, and body mass index (BMI); tumor-related features including the number of radiotherapy sessions before surgery, preoperative combined chemotherapy, the time interval between recurrence and the last session of radiotherapy, rT stage, status of lymph node metastasis (LNM) at the time of recurrence, pathological type, status of tumor necrosis, surgical margins, tumor invasion into the ICA, the use of pedicled flaps to repair the skull base defect, postoperative adjuvant therapy, progression-free survival (PFS) and overall survival (OS); and serological parameters, i.e., hemoglobin (Hb) levels, neutrophil-to-lymphocyte ratio (NLR), and serum alkaline phosphatase levels.

Statistical Analysis

The curves of OS and PFS were plotted using the Kaplan–Meier method, and the significance of the differences among rNPC patients with regard to the prognostic factors was analyzed using the Log-rank tests. A Cox regression model was used to perform multivariate survival analyses. The predicted values of the parameters were determined by means of the receiver operating characteristic (ROC) curve analysis. The follow-up period was defined as the time period from the initial diagnosis at our institution to the date of death or last contact.

RESULTS

Study Population

A summary of the details regarding the patients involved in the present study is presented in **Table 1**. A total of 120 patients were identified; 88 (73.3%) male subjects and 32 (26.7%) female subjects. Among the aforementioned patients, the number of

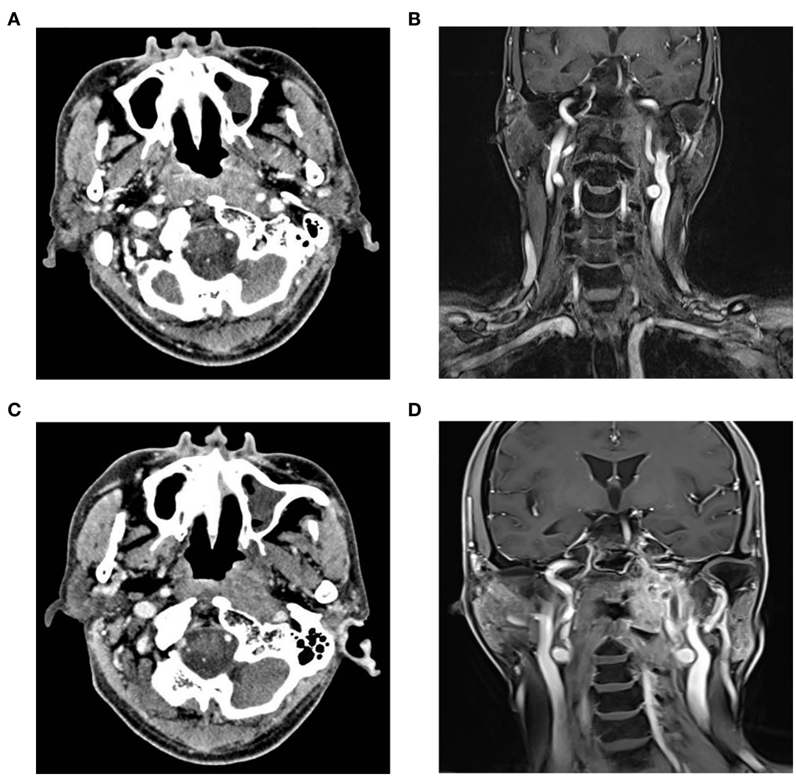

FIGURE 1 | Imaging examination of ICA before and after embolization **(A)** Horizontal enhanced CT showed that the tumor partially wrapped the left ICA; **(B)** Coronal enhanced MRI exhibited that the tumor invaded the left pharyngeal recess, parapharyngeal space, the longus capitis, sphenoid body and skull base, and partially surrounded the left ICA; **(C, D)** Horizontal enhanced CT and coronal enhanced MRI showed the undeveloped cavenous, lacerum, petrous and cervical segments of the left ICA. CT, Computer Tomography; MRI, Magnetic resonance imaging; ICA, Internal carotid artery.

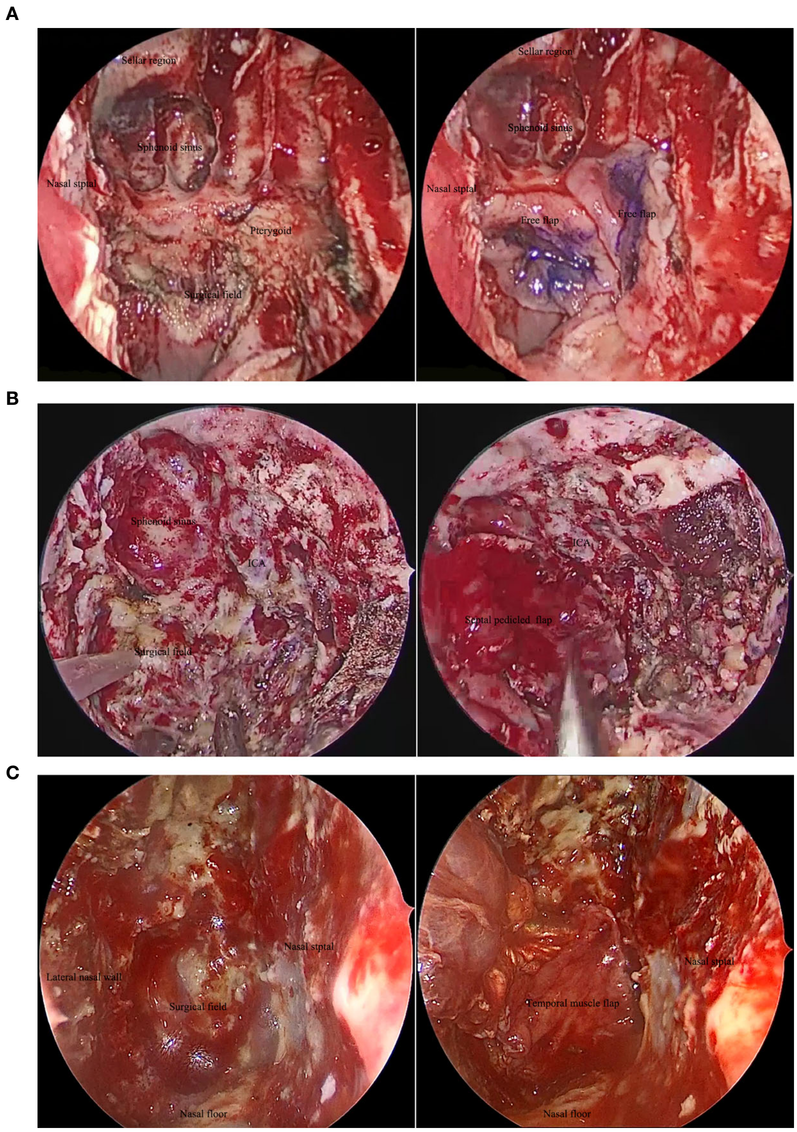

FIGURE 2 | Reconstruction of skull base defect after salvage surgery for recurrent nasopharyngeal carcinoma: **(A)** nasal free flap; **(B)** septal pedicled flap; and **(C)** temporal muscle flap. ICA, Internal carotid artery.

patients with age ≥50 years, a history of smoking, alcohol consumption, diabetes, and hypertension were sixty-five, thirty, twenty-one, four, and thirty, respectively. In the present study, the normal range of BMI was set at 18.5–24.9 kg/m^2; 26, 80, and 14 patients had high, normal, and low BMI, respectively. Regarding the serologic parameters, forty-two, forty, and six patients had low hemoglobin (<120 g/L) levels, high NLR (≥6), and low serum alkaline phosphatase (<50 mmol/L) levels, respectively. The time interval between recurrence and the last radiotherapy session was more than three years in sixty-eight patients.

Among the study subjects, 99 patients received adjuvant chemotherapy along with preoperative radiotherapy. The most frequent histological subtype of the tumor encountered in the current study was World Health Organization (WHO) type III (n=77, 64.2.0%), followed by WHO type II (n=43, 45.8%). In the current study, the tumors were staged on the basis of the rTNM staging system by the American Joint Committee on Cancer (AJCC/UICC) (7th edition, published in 2010) as follows: rT3 (n=75) and rT4 (n=45). The current study detected lymph node metastases in 28 patients (23.3%). The presence of tumor necrosis was observed in 64 patients (53.5%).

Preoperative tumor invasion into the ICA was observed in 41 patients (34.2%), including 13 cases with ICA embolization and 28 cases without ICA embolization. Moreover, in 79 patients, the tumor did not invade the ICA (63.8%). Among the 120 patients,

TABLE 1 | Characteristics of patients with advanced rNPC.

Characteristics	Total = 120	%
Gender		
Male	88	73.3
Female	32	26.7
Age (years)		
≥50	65	54.2
<50	55	18.3
Smoking history		
Yes	30	25.0
NO	90	75.0
Drinking history		
Yes	21	17.5
No	99	82.5
Diabetes mellitus		
Yes	116	96.7
No	4	3.3
Hypertension		
Yes	90	75.0
No	30	25.0
BMI		
18.5–24.9	80	66.7
<18.5	14	11.7
>24.9	26	21.7
Hemoglobin		
≥120	78	65.0
<120	42	35.0
NLR		
≥6	40	33.3
<6	80	66.7
Alkaline phosphatase		
<50	6	5.0
≥50	114	95.0
Period between recurrence and the last session of radiotherapy (year)		
≥3	68	56.7
<3	52	43.3
Preoperative combined chemotherapy		
Yes	99	82.5
No	21	17.5
Histological subtype		
WHO type II	43	35.8
WHO type III	77	64.2
rT stage		
rT3	75	62.5
rT4	45	37.5
LNM		
Yes	28	23.3
NO	92	76.7
Tumor necrosis		
Yes	64	53.3
No	56	46.7
Tumor invasion of the ICA		
No invasion	79	65.8
Invasion	28	23.3
Invasion, but ICA was embolized	13	10.8
The use of pedicled flap		
Yes	55	45.8
No	65	54.2
Surgical margin		
Negative margin	85	70.8
Positive margin	35	29.2
Postoperative radiotherapy		
No	112	93.3
Yes	8	6.7
Postoperative chemotherapy		
No	94	78.3
Yes	26	21.7
Postoperative PD-1 treatment		
No	111	92.5
Yes	9	7.5
All patients with follow-up (mean months of survival) range)	18 (2-81)	
Outcome		
Remission	39	32.5
Deceased	40	33.3
Alive with disease	41	34.2

(Continued)

rNPC, recurrent nasopharyngeal carcinoma; BMI, Body mass index; NLR, Neutrophil to lymphocyte ratio; LNM, lymph node metastasis; ICA, Internal carotid artery.

84 (70.0%) underwent repair of the postoperative nasopharyngeal defect. The pedicled flap was used in 55 cases (45.8%), including 41 cases of pedicled septal mucosal flap and 14 cases of temporal muscle flap. The pedicled flap was not employed to repair skull base defect in 65 patients, including 29 cases that underwent repair using nasal free mucosal flap and 36 cases without any intervention. Furthermore, eight, twenty-six, and nine patients received postoperative radiotherapy, chemotherapy, and programmed cell death protein 1 (PD-1) treatment, respectively.

Among the study subjects, 85 (70.8%) patients had negative surgical margins. The relationship between surgical margin and ICA embolization in patients with tumor invasion of the ICA is shown in **Table 2**. A higher rate of negative margins (11/13, 84.6%) was observed in the patients with ICA embolization, compared to those without embolization (15/28, 53.6%). However, there was no significant difference between the two groups (P=0.084).

Postoperative Complications

In this study, no patient died during the perioperative period. Although the post-operative period was uneventful, there still remain some complications. Most patients have wound scab, dry nose and headache in the first few days after surgery. The use of antibiotics and nasal irrigation gradually relieved these symptoms in about 4 weeks. In addition, 16 cases (13.3%) developed nasopharyngeal necrosis, which is a serious postoperative complication caused by surgical wound infection

TABLE 2 | The relationship between surgical margin and ICA embolization in rNPC patients with tumor invasion of ICA.

Embolization of ICA	Surgical margin		P value
	Negative margin	Positive margin	
No (n)	15	13	0.084
Yes (n)	11	2	

rNPC, recurrent nasopharyngeal carcinoma; ICA, Internal carotid artery.

and difficult to heal due to previous radiotherapy. 15 patients (12.5%) had dyskinesia of masticatory muscle or limitation of mouth opening due to the mandibular branch injury of trigeminal nerve. One patient occurred cerebral infarction after ICA embolization.

Overall Survival and Progression-Free Survival

The median duration of follow-up in the current study was 18 months (range: 2–81 months). Among the 40 patients who expired during the course of the study, 19 patients expired due to tumor progression at the local site (n=12) or the brain (n=5), the cause of mortality in 15 patients was postoperative ICA hemorrhage, three patients expired due to lung metastasis, one patient died as a result of skull base necrosis, one patient died of brain necrosis, and one patient expired by reason of cerebral infarction. Remission was confirmed by means of physical examination and enhanced magnetic resonance in 39 patients (32.5%), and 41 patients (34.2%) survived with the disease. The 1-year,2-year and 3-year OS pertaining to all the patients were 81.1%, 67.1% and 55.2%, respectively. In addition, the 1-year, 2-year and 3-year PFS were 54.7%, 37.3% and 29.4%, respectively (**Figure 3**).

Prognostic Analysis

The log-rank tests for prognostic factors pertaining to advanced rNPC are shown in **Table 3**. Age ≥50 years (**Figure 4A**), low BMI (**Figure 4B**), rT4 disease (**Figure 4C**), tumor necrosis (**Figure 4D**), tumor invasion into the ICA (**Figure 4E**), the use of pedicled flap (**Figure 4F**) and positive surgical margins (**Figure 4G**) were associated with a poor prognosis of OS. In addition, Age ≥50 years (**Figure 5A**), low BMI (**Figure 5B**) and rT4 disease (**Figure 5C**) were found to be significantly associated with worse PFS.

The variables that were considered to be significant in the Cox univariate analyses were age, BMI, rT stage, tumor necrosis, tumor invasion into the ICA, the use of pedicled flaps to repair the defect, and positive surgical margins. Subsequently, Cox multivariate analyses were performed using the aforementioned seven variables. A total of five variables (age, BMI, T stage, tumor necrosis, and tumor invasion into the ICA) were proven to be independent prognostic factors in the multivariate Cox regression model (**Table 4**). Moreover, based on the factors affecting OS, the predictive values were analyzed by means of the ROC analysis, which revealed that the rT stage was the best predictor for OS. The area under the ROC curve for rT stage with regard to the OS was 0.669 (95% confidence interval [CI], 0.563–0.774; *P*=0.003). The prognostic values pertaining to the other factors are shown in **Figure 6**. In addition, multivariable analysis revealed that patients with BMI and rT stage were significantly related to PFS (**Table 5**).

DISCUSSION

Aggressive salvage treatment is recommended for the management of locally rNPC, owing to the fact that many patients can still achieve long-term survival (4). The most common therapeutic modalities used for the management of rNPC are salvage surgery and re-irradiation with IMRT. Moreover, several studies have reported that IMRT is the most effective treatment for the management of advanced rNPC. Salvage surgery is only employed in the scenarios involving resectable, early-stage rNPC, such as rT1 disease, rT2–3 disease with limited parapharyngeal space involvement, or disease confined to the base of the sphenoid sinus (11, 12). However, advanced rNPC is characteristically more radioresistant, compared to the primary tumor, which can be attributed to

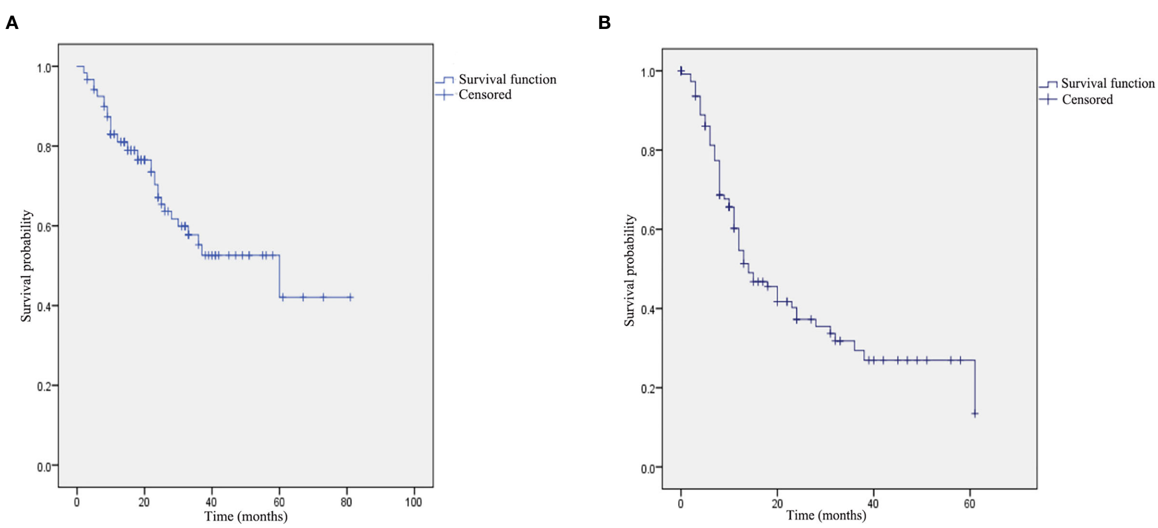

FIGURE 3 | Kaplan–Meier curve pertaining to the survival in patients with advanced recurrent nasopharyngeal carcinoma: **(A)** overall survival: and **(B)** progression-free survival.

TABLE 3 | Log-rank test of prognostic factors for rNPC.

Prognostic factors	OS (%)			P value	PFS (%)			P value
	1-year	2-year	3-year		1-year	2-year	3-year	
Sex				0.110				0.640
Male	83.5	73.8	60.4		56.9	36.0	31.4	
Female	74.1	61.4	45.5		48.1	39.2	23.5	
Age (year)				0.040				0.027
≥50	74.1	54.9	45.7		46.6	27.2	21.7	
<50	88.9	77.1	62.7		63.0	46.7	37.0	
Smoking history				0.120				0.127
Yes	89.3	80.3	70.3		55.6	41.1	33.2	
NO	78.2	63.4	51.8		51.4	24.0	18.0	
Drinking history				0.220				0.846
Yes	90.5	90.5	77.6		54.1	37.1	29.8	
NO	79.1	63.2	51.9		57.1	38.1	28.6	
Diabetes mellitus				0.926				0.815
Yes	100	50	50		66.7	33.3	33.3	
NO	80.5	67.3	55.4		54.0	37.2	29.3	
Hypertension				0.847				0.670
Yes	82.9	78.0	59.4		54.6	31.9	31.9	
No	80.4	63.9	54.4		54.6	38.8	28.9	
BMI				<0.001				0.004
18.5–24.9	81.7	69.5	53.2		58.2	44.9	33.3	
<18.5	57.1	32.7	16.3		35.9	0	0	
>24.9	92.3	92.3	92.3		54.4	34.6	34.6	
Hemoglobin				0.461				0.115
≥120	81.5	67.9	57.5		59.4	41.2	33.7	
<120	80.2	64.9	47.3		45.9	32.2	16.1	
NLR				0.137				0.644
≥6	72.5	56.1	42.1		38.7	38.7	29.0	
<6	83.4	70.2	58.7		59.0	36.7	29.6	
Alkaline phosphatase				0.899				0.428
<50	83.3	83.3	41.7		60.0	60.0	60.0	
≥50	81.0	66.2	55.6		54.3	36.1	28.0	
Preoperative combined chemotherapy chemotherapy				0.067				0.541
Yes	84.1	69.2	57.4		52.4	40.7	31.6	
No	66.7	55.6	41.7		65.9	13.8	13.8	
Period between recurrence and the last session of radiotherapy (year)				0.433				0.291
≥3	80.4	72.4	68.8		60.6	43.7	30.9	
<3	81.8	62.9	43.2		47.9	30.6	27.2	
Histological subtype				0.406				0.340
WHO type II	73.9	63.5	57.7		59.0	44.1	35.3	
WHO type III	86.6	69.2	54.5		52.2	34.1	26.0	
rT stage				0.001				0.020
rT3	88.8	75.3	68.8		63.7	43.8	40.6	
rT4	68.4	53.7	36.9		41.8	28.2	15.1	
LNM				0.216				0.159
Yes	78.2	60.0	40.0		55.7	28.6	14.3	
No	81.9	69.2	60.0		54.1	40.4	33.1	
Tumor necrosis				0.001				0.698
Yes	71.8	53.4	38.6		58.7	36.2	25.6	
No	88.8	78.0	67.9		50.4	39.6	39.6	
Tumor invasion of the ICA				<0.001				0.192
No invasion	89.6	79.2	65.1		57.6	39.6	34.8	
Invasion	49.5	23.6	15.7		39.9	23.3	11.7	
Invasion, but ICA was embolized	100	100	100		68.6	57.1	28.6	
The use of pedicled flap				0.024				0.513
Yes	92.6	77.8	60.5		50.9	33.7	23.6	
No	71.8	58.7	50.5		57.6	40.2	34.0	
Surgical margin				0.017				0.139
Negative margin	86.6	75.2	61.9		55.2	43.0	36.3	
Positive margin	67.8	50.8	41.9		53.4	25.1	15.1	

(Continued)

TABLE 3 | Continued

Prognostic factors	OS (%)			P value	PFS (%)			P value
	1-year	2-year	3-year		1-year	2-year	3-year	
Postoperative radiotherapy				0.655				0.200
No	81.5	68.3	55.6		56.6	38.1	29.6	
Yes	75.0	50.0	50.0		31.3	31.3	31.3	
Postoperative chemotherapy				0.134				0.248
No	79.1	65.8	51.1		58.3	39.1	34.0	
Yes	87.7	71.7	71.7		42.4	31.4	16.7	
Postoperative PD-1 treatment				0.238				0.675
No	79.5	66.2	53.7		54.9	38.3	32.5	
Yes	100	83.3	83.3		51.9	25.9	25.9	

rNPC, recurrent nasopharyngeal carcinoma; OS, Overall survival; PFS, Progress free survival; BMI, Body mass index; NLR, Neutrophil to lymphocyte ratio; LNM, lymph node metastasis; ICA, Internal carotid artery.

the poor blood supply and hypoxia, and a suboptimal dose distribution resulting from the protection of critical structures. Re-irradiation for the management of these bulky tumors warrants a higher radiation dose and wider treatment range to include a 1–1.5 cm margin, thereby compromising adjacent critical structures, which leads to severe radiotherapy-related toxicity and poor survival outcomes (13–15).

Over the recent years, several studies have suggested that salvage surgery could be used in patients with advanced rNPC (9, 10, 12, 16). Wong et al. reported favorable patient outcomes in fifteen patients with advanced rNPC (two rT3 and thirteen rT4 tumors) who underwent surgery by means of the endoscopic approach; the two-year OS was 66.7% (10). In our study, the three-year OS in patients with advanced rNPC was 55.2%, which was higher, compared to the patients who underwent salvage IMRT (17–19). Furthermore, the three-year OS in patients with rT3 and rT4 tumors were 68.8% and 36.9%, respectively, which were higher, compared to the patients who underwent salvage IMRT pertaining to rT3 and rT4 tumors, i.e., of 49.5% and 33.9%, reported by Hua et al. (18) However, many patients who received salvage surgery were given postoperative multimodal treatment including chemotherapy, radiotherapy or anti-PD-1 drugs. In addition, this study lacked a comparison cohort between salvage surgery and IMRT. Thus, case matching studies and prospective studies with larger clinical samples are required to further evaluate the efficacy of endoscopic surgery compared with re-irradiation in advanced rNPC.Postoperative ICA hemorrhage is one of the major causes of mortality after

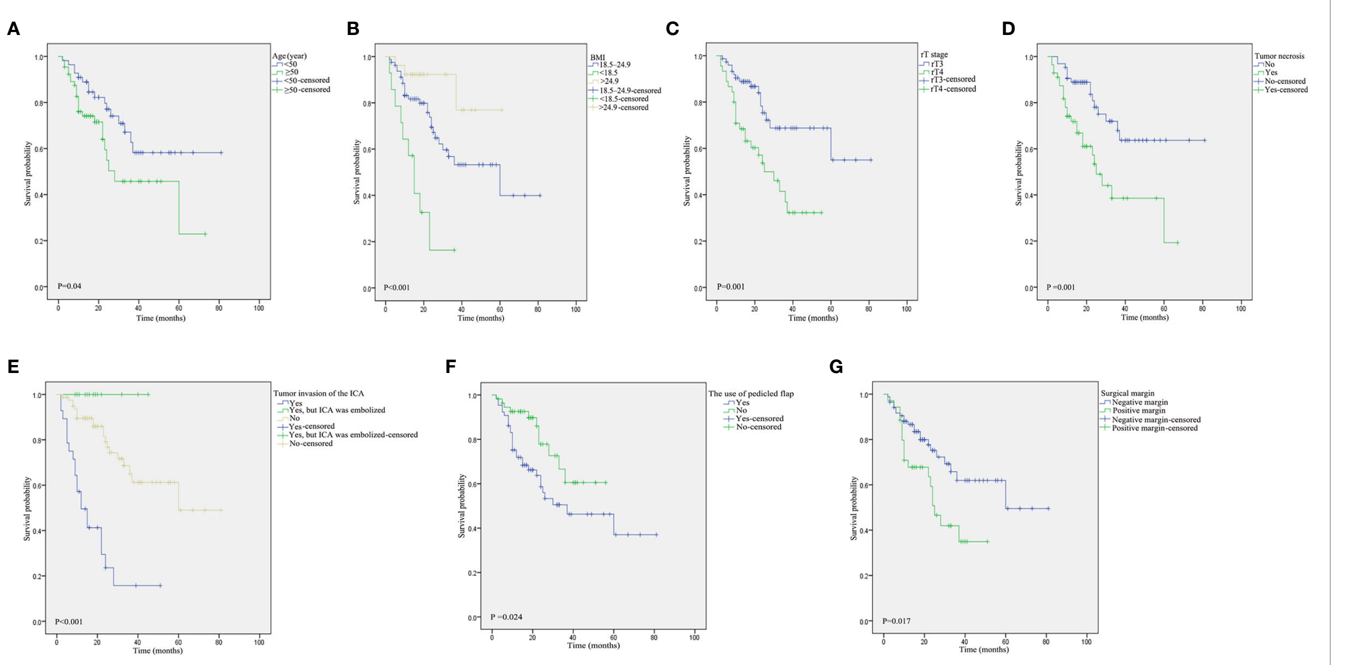

FIGURE 4 | Kaplan–Meier curves pertaining to the overall survival in patients with recurrent nasopharyngeal carcinoma: **(A)** age (≥50 *vs*. <50 years); **(B)** body mass index (BMI); **(C)** rT stage (rT3 *vs*. rT4); **(D)** tumor necrosis; **(E)** tumor invasion into the ICA; **(F)** the use of pedicled flap; and **(G)** surgical margins.

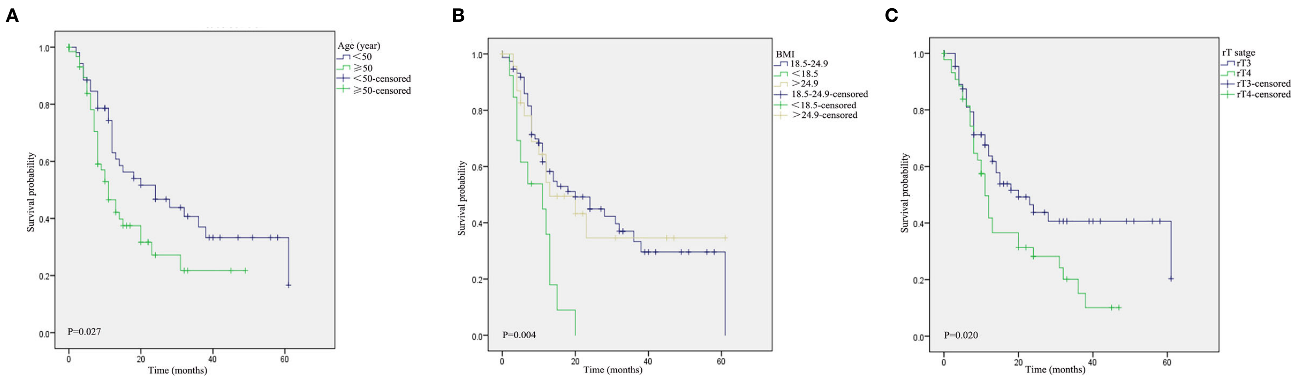

FIGURE 5 | Kaplan–Meier curves pertaining to the progression-free survival in patients with recurrent nasopharyngeal carcinoma: **(A)** age (≥50 *vs*. <50 years); **(B)** body mass index (BMI); and **(C)** rT stage (rT3 *vs*. rT4).

TABLE 4 | Univariate and multivariate Cox regression analyses of OS in patients with rNPC.

Variable	Univeriate			Multivariate		
	HR	95%CI	P	HR	95%CI	P
Age (year)						
≥50	1		Reference	1		Reference
<50	0.517	0.272-0.985	0.045	0.462	0.235-0.908	0.025
BMI						
18.5–24.9	1		Reference	1		Reference
<18.5	3.693	1.745-7.817	0.001	2.981	1.282-6.931	0.011
>24.9	0.348	0.105-1.147	0.083	0.570	0.159-2.047	0.388
T stage						
rT3	1		Reference	1		Reference
rT4	2.827	1.483-5.391	0.002	2.396	1.140-5.037	0.021
Tumor necrosis						
Yes	1		Reference	1		Reference
No	0.361	0.189-0.688	0.002	0.488	0.249-0.960	0.038
Tumor invaded the ICA						
No invasion	1		Reference	1		Reference
Invasion	5.164	2.713-9.827	0.000	2.445	1.093-5.469	0.030
Invasion, but ICA was embolized.	<0.001	/	0.968	<0.001	/	0.971
Surgical margin						
Negative margin	1		Reference	1		Reference
Positive margin	2.108	1.123-3.959	0.020	1.017	0.478-2.162	0.965
The use of pedicled flap						
Yes	1		Reference	1		Reference
No	2.179	1.085-4.379	0.029	1.405	0.666 -2.968	0.372
Sex						
Male	1		Reference			
Female	1.667	0.876-3.171	0.119			
Smoking history						
Yes	1		Reference			
No	2.064	0.805-5.295	0.132			
Drinking history						
Yes	1		Reference			
No	2.439	0.751-7.926	0.138			
Diabetes mellitus						
Yes	1		Reference			
No	0.911	0.124-6.685	0.911			
Hypertension						
Yes	1		Reference			
NO	0.933	0.455-1.910	0.849			
Hemoglobin						
<120	1		Reference			

(Continued)

TABLE 4 | Continued

Variable	Univeriate			Multivariate		
	HR	95%CI	P	HR	95%CI	P
≥120	0.783	0.405-1.511	0.466			
NLR						
≥6	1		Reference			
<6	0.593	0.294-1.198	0.145			
Alkaline phosphatase						
<50	1		Reference			
≥50	1.096	0.264-4.552	0.900			
The time between recurrence and the last radiotherapy (year)						
≥3	1		Reference			
<3	1.282	0.684-2.405	0.438			
Preoperative combined chemotherapy before surgery						
Yes	1		Reference			
No	1.922	0.937-3.941	0.075			
Histological subtype						
WHO type II	1		Reference			
WHO type III	0766	0.405-1.447	0.411			
LNM						
Yes	1		Reference			
No	0.657	0.334-1.292	0.068			
Postoperative radiotherapy						
No	1		Reference			
Yes	1.305	0.401-4.240	0.658			
Postoperative chemotherapy						
No	1		Reference			
Yes	0.498	0.195-1.273	0.145			
Postoperative PD-1 treatment						
No	1		Reference			
Yes	0.324	0.044-2.366	0.267			

rNPC, recurrent nasopharyngeal carcinoma; OS, Overall survival; BMI, Body mass index; NLR, Neutrophil to lymphocyte ratio; LNM, lymph node metastasis; ICA, Internal carotid artery; HR, hazard ratio; CI, confidence interval.

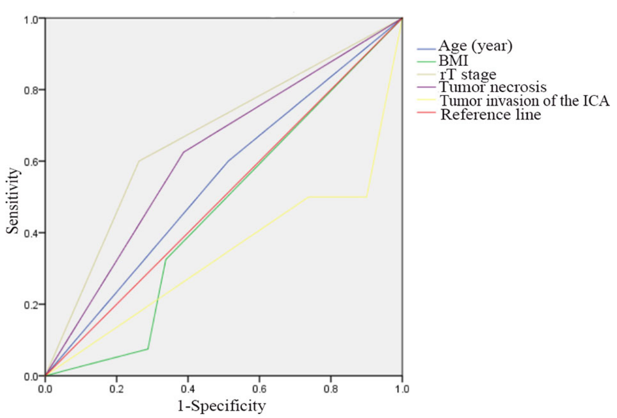

Variables	AUC	SE	95% CI	P value
Age	0.544	0.056	0.435-0.653	0.436
BMI	0.460	0.054	0.354-0.565	0.473
rT stage	0.669	0.054	0.563-0.774	0.003
Tumor necrosis	0.619	0.054	0.512-0.726	0.034
Tumor invasion of the ICA	0.341	0.057	0.229-0.453	0.005

FIGURE 6 | Receiver operating characteristic analysis revealed that the rT stage was the best predictor for overall survival (OS). The area under the ROC curve for rT stage was 0.669 (P = 0.003).

salvage surgery in patients with advanced rNPC. Consequently, tumor invasion into the ICA presents a difficult undertaking with regard to surgery. During the early years of the current research, the present study adopted the vidian nerve and eustachian tube as consistent and reliable ICA markers in the patients undergoing such high-risk surgical procedures (20). According to the relationship between the aforementioned markers, the parapharyngeal segment and petrous segment can be safely identified during the surgical procedure. However, the tumor resection had limitations; the tumor close to the ICA could only be removed as much as possible. Inevitably, some patients had tumor recurrence or postoperative ICA hemorrhage, which affects the OS in patients with advanced rNPC.

Recently, the authors proposed a new surgical procedure for the management of rNPC, namely, the embolization of ICA and the resection of tumor invading the ICA. This innovative technique can expand the scope of surgical resection and completely remove the tumor on the ICA, so as to ensure the negative margin, and reduce the probability of residual tumor and recurrence. In addition, it can avoid the occurrence of ICA hemorrhage in the process of tumor dissection, thus reduce the risk of surgery. More importantly, preoperative radiotherapy and previous surgical trauma have a great influence on the blood supply to the skull base, and postoperative cavity infection can occur easily. When the focus of infection invades the ICA, it leads to fatal ICA hemorrhage. Consequently, ICA embolization can

TABLE 5 | Univariate and multivariate Cox regression analyses of PFS in patients with rNPC.

Variable	Univeriate			Multivariate		
	HR	95%CI	P	HR	95%CI	P
Age (year)						
≥50	1		Reference	1		Reference
<50	0.580	0.352-0.957	0.033	0.610	0.368-1.010	0.055
BMI						
18.5–24.9	1		Reference	1		Reference
<18.5	2.795	1.445-5.409	0.002	2.462	1.267-4.784	0.008
>24.9	1.019	0.544-1.908	0.953	0.904	0.480-1.703	0.755
T stage						
rT3	1		Reference	1		Reference
rT4	1.750	1.075-2.850	0.024	1.648	1.010-2.689	0.046
Sex						
Male	1		Reference			
Female	0.881	0.511-1.518	0.648			
Smoking history						
Yes	1		Reference			
No	0.662	0.384-1.142	0.138			
Drinking history						
Yes	1		Reference			
No	0.849	0.477-1.839	0.849			
Diabetes mellitus						
Yes	1		Reference			
No	0.849	0.207-3.480	0.849			
Hypertension						
Yes	1		Reference			
No	0.677	0.496-1.578	0.677			
Hemoglobin						
<120	1		Reference			
≥120	0.670	0.401-1.119	0.126			
NLR						
≥6	1		Reference			
<6	0.872	0.482-1.579	0.652			
Alkaline phosphatase						
<50	1		Reference			
≥50	1.732	0.424-7.084	0.444			
The time between recurrence and the last radiotherapy (year)						
≥3	1		Reference			
<3	1.292	0.794-2.101	0.303			
Preoperative combined chemotherapy before surgery						
Yes	1		Reference			
No	1.211	0.645-2.275	0.551			
Histological subtype						
WHO type II	1		Reference			
WHO type III	1.289	0.755-2.200	0.353			
LNM						
Yes	1		Reference			
No	0.688	0.402-1.175	0.171			
Postoperative radiotherapy						
No	1		Reference			
Yes	0.559	0.223-1.402	0.215			
Postoperative chemotherapy						
No	1		Reference			
Yes	1.374	0.790-2.390	0.261			
Postoperative PD-1 treatment						
No	1		Reference			
Yes	0.839	0.361-1.947	0.683			
Tumor necrosis						
Yes	1		Reference			
No	0.910	0.558-1.483	0.705			

(Continued)

TABLE 5 | Continued

Variable	Univeriate			Multivariate		
	HR	95%CI	P	HR	95%CI	P
Tumor invaded the ICA						
No invasion	1		Reference			
Invasion	1.554	0.888-2.718	0.122			
Invasion, but ICA was embolized.	0.774	0.306-1.959	0.589			
Surgical margin						
Negative margin	1		Reference			
Positive margin	1.444	0.875-2.383	0.150			
The use of pedicled flap						
Yes	1		Reference			
No	0.853	0.523-1.391	0.853			

rNPC, recurrent nasopharyngeal carcinoma; PFS, progress free survival; BMI, Body mass index; NLR, Neutrophil to lymphocyte ratio; LNM, lymph node metastasis; ICA, Internal carotid artery; HR, hazard ratio; CI, confidence interval.

also prevent postoperative ICA rupture. In this series, the three-year OS rate pertaining to the patients without ICA invasion, invasion into ICA, and embolization of ICA were 65.1%, 15.7%, and 100%, respectively. Multivariate Cox regression analysis showed that ICA invasion was an independent risk factor for OS. Hence, it was concluded that the patients with rNPC with ICA invasion who undergo preoperative ICA embolization might have a better survival prognosis after salvage nasopharyngectomy.

BMI is a simple weight-for-height calculation that is often used to evaluate the nutritional status in adults. Several studies have reported that lower BMI is an independent risk factor for tumor recurrence or distant metastasis after radiotherapy in NPC patients (21, 22). A previous study regarding metastatic NPC by Li et al. demonstrated that the overweight/obese status was associated with longer OS, compared to the underweight or normal weight status. Overweight patients experience adverse treatment outcomes to a lesser extent and are less likely to experience malnutrition, cachexia, and increased tolerance to cancer treatment (23). The current study observed that rNPC patients with low BMI displayed worse OS after endoscopic surgery, compared to the patients with normal BMI. The patients with low BMI should receive further assessment, intensive counseling, and nutrition support. However, the current study did not observe any significant difference between the patients with high BMI and normal BMI with regard to OS, which was consistent with our preliminary report (24, 25).

CONCLUSION

Generally, Salvage treatment using endoscopic nasopharyngectomy appears to be an effective treatment in the management of patients with advanced rNPC. The independent risk factors pertaining to the OS were age (above 50 years), low BMI, rT4 stage, tumor necrosis, and tumor invasion into the ICA. In addition, case matching studies and prospective studies with larger clinical samples are required to further evaluate the efficacy of endoscopic surgery compared with re-irradiation in advanced rNPC.

DATA AVAILABILITY STATEMENT

The original contributions presented in the study are included in the article/supplementary material. Further inquiries can be directed to the corresponding authors.

ETHICS STATEMENT

The studies involving humans were reviewed and approved by the Institutional Review Board of AEENTH at Fudan University. The patients/participants provided their written informed consent to participate in this study.

AUTHOR CONTRIBUTIONS

DW, HY, and XS conceived, designed, and supervised the study. WL conceived and designed the study, performed the statistical analysis, and drafted the manuscript. HZ conceived and designed the study and drafted the manuscript. HLu acquired the data. YG and HLi drafted the manuscript. All authors contributed to the article and approved the submitted version.

FUNDING

This work was financially supported by the National Natural Science Foundation of China (No. 81870703), Shanghai Shen Kang Hospital Development Center (SHDC12018118), Clinical Research Plan of SHDC (SHDC2020CR2005A), Research Units of New Technologies of Endoscopic Surgery in Skull Base Tumor (2018RU003) supported by the Chinese Academy of Medical Sciences, Science and Technology Commission of Shanghai Municipality (20Y11902000, 21ZR1411700), and Shanghai Municipal Health Commission (201940143).

ACKNOWLEDGMENTS

We thank all the participants for their contribution and participation.

REFERENCES

1. Chen YP, Chan ATC, Le QT, Blanchard P, Sun Y, Ma J. Nasopharyngeal Carcinoma. *Lancet* (2019) 394:64–80. doi: 10.1016/S0140-6736(19)30956-0
2. Kong L, Lu JJ. Reirradiation of Locally Recurrent Nasopharyngeal Cancer: History, Advances, and Promises for the Future. *Chin Clin Oncol* (2016) 5:26. doi: 10.21037/cco.2016.03.19
3. Lu TX, Mai WY, Teh BS, Zhao C, Han F, Huang Y, et al. Initial Experience Using Intensity-Modulated Radiotherapy for Recurrent Nasopharyngeal Carcinoma. *Int J Radiat Oncol Biol Phys* (2004) 58:682–7. doi: 10.1016/S0360-3016(03)01508-6
4. Yu KH, Leung SF, Tung SY, Zee B, Chua DT, Sze WM, et al. Survival Outcome of Patients With Nasopharyngeal Carcinoma With First Local Failure: A Study by the Hong Kong Nasopharyngeal Carcinoma Study Group. *Head Neck* (2005) 27:397–405. doi: 10.1002/hed.20161
5. You R, Zou X, Hua YJ, Han F, Li L, Zhao C, et al. Salvage Endoscopic Nasopharyngectomy Is Superior to Intensity-Modulated Radiation Therapy for Local Recurrence of Selected T1-T3 Nasopharyngeal Carcinoma - A Case-Matched Comparison. *Radiother Oncol* (2015) 115:399–406. doi: 10.1016/j.radonc.2015.04.024
6. Hao CY, Hao SP. The Management of rNPC: Salvage Surgery vs. Re-Irradiation. *Curr Oncol Rep* (2020) 22:86. doi: 10.1007/s11912-020-00949-0
7. Liu YP, Wen YH, Tang J, Wei Y, You R, Zhu XL, et al. Endoscopic Surgery Compared With Intensity-Modulated Radiotherapy in Resectable Locally Recurrent Nasopharyngeal Carcinoma: A Multicentre, Open-Label, Randomised, Controlled, Phase 3 Trial. *Lancet Oncol* (2021) 22:381–90. doi: 10.1016/S1470-2045(20)30673-2
8. Li W, Lu H, Liu J, Liu Q, Wang H, Zhang H, et al. Quality of Life Following Salvage Endoscopic Nasopharyngectomy in Patients With Recurrent Nasopharyngeal Carcinoma: A Prospective Study. *Front Oncol* (2020) 10:437. doi: 10.3389/fonc.2020.00437
9. Wong EHC, Liew YT, Loong SP, Prepageran N. Five-Year Survival Data on the Role of Endoscopic Endonasal Nasopharyngectomy in Advanced Recurrent Rt3 and Rt4 Nasopharyngeal Carcinoma. *Ann Otol Rhinol Laryngol* (2020) 129:287–93. doi: 10.1177/0003489419887410
10. Wong EHC, Liew YT, Abu Bakar MZ, Lim EYL, Prepageran N. A Preliminary Report on the Role of Endoscopic Endonasal Nasopharyngectomy in Recurrent Rt3 and Rt4 Nasopharyngeal Carcinoma. *Eur Arch Otorhinolaryngol* (2017) 274:275–81. doi: 10.1007/s00405-016-4248-2
11. Lee AWM, Ng WT, Chan JYW, Corry J, Makitie A, Mendenhall WM, et al. Management of Locally Recurrent Nasopharyngeal Carcinoma. *Cancer Treat Rev* (2019) 79:101890. doi: 10.1016/j.ctrv.2019.101890
12. Chan JYW, Wong STS, Wei WI. Surgical Salvage of Recurrent T3 Nasopharyngeal Carcinoma: Prognostic Significance of Clivus, Maxillary, Temporal and Sphenoid Bone Invasion. *Oral Oncol* (2019) 91:85–91. doi: 10.1016/j.oraloncology.2019.02.023
13. Wang Y, Wang ZQ, Jiang YX, Wang FH, Luo HY, Liang Y, et al. A Triplet Chemotherapy Regimen of Cisplatin, Fluorouracil and Paclitaxel for Locoregionally Recurrent Nasopharyngeal Carcinoma Cases Contraindicated for Re-Irradiation/Surgery. *Expert Opin Pharmacother* (2016) 17:1585–90. doi: 10.1080/14656566.2016.1204293
14. Yue Q, Zhang M, Chen Y, Zheng D, Chen Y, Feng M. Establishment of Prognostic Factors in Recurrent Nasopharyngeal Carcinoma Patients Who Received Salvage Intensity-Modulated Radiotherapy: A Meta-Analysis. *Oral Oncol* (2018) 81:81–8. doi: 10.1016/j.oraloncology.2018.04.017
15. Tian YM, Huang WZ, Yuan X, Bai L, Zhao C, Han F. The Challenge in Treating Locally Recurrent T3-4 Nasopharyngeal Carcinoma: The Survival Benefit and Severe Late Toxicities of Re-Irradiation With Intensity-Modulated Radiotherapy. *Oncotarget* (2017) 8:43450–7. doi: 10.18632/oncotarget.15896
16. Chen Z, Qiu Q. Analysis of Clinical Efficacy and the Quality of Life After Endoscopic Nasopharyngectomy for Residual or Recurrent Nasopharyngeal Carcinoma. *Zhonghua Er Bi Yan Hou Tou Jing Wai Ke Za Zhi* (2015) 50:896–903. doi: 10.3760/cma.j.issn.1673-0860.2015.11.004
17. Kong F, Zhou J, Du C, He X, Kong L, Hu C, et al. Long-Term Survival and Late Complications of Intensity-Modulated Radiotherapy for Recurrent Nasopharyngeal Carcinoma. *BMC Cancer* (2018) 18:1139. doi: 10.1186/s12885-018-5055-5
18. Hua YJ, Han F, Lu LX, Mai HQ, Guo X, Hong MH, et al. Long-Term Treatment Outcome of Recurrent Nasopharyngeal Carcinoma Treated With Salvage Intensity Modulated Radiotherapy. *Eur J Cancer* (2012) 48:3422–8. doi: 10.1016/j.ejca.2012.06.016
19. Chan OS, Sze HC, Lee MC, Chan LL, Chang AT, Lee SW, et al. Reirradiation With Intensity-Modulated Radiotherapy for Locally Recurrent T3 to T4 Nasopharyngeal Carcinoma. *Head Neck* (2017) 39:533–40. doi: 10.1002/hed.24645
20. Liu J, Sun X, Liu Q, Wang D, Wang H, Ma N. Eustachian Tube as a Landmark to the Internal Carotid Artery in Endoscopic Skull Base Surgery. *Otolaryngol Head Neck Surg* (2016) 154:377–82. doi: 10.1177/0194599815616799
21. Tang LQ, Li CF, Li J, Chen WH, Chen QY, Yuan LX, et al. Establishment and Validation of Prognostic Nomograms for Endemic Nasopharyngeal Carcinoma. *J Natl Cancer Inst* (2016) 108:djv291. doi: 10.1093/jnci/djv291
22. Huang PY, Zeng Q, Cao KJ, Guo X, Guo L, Mo HY, et al. Ten-Year Outcomes of a Randomised Trial for Locoregionally Advanced Nasopharyngeal Carcinoma: A Single-Institution Experience From an Endemic Area. *Eur J Cancer* (2015) 51:1760–70. doi: 10.1016/j.ejca.2015.05.025
23. Li W, Shen LJ, Chen T, Sun XQ, Zhang Y, Wu M, et al. Overweight/obese Status Associates With Favorable Outcome in Patients With Metastatic Nasopharyngeal Carcinoma: A 10-Year Retrospective Study. *Chin J Cancer* (2016) 35:75. doi: 10.1186/s40880-016-0139-6
24. Li W, Lu H, Liu J, Liu Q, Wang H, Zhang H, et al. A Novel Nomogram to Predict Survival in Patients With Recurrent Nasopharyngeal Carcinoma After Salvage Endoscopic Surgery. *Oral Oncol* (2020) 111:104922. doi: 10.1016/j.oraloncology.2020.104922
25. Li W, Lu H, Wang H, Zhang H, Sun X, Hu L, et al. Salvage Endoscopic Nasopharyngectomy in Recurrent Nasopharyngeal Carcinoma: Prognostic Factors and Treatment Outcomes. *Am J Rhinol Allergy* (2021) 35:1458–66. doi: 10.1177/1945892420964054

Conflict of Interest: The authors declare that the research was conducted in the absence of any commercial or financial relationships that could be construed as a potential conflict of interest.

frontiers in Oncology

ORIGINAL RESEARCH
published: 09 August 2021
doi: 10.3389/fonc.2021.708235

Unilateral Subfrontal Approach for Giant Tuberculum Sellae Meningioma: Single Center Experience and Review of the Literature

Feng Xiao[†], Jie Shen[†], Luyuan Zhang[†], Jiqi Yang, Yuxiang Weng, Zebin Fang, Chao Zhang, Hongxing Ye, Renya Zhan* and Xiujue Zheng*

Department of Neurosurgery, The First Affiliated Hospital, Zhejiang University School of Medicine, Hangzhou, China

OPEN ACCESS

Edited by:
Weihong Jiang, Central South University, China

Reviewed by:
Tianwen Gao, Nanjing Medical University, China
Jian Xie, Capital Medical University, China

***Correspondence:**
Renya Zhan
1196057@zju.edu.cn
Xiujue Zheng
zxj8065@zju.edu.cn

[†]These authors have contributed equally to this work

Specialty section:
This article was submitted to Surgical Oncology, a section of the journal Frontiers in Oncology

Received: *11 May 2021*
Accepted: *19 July 2021*
Published: *09 August 2021*

Citation:
Xiao F, Shen J, Zhang L, Yang J, Weng Y, Fang Z, Zhang C, Ye H, Zhan R and Zheng X (2021) Unilateral Subfrontal Approach for Giant Tuberculum Sellae Meningioma: Single Center Experience and Review of the Literature. Front. Oncol. 11:708235. doi: 10.3389/fonc.2021.708235

Background: Microsurgical Transcranial approach (mTCA) is the primary choice for the resection of giant Tuberculum Sellae Meningiomas (TSM). The objective of this study is to explore surgical details of unilateral subfrontal approach.

Methods: Ten patients with giant TSM treated by unilateral subfrontal approach were included from January 2018 to June 2021. Demographic characteristics, surgical data, post-procedure complications and outcomes of patients have been descriptive analyzed, combined with systematic literature review to explore the surgical details and the prognosis of unilateral subfrontal approach.

Results: Ten patients include six male and four females, age range from 35 to 77 years, duration of visual impairment from 1 to 12 months, were all performed unilateral subfrontal approach. Nine patients achieved radical resection (Simpson grades I-II) through post-operative imaging confirmation, and Simpson IV resection was performed in the remaining one due to cavernous sinus invasion. The postoperative visual acuity was improved or maintained in 8 patients. Visual acuity decreased in 2 cases, including 1 case of optic nerve atrophy and the other case of optic canal not opening. Five cases with frontal sinus opened were repaired during the operation and there was no postoperative cerebrospinal fluid leakage or intracranial infection. One patient suffered from postoperative anosmia, one patient developed left limb weakness, but their symptoms have improved in the follow-up.

Conclusion: Summarize the experience of our center and previous literature, unilateral forehead bottom craniotomy is a feasible surgical approach for giant tuberculum sellae meningioma. Intraoperative application of EC glue and pedicled fascia flap to repair the frontal sinus can prevent complications associated with frontal sinus opening. Optic canal unroofing has huge advantage in visual improvement.

Keywords: giant tuberculum sellae meningiomas, frontal sinus repair, unilateral subfrontal approach, optic canal decompression, microsurgical transcranial approach

INTRODUCTION

Meningiomas are the most common tumors arising from the meninges by far, accounting for 13%-26% in primary intracranial tumors, more common among female (1, 2). The clinical manifestation and course of disease may be quite different on individuals, a portion are characterized by asymptomatic lesions with slow growth which found by incidental computerized tomography, some present a headache, but sometimes, the progressive enlargement of tumors may lead to seizures, neurological deficits occurred after adjacent nerve tissues compressed, disorder of hormone secretion caused by impairment of pituitary (1, 3). Tuberculum sellae meningiomas (TSM) approximately account for 5%-10% in all meningiomas, occur in the sphenoidal platform, anterior bed, saddle nodule, and saddle septum (3–7). Microsurgical resection is still the first choice for tuberculum sellae meningioma. The anatomy location of giant TSMs (maximum diameter ≥ 3cm) are deeper and more complex, some of giant TSMs often wraps around optic nerve, internal carotid artery and branches, oculomotor nerve, pituitary gland and pituitary stalk (8). As a result, the difficulty of total resection of the tumor is greatly increased, and postoperative complications are difficult to completely avoid. There are still great challenges in clinical practice on how to achieve the maximum excision of tumors, protect blood vessels and nerves, and reduce postoperative complications. Microsurgical craniotomy has always been the main surgical method for the treatment of tuberosity sellae meningioma due to its good total tumor resection rate, however, it also has disadvantages such as large surgical trauma and easy traction of the optic nerve. We present a case series of 10 patients with giant tuberculum sellae meningiomas and summarize literature to explore the surgical details of unilateral subfrontal approach.

MATERIALS AND METHODS

Study Population

Patients diagnosed with TSM and treated by microsurgical transcranial resection between January 2018 to June 2021 in Department of Neurosurgery, The First Affiliated Hospital, College of Medicine, Zhejiang University were included in this case series report. Of 39 patients with TSM in our center, 10 patients met the following inclusion criteria: MRI showed that a space-occupying lesion with a diameter of more than 3 cm was observed in the saddle nodule; Postoperative pathology of tumor revealed meningioma. Written informed consent was obtained from all individual participants before procedures and permission for the publication. Giant TSM were all resected by the same surgeon using unilateral subfrontal approach. Patients whose giant TSM resected by other surgical approaches were excluded, and also those absence of important medical information.

Clinical Therapeutic Protocol

All patients' meningiomas were resected by the same experienced surgeons using unilateral subfrontal approach (**Figure 1**). The repair process of frontal sinus is as follows (**Figure 2**): Ear-cerebrum (EC) glue was dripped into the gelatin sponge and filled the open frontal sinus cavity with gelatin sponge containing EC glue. Finally, the open frontal sinus was covered by subcutaneous fascia of the forehead and then sutured with the meninges. Optic canal unroofing was taken in patients with tuberculum sellae meningiomas which invaded optic canal.

Clinical Variables and Definition

The demographic features of the patients, symptoms upon admission, duration of visual impairment, visual acuity and visual field, surgical approaches, intraoperative video, size of meningiomas are reviewed and described. Some potential postoperative complications such as anosmia, cerebrospinal fluid (CSF) leakage, cerebral infection, epilepsy, artery injury, endocrine hormones disorder and so on were carefully examined in every patient. Anosmia was tested using the UPSIT (9). Odor identification refers to a person's ability to produce and attach a verbal label to an odor, or to identify an odor that matches a verbal or nonverbal (picture) label provided by another person (10).

Outcome Measures

Postoperative magnetic resonance imaging was the preferred investigation of choice to assess the gross resection rate of tumors, residual and recurrence of tumor. The extent of meningioma resection was assessed by Simpson classification criteria (11). The visual acuity prognosis was assessed by a neurosurgeon using visual acuity chart on discharge and three months after discharge *via* telephone call or outpatient appointment.

RESULT

Ten cases of TSM were included, including 6 males and 4 females (**Table 1**), with an average age of 54 ± 3.7 years old. All of them were giant TSM with maximum diameter (calculated according to the maximum diameter of sagittal MRI tumor) ≥ 30mm, with an average size of 34.3 ± 1.03 mm. **Table 1** summarizes the patients' characteristics. Simpson I-II resection was performed in 9 cases (**Table 1**, **Figure 3**). Neurosurgeon resected the main tumors and the meningeal invasion site during the operation and cauterize the tumor attachment site by electrocoagulation at the same time. The remaining 1 case underwent Simpson IV resection because the tumor invaded the cavernous sinus and grew into the cavernous sinus. There was still residual tumor in cavernous sinus after operation. Eight patients' optic canal were invaded by the tumor, all of them performed unilateral optic canal unroofing and enlargement, incised falciform ligament and resected peripheral tumors of optic nerve (**Figure 4**). And all of these eight patients had visual acuity improved after operation.

Abbreviations: mTCA, Microsurgical Transcranial approach; TSM, Tuberculum Sellae Meningiomas; CSF, Cerebrospinal fluid; EC, Ear-cerebrum; UPSIT, University of Pennsylvania Smell Identification Test; EEA, endoscopic endonasal approach; VIS, visual impairment score; GTR, gross total resection; DVI, Duration of visual impairment; VAO, Visual symptom after operation.

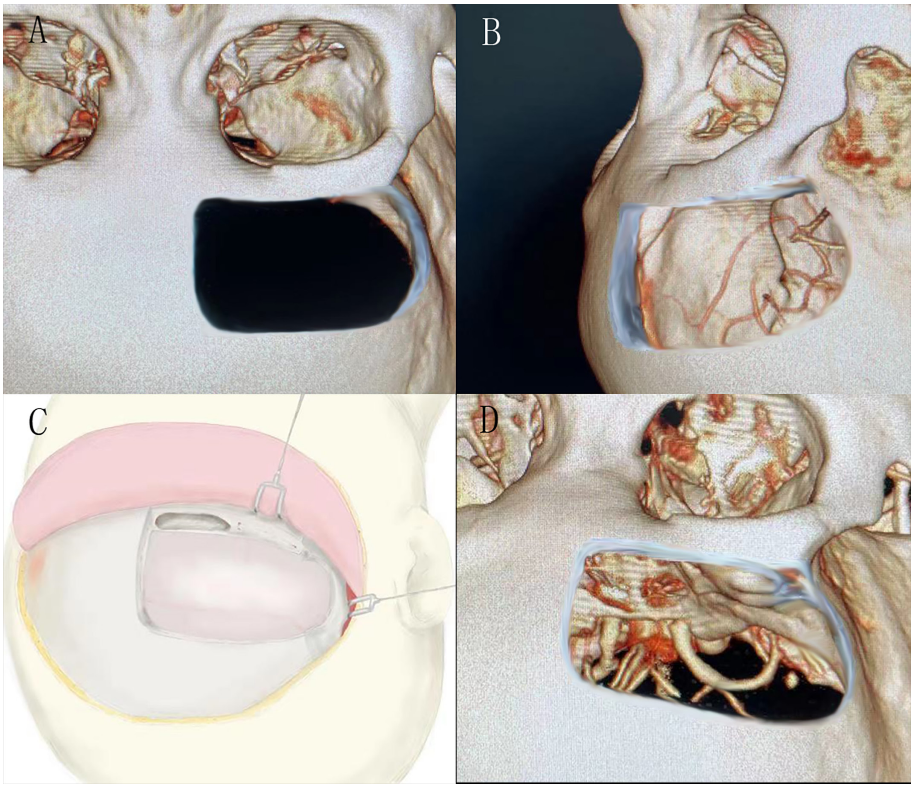

FIGURE 1 | **(A)** and **(B)** showed the bone window of the unilateral subfrontal approach, the larger extension to the temporal side, the more fields of surgical view exposed. **(C)** showed the schematic diagram of unilateral frontal floor craniotomy. **(D)** showed the visual field of sellar area by unilateral subfrontal approach.

Two cases suffered varying degrees of vision loss: One case had only preoperative light perception, the tumor was huge and the optic nerve was obviously compressed and pushed and thinner than normal, these suggested that optic nerve atrophy; Another case may have optic canal invasion, but the optic canal was not unroofed during the operation. The frontal sinus was opened in 5 cases during the operation, all of which were filled and repaired with EC glue, and covered with frontal subcutaneous pedicled fascia flap (**Figure 2**). There was no cerebrospinal fluid leakage and intracranial infection in these 5 patients. In one case, surgeon was obliged to stretched the frontal lobe due to the huge tumor. As a result, there was extensive edema of the frontal lobe after the operation, and the muscle strength of the left limb decreased. After 6 months of rehabilitation, patient's muscle strength of the limb improved. In another case, transient loss of smell occurred after the operation, and the olfactory function was improved after 6 months follow-up.

DISCUSSION

TSM is a general term for meningioma originating from the skull base and the saddle area transition zone. Since Cushing completed the first resection of tuberculum sellae meningioma in 1916, surgery has been the preferred treatment for tuberculum sellae meningioma (1, 5, 6, 12). The surgical approach for tuberculum sellae meningioma mainly depends on the size, growth direction and neurovascular invasion of tumor. At present, the most commonly used surgical approaches include subfrontal approach (13), anterior interhemispheric approach (14, 15), pterional approach (16, 17), supraorbital keyhole approach (7, 18), and endoscopic endonasal approach (EEA) (12, 19). There are many disputes about the choice of surgical approach at present, but microsurgery is the key to totally remove tumors.

Unilateral or bilateral subfrontal approach was usually selected in earlier microsurgery to resect TSM (13). The subfrontal approach can provide a wide and direct field of vision, clearly expose bilateral optic nerve, internal carotid artery, anterior cerebral artery and anterior communicating artery to protect visual nerve and adjacent vessels, facilitate the reconstruction of anterior cranial fossa base. In a long-term follow-up study of subfrontal approach for TSM patients (13), radical resection (Simpson Grades I and II) was achieved in 79% of patients and 91% of patients with preoperative visual impairment showed significantly improved postoperative visual impairment score (VIS). In previous literature, bilateral subfrontal approach can achieve visual improvement more effective than other surgical approaches (6, 13, 20). Unilateral subfrontal approach can expose bilateral optic nerves at the same

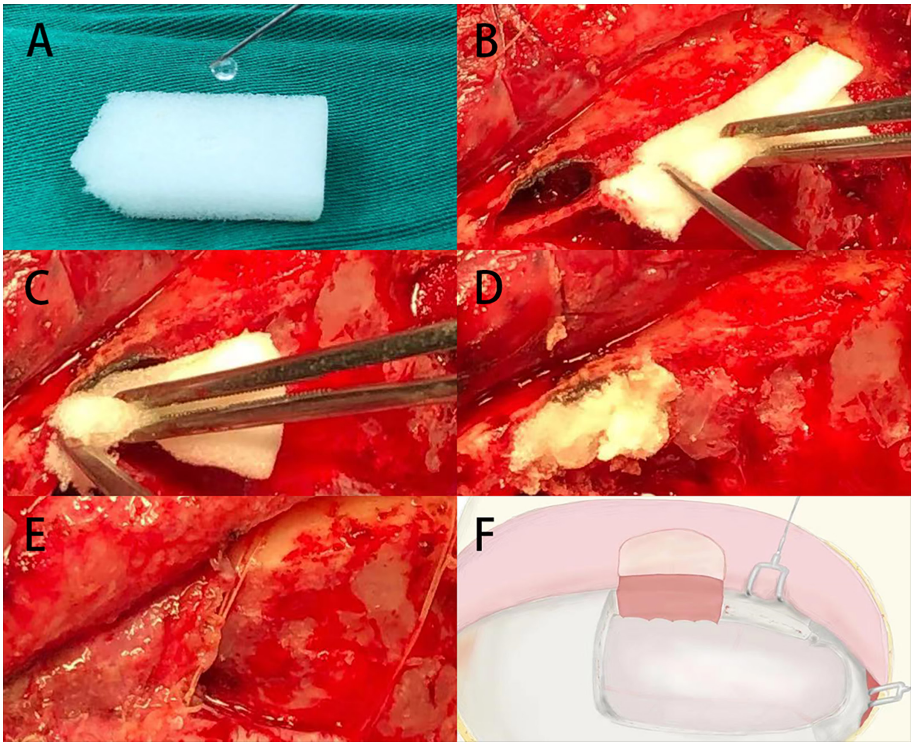

FIGURE 2 | **(A)** The gelatin sponge was dripped with EC glue. **(B–D)** The open frontal sinus cavity was filled with gelatin sponge containing EC glue. **(E, F)** The open frontal sinus was covered by subcutaneous pedicle and sutured with the frontal meninges.

TABLE 1 | Clinical characteristics of patients and tumors.

Case	Gender	Age (year)	DVI (month)	Size/mm	Simpson Grade	VOA	Complications
1	M	35	Normal	33	I	stable	
2	M	46	Normal	32	I	stable	
3	F	67	1	32	I	improved	
4	M	77	12	39	II	stable	left limb weakness
5	M	54	3	30	II	stable	anosmia
6	M	55	6	31	I	stable	
7	F	48	10	37	II	right deteriorated, left stable	
8	F	48	2	39	IV	improved	
9	F	57	6	36	II	right stable, left deteriorated	
10	M	53	1	34	II	stable	

DVI, Duration of visual impairment; VAO, Visual sympton after operation.

time and perform decompression of bilateral optic canal, there is no obvious disadvantage compared with bilateral frontal floor approach. Although the visual field of unilateral subfrontal approach is smaller than that of bilateral frontal floor approach, the scope of craniotomy is smaller and the surgical trauma is smaller. And there is no need to ligate the sagittal sinus, the contralateral olfactory nerve can also be reserved, so the possibility of postoperative olfactory dysfunction is reduced. In our case series, one patient had postoperative olfactory loss, but then improved after discharge.

Pterional approach is a classic approach for skull base surgery. Studies have shown that pterional approach is more suitable for sellae meningiomas with tumors growing on one side and posterior sellae region (5, 16, 17). The pterional approach has three main advantages: First, it can minimize the damage to the olfactory nerve through fully exposing of the ipsilateral olfactory nerve without cutting off the olfactory tract. Second, the frontal bone window edge is generally far from the frontal sinus, and the risk of cerebrospinal fluid leakage or frontal sinus infection is low. Third, this approach has the shortest distance to the sellae region. However, a large number of huge sellae tubercle meningiomas often adhere to the optic nerve and invade the optic foramen, which makes pterional approach for resection of sellae tubercle meningiomas prone to residual (21). And ipsilateral optic nerve and inferior surface of the optic chiasma cannot be fully exposed, previous literature shows that about

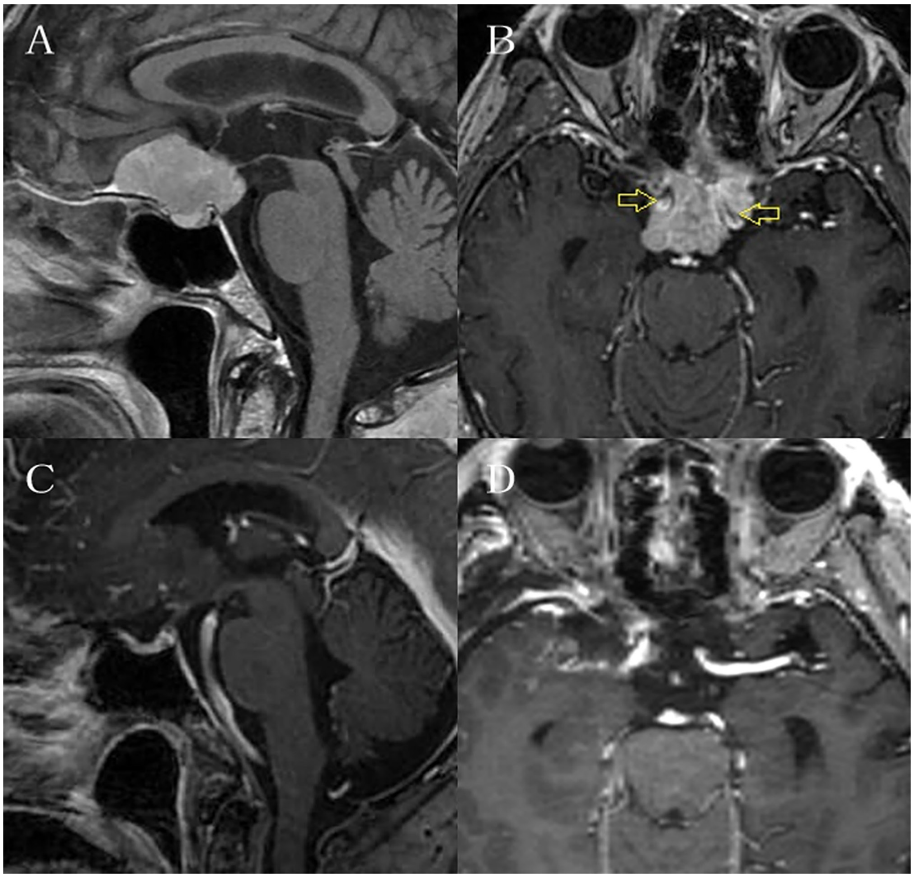

FIGURE 3 | It is the preoperative and postoperative MRI enhancement figure of one case. **(A)** and **(B)** showed the tumor was huge and surrounded bilateral internal carotid arteries. **(C)** and **(D)** showed total resection of the tumor.

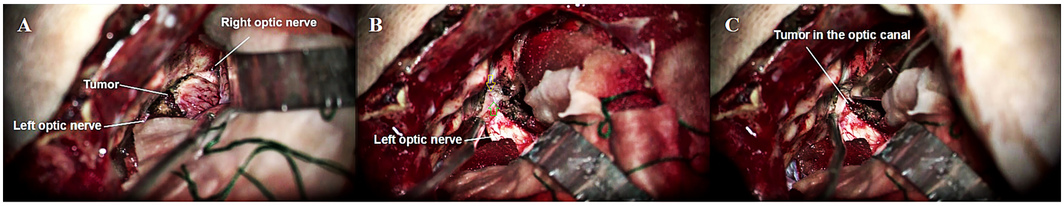

FIGURE 4 | **(A)** Exposure of bilateral optic nerves and tumors *via* left subfrontal approach. **(B)** Open the left optic canal (Yellow arrow) and the left falciform ligament (Green arrow). **(C)** The left falciform ligament was incised to expose the optic canal tumor.

10% to 20% of patients with pterional approach may have visual impairment after surgery (22–26). However, by using a unilateral frontal approach, attaining a fuller anatomy exposure on optic nerve areas, the inferior surface of the optic nerve can be clearly visualized under the microscope and its perforators can be carefully preserved. Thus, the improvement of visual function is better in unilateral frontal approach. In addition, unilateral frontal approach has more widely vision of sphenoid plateau and sellae tubercle compared with pterional approach, and its field of obtained vision during the operation is also wider. At the same time, unilateral frontal approach is more beneficial for the protection of blood vessels in the sellae area because of the clearly exposure of the lateral field of internal carotid artery.

Anterior interhemispheric approach was first used in anterior communicating artery aneurysm clipping (27). With the progress of microsurgery, it has become an alternative surgical approach for tuberculum sellae meningiomas (7). It provides a broad and direct surgical approach to the entire optic nerve apparatus and its surrounding structures, including the tubercle sellae, and without excessive frontal lobe contraction. Current literature has reported that the gross total resection (GTR) of this approach for tuberculum sellae meningiomas is over 90% (14, 15). In addition, the interhemispheric fissure approach has more visual enhancement benefits, at least, fewer visual deterioration after surgery (28). And without opening the frontal sinus during surgery, cerebrospinal fluid leakage is also rare. The shortcomings of this approach is that surgeon require more elaborate micromanipulation and longer operative time to dissect the anterior hemispheric fissure and more chance to occur anosmia after interhemispheric approach (28). Moreover, the longitudinal fissure approach is relatively difficult to expose the lateral side of the tumor compared with the unilateral subfrontal approach.

The endoscopic endonasal approach has become a new alternative technology different from transcranial approach (3, 29, 30). EEA offers several advantages over TCA, such as maximize the removal of all bone and dura involved by tumor; less manipulation of the optic nerves, optic chiasm, and brain; improved visualization of the medial optic canal and without skin incision, more aesthetically pleasing (31–34). However, in the early period, the outcome of tuberculum sellae meningiomas resected by EEA is not satisfactory. Prior to 2012, a meta-analysis comprised 60 series and 1426 patients revealed the GTR of TSM was higher in patients undergoing microsurgical transcranial surgery compared those undergoing EEA (84.1% *vs* 74.7%; p = 0.041) (35). In another meta-analysis included 64 case series which published before 2017, found no significant statistical significance in GTR between mTCA and EEA for patients with TSM (EEA: 83.0% *vs* mTCA: 85.8%, p = 0.34), however, visual improvement was higher in EEA than mTCA for patients with TSM (77.7% *vs* 60.7%, p < 0.01) (12). The mainly advantages of EEA are the protection of optic nerve and the improvement of visual acuity after surgery, but its main problems of EEA are the high incidence of cerebrospinal fluid leakage and meningitis. Most of the current studies consistently confirm that EEA provides better results at the expense of higher CSF leakage rates in visual restoration and preservation (12, 13, 34–36). It is worth mentioning that the risk of cerebrospinal fluid leakage after EEA has been gradually reduced with the improvement and standardization of reconstruction techniques of nasal septal flaps (37, 38). The prominent drawback of EEA is difficult to resect giant tumor (the largest diameter ≥ 30mm), tumor with tough texture or the lateral growth tumor that invades the optic canal and surrounds the internal carotid artery. Therefore, craniotomy is still the first choice for giant complex tuberculum sellae meningiomas.

Unilateral subfrontal approach requires fully exposing the base of anterior cranial fossa to reduce the traction of the frontal lobe, so the frontal sinus will be opened in most cases. Some researches pointed out the potential risk of cerebrospinal fluid leakage, meningitis, olfactory nerve injury caused by intraoperative frontal sinus opening, and the chance of venous infarction caused by occlusion of the superior sagittal sinus (6). Nevertheless, these complications are not specific to subfrontal approach and, indeed, also exist in the series reports of other surgical approach. And in fact, as long as a better exposure of sellae structure, frontal sinus could be repaired with free fat tissues, the effect of preventing CSF leakage and frontal sinus infections were satisfactory (39, 40). Opening the frontal sinus combined with preoperative navigation to determine the path of the milling cutter to ensure the integrity of the frontal sinus mucosa is a reasonable option. However, it is difficult to completely preserve the frontal sinus mucosa in cases where the frontal sinus is well developed and the top is taller and wider. The procedure of frontal sinus repair in our center is as follows: frontal sinus mucosa was separated and pushed downward during the operation; EC glue was dripped into the dry gelatin sponge and tightly packed in the open frontal sinus orifice; finally, the subcutaneous tissue of the frontal scalp was taken to form a pedicled tissue flap to cover the open frontal sinus orifice, and sutured with the meninges on the inner side of the skull. No cerebrospinal fluid rhinorrhea or frontal sinus associated infection occurred in all cases.

The optimal surgical goal for tuberculum sellae meningioma is to resect as much tumors as possible while preserving good neurological function. In this case series, 9 cases of tumor achieved Simpson I-II resection, and no obvious residual was found on MRI after 3 months of operation, which shows that unilateral subfrontal approach will not reduce the total resection rate of tumor. The effectiveness of radiotherapy as an adjuvant therapy for remnant meningiomas has already been confirmed (41–43). Therefore, when we could not attain gross total resection for tumor, it is more meaningful to preserve the neural function and ensure the self-care ability of patients. According to statistics, the proportion of vision deterioration after surgery for tuberculum sellae meningioma can reach 10 to 40%. Several influence variables of postoperative visual outcome include tumor size (44), the site and extension of the tumor (45), patient age (24), duration and degree of visual compromise (24), and probably also the surgical technique (25, 44). Thus, early treatment and optimal surgical planning for tuberculum sellae meningioma is very important to improve visual acuity. The ischemic, compression, or demyelination of the optic nerve are main causes of optic nerve dysfunction (46). Compression of the nerve could lead to small vessel lesions and demyelinating lesions, thus, some patients optic function might not recover even after decompression. Similarly, a partially demyelinated optic nerve may remyelinate itself after excision of the compressive mass. Previous studies about involvement of the optic canal in cases of tuberculum sellae meningiomas have all recommended opening of the optic canal and resection of the intracanalicular portion of the tumor (25, 47–49). Reviewing the literature, we can find that more than 85% of the patients with TSM who underwent optic nerve unroofing have improved and/or retained their visual acuity after surgery (13, 48–50). In our case series, eight patients performed unilateral optic canal unroofing and all of them had visual acuity improved and/or retained their visual acuity after operation. Intraoperative protection of optic nerve, separation and retention of feeding arteries of optic nerve, optic canal unroofing to relieve compression are vital for improving the visual acuity.

There are some limitations in this study. The clinical data were retrospectively collected and the results only represent the subgroup of giant tuberculum sellae meningioma patients. With regard to outcomes, if data on long-term follow-up can be acquired, the conclusion will be more accurate. Furthermore, the case series were small and acquired from a single center, and only descriptive analysis but without statistical analysis, which may lead to some inevitable bias in the conclusion.

CONCLUSION

Summarize the experience of our center and previous literature, unilateral subfrontal approach can completely remove the giant sellae nodule meningioma (the maximum diameter is ≥ 30mm), and has good visual retention rate and low postoperative complication rate. It is a feasible surgical treatment for giant TSM. Intraoperative application of EC glue and pedicled fascia flap to repair the frontal sinus can significantly prevent cerebrospinal fluid leakage and frontal sinus infection. Optic canal unroofing has huge advantage in visual improvement especially for patients with visual impairment.

DATA AVAILABILITY STATEMENT

The original contributions presented in the study are included in the article/supplementary material. Further inquiries can be directed to the corresponding authors.

ETHICS STATEMENT

The studies involving human participants were reviewed and approved by Clinical Research Ethics Committee of the First Affiliated Hospital, Zhejiang University School of Medicine. Written informed consent for participation was not required for this study in accordance with the national legislation and the institutional requirements.

AUTHOR CONTRIBUTIONS

FX has contributed in conceptualization, methodology, writing - review & editing and visualization. JS has contributed in writing - original draft. LZ has contributed in formal analysis and visualization. JY has contributed in visualization. YW has contributed in data curation. ZF has contributed in data curation. CZ has contributed in data curation. HY has contributed in data curation. RZ has contributed in conceptualization, validation, and supervision. XZ has contributed in conceptualization, validation, and supervision. All authors contributed to the article and approved the submitted version.

REFERENCES

1. Whittle IR, Smith C, Navoo P, Collie D. Meningiomas. *Lancet* (2004) 363 (9420):1535–43. doi: 10.1016/S0140-6736(04)16153-9
2. Marosi C, Hassler M, Roessler K, Reni M, Sant M, Mazza E, et al. Meningioma. *Crit Rev Oncol Hematol* (2008) 67(2):153–71. doi: 10.1016/j.critrevonc.2008.01.010
3. de Divitiis E, Esposito F, Cappabianca P, Cavallo L, dD O. Tuberculum Sellae Meningiomas: High Route or Low Route? A Series of 51 Consecutive Cases. *Neurosurgery* (2008) 62:556–63. doi: 10.1227/01.neu.0000317303.93460.24
4. Bowers CA, Altay T, Couldwell WT. Surgical Decision-Making Strategies in Tuberculum Sellae Meningioma Resection. *Neurosurg Focus* (2011) 30(5):E1. doi: 10.3171/2011.2.FOCUS1115
5. Jallo GBV. Tuberculum Sellae Meningiomas: Microsurgical Anatomy and Surgical Technique. *Neurosurgery* (2002) 51:1432–40. doi: 10.1097/00006123-200212000-00013
6. Nakamura M, Roser F, Struck M, Vorkapic P, Samii M. Tuberculum Sellae Meningiomas: Clinical Outcome Considering Different Surgical Approaches. *Neurosurgery* (2006) 59(5):1019–28; discussion 1028–9. doi: 10.1227/01.NEU.0000245600.92322.06
7. Romani R, Laakso A, Kangasniemi M, Niemela M, Hernesniemi J. Lateral Supraorbital Approach Applied to Tuberculum Sellae Meningiomas: Experience With 52 Consecutive Patients. *Neurosurgery* (2012) 70(6):1504–18. doi: 10.1227/NEU.0b013e31824a36e8
8. da Silva CE, de Freitas PE. Large and Giant Skull Base Meningiomas: The Role of Radical Surgical Removal. *Surg Neurol Int* (2015) 6:113. doi: 10.4103/2152-7806.159489
9. Doty RL, Shaman P MD. Development of the University of Pennsylvania Smell Identification Test: A Standardized Microencapsulated Test of Olfactory Function. *Physiol Behav* (1984) 32:489–502. doi: 10.1016/0031-9384(84)90269-5
10. Martin GE, Junque C, Juncadella M, Gabarros A, de Miquel MA, Rubio F. Olfactory Dysfunction After Subarachnoid Hemorrhage Caused by Ruptured Aneurysms of the Anterior Communicating Artery. Clinical Article. *J Neurosurg* (2009) 111(5):958–62. doi: 10.3171/2008.11.JNS08827
11. Simpson D. The Recurrence of Intracranial Meningiomas After Surgical Treatment. *J Neurol Neurosurg Psychiatry* (1957) 20:22–39. doi: 10.1136/jnnp.20.1.22
12. Muskens IS, Briceno V, Ouwehand TL, Castlen JP, Gormley WB, Aglio LS, et al. The Endoscopic Endonasal Approach Is Not Superior to the Microscopic Transcranial Approach for Anterior Skull Base Meningiomas-A Meta-Analysis. *Acta Neurochir (Wien)* (2018) 160:59–75. doi: 10.1007/s00701-017-3390-y
13. Chokyu I, Goto T, Ishibashi K, Nagata T, Ohata K. Bilateral Subfrontal Approach for Tuberculum Sellae Meningiomas in Long-Term Postoperative Visual Outcome. *J Neurosurg* (2011) 115(4):802–10. doi: 10.3171/2011.5.JNS101812
14. Curey S, Derrey S, Hannequin P, Hannequin D, Freger P, Muraine M, et al. Validation of the Superior Interhemispheric Approach for Tuberculum Sellae Meningioma: Clinical Article. *J Neurosurg* (2012) 117(6):1013–21. doi: 10.3171/2012.9.JNS12167
15. Terasaka S, Asaoka K, Kobayashi H, Yamaguchi S. Anterior Interhemispheric Approach for Tuberculum Sellae Meningioma. *Neurosurgery* (2011) 68(1 Suppl Operative):84–8. doi: 10.1227/NEU.0b013e31820781e1
16. Bitter AD, Stavrinou LC, Ntoulias G, Petridis AK, Dukagjin M, Scholz M, et al. The Role of the Pterional Approach in the Surgical Treatment of Olfactory Groove Meningiomas: A 20-Year Experience. *J Neurol Surg B Skull Base* (2013) 74(2):97–102. doi: 10.1055/s-0033-1333618
17. Muhammad Zafrullah A, Ignatius M, Sidabutar R, Atmadja Wirjomartani B, Faried A. Pterional Approach *Versus* Unilateral Frontal Approach on Tuberculum Sellae Meningioma: Single Centre Experiences. *Asian J Neurosurg* (2012) 7(1):21–4. doi: 10.4103/1793-5482.95691
18. Reisch R, Perneczky A, Filippi R. Surgical Technique of the Supraorbital Key-Hole Craniotomy. *Surg Neurol* (2003) 59:223–7. doi: 10.1016/S0090-3019(02)01037-6
19. Schwartz TH, Morgenstern PF, Anand VK. Lessons Learned in the Evolution of Endoscopic Skull Base Surgery. *J Neurosurg* (2019) 130(2):337–46. doi: 10.3171/2018.10.JNS182154
20. Jang WY, Jung S, Jung TY, Moon KS, Kim IY. The Contralateral Subfrontal Approach can Simplify Surgery and Provide Favorable Visual Outcome in Tuberculum Sellae Meningiomas. *Neurosurg Rev* (2012) 35(4):601–7; discussion 607-608. doi: 10.1007/s10143-012-0397-y
21. Goel A, Muzumdar D, Desai KI. Tuberculum Sellae Meningioma: A Report on Management on the Basis of a Surgical Experience With 70 Patients. *Neurosurgery* (2002) 51:1358–63. doi: 10.1097/00006123-200212000-00005

22. Benjamin V, Russell SM. The Microsurgical Nuances of Resecting Tuberculum Sellae Meningiomas. *Neurosurgery* (2005) 56(2 Suppl):411–7. doi: 10.1227/01.NEU.0000144783.07688.BC
23. Fahlbusch R, Schott W. Pterional Surgery of Meningiomas of the Tuberculum Sellae and Planum Sphenoidale: Surgical Results With Special Consideration of Ophthalmological and Endocrinological Outcomes. *J Neurosurg* (2002) 96:235–43. doi: 10.3171/jns.2002.96.2.0235
24. Pamir MN, Ozduman K, Belirgen M, Kilic T, Ozek MM. Outcome Determinants of Pterional Surgery for Tuberculum Sellae Meningiomas. *Acta Neurochir (Wien)* (2005) 147(11):1121–30; discussion 1130. doi: 10.1007/s00701-005-0625-0
25. Mathiesen T, Kihlstrom L. Visual Outcome of Tuberculum Sellae Meningiomas After Extradural Optic Nerve Decompression. *Neurosurgery* (2006) 59(3):570–6. doi: 10.1227/01.NEU.0000228683.79123.F9
26. Park CK, Jung HW, Yang SY, Seol HJ, Paek SH, Kim DG. Surgically Treated Tuberculum Sellae and Diaphragm Sellae Meningiomas: The Importance of Short-Term Visual Outcome. *Neurosurgery* (2006) 59(2):238–43. doi: 10.1227/01.NEU.0000223341.08402.C5
27. Diraz A, Kobayashi S, Toriyama T, Ohsawa M, Hokama M, Kitazama K. Surgical Approaches to the Anterior Communicating Artery Aneurysm and Their Results. *Neurol Res* (1993) 15:273–80. doi: 10.1080/01616412.1993.11740148
28. Ganna A, Dehdashti AR, Karabatsou K, Gentili F. Fronto-Basal Interhemispheric Approach for Tuberculum Sellae Meningiomas; Long-Term Visual Outcome. *Br J Neurosurg* (2009) 23(4):422–30. doi: 10.1080/02688690902968836
29. Attia M, Kandasamy J, Jakimovski D, Bedrosian J, Alimi M, Lee DL, et al. The Importance and Timing of Optic Canal Exploration and Decompression During Endoscopic Endonasal Resection of Tuberculum Sella and Planum Sphenoidale Meningiomas. *Neurosurgery* (2012) 71(1 Suppl Operative):58–67. doi: 10.1227/NEU.0b013e318258e23d
30. Khan OH, Anand VK, Schwartz TH. Endoscopic Endonasal Resection of Skull Base Meningiomas: The Significance of a "Cortical Cuff" and Brain Edema Compared With Careful Case Selection and Surgical Experience in Predicting Morbidity and Extent of Resection. *Neurosurg Focus* (2014) 37(4):E7. doi: 10.3171/2014.7.FOCUS14321
31. Laufer I, Anand V, Schwartz T. Endoscopic, Endonasal Extended Transsphenoidal, Transplanum Transtuberculum Approach for Resection of Suprasellar Lesions. *J Neurosurg* (2007) 106(3):400–6. doi: 10.3171/jns.2007.106.3.400
32. Mascarenhas L, Moshel YA, Bayad F, Szentirmai O, Salek AA, Leng LZ, et al. The Transplanum Transtuberculum Approaches for Suprasellar and Sellar-Suprasellar Lesions: Avoidance of Cerebrospinal Fluid Leak and Lessons Learned. *World Neurosurg* (2014) 82(1-2):186–95. doi: 10.1016/j.wneu.2013.02.032
33. Song SW, Kim YH, Kim JW, Park CK, Kim JE, Kim DG, et al. Outcomes After Transcranial and Endoscopic Endonasal Approach for Tuberculum Meningiomas-A Retrospective Comparison. *World Neurosurg* (2018) 109:e434–45. doi: 10.1016/j.wneu.2017.09.202
34. Bander ED, Singh H, Ogilvie CB, Cusic RC, Pisapia DJ, Tsiouris AJ, et al. Endoscopic Endonasal *Versus* Transcranial Approach to Tuberculum Sellae and Planum Sphenoidale Meningiomas in a Similar Cohort of Patients. *J Neurosurg* (2018) 128(1):40–8. doi: 10.3171/2016.9.JNS16823
35. Komotar RJ, Starke RM, Raper DM, Anand VK, Schwartz TH. Endoscopic Endonasal *Versus* Open Transcranial Resection of Anterior Midline Skull Base Meningiomas. *World Neurosurg* (2012) 77(5-6):713–24. doi: 10.1016/j.wneu.2011.08.025
36. Kong DS, Hong CK, Hong SD, Nam DH, Lee JI, Seol HJ, et al. Selection of Endoscopic or Transcranial Surgery for Tuberculum Sellae Meningiomas According to Specific Anatomical Features: A Retrospective Multicenter Analysis (KOSEN-002). *J Neurosurg* (2018) 130(3):838–47. doi: 10.3171/2017.11.JNS171337
37. Hadad G, Bassagasteguy L, Carrau RL, Mataza JC, Kassam A, Snyderman CH, et al. A Novel Reconstructive Technique After Endoscopic Expanded Endonasal Approaches: Vascular Pedicle Nasoseptal Flap. *Laryngoscope* (2006) 116(10):1882–6. doi: 10.1097/01.mlg.0000234933.37779.e4
38. Ottenhausen M, Banu MA, Placantonakis DG, Tsiouris AJ, Khan OH, Anand VK, et al. Endoscopic Endonasal Resection of Suprasellar Meningiomas: The Importance of Case Selection and Experience in Determining Extent of Resection, Visual Improvement, and Complications. *World Neurosurg* (2014) 82(3-4):442–9. doi: 10.1016/j.wneu.2014.03.032
39. Black P. Cerebrospinal Fluid Leaks Following Spinal or Posterior Fossa Surgery: Use of Fat Grafts for Prevention and Repair. *Neurosurg Focus* (2000) 9(1):e4. doi: 10.3171/foc.2000.9.1.4
40. Weber R, Draf W, Keerl R, Kahle G, Schinzel S, Thomann S, et al. Osteoplastic Frontal Sinus Surgery With Fat Obliteration: Technique and Long-Term Results Using Magnetic Resonance Imaging in 82 Operations. *Laryngoscope* (2000) 110(6):1037–44. doi: 10.1097/00005537-200006000-00028
41. Elia AE, Shih HA, Loeffler JS. Stereotactic Radiation Treatment for Benign Meningiomas. *Neurosurg Focus* (2007) 23(4):E5. doi: 10.3171/FOC-07/10/E5
42. Di Maio S, Ramanathan D, Garcia-Lopez R, Rocha MH, Guerrero FP, Ferreira M, et al. Evolution and Future of Skull Base Surgery: The Paradigm of Skull Base Meningiomas. *World Neurosurg* (2012) 78(3-4):260–75. doi: 10.1016/j.wneu.2011.09.004
43. Minniti G, Amichetti M, Enrici RM. Radiotherapy and Radiosurgery for Benign Skull Base Meningiomas. *Radiat Oncol* (2009) 4:42. doi: 10.1186/1748-717X-4-42
44. Kitano M, Taneda M, Nakao Y. Postoperative Improvement in Visual Function in Patients With Tuberculum Sellae Meningiomas: Results of the Extended Transsphenoidal and Transcranial Approaches. *J Neurosurg* (2007) 107(2):337–46. doi: 10.3171/JNS-07/08/0337
45. Schick U, Hassler W. Surgical Management of Tuberculum Sellae Meningiomas: Involvement of the Optic Canal and Visual Outcome. *J Neurol Neurosurg Psychiatry* (2005) 76(7):977–83. doi: 10.1136/jnnp.2004.039974
46. Lee JH, Jeun SS, Evans J, Kosmorsky G. Surgical Management of Clinoidal Meningiomas. *Neurosurgery* (2001) 48(5):1012–9. doi: 10.1227/00006123-200105000-00009
47. Sade B, Lee JH. High Incidence of Optic Canal Involvement in Tuberculum Sellae Meningiomas: Rationale for Aggressive Skull Base Approach. *Surg Neurol* (2009) 72(2):118–23. doi: 10.1016/j.surneu.2008.08.007
48. Mahmoud M, Nader R, Al-Mefty O. Optic Canal Involvement in Tuberculum Sellae Meningiomas: Influence on Approach, Recurrence, and Visual Recovery. *Neurosurgery* (2010) 67(3 Suppl Operative):ons108–19. doi: 10.1227/01.NEU.0000383153.75695.24
49. Nozaki K, Kikuta K-I, Takagi Y, Mineharu Y, Takahashi JA, Hashimoto N. Effect of Early Optic Canal Unroofing on the Outcome of Visual Functions in Surgery for Meningiomas of the Tuberculum Sellae and Planum Sphenoidale. *Neurosurgery* (2008) 62(4):839–46. doi: 10.1227/01.neu.0000318169.75095.cb
50. Attia M, Umansky F, Paldor I, Dotan S, Shoshan Y, Spektor S. Giant Anterior Clinoidal Meningiomas: Surgical Technique and Outcomes. *J Neurosurg* (2012) 117(4):654–65. doi: 10.3171/2012.7.JNS111675

Conflict of Interest: The authors declare that the research was conducted in the absence of any commercial or financial relationships that could be construed as a potential conflict of interest.

frontiers in Surgery

METHODS
published: 10 August 2021
doi: 10.3389/fsurg.2021.693774

Treatment of Recurrent Undifferentiated Pleomorphic Sarcoma of Infratemporal Fossa by Surgery Combined With Carbon Ion Radiotherapy: One Case Report

Zaixing Wang[1†], *Zhiyuan Tang*[1†], *Hailiang Zhao*[1], *Xianhai Zeng*[1*], *Xiaodong Han*[1] *and Qiuhang Zhang*[2*]

[1] *Institute of ENT and Shenzhen Key Laboratory of ENT, Longgang ENT Hospital, Shenzhen, China,* [2] *Center of Skull Base Surgery, China INN and Department of Otolaryngology-Head and Neck Surgery, Xuanwu Hospital, Capital Medical University, Beijing, China*

OPEN ACCESS

Edited by:
Weihong Jiang,
Central South University, China

Reviewed by:
Jianfeng Liu,
China-Japan Friendship Hospital, China
Jiang Yan,
The Affiliated Hospital of Qingdao University, China
Zhihai Xie,
Central South University, China

***Correspondence:**
Xianhai Zeng
zxhklwx@163.com
Qiuhang Zhang
entzqh330@126.com

[†] *These authors have contributed equally to this work*

Specialty section:
This article was submitted to Surgical Oncology, a section of the journal Frontiers in Surgery

Received: *10 May 2021*
Accepted: *09 July 2021*
Published: *10 August 2021*

Citation:
Wang Z, Tang Z, Zhao H, Zeng X, Han X and Zhang Q (2021) Treatment of Recurrent Undifferentiated Pleomorphic Sarcoma of Infratemporal Fossa by Surgery Combined With Carbon Ion Radiotherapy: One Case Report. Front. Surg. 8:693774. doi: 10.3389/fsurg.2021.693774

We retrospectively analyzed the diagnosis and treatment process of one patient with recurrent undifferentiated pleomorphic sarcoma (UPS) of infratemporal fossa and made a definite diagnosis by combining the imaging and pathological examination results. After treatment failure with 2 cycles of chemotherapy and several surgeries, UPS was eventually treated by surgery + carbon ion radiotherapy, and MRI reexamination showed no relapse. Head and neck UPS is located deeply, easily recurs after operation, and difficult to be resected completely by surgery, with a gradually shortened interval of relapse over the number of surgeries, which becomes a treatment challenge. After the last surgery, the patient received carbon ion radiotherapy, with a good therapeutic effect, and no sign of relapse just before sending this article. Based on the above advantages, we have concluded that surgery + carbon ion radiotherapy is a new effective pathway to treat head and neck UPS.

Keywords: undifferentiated pleomorphic sarcoma, infratemporal fossa, operation combined with carbon-ion radiotherapy, otolaryngology head and neck surgery, recurrent

HIGHLIGHTS

- Surgical excision of UPS alone cannot achieve the goal of cure.
- The UPS of head and neck region is not sensitive to chemotherapy.
- The UPS could be controlled and cured by operation with carbon-ion radiotherapy, However, long-term efficacy remains to be seen.

INTRODUCTION

Undifferentiated pleomorphic sarcoma (UPS) may occur in any organ, most frequently in soft tissues of limbs and retroperitoneal space, but rarely in head and neck (higher malignancy, easier relapse and metastasis, and poorer prognosis); it originates from mesenchymal tissues, and its incidence rate accounts for 1% of all malignant tumors (1). One case of recurrent UPS treated by surgery + carbon ion radiotherapy was reported to explore the clinical significance of such new combination.

CASE REPORT

The patient, female, 60 years old, was admitted to the hospital due to nearly 2 months after several surgeries for UPS of left infratemporal fossa and just after 1 cycle of chemotherapy. In January 2016, the patient felt sore and bursting at left cheek but paid no attention and received no examination and treatment.

On 7 March 2016, the patient paid a medical visit to Otolaryngology Hospital—the First Affiliated Hospital, Sun Yat-sen University, and then received rhinoscopic skull base tumor biopsy. The pathological examination results of HE-stained tissue sections indicated that tumor cells were short fusiform or elliptical and significantly atypical, with visible pathological mitosis, mononuclear or multinuclear tumor giant cells, thus morphologically complying with malignant tumor; immunohistochemistry (tumor cells) showed Vimentin (+), desmin (less) (+), Ki67 50% (+), CK (–), GFAP (–), S-100 (–), CD34 (–), Actin (–). The above findings met the diagnostic criteria of (skull base) UPS (**Figures 1A,B**).

On 5 and 25 April 2016, the patient successfully completed 2 cycles of chemotherapy with IFO+mesna+doxil in Sun Yat-sen University Cancer Center. Skull base MRI examination in May 2016 showed compression-caused displacement of left temporal lobe, and a mass shadow in left infratemporal fossa—middle cranial fossa, with non-uniform signals, predominantly T1 and T2 equisignals in the lesion, patchy slightly low T1 and significantly high T2 signals in the lesion center, nearly a clear and smooth border, and localized mild lobulation, in a size of 30.5 mm (AP) × 39.2 mm (LR) × 29.5 mm (HL), and surrounded by multiple circuitously routing flowing-void vascular shadows. Enhanced scan indicated a significantly enhanced mass in left infratemporal fossa—middle cranial fossa, a patchy low signal non-enhancement area in the center, and linear enhancement nearby meninges. The size of lesion had no significant change as compared with before chemotherapy (**Figure 2**).

On 25 May 2016, the patient underwent endoscopic transnasal resection for left infratemporal fossa—middle cranial fossa tumor in Otolaryngology Hospital (Longgang District, Shenzhen, Guangdong, China), and the postoperative pathology indicated that the lesion complied with UPS. After operation, the lesion recurred.

On 13 October 2016, the patient underwent subtemporal-preauricular resection for left infratemporal fossa—middle cranial fossa tumor in the same hospital, and the postoperative pathology indicated that the lesion complied with common osteosarcoma (co-presence of chondroblastic osteosarcoma and fibroblastic osteosarcoma). After operation, the lesion recurred.

On 14 October 2017, the patient underwent subtemporal-preauricular resection for left infratemporal fossa—middle cranial fossa tumor in the same hospital, and the postoperative pathology indicated that the lesion complied with common osteosarcoma. After operation, the lesion recurred again.

According to skull base MRI examination in May 2018, there were changes after surgeries for left infratemporal fossa—middle cranial fossa tumor, local bone defect in left maxillary sinus wall, cribriform plate, sphenoid bone and middle nasal concha, compression-caused displacement of left temporal lobe, and an enlarged mass shadow in left infratemporal fossa—middle cranial fossa, with non-uniform signals, predominantly T1 and T2 equisignals in the lesion, patchy slightly low T1 and significantly high T2 signals in the lesion center, nearly a clear and smooth border, and localized mild lobulation, in a size of 35.6 mm (AP) × 42.3 mm (LR) × 35.9 mm (HL), and surrounded by multiple circuitously routing flowing-void vascular shadows. Enhanced scan indicated a significantly enhanced mass in left infratemporal fossa—middle cranial fossa, a patchy low signal non-enhancement area in the center, linear enhancement nearby meninges, a few long T2 abnormal signals in left middle ear and mastoid process, thickened mucosa in bilateral maxillary sinus and ethmoid sinus as well as left sphenoid sinus, a cerebral spinal fluid (CSF)-like signal shadow in sellar region, and compression-caused flattened pituitary. Tumor relapse was considered (**Figures 2A–C**).

On 21 May 2018, the patient underwent subtemporal (preauricular) resection for left infratemporal fossa—middle cranial fossa tumor in the same hospital. The surgical procedures were as follows: The patient was in a supine position. After successful tracheal intubation and general anesthesia, the patient was routinely kept in a required position with left ear upward, followed by routine disinfection with iodophor and draping. A "C" surgical incision was made at the original incision scar on the hairline of anterior left ear edge and extended to left external acoustic meatus orifice, the skin, subcutaneous tissue and superficial fascia were dissected layer by layer using low-temperature plasma radiofrequency ablation, the skin flap was dissociated, zygomatic arch was exposed at lateral inferior parotid gland, and then its superficial muscular fasciae was dissected. Subsequently, the incision was dilated with a distracter, and the operation space was exposed under endoscope, observing a white fish-like mass with a smooth surface. Then, the mass border was dissected using a stripper upward to cerebral dura mater, and the mass was cut open at the center and mostly resected with a curette. Thereafter, under endoscopic view, the inferior tumor was resected to mandibular ramus and lateral pterygoid of infratemporal fossa and medially to os petrosum, internal carotid artery of os petrosum was exposed, and tumor tissues were fully curetted with a curette at middle cranial fossa base in an up-to-down manner along middle skull base meninges, without residual tumor. During operation, cerebral dura mater of middle cranial fossa base wall was thin, and there were no CSF leakage but slight blood exudation; full hemostasis was performed using bipolar coagulation scalpel, the operation space was rinsed with iodophor and physiological saline and then filled with iodoform gauzes after cerebral dura mater was covered with SURGICEL Absorbable Hemostat and Biodesign Surgisis Dural Graft, these gauzes were withdrawn from external auditory meatus, and the subcutaneous tissue and skin were sutured layer by layer after finishing the surgical count of instruments and gauzes. The surgery was successful, the intraoperative bleeding volume was 1,200 ml, and the resected tumor was sent for pathological examination.

From 16 July to 13 August 2018 after operation, the patient received carbon ion radiotherapy (70 GyE, 20 Fx) for recurrent tumor and treatment-extending safe area. In March 2019,

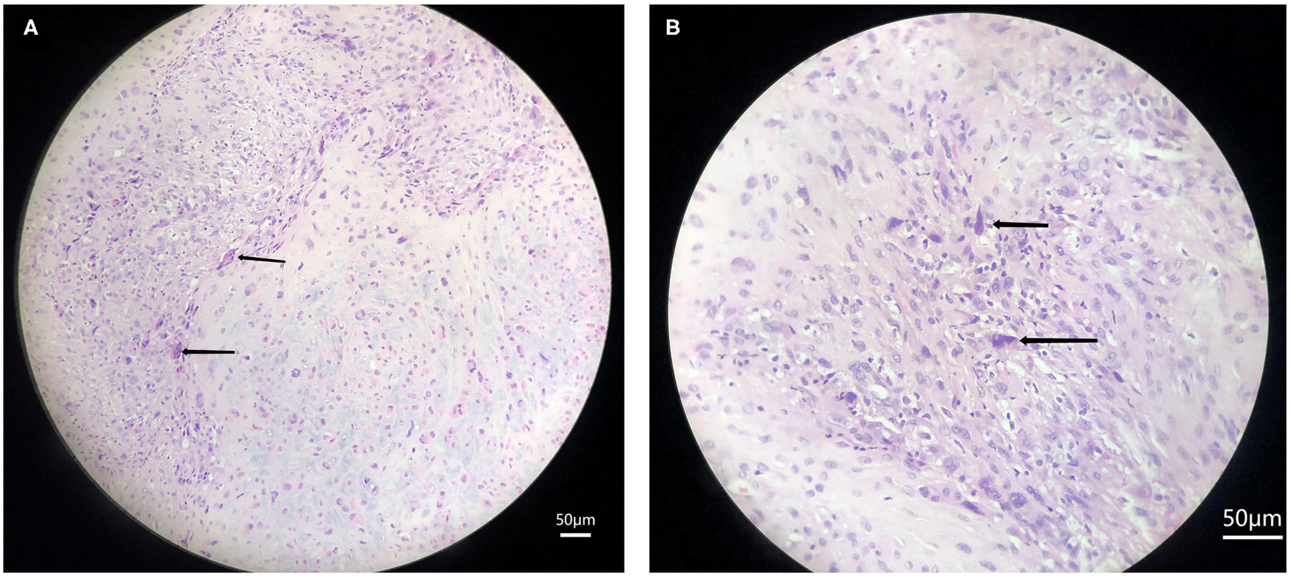

FIGURE 1 | Pathological slice of undifferentiated pleomorphic sarcoma. Arrows indicate that the tumor cells have obvious nuclear atypia and pathological nuclear mitosis. **(A)** 20X HE stain, **(B)** 40X HE stain.

brain MRI reexamination showed no recurrent tumor lesion (**Figures 2D–F**).

The above examination and treatment items have obtained the informed consent from the patient who participated in clinical investigations.

DISCUSSION

UPS, also known as malignant fibrous histiocytoma (MFH), is an extremely rare soft tissue malignant tumor. According to WHO latest classification standard in 2013, the concept of MFH was replaced by UPS (2). UPS highly occurs at an age of 60–70 years, with a similar morbidity in males and females; it is frequently seen in limbs, trunk, head and neck, and other organs and tissues, and located deeply, has a high tumor grade and high malignancy, and easily recurs after operation (3). After diagnosis, this case was treated by chemotherapy (no good response) and several surgeries, but the treatment effect was poor, and the patient experienced several relapses with a gradually shortened interval, which complied with the easy recurrence character of UPS.

UPS patients often have a low 5 year survival rate, i.e., 30–50% (3). Peiper et al. (4) investigated 97 patients with a diagnosis of UPS, and their study results showed that the local relapse rate of UPS and the relapse rate of distant metastasis in 13 months (on average) were 31 and 30%, the mean survival was 84 months, and the 5 year survival rate was 70%. Canter et al. (5) also agreed to a low 5 year survival rate of UPS patients as abovementioned. As shown by the study of Lehnhardt et al. (6) which involved 140 cases of UPS in limbs, the 5 year overall survival rate was 72%. In this case, the patient survival could be continuously followed up.

According to the study of Clark et al. (7), head and neck UPS had strong invasiveness and poor prognosis. Sabesan et al. (8) retrospectively analyzed UPS in head and neck and other body parts and drew a conclusion consistent with Clark, which may be attributed to a smaller distance between head and neck tumors and critical structures and a bigger difficulty in surgically resecting complete tumors. Compared with tumors in body trunk and limbs, head and neck tumors are more easily detected at the early stage and thus often have a smaller size and a lower grade. In this case, however, the tumor was located deeply at infratemporal fossa and thus difficult to be completely resected by surgery; considering no distant metastasis, the treatment was surgery + radiotherapy, without requiring chemotherapy.

In the recent years, heavy ion radiotherapy has gradually become a leading technique in the field of tumor radiotherapy, and heavy ions refer to ionized particles heavier than helium element. Carbon ion radiation kills tumor cells via the abovementioned cluster injury, while traditional low-LET-radiation X ray injures tumor cells mainly by independently destroying DNA single-strand or double-strand; tumor cells can repair the injury caused by the later, but are incapable to repair more complicated and diverse DNA cluster injury caused by the former; thus, DNA cluster injury is an important mechanism of carbon ions killing tumor cells (9). In the past nearly 20 years, the National Institute of Radiation Medicine (Japan) has intermittently conducted the clinical studies of carbon ion radiotherapy for head and neck tumors, involving 175 cases of adenoid cystic carcinoma, 102 cases of malignant mucosal melanoma, and 50 cases of adenocarcinoma, separately located in paranasal sinus, nasal cavity, major salivary glands and throat, of which nearly 74% could not be treated by surgery; the 5 year local control rate (LCR) and 5 year overall survival rate (OSR) were

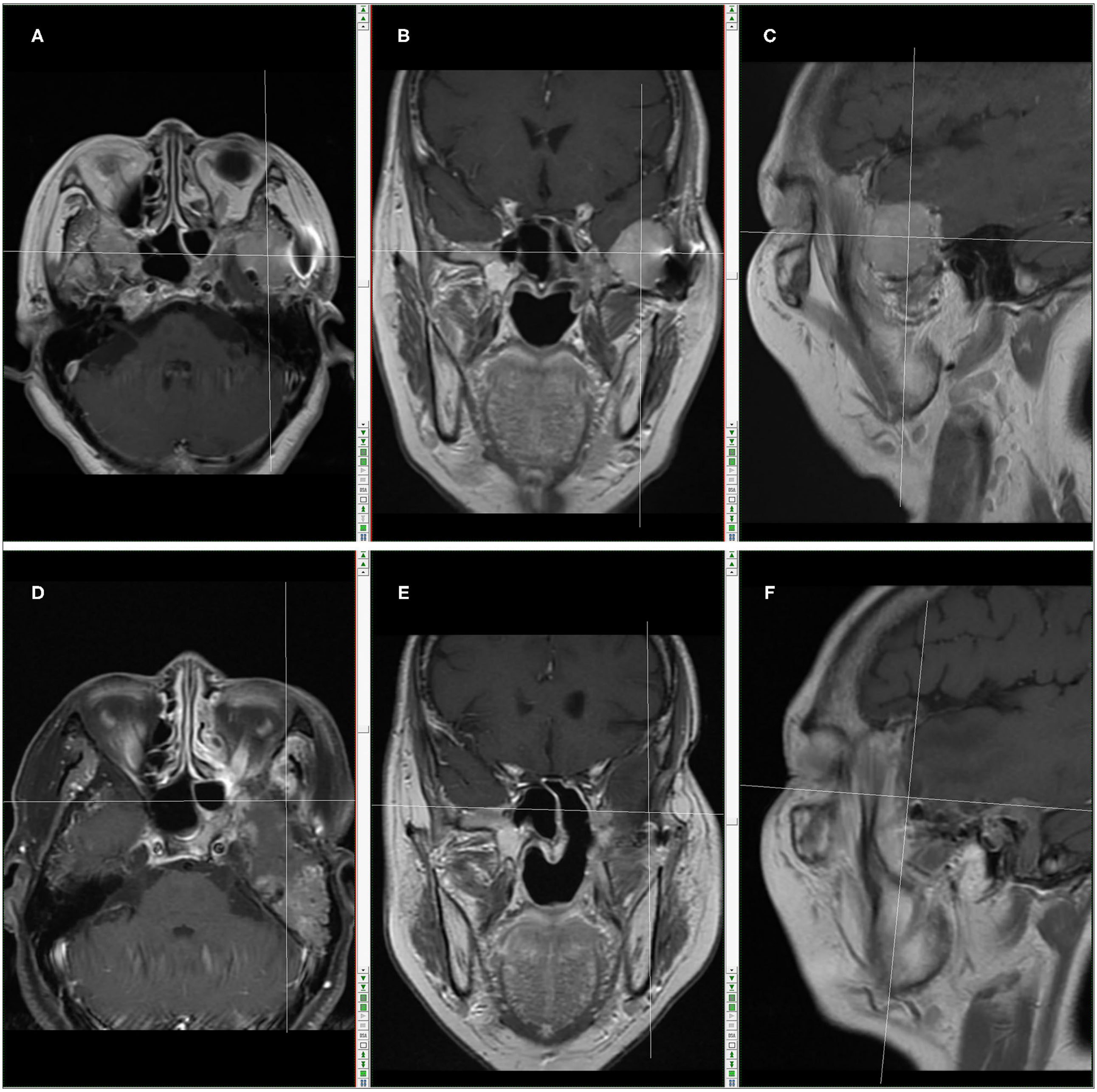

FIGURE 2 | Skull base MRI in May, 2018 (Before the operation combined with carbon-ion radiotherapy): **(A)** MR images in transection. **(B)** MR images in coronal plane; **(C)** MR images in sagittal plane. The cross location denotes the recurring tumor. Skull base MRI in March, 2019 (After the operation combined with carbon-ion radiotherapy): **(D)** MR images in transection; **(E)** MR images in coronal plane; **(F)** MR images in sagittal plane. The cross location denotes no recurrent tumor.

74, 79, 81, and 72, 33, 57%, respectively (10). In another study totally including 76 cases of malignant skull base tumor (44 cases of chordoma, 14 cases of chondrosarcoma, 9 cases of olfactory neuroblastoma, 7 cases of malignant meningioma, 1 case of giant cell tumor, and 1 case of neuroendocrine carcinoma), the treatment was NIRS + carbon ion radiotherapy, the 5-year LCRA and OSR were 88% and 82%, and none of patients experienced serious adverse reactions (11).

The major therapy for malignant tumors of head and neck and skull base is traditionally surgical resection, but complete resection is difficult for tumors with deep invasion and special locations, and surgical treatment will occasionally damage the face of patients and thus seriously influence the quality of life; therefore, radiotherapy is required to improve the LCR. A part of tumors, such as UPS, chordoma and adenoid cystic carcinoma, are resistant to conventional X-rays, and their local control needs a dose of 60 GyE or above (12). In this case, several surgical resections + postoperative 70 GyE radiotherapy realized the purpose of controlling tumor relapse; no sign of tumor relapse was observed before sending this article, and the patient could be continuously followed up. Traditional radiotherapy is incapable to safely release the above dose because of influence from surrounding dangerous organs (spinal cord, brain stem, optic neuropathway, etc.), while carbon ion beam can achieve the local control efficacy, without injuring these organs and changing the face of patients.

In this case, multiple surgical resections and a gradually shortened interval of tumor relapse brought to a challenge for treating UPS, but it was noted that heavy ion radiotherapy after the last surgery achieved a good therapeutic effect, and no sign of relapse was found before sending this article. Based on the above advantages, we have concluded that surgery + carbon ion radiotherapy is a new effective pathway to treat head and neck UPS.

DATA AVAILABILITY STATEMENT

The raw data supporting the conclusions of this article will be made available by the authors, without undue reservation.

ETHICS STATEMENT

Written informed consent was obtained from the individual(s) for the publication of any potentially identifiable images or data included in this article.

AUTHOR CONTRIBUTIONS

ZW, ZT, and QZ: concept and design. ZW, ZT, HZ, XZ, and QZ: supervision. ZW, ZT, HZ, XZ, XH, and QZ: resources. ZW, ZT, XH, and QZ: materials. ZW and ZT: data collection and processing, analysis and interpretation, literature search, and writing manuscript. QZ: critical review. All authors contributed to the article and approved the submitted version.

FUNDING

This study was supported by the Shenzhen Key Medical Discipline Construction Fund (SZXK039) and the Health Science and Technology Program of Shenzhen Longgang District (LGKCYLWS2020097).

REFERENCES

1. Liu SR, Cai XR, Qiu L. WHO bone tumor classification interpretation. *Magn Reson Imaging*. (2020) 11:1086–91. doi: 10.12015/issn.1674-8034.2020.12.002
2. Fang SG, Zhou XJ. Reading a new version of the WHO (2013) classification of bone tumors. *Int J Clin Exp Pathol*. (2014) 30:119–22.
3. Nakayama Y, Minagawa N, Torigoe T, Yamaguchi K. Malignant fibrous histiocytoma originating from the mesorectum: a case report. *World J Surg Oncol*. (2011) 9:15. doi: 10.1186/1477-7819-9-15
4. Peiper M, Zurakowski D, Knoefel WT, Izbicki JR. Malignant fibrous histiocytoma of the extremities and trunk: an institutional review. *Surgery*. (2004) 135:59–66. doi: 10.1016/S0039-6060(03)00325-8
5. Canter RJ, Beal S, Borys D, Martinez SR, Bold RJ, Robbins AS. Interaction of histologic subtype and histologic grade in predicting survival for soft tissue sarcomas. *J Am Coll Surg*. (2010) 210:191–8. doi: 10.1016/j.jamcollsurg.2009.10.007
6. Lehnhardt M, Daigeler A, Homann HH, Schwaiberger V, Goertz O, Kuhnen C, et al. MFH revisited: outcome after surgical treatment of undifferentiated pleomorphic or not otherwise specified (NOS) sarcomas of the extremities– an analysis of 140 patients. *Langen becks Arch Surg*. (2009) 394:313–20. doi: 10.1007/s00423-008-0368-5
7. Clark DW, Moore BA, Patel SR, Guadagnolo BA, Roberts DB, Sturgis EM, et al. Malignant fibrous histiocytoma of the head and neck region. *Head Neck*. (2011) 33:303–8. doi: 10.1002/hed.21449
8. Sabesan T, Xuexi W, Yongfa Q, Pingzhang T, Ilankovan V. Malignant fibroushistiocytoma: outcome of tumours in the head and neck compared with those in the trunk and extremities. *Br J Oral Maxillofac Surg*. (2006) 44:209–12. doi: 10.1016/j.bjoms.2005.06.006
9. Brenner DJ, Ward JF. Constraints on energy deposition and target size of multiply damaged sites associated with DNA double-strand break. *Int J Radiat Biol*. (1992) 61:737–48. doi: 10.1080/09553009214551591
10. Zhang J, Xiong Z, Zhang F, Feng L, Tang G. Prognostic correlation of MRI characteristics and Ki-67 expression in undifferentiated pleomorphic sarcoma. *J Pract Radiol*. (2016) 32:396–9. doi: 10.3969/j.issn.1002-1671.2016.03.018
11. Fang S, Li Y, Ma Q, Lin L, Zeng Y, Xiao H. Undifferentiated high-grade pleomorphic sarcoma of bone: a clinicopathological analysis of 8 cases. *Chin J Clin Exp Pathol*. (2014) 30:171–5. doi: 10.13315/j.cnki.cjcep.2014.02.013
12. Xi RQ, Guo MF, Xie DH, Chu W, Kang SY. Pathologic and X-ray features of primary palignant fibrous histiocytoma of bone – a report of 16 cases. *Chin J Cancer*. (2006) 25:614–18. doi: 10.3969/j.issn.1000-467X.2006.05.019

Conflict of Interest: The authors declare that the research was conducted in the absence of any commercial or financial relationships that could be construed as a potential conflict of interest.

frontiers in Surgery

ORIGINAL RESEARCH
published: 03 September 2021
doi: 10.3389/fsurg.2021.720506

Low-Dosage Bevacizumab Treatment: Effect on Radiation Necrosis After Gamma Knife Radiosurgery for Brain Metastases

Yuxiang Weng[1†], Jie Shen[1†], Luyuan Zhang[1†], Zebin Fang[1], Feng Xiao[1], Chao Zhang[1], Zuoxu Fan[1], Kaiyuan Huang[1], Liyun Wang[2], Bin Huang[3], Fan Wu[1], Tiesong Zhang[1] and Qingsheng Xu[1]*

[1] Department of Neurosurgery, College of Medicine, The First Affiliated Hospital, Zhejiang University, Hangzhou, China, [2] Department of Neurosurgery, Shengzhou People's Hospital, Shaoxing, China, [3] Department of Neurosurgery, Xinchang Hospital of Traditional Chinese Medicine, Shaoxing, China

OPEN ACCESS

Edited by:
Weihong Jiang,
Central South University, China

Reviewed by:
Xin Wang,
Capital Medical University, China
Mei Luo,
Central South University, China

***Correspondence:**
Qingsheng Xu
xuqingsheng79@zju.edu.cn

[†] These authors have contributed equally to this work

Specialty section:
This article was submitted to Surgical Oncology, a section of the journal Frontiers in Surgery

Received: 04 June 2021
Accepted: 15 July 2021
Published: 03 September 2021

Citation:
Weng Y, Shen J, Zhang L, Fang Z, Xiao F, Zhang C, Fan Z, Huang K, Wang L, Huang B, Wu F, Zhang T and Xu Q (2021) Low-Dosage Bevacizumab Treatment: Effect on Radiation Necrosis After Gamma Knife Radiosurgery for Brain Metastases. Front. Surg. 8:720506. doi: 10.3389/fsurg.2021.720506

Cerebral radiation necrosis (RN), a complication of Gamma Knife radiosurgery, is difficult to treat, although bevacizumab seems to be effective. However, clinical data pertaining to bevacizumab treatment for RN are scarce, and its high price is problematic. This study explored the effectiveness of low-dose bevacizumab for RN caused by Gamma Knife. We retrospectively analyzed 22 patients who suffered cerebral RN post-Gamma Knife, and received bevacizumab treatment because of the poor efficacy of glucocorticoids. Low-dose bevacizumab (3 mg/kg) was administered for two cycles at 2-week intervals. T1- and T2-enhanced magnetic resonance imaging (MRI) images were examined for changes in RN status. We also monitored the dose of glucocorticoid, Karnofsky Performance Status (KPS) score, and adverse drug reactions. The mean volume of RN lesions decreased by 45% on T1-weighted images with contrast enhancement, and by 74% on T2-weighted images. All patients discontinued the use of glucocorticoids. According to the KPS scores, all patients showed an improvement in their symptoms and neurological function. No side effects were observed. Low-dosage bevacizumab at a dose of 3 mg/kg every 2 weeks is effective for treating cerebral RN after Gamma knife for brain metastases.

Keywords: low-dosage, bevacizumab, radiation necrosis, gamma knife, brain metastase

INTRODUCTION

Gamma Knife, a type of stereotactic radiosurgery (SRS), is effective for local control of brain metastases (1). Unfortunately, Gamma Knife leads to the intractable complication of radiation necrosis (RN) (2). At present, glucocorticoids are the standard treatment for cerebral RN, in spite of their adverse side effects and limited treatment efficacy (3). The efficacy of other non-invasive treatments, including antiplatelet, anticoagulation and hyperbaric oxygenation, is considered controversial (1, 2, 4, 5). Surgical management can relieve clinical symptoms due to removal of the mass and reduced intracranial hypertension; however, surgery carries risks and causes neurological damage (6).

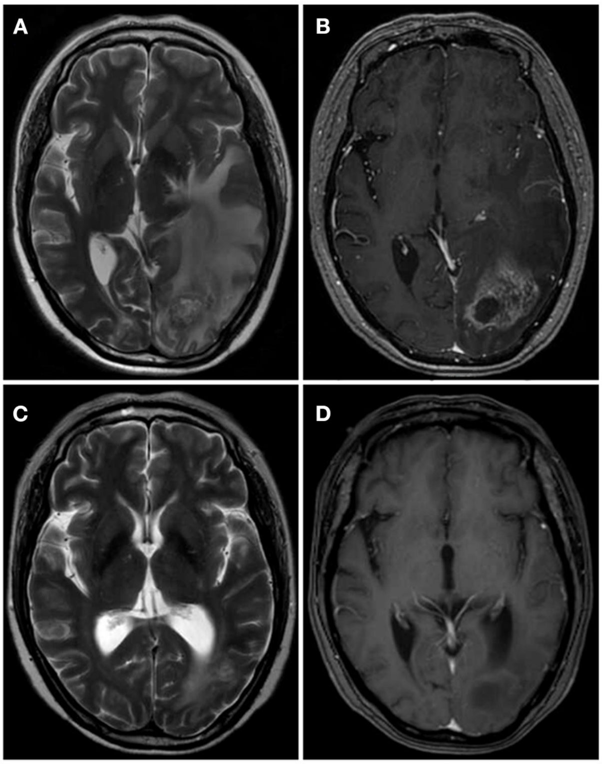

FIGURE 1 | One case of RN after Gamma Knife before and after bevacizumab treatment. **(A,B)** MRI showed the lesion was located in left occipital with large edema area and obvious enhancement surrounding the tumor. **(C,D)** After the therapy of bevacizumab (3 mg/kg) for 2 cycles, the zone of lesion reduced dramatically.

Recently, because of its ability to block vascular endothelial growth factor (VEGF), bevacizumab has proved to be an effective treatment for RN, in large dosage of 5–10 mg/kg every 2 weeks for 2–6 cycles (7–14). However, data on bevacizumab as a therapy for RN are still limited. In addition, bevacizumab is expensive, which creates a large economic burden for patients and society overall. In this study, we evaluated the efficacy of low-dosage bevacizumab treatment for RN following Gamma Knife in patients with brain metastases.

MATERIALS AND METHODS

Patients' Characteristics

We analyzed 22 patients treated with bevacizumab for cerebral RN, caused by Gamma Knife in our center, between January 2013 and December 2017 (**Table 1**). All patients had metastatic brain tumors 13 from lung adenocarcinoma, 2 from Small cell lung cancer, 1 from neuroendocrine lung cancer, 2 from breast cancer, 1 from renal clear cell carcinoma, 1 from maxillary sinus carcinoma and 1 from esophageal Cancer, 1 from ovarian cancer, and long-term glucocorticoid treatment yielded unsatisfactory results.

Diagnostic Criteria of RN

Pathology is the gold standard for a diagnosis of RN, although it is difficult to obtain biopsy specimens. Therefore, RN is usually diagnosed with the help of medical imaging (14, 15). In our study, the final diagnosis of RN was based on history of receiving Gamma Knife, clinical symptoms, physical examination, imaging, and biopsy. Low T1-weighted and high T2-weighted magnetic resonance imaging (MRI) images revealed cerebral edema surrounding the tumor and an enhanced irradiated field (**Figure 1**). Perfusion computed tomography (PCT) demonstrated low cerebral blood volume (CBV), low cerebral blood flow (CBF) and higher mean transit time (MTT) in RN (16).

Therapeutic Regimen Based on Bevacizumab

All patients received two low dosage of bevacizumab (3 mg/kg), 2 weeks apart, for 2–4 courses. Two patients had two separate cycles of bevacizumab because RN recurred during the 6 months follow-up after bevacizumab discontinuation. All patients were hospitalized for observation of adverse drug reactions.

Treatment Assessment

Enhanced MRI was performed before and after bevacizumab treatment, and was then repeated 2 months after the end of bevacizumab therapy in the two patients with repeated cycles. When patients developed neurological symptoms, MRI scans were evaluated immediately. We calculated the volume of RN lesions on T1 and T2 sequences, and compared the findings to those based on images acquired before bevacizumab was started. When patients underwent MRI scans pre- and post-bevacizumab, or to check for the onset of new symptoms, we could analyze the clinical data in terms of changes in neurological symptoms, glucocorticoid dosage, Karnofsky Performance Status (KPS) score, and clinical outcome.

RESULTS

Table 1 shows patients ranged in age from 48 to 79 years (median: 64 years old). Eleven patients were male and others were female; all patients had undergone Gamma Knife with the prescription dosage of 15–25 Gy (median dosage: 20 Gy). In these patients, sixteen (72.7%) patients had brain metastases from lung cancer (**Figure 2**). Among 22 patients, 7 (31.8%) patients had metastases located in the frontal lobe, and 4 (18.2%) patients had metastases located in the parietal lobe (**Figure 2**). The mean volume of the RN lesions was 14.5 cm^3 (range from 3.1 to 45.9 cm^3) on T1 images post-gadolinium, and 109.25 cm^3 (range: 26.7–266.8 cm^3) on T2 images before bevacizumab treatment. After bevacizumab therapy, the average lesion volume was 6.99 cm^3 (range: 0.7–20.6 cm^3) on T1 contrast images and 26.1 cm^3 (range: 5.6–60.8 cm^3) on T2 images. Therefore, the average volume of RN lesions was reduced by 45% on T1-weighted contrast images and 74% on T2-weighted images (**Figure 3**). All patients discontinued the use of glucocorticoids after receiving two cycles of bevacizumab therapy. KPS scores were increased by an average of 31.8 in all patients' post-therapy (**Figure 3**). No side effects were observed.

TABLE 1 | Characteristics of patients with radiation necrosis after Gamma Knife for brain metastases.

No.	Sex	Original tumor	Metastatic site	Prescription dose (Gy)	% Decrease in gadolinium	% Decrease in T2	KPS change
1	F	Lung adenocarcinoma	Left temporal and parietal	22	21	86	50
2	F	Lung adenocarcinoma	Left occipital	20	18	83	50
3	F	Lung adenocarcinoma	Right parietal	18	27	45	40
4	M	Lung adenocarcinoma	Left frontal	15	82	59	50
5	F	Lung adenocarcinoma	Right frontal and parietal	20	34	52	20
6	F	Lung adenocarcinoma	Left occipital	20	55	72	10
7	M	Lung adenocarcinoma	Right frontal	18	10	64	10
8	M	Neuroendocrine lung cancer	Right parietal	24	34	61	40
9	M	Small cell lung cancer	Left posteior horn of lateral ventricle	24	82	80	40
10	M	Small cell lung cancer	Right parietal and occipital	25	49	79	40
11	F	Breast cancer	Left frontal	24	38	81	40
12	M	Renal clear cell carcinoma	Left frontal	22	31	69	40
13	M	Maxillary sinus carcinoma	Right temporal	15	42	79	50
14	M	Esophageal cancer	Right occiptal	24	56	83	10
15	M	Lung adenocarcinoma	Right parietal	20	23	82	40
16	M	Lung adenocarcinoma	Left parietal	18	70	90	30
17	F	Lung adenocarcinoma	Right frontal	22	73	85	40
18	M	Lung adenocarcinoma	Right posteior horn of lateral ventricle	15	33	85	20
19	F	Lung adenocarcinoma	Left frontal	22	67	66	20
20	F	Lung adenocarcinoma	Right posteior horn of lateral ventricle	22	81	85	20
21	F	Breast cancer	Right frontal	15	30	78	30
22	F	Ovarian cancer	Left temporal	20	28	68	20

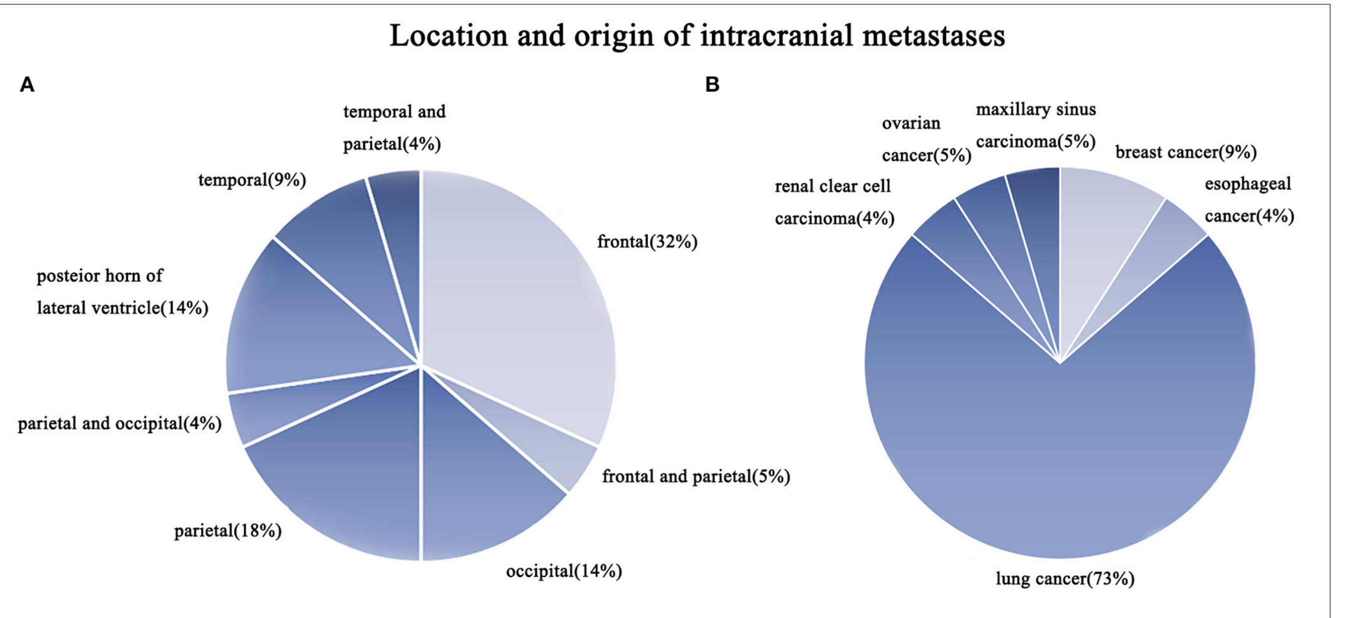

FIGURE 2 | (A) The location of the intracranial metastases in this series of cases, with the frontal lobe having the most lesions, followed by the temporal lobe. **(B)** The source of metastases in this series of cases, with lung cancer having the most brain metastases (73%).

DISCUSSION

RN is the most common complication in patients with brain metastases treated by SRS (2). The main factors associated with RN are irradiation dosage, treatment duration, volume of irradiation and fractionation regimen (17, 18). RN usually occurs 3 or more months after radiotherapy (mean: 11.6 months) and 13–17% of patients develop some degree of RN after receiving SRS therapy for 1 year (19, 20). A meta-analysis of RN found that the most common necrotic

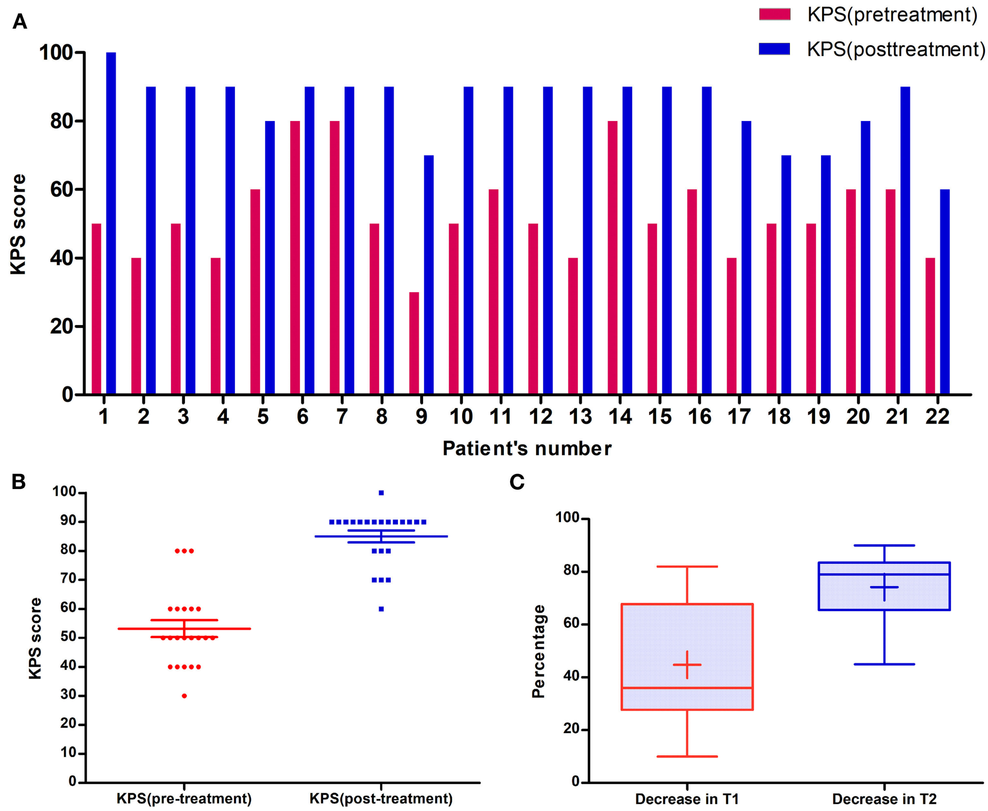

FIGURE 3 | (A) The change of each patient's KPS score after bevacizumab treatment. **(B)** Scatter plot of KPS scores of patients in cohort before and after bevacizumab treatment: the median KPS score of patients before bevacizumab treatment was 50, however, median KPS score increased to 90 after bevacizumab treatment. **(C)** Boxplot of imageology of patients in cohort before and after bevacizumab treatment. After bevacizumab treatment, the volume of nidus in Gadolinium and T2 sequence decreased by 44.7 and 74.2%, respectively.

sites were the frontal lobe (25%), temporal lobe (24%), and parietal lobe (10%). RN causes symptoms including focal or systemic neurological deficits. In severe cases, patients may experience a major decrease in quality of life (17, 21).

The mechanism of RN is unclear. At present, it is believed that RN progresses continuously from endothelial cell dysfunction to tissue hypoxia and necrosis, accompanied by the release of cytokines, such as VEGF (2, 14, 17, 18), which can lead to destruction of the blood-brain barrier permeability and cerebral edema (22, 23). Both animal and human models of RN have shown that high levels of VEGF occur due to blood-brain barrier dysfunction (24, 25). Nordal et al. reported that lab rats without the gene encoding VEGF were more resistant to radiation damage (26). Early blocking of VEGF can lower the risk of RN by reducing vascular permeability. This may help reverse pathological mechanisms, improve symptoms and prevent further disease progression. Bevacizumab seems to be an effective new treatment for RN, which exerts its effects through angiogenesis inhibition.

Data on the efficacy of bevacizumab treatment for RN are limited. However, recent literature has suggested that bevacizumab plays an important role in preventing RN. Gonzalez et al. were the first to report a potential benefit of bevacizumab treatment on RN. After treatment with bevacizumab at a dosage of 5 mg/kg every 2 weeks, or 7.5 mg/kg every 3 weeks, the neurological symptoms of eight patients affected by cerebral RN improved. The average reduction in the abnormal area on T1-weighted post-gadolinium images was 48%, compared to 60% on fluid-attenuated inversion recovery (FLAIR) images (3). Torcuator et al. assessed six biopsy-confirmed RN patients who received low-dosage bevacizumab; follow-up MRI showed an improvement in RN, with an average reduction in the abnormal area on T1-weighted post-gadolinium and FLAIR images of 79 and 49%, respectively (27). In a randomized, double-blind, placebo-controlled study, after bevacizumab treatment (7.5 mg/kg every 3 weeks) 14 patients with biopsy-confirmed RN showed a median reduction in edema volume of 59 and 63% on T2-FLAIR and T1-weighted post-gadolinium images, respectively. In addition, although some complications occurred after bevacizumab treatment, these 14 patients showed improvements in clinical symptoms (15). Delishaj et al. reviewed 125 patients, 114 (91.2%) of whom showed an improvement in neurological symptoms (17). In our study, the mean lesion volume decreased by 41 and 71% on T1-weighted contrast images and T2-weighted images, respectively. The KPS scores of all patients improved by > 30. Previous studies reported that patient dependence on glucocorticoids decreased after bevacizumab treatment, and that the dosage of glucocorticoids could be reduced (7, 23, 28). In our center, all patients gradually tapered off glucocorticoids after two cycles of bevacizumab treatment. Our data are consistent with previous studies, and therefore support a role of bevacizumab in the treatment of RN after Gamma Knife treatment for cerebral metastases.

In a prospective phase II clinical study, bevacizumab at a dosage of 1 mg/kg was used to treat cerebral RN. The regimen included three treatment cycles and one infusion every 3 weeks. Preliminary results showed that the severity of the symptoms decreased after bevacizumab treatment in 90% of patients (29). This suggests that ultra-low dosage bevacizumab could be a valid alternative to the standard dosage. At present, bevacizumab is regarded as a treatment that can be applied subsequent to RN diagnosis; whether it could also be used as a preventive treatment is rarely mentioned. A study including 54 adults male Wistar rats reported less severe RN in animals receiving prophylactic bevacizumab treatment before a 100-Gy radiation dosage (30). If further clinical research confirms these findings, it may be possible to consider bevacizumab as a preventive rather than purely treatment modality.

Bevacizumab has few side effects; however, patients who receive this agent are at risk of gastrointestinal perforation, delayed wound healing, thromboembolic events, asymptomatic ischemic changes, and even symptomatic ischemic changes such as hemiplegia (5, 31). The rate of adverse events (9.5%) reported by Bodensohn et al. (23) was not replicated in our study; in fact, no adverse events were observed in any of the 14 patients treated with low-doage bevacizumab. However, this finding is likely related to the small number of patients and relatively short follow-up time.

Our study had several limitations, including the small sample, which was recruited from a single-center with a descriptive analysis. This may have biased the analysis and conclusions. Larger studies are needed to confirm our findings and determine the optimal bevacizumab treatment schedule for RN.

CONCLUSIONS

In conclusion, low-dosage bevacizumab at a dosage of 3 mg/kg every 2 weeks is effective for the treatment of cerebral RN after Gamma Knife for brain metastases.

DATA AVAILABILITY STATEMENT

The original contributions presented in the study are included in the article/supplementary material, further inquiries can be directed to the corresponding author/s.

ETHICS STATEMENT

Ethics approval has been obtained from the ethics committee of the First Affiliated Hospital of Zhejiang University. The patients/participants provided their written informed consent to participate in this study.

AUTHOR CONTRIBUTIONS

QX is guarantor of integrity of the entire study. YW, JS, and LZ designed the study and prepare manuscript. ZFang and CZ collected the patient's information. FX, ZFan, and KH are response to statistical analysis. BH, LW, and TZ contributed to literature research. All authors agreed to be accountable for the content of the work.

REFERENCES

1. Frazier JL, Batra S, Kapor S, Vellimana A, Gandhi R, Carson KA, et al. Stereotactic radiosurgery in the management of brain metastases: an institutional retrospective analysis of survival. *Int J Radiat Oncol Biol Phys.* (2010) 76:1486–92. doi: 10.1016/j.ijrobp.2009.03.028
2. Le Rhun E, Dhermain F, Vogin G, Reyns N, Metellus P. Radionecrosis after stereotactic radiotherapy for brain metastases. *Expert Rev Neurother.* (2016) 16:903–14. doi: 10.1080/14737175.2016.1184572
3. Gonzalez J, Kumar AJ, Conrad CA, Levin VA. Effect of bevacizumab on radiation necrosis of the brain. *Int J Radiat Oncol Biol Phys.* (2007) 67:323–6. doi: 10.1016/j.ijrobp.2006.10.010
4. Ohguri T, Imada H, Kohshi K, Kakeda S, Ohnari N, Morioka T, et al. Effect of prophylactic hyperbaric oxygen treatment for radiation-induced brain injury after stereotactic radiosurgery of brain metastases. *Int J Radiat Oncol Biol Phys.* (2007) 67:248–55. doi: 10.1016/j.ijrobp.2006.08.009
5. Lubelski D, Abdullah KG, Weil RJ, Marko NF. Bevacizumab for radiation necrosis following treatment of high grade glioma: a systematic review of the literature. *J Neuro-Oncol.* (2013) 115:317–22. doi: 10.1007/s11060-013-1233-0
6. McPherson C, Warnick R. Results of contemporary surgical management of RN using frameless stereotaxis and intraoperative magnetic resonance imaging. *J Neurooncol.* (2004) 68:41–7. doi: 10.1023/B:NEON.0000024744.16031.e9
7. Wang Y, Pan L, Sheng X, Mao Y, Yao Y, Wang E, et al. Reversal of cerebral radiation necrosis with bevacizumab treatment in 17 Chinese patients. *Eur J Med Res.* (2012) 17:25. doi: 10.1186/2047-783X-17-25
8. Boothe D, Young R, Yamada Y, Prager A, Chan T, Beal K. Bevacizumab as a treatment for radiation necrosis of brain metastases post stereotactic radiosurgery. *Neuro Oncol.* (2013) 15:1257–63. doi: 10.1093/neuonc/not085
9. Furuse M, Nonoguchi N, Kawabata S, Yoritsune E, Takahashi M, Inomata T, et al. Bevacizumab treatment for symptomatic radiation necrosis diagnosed by amino acid PET. *Jpn J Clin Oncol.* (2013) 43:337–41. doi: 10.1093/jjco/hys231
10. Bostrom JP, Seifert M, Greschus S, Schafer N, Glas M, Lammering G, et al. Bevacizumab treatment in malignant meningioma with additional radiation necrosis. an MRI diffusion and perfusion case study. *Strahlenther Onkol.* (2014) 190:416–21. doi: 10.1007/s00066-013-0505-0
11. Delishaj D, Ursino S, Pasqualetti F, Pesaresi I, Desideri I, Cosottini M, et al. The effectiveness of bevacizumab in radionecrosis after radiosurgery of a single brain metastasis. *Rare Tumors.* (2015) 7:6018. doi: 10.4081/rt.2015.6018
12. Sadraei NH, Dahiya S, Chao ST, Murphy ES, Osei-Boateng K, Xie H, et al. Treatment of cerebral radiation necrosis with bevacizumab:

the Cleveland clinic experience. *Am J Clin Oncol.* (2015) 38:304–310. doi: 10.1097/COC.0b013e31829c3139
13. Xiang-Pan L, Yuxin C, Xiao-Fei W, Na L, Tang-Peng X, Xiao-Tao X, et al. Bevacizumab alleviates radiation-induced brain necrosis: a report of four cases. *J Cancer Res Ther.* (2015) 11:485–7. doi: 10.4103/0973-1482.140782
14. Zhuang H, Yuan X, Zheng Y, Li X, Chang JY, Wang J, et al. A study on the evaluation method and recent clinical efficacy of bevacizumab on the treatment of radiation cerebral necrosis. *Sci Rep.* (2016) 6:24364. doi: 10.1038/srep24364
15. Levin VA, Bidaut L, Hou P, Kumar AJ, Wefel JS, Bekele BN, et al. Randomized double-blind placebo-controlled trial of bevacizumab therapy for radiation necrosis of the central nervous system. *Int J Radiat Oncol Biol Phys.* (2011) 79:1487–1495. doi: 10.1016/j.ijrobp.2009.12.061
16. Chernov M, Ono Y, Abe K, Usukura M, Hayashi M, Izawa M, et al. Differentiation of tumor progression and radiation-induced effects after intracranial radiosurgery. *Acta Neurochir Suppl.* (2013) 116:193–210. doi: 10.1007/978-3-7091-1376-9_29
17. Delishaj D, Ursino S, Pasqualetti F, Cristaudo A, Cosottini M, Fabrini MG, et al. Bevacizumab for the treatment of radiation-induced cerebral necrosis: a systematic review of the literature. *J Clin Med Res.* (2017) 9:273–80. doi: 10.14740/jocmr2936e
18. Ali FS, Arevalo O, Zorofchian S, Patrizz A, Riascos R, Tandon N, et al. Cerebral radiation necrosis: incidence, pathogenesis, diagnostic challenges, and future opportunities. *Curr Oncol Rep.* (2019) 21:66. doi: 10.1007/s11912-019-0818-y
19. Sneed PK, Mendez J, Vemer-van den Hoek JGM, Seymour ZA, Ma L, Molinaro AM, et al. Adverse radiation effect after stereotactic radiosurgery for brain metastases: incidence, time course, and risk factors. *J Neurosurg.* (2015) 123:373–86. doi: 10.3171/2014.10.JNS141610
20. Kohutek ZA, Yamada Y, Chan TA, Brennan CW, Tabar V, Gutin PH, et al. Long-term risk of radionecrosis and imaging changes after stereotactic radiosurgery for brain metastases. *J Neurooncol.* (2015) 125:149–56. doi: 10.1007/s11060-015-1881-3
21. Matuschek C, Bolke E, Nawatny J, Hoffmann TK, Peiper M, Orth K, et al. Bevacizumab as a treatment option for radiation-induced cerebral necrosis. *Strahlenther Onkol.* (2011) 187:135–9. doi: 10.1007/s00066-010-2184-4
22. Coderre JA, Morris GM, Micca PL, Hopewell JW, Verhagen I, Kleiboer BJ, et al. Late effects of radiation on the central nervous system: role of vascular endothelial damage and glial stem cell survival. *Radiat Res.* (2006) 166:495–503. doi: 10.1667/RR3597.1
23. Bodensohn R, Hadi I, Fleischmann DF, Corradini S, Thon N, Rauch J, et al. Bevacizumab as a treatment option for radiation necrosis after cranial radiation therapy: a retrospective monocentric analysis. *Strahlenther Onkol.* (2019) 196:70–6. doi: 10.1007/s00066-019-01521-x
24. Kim J, Chung Y, Kim C, Kim H, Lee H. Upregulation of VEGF and FGF2 in normal rat brain after experimental intraoperative radiation therapy. *J Korean Med Sci.* (2004) 19:879–86. doi: 10.3346/jkms.2004.19.6.879
25. Gerstner ER, Duda DG, di Tomaso E, Ryg PA, Loeffler JS, Sorensen AG, et al. VEGF inhibitors in the treatment of cerebral edema in patients with brain cancer. *Nat Rev Clin Onco.* (2009) 6:229–36. doi: 10.1038/nrclinonc.2009.14
26. Nordal R, Nagy A, Pintilie M, Wong C. Hypoxia and hypoxia-inducible factor-1 target genes in central nervous system radiation injury: a role for vascular endothelial growth factor. *Clin Cancer Res.* (2004) 10:3342–53. doi: 10.1158/1078-0432.CCR-03-0426
27. Torcuator R, Zuniga R, Mohan YS, Rock J, Doyle T, Anderson J, et al. Initial experience with bevacizumab treatment for biopsy confirmed cerebral radiation necrosis. *J Neurooncol.* (2009) 94:63–8. doi: 10.1007/s11060-009-9801-z
28. Jeyaretna D, Curry WT J, Batchelor T, Stemmer-Rachamimov A, Plotkin S. Exacerbation of cerebral radiation necrosis by bevacizumab. *J Clin Oncol.* (2011) 29:E159–E62. doi: 10.1200/JCO.2010.31.4815
29. Zhuang H, Zhuang H, Shi S, Wang Y. Ultra-low-dose bevacizumab for cerebral radiation necrosis: a prospective phase II clinical study. *OncoTargets Therap.* (2019) 12:8447–53. doi: 10.2147/OTT.S223258
30. Aslan A, Kaya ZB, Bulduk EB, Ocal O, Ucar M, Erpolat OP, et al. Prophylactic bevacizumab may mitigate radiation injury: an experimental study. *World Neurosurg.* (2018) 116:e791–800. doi: 10.1016/j.wneu.2018.05.094
31. Tye K, Engelhard HH, Slavin KV, Nicholas MK, Chmura SJ, Kwok Y, et al. An analysis of radiation necrosis of the central nervous system treated with bevacizumab. *J Neurooncol.* (2014) 117:321–7. doi: 10.1007/s11060-014-1391-8

Conflict of Interest: The authors declare that the research was conducted in the absence of any commercial or financial relationships that could be construed as a potential conflict of interest.

Publisher's Note: All claims expressed in this article are solely those of the authors and do not necessarily represent those of their affiliated organizations, or those of the publisher, the editors and the reviewers. Any product that may be evaluated in this article, or claim that may be made by its manufacturer, is not guaranteed or endorsed by the publisher.

frontiers in Oncology

ORIGINAL RESEARCH
published: 22 September 2021
doi: 10.3389/fonc.2021.743370

Reconstruction of Complex Lateral Skull Base Defects After Oral Cancer Resection With Individualized Anterolateral Thigh Flap

Zhaojian Gong[1*†], *Shanshan Zhang*[2*†], *Chang Chen*[1], *Yuan Zhi*[1] *and Moxin Zi*[1]

[1] *Department of Stomatology, The Second Xiangya Hospital, Central South University, Changsha, China,* [2] *Department of Stomatology, Xiangya Hospital, Central South University, Changsha, China*

Objectives: Complex lateral skull base defects resulting from advanced or recurrent oral cancer resection are continuously challenging reconstructive surgeons. This study aimed to use reconstructive methods for lateral skull base defects, explore their feasibility, and evaluate the efficacy of defect reconstruction using anterolateral thigh (ALT) flaps.

Patients and Methods: We performed a retrospective case series of 37 patients who underwent lateral skull base defect reconstruction using the ALT/anteromedial thigh (AMT) flap between March 2016 and May 2021 at the Second Xiangya Hospital. The design and harvest of the flaps, methods for defect reconstruction, and reconstructive efficacy are described.

Results: Of the 37 patients, 3 were women and 34 were men, with a mean age of 51.7 years. Among the defects, 26 were through-and-through defects and were reconstructed using ALT chimeric flaps, double ALT flaps, folded ALT flap, combined ALT chimeric flaps and AMT flaps, or combined ALT chimeric flaps and pectoralis major flaps; the large lateral skull base dead spaces were filled with muscle tissues or fatty tissues. Postoperatively, 38 of the 39 ALT/AMT flaps survived completely, and the remaining flap experienced partial necrosis. Venous compromise occurred in one patient who was salvaged after operative exploration. Oral and maxillofacial wound infections occurred in two patients, salivary fistula in three patients, and thigh wound effusion in three patients. The wounds healed gradually in all patients after repeated dressing changes. Thirty-three patients were followed up for approximately 3–60 months; their oral functions and appearance were acceptable, and thigh motor dysfunction was not observed.

Conclusions: With the convenient flap design and muscle flap harvest, large and individualized tissue supply, feasible combination with other flaps, effective reduction or avoidance of wound complications, and acceptable donor site morbidity, the ALT flap is an appropriate choice for complex lateral skull base defect reconstruction.

Keywords: oral cancer, lateral skull base, anterolateral thigh flap, defect, reconstruction

Edited by:
Xiaobiao Zhang,
Fudan University, China

Reviewed by:
Xu Qin,
Huazhong University of Science and Technology, China
Yuefeng Li,
Jiangsu University, China

***Correspondence:**
Zhaojian Gong
gongzhaojian4458@csu.edu.cn
Shanshan Zhang
zhangshanshan@csu.edu.cn

[†]*These authors have contributed equally to this work*

Specialty section:
This article was submitted to Surgical Oncology, a section of the journal Frontiers in Oncology

Received: *18 July 2021*
Accepted: *01 September 2021*
Published: *22 September 2021*

Citation:
Gong Z, Zhang S, Chen C, Zhi Y and Zi M (2021) Reconstruction of Complex Lateral Skull Base Defects After Oral Cancer Resection With Individualized Anterolateral Thigh Flap. Front. Oncol. 11:743370. doi: 10.3389/fonc.2021.743370

INTRODUCTION

Oral cancer is a group of malignant diseases arising from the surface of the tongue, gums, buccal mucosa, floor of the mouth, palate, and lips (1, 2). Current therapies for oral cancer include surgery, radiotherapy, chemotherapy, and combination therapy (1, 3). In general, surgery is the primary treatment modality in most cases. The wide local excision of tumors often results in large and complex oral and maxillofacial defects, severely damaging the function and appearance and even leading to psychological disorders (4). In particular, complex multitissue defects resulting from the radical resection of some recurrent or locally advanced-stage tumors may also involve the lateral skull base. Varying-sized dead spaces are often left in these lateral skull base defects, leading to wound infection or effusion and even more serious complications (4). The reconstruction of such defects remains a reconstructive challenge because of the limited local tissue supply and extremely visible location (5–7).

Several free or pedicle flaps, such as radial forearm flap (8), latissimus dorsi flap (9), anterolateral thigh (ALT) flap (4, 10–12), and pectoralis major flap (13), have been used to repair oral and maxillofacial soft-tissue defects. Among them, the ALT flap, which was first introduced in 1984 by Song et al. (14), is a good candidate. With noticeable advantages and acceptable donor site morbidity, this flap has been increasingly applied in recent years (5, 7, 15–17). The ALT flap is nourished by the lateral circumflex femoral artery (LCFA), and the classic ALT flap or its chimeric flaps are pedicled with the descending branch (DB), the largest and longest branch of the LCFA (4, 17). Therefore, various-sized muscles or adipose tissue can be raised simultaneously with the ALT flap, which is crucial for dead space filling and beneficial for wound healing (4).

ALT flaps have been used to repair lateral skull base defects for some time in our department; they are suitable for the reconstruction of such large and complex defects, which are often caused by extensive resection of recurrent or advanced oral cancer. With the large muscle and/or adipose tissue for dead space filling, reconstruction can result in acceptable esthetic and functional outcomes as well as reduced postoperative complications. Herein, we report our experience with 37 patients who underwent complex lateral skull base defect reconstruction using ALT/anteromedial thigh (AMT) flaps or their chimeric flaps from March 2016 to May 2021.

PATIENTS AND METHODS

Study Design

We designed and implemented a retrospective study to address our research aims. The study population included all patients who presented for management and evaluation of lateral skull base defects and underwent reconstruction using the ALT flap or its chimeric flaps from March 2016 to May 2021 at the Second Xiangya Hospital of Central South University. The inclusion criteria of the study included the following: defects involving the lateral skull base, defects resulting from the resection of locally advanced-stage or recurrent tumors, and defects repaired using ALT flaps or combined ALT flap and other flaps. Moreover, the exclusion criteria were defects not caused by tumor resection or those not reconstructed using ALT flaps. The hospital institutional review board approved this project, and the study followed the guidelines set forth in the Declaration of Helsinki.

Surgical Technique

The flaps were harvested simultaneously with tumor ablation and/or neck dissection in two groups, and the methods for flap design and elevation were as previously described (4, 17). After sectioning of the skin, subcutaneous fat, and fascia, the lateral and/or medial fascia lata were opened, and sizable cutaneous perforators were explored for the ALT and/or AMT flaps. The ALT flaps or their chimeric flaps were harvested accordingly, with the flaps aimed at reconstructing intraoral mucosal and extraoral skin defects and the muscle and/or fat tissue at filling the lateral skull base dead space (**Figures 1**, **2**). Through-and-through defects were repaired using ALT chimeric flaps, double ALT flaps, folded ALT flap, and combined ALT chimeric flaps and AMT flaps and very large defects using combined ALT chimeric flaps and pectoralis major flaps. For some patients, the entire rectus femoris was harvested to fill the dead spaces, which were located in the temporal, subzygomatic, lateral skull base, and submandibular regions. Additionally, the individualized muscle flaps were harvested with the distal end of the vascular pedicles, which are usually the DB and long enough for all oral and maxillofacial dead spaces. Postoperatively, all flaps were strictly and carefully monitored as previously described, and salvage surgery was immediately performed when flap compromise occurred (12).

RESULTS

Among the 37 patients, 3 were women and 34 were men, with a mean age of 51.7 years (range, 40–64 years). At presentation, 25 patients had buccal squamous cell carcinoma (SCC), 1 patient had mandibular SCC, 1 patient had palate SCC, 1 patient had gingival SCC, and 9 patients had recurrent oral SCC.

All 37 complex defects involving the lateral skull base, including 26 through-and-through defects, were repaired using 39 ALT/AMT flaps or their chimeric flaps and 1 pectoralis major flap. The skin paddles of the ALT/AMT flaps were 5 × 9 −11 × 14 cm in size. The through-and-through defects were repaired using ALT chimeric flaps in 22 cases, double ALT flaps in 1 case, folded ALT flap in 1 case, combined ALT chimeric flaps and AMT flaps in 1 case, and combined ALT chimeric flaps and pectoralis major flaps in 1 case, with separate flaps or folded flap for extraoral skin and intraoral mucosal reconstructions. The muscle and fat tissue, such as the rectus femoris and vastus lateralis flaps, were individually designed and harvested to fill the temporal, lateral skull base, subzygomatic, and submandibular dead spaces. The entire rectus femoris was harvested in 20 patients.

Postoperatively, 38 of the 39 ALT/AMT flaps and 1 pectoralis major flap survived completely, and the remaining ALT flap

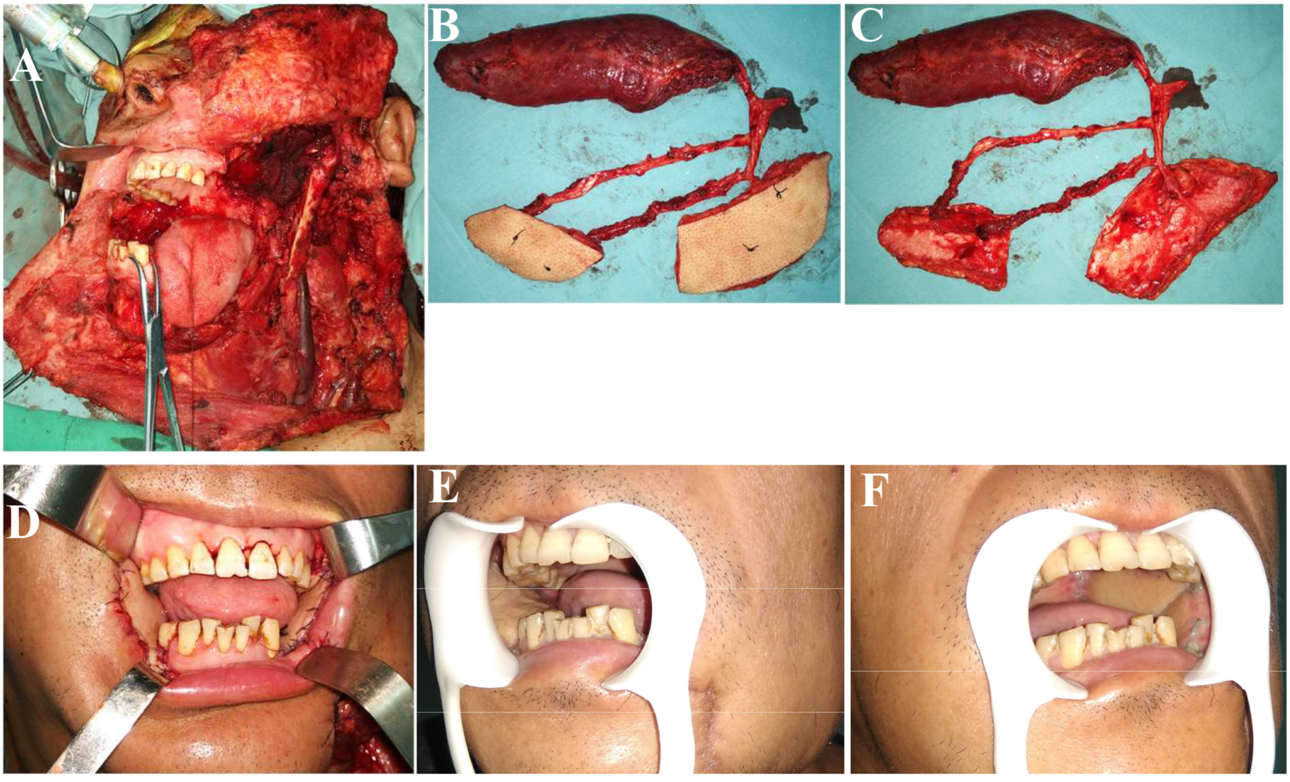

FIGURE 1 | Reconstruction of complex bilateral buccal mucosal defects (involving the lateral skull base) using ALT chimeric flaps. **(A)** Left lateral skull base defects and right buccal mucosal defects resulting from bilateral buccal squamous cell carcinoma resection. **(B, C)** Chimeric ALT, ALT, and rectus femoris flaps (entire rectus femoris). **(D)** Reconstruction of complex defects using ALT chimeric flaps, separate flaps for bilateral buccal mucosal reconstruction, and rectus femoris flap for lateral skull base dead space filling. **(E, F)** One month postoperatively. ALT, anterolateral thigh.

experienced partial necrosis. Venous compromise occurred in 1 patient, which was salvaged after operative exploration, and partial necrosis of the flap then occurred. Of the donor sites (thigh and chest), 35 were primarily closed, resulting in only linear scars, and the other 2 (thigh) were closed using full-thickness skin grafts due to larger defects. In 1 of these 2 cases, the chimeric ALT plus ALT flaps (nourished by the LCFA) and AMT flap (supplied by a branch of the femoral artery) were elevated in the same thigh, and they were then combined in tandem *via* additional vascular anastomoses and used for large defect reconstruction. Oral and maxillofacial wound infections occurred in 2 patients, salivary fistula in 3 patients, and thigh wound effusion in 3 patients. The wounds healed gradually in all patients after repeated dressing changes.

Thirty-three patients were followed up for approximately 3 to 60 months, and their oral functions and appearance were acceptable. Thigh scars caused by flap harvest were not readily visible, and thigh dyskinesia was not observed. Tumor recurrence and/or metastasis occurred in 16 patients during follow-up. Of them, 12 patients received non-surgical treatment or refused further treatment, and the other 4 patients underwent reoperation, including tumor resection and/or contralateral neck dissection.

DISCUSSION

The reconstruction of massive defects resulting from locally advanced-stage or recurrent oral cancer resection is still a difficult challenge owing to the limited local tissue supply, extensive skin and soft-tissue defects, and especially the complex oral and maxillofacial structures, including the existence of the zygomatic bone, zygomatic arch, maxilla, mandible, and other bone tissues (4–6). Large dead spaces are often left in defects involving the lateral skull base, easily leading to wound infection or effusion and even other potentially life-threatening complications (4). Owing to the convenient and individualized flap design, large skin territory, sufficient soft-tissue supply, long pedicle and suitable vessel caliber, minimal and acceptable donor site morbidity, and high success rate of transplantation, the ALT flap has been referred to as a "versatile soft-tissue flap" (4, 18). Many groups, including ourselves, have considered the ALT flap or its chimeric flaps as the preferred choice for oral and maxillofacial soft-tissue defect reconstruction after tumor resection (7, 15).

The wide surgical excision of oral cancer often results in large dead spaces and may lead to wound effusion or infection. In particular, for some locally advanced-stage or recurrent tumors,

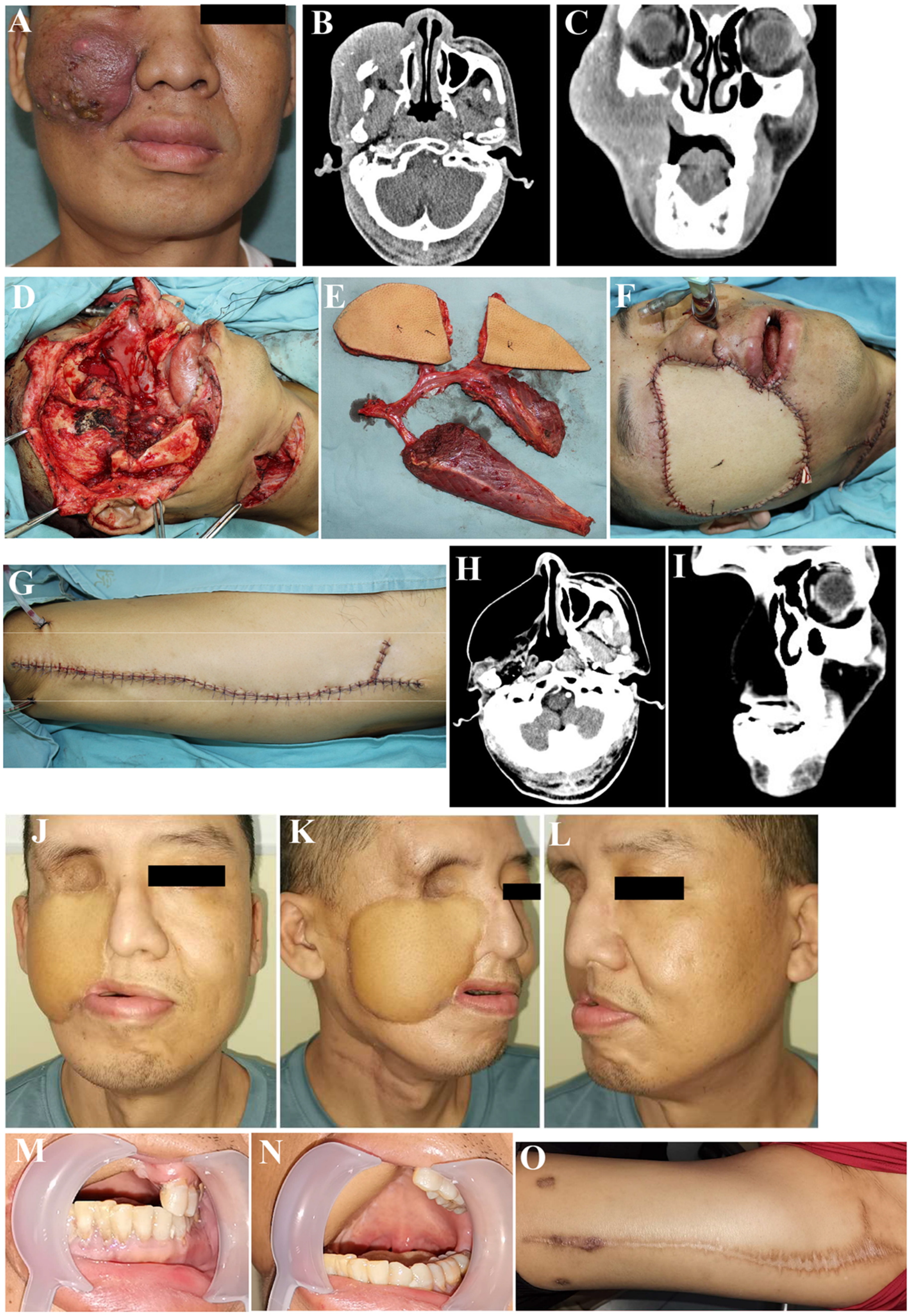

FIGURE 2 | Reconstruction of complex lateral skull base defects using ALT chimeric flaps. **(A)** Recurrence of maxillary gingival squamous cell carcinoma, postoperatively after radiation therapy. **(B, C)** Preoperative CT. **(D)** Through-and-through cheek and lateral skull base defects after tumor resection. **(E)** Chimeric ALT, ALT, and rectus femoris flaps (entire rectus femoris). **(F)** Defects reconstruction using ALT chimeric flaps, separate flaps for intraoral mucosal and extraoral skin reconstruction, and rectus femoris flap for lateral skull base dead space filling. **(G)** Primary closure of the donor site. **(H, I)** Postoperative CT, 52 months postoperatively. **(J–O)**. Sixty months postoperatively. ALT, anterolateral thigh.

defects often involve the lateral skull base and thus complicate defect reconstruction. These dead spaces, including lateral skull base defects, usually require sufficient muscle and/or fat tissue to be filled. The use of ALT flaps or their chimeric flaps for various defect reconstructions can be accomplished *via* incorporating different soft-tissue components, including the skin, fat, fascia, muscle, and nerve (18, 19). According to our previous reports, muscle tissues of various sizes, including the rectus femoris, vastus medialis, and vastus lateralis, could be easily raised with the flap (4, 17). Moreover, the individually designed fat flaps can also be harvested concomitantly or independently, with the flap or other cutaneous perforators originating from the same vascular pedicle (5, 17). This is excellent for the reconstruction of complex oral and maxillofacial defects in which varying-sized dead spaces are often included. The long vascular pedicle, which permits better convenience and freedom in defect reconstruction, is an obvious advantage of the ALT flap (6, 7). With the long pedicle and individually designed muscle flap and/or fat flap, almost all of the dead spaces resulting from oral cancer ablation, such as the temporal region, lateral skull base, subzygomatic region, submandibular region, and floor of the mouth, can be well filled. In our experience, the rectus femoris branch vessel, which arises from the DB of the LCFA and nourishes the rectus femoris, is relatively constant; thus, the elevation of the rectus femoris flap is safe and straightforward (4, 20). With the separated pedicle, rectus femoris branch vessel, and a large amount of muscle tissue with a sufficient length, the rectus femoris flap could be flexibly used either to fill the dead spaces in any position of the oral and maxillofacial region or to cover the major cervical vessels and/or titanium plate (4). Additionally, the ALT flaps were mainly pedicled with the DB, the longest branch of the LCFA; thus, the muscle flaps that elevated with the distal end of the pedicles can also be used flexibly, similar to the rectus femoris flaps. This is particularly useful for the temporal region, subzygomatic region, and lateral skull base reconstructions in which the temporalis muscle is completely removed because of the tumor. In our series, all dead spaces were obliterated with sufficient muscle and/or fat tissue, and the entire rectus femoris was used in 20 patients. Only 2 and 3 patients developed wound infection and salivary fistula, respectively, which eventually healed following repeated dressing changes. One case of wound infection was caused by flap compromise and partial necrosis.

The reconstruction of lateral skull base defects after oral cancer resection is cosmetically, technically, and functionally challenging, especially when presented with through-and-through defects. In addition to the three-dimensional dead spaces that require sufficient muscle and/or fat tissue, the complex intraoral mucosal and extraoral skin defects also require large and separated skin paddles. Although single skin paddle, such as folded ALT flap, can also repair these defects, good outcomes cannot always be accomplished, particularly if the defects are very large or the corners of the mouth are excised (5). The use of separated skin paddles to repair extraoral skin and intraoral mucosal defects can effectively improve the reconstruction, with acceptable appearance, good functions, and a high degree of patient satisfaction (5). According to our experience, ALT chimeric flaps can be easily raised to reconstruct through-and-through defects (17). Chimeric ALT plus AMT flaps or chimeric ALT plus ALT flaps can be designed according to the location of the cutaneous perforators in the thigh. Although ALT chimeric flaps are a good candidate for through-and-through defect reconstruction, chimeric flaps cannot always be successfully elevated in some patients. Double ALT flaps can also be used. They can either be combined with each other through additional vascular anastomosis or be separately used with the respective vascular anastomosis to the cervical vessels. In cases in which the defects are very large, the ALT flap or its chimeric flaps can also be combined with other flaps, such as the pectoralis major flap. Among the 26 through-and-through defects in our series, 22 were reconstructed using ALT chimeric flaps, 1 using double ALT flaps, 1 using folded ALT flap, 1 using combined ALT chimeric flaps and AMT flaps, and 1 using combined ALT chimeric flaps and pectoralis major flaps. With separated skin paddles for the reconstruction of extraoral skin and intraoral mucosal defects, the functional and esthetic outcomes are acceptable. Moreover, the combined ALT flap and pectoralis major flaps can serve as a good choice for the reconstruction of very large oral and maxillofacial through-and-through defects.

Sometimes, a few patients may present with multiple oral mucosal lesions, resulting in complex multiple and non-adjacent defects. The reconstruction of such complex defects remains a major surgical challenge because of the need for flexible and feasible chimeric flaps (21). Although double or more flaps from different donor sites can meet the requirements, the operating time, difficulty, and local damage are increased due to the need of additional donor sites (5). Moreover, two or more sets of recipient vessels are needed; thus, this strategy cannot be achieved in cases with a single available recipient vessel (6). With the long pedicle and consequent freedom in position, the different skin paddles of ALT chimeric flaps can usually be separated at a distance; thus, these flaps can be used to repair multiple non-adjacent defects. As shown in **Figure 1**, ALT chimeric flaps were successfully used to reconstruct bilateral buccal mucosal defects. The use of ALT chimeric flaps to repair multiple and non-adjacent oral and maxillofacial defects not only resulted in reconstruction with acceptable appearance and oral functions but also effectively avoided the use of additional donor sites, thus reducing local damage.

One of the prominent advantages of the ALT flap over other flaps is reduced and acceptable donor site morbidity (6, 19, 22). Normally, thigh donor site defects narrower than 8 cm and even defects larger than 8 cm can be closed directly (6). In our series, only 2 thigh donor sites were closed using full-thickness skin grafts due to larger defects, while the other 35 donor sites were primarily closed, resulting in only linear scars. In 1 patient, the skin graft was raised from the upper part of the same donor site without additional donor sites. In the other patient, in whom the chimeric ALT plus ALT flaps and AMT flap were elevated in the same thigh, the skin graft was harvested from the abdomen. All donor sites healed well, without significant morbidity. The harvest of the rectus femoris did not significantly increase thigh motor dysfunction, without patient complaints regarding inconvenience in daily life. In addition, it is interesting that such harvest, which reduces the amount of thigh tissue, is conducive to the direct suture of donor site defects (4).

Any type of flap, including the ALT flap, has disadvantages. The harvest of the ALT flap is often more complex and riskier than that of other flaps because of the complicated perforator dissection and high perforator variation. In addition, the ALT chimeric flaps with separated skin paddles cannot always be successfully harvested owing to the lack of adequate cutaneous perforators.

CONCLUSIONS

With the convenient flap design and muscle flap harvest, large and individualized tissue supply, feasible combination with other flaps, effective reduction or avoidance of wound complications, and acceptable donor site morbidity, the ALT flap is an appropriate choice for complex lateral skull base defect reconstruction.

DATA AVAILABILITY STATEMENT

The original contributions presented in the study are included in the article/supplementary material. Further inquiries can be directed to the corresponding authors.

ETHICS STATEMENT

The studies involving human participants were reviewed and approved by the Ethics Committee of the Second Xiangya Hospital, Central South University. Written informed consent for participation was not required for this study in accordance with the national legislation and the institutional requirements. Written informed consent was obtained from the individual(s) for the publication of any potentially identifiable images or data included in this article.

AUTHOR CONTRIBUTIONS

Study concepts and design: ZG and SZ. Data acquisition: CC, YZ, and MZ. Quality control of data and algorithms: CC, YZ, and MZ. Data analysis and interpretation: ZG, CC, YZ, and MZ. Manuscript preparation and editing: ZG, SZ, and CC. All authors contributed to the article and approved the submitted version.

ACKNOWLEDGMENTS

We thank Hanjiang Wu, Zhaofu Zhu, Jinbing Liu, and Xiangqing Wu for their excellent technical assistance.

REFERENCES

1. Haddad RI, Shin DM. Recent Advances in Head and Neck Cancer. *N Engl J Med* (2008) 359(11):1143–54. doi: 10.1056/NEJMra0707975
2. Chen SH, Hsiao SY, Chang KY, Chang JY. New Insights Into Oral Squamous Cell Carcinoma: From Clinical Aspects to Molecular Tumorigenesis. *Int J Mol Sci* (2021) 22(5):2252. doi: 10.3390/ijms22052252
3. Yasukawa M, Fujihara H, Fujimori H, Kawaguchi K, Yamada H, Nakayama R, et al. Synergetic Effects of PARP Inhibitor AZD2281 and Cisplatin in Oral Squamous Cell Carcinoma *in Vitro* and *in Vivo*. *Int J Mol Sci* (2016) 17 (3):272. doi: 10.3390/ijms17030272
4. Li P, Zhang S, Liu J, Xu Y, Wu H, Gong Z. Chimeric Anterolateral Thigh and Rectus Femoris Flaps for Reconstruction of Complex Oral and Maxillofacial Defects. *J Craniofac Surg* (2021) 32(5):1841–4. doi: 10.1097/SCS.0000000000007228
5. Gong ZJ, Zhang S, Wang K, Tan HY, Zhu ZF, Liu JB, et al. Chimeric Flaps Pedicled With the Lateral Circumflex Femoral Artery for Individualised Reconstruction of Through-and-Through Oral and Maxillofacial Defects. *Br J Oral Maxillofac Surg* (2015) 53(2):148–52. doi: 10.1016/j.bjoms.2014.10.017
6. Gong ZJ, Zhang S, Zhang S, Liu J, Xu YM, Wu HJ. Reconstruction of Through-And-Through Oromandibular Defects With Combined Fibula Flap and Anterolateral Thigh Flap. *J Oral Maxillofac Surg* (2017) 75(6):1283–92. doi: 10.1016/j.joms.2016.11.025
7. Gong Z, Zhang S, Li P, Liu J, Xu Y. Femoral Artery-Nourished Anteromedial Thigh Flap: A New Perspective in Oral and Maxillofacial Defect Reconstruction. *Oral Oncol* (2021) 117:105295. doi: 10.1016/j.oraloncology.2021.105295
8. Gerressen M, Pastaschek CI, Riediger D, Hilgers RD, Holzle F, Noroozi N, et al. Microsurgical Free Flap Reconstructions of Head and Neck Region in 406 Cases: A 13-Year Experience. *J Oral Maxillofac Surg* (2013) 71(3):628–35. doi: 10.1016/j.joms.2012.07.002
9. Janus JR, Carlson ML, Moore EJ. The Scapular, Parascapular, and Latissimus Dorsi Flap as a Single Osteomyocutaneous Flap for Repair of Complex Oral Defects. *Clin Anat* (2012) 25(1):120–8. doi: 10.1002/ca.21260
10. Gong ZJ, Chen YR, Wang K, Zhang S, Ren ZH, Wu HJ. Longitudinal Contraction Venoplasty in Prevention of Internal Jugular Vein Thrombosis After Free Flap Vascular Anastomosis. *J Oral Maxillofac Surg* (2016) 74 (6):1277–83. doi: 10.1016/j.joms.2016.01.006
11. Liu C, Li P, Liu J, Xu Y, Wu H, Gong Z. Management of Intraoperative Failure of Anterolateral Thigh Flap Transplantation in Head and Neck Reconstruction. *J Oral Maxillofac Surg* (2020) 78(6):1027–33. doi: 10.1016/j.joms.2020.02.010
12. Xu YM, Liu J, Qiu XW, Liu C, Wu HJ, Gong ZJ. Characteristics and Management of Free Flap Compromise Following Internal Jugular Venous Thrombosis. *J Oral Maxillofac Surg* (2018) 76(11):2437–42. doi: 10.1016/j.joms.2018.05.006
13. Sahu PK, Kumar S. Bipaddle Pectoralis Major Myocutaneous Flap for Single Stage Reconstruction of Oromandibular Defects. *Indian J Otolaryngol Head Neck Surg* (2020) 72(1):44–8. doi: 10.1007/s12070-019-01731-w
14. Song YG, Chen GZ, Song YL. The Free Thigh Flap: A New Free Flap Concept Based on the Septocutaneous Artery. *Br J Plast Surg* (1984) 37(2):149–59. doi: 10.1016/0007-1226(84)90002-X
15. Gong ZJ, Ren ZH, Wang K, Tan HY, Zhang S, Wu HJ. Reconstruction Design Before Tumour Resection: A New Concept of Through-and-Through Cheek Defect Reconstruction. *Oral Oncol* (2017) 74:123–9. doi: 10.1016/j.oraloncology.2017.09.023
16. Gong ZJ, Wang K, Tan HY, Zhang S, He ZJ, Wu HJ. Application of Thinned Anterolateral Thigh Flap for the Reconstruction of Head and Neck Defects. *J Oral Maxillofac Surg* (2015) 73(7):1410–9. doi: 10.1016/j.joms.2015.01.006
17. Gong ZJ, Wu HJ. Measurement for Subcutaneous Fat and Clinical Applied Anatomic Studies on Perforators in the Anterior Thigh Region. *J Oral Maxillofac Surg* (2013) 71(5):951–9. doi: 10.1016/j.joms.2012.12.003
18. Wei FC, Jain V, Celik N, Chen HC, Chuang DC, Lin CH. Have We Found an Ideal Soft-Tissue Flap? An Experience With 672 Anterolateral Thigh Flaps. *Plast Reconstr Surg* (2002) 109(7):2219–26; discussion 2227–30. doi: 10.1097/00006534-200206000-00008
19. Zhang S, Li P, Liu C, Wu H, Gong Z. Application of Suprafascially Harvested Anterolateral Thigh Perforator Flap for the Reconstruction of Oral and Maxillofacial Defects. *J Craniofac Surg* (2020) 31(7):e673–6. doi: 10.1097/SCS.0000000000006511
20. Gong ZJ, Zhang S, Ren ZH, Zhu ZF, Liu JB, Wu HJ. Application of Anteromedial Thigh Flap for the Reconstruction of Oral and Maxillofacial Defects. *J Oral Maxillofac Surg* (2014) 72(6):1212–25. doi: 10.1016/j.joms.2013.11.017
21. Jiang C, Guo F, Li N, Liu W, Su T, Chen X, et al. Multipaddled Anterolateral Thigh Chimeric Flap for Reconstruction of Complex Defects in Head and Neck. *PloS One* (2014) 9(9):e106326. doi: 10.1371/journal.pone.0106326
22. Kuo YR, Jeng SF, Kuo MH, Huang MN, Liu YT, Chiang YC, et al. Free Anterolateral Thigh Flap for Extremity Reconstruction: Clinical Experience

and Functional Assessment of Donor Site. *Plast Reconstr Surg* (2001) 107 (7):1766–71. doi: 10.1097/00006534-200106000-00019

Conflict of Interest: The authors declare that the research was conducted in the absence of any commercial or financial relationships that could be construed as a potential conflict of interest.

Publisher's Note: All claims expressed in this article are solely those of the authors and do not necessarily represent those of their affiliated organizations, or those of the publisher, the editors and the reviewers. Any product that may be evaluated in this article, or claim that may be made by its manufacturer, is not guaranteed or endorsed by the publisher.

frontiers in Oncology

ORIGINAL RESEARCH
published: 26 October 2021
doi: 10.3389/fonc.2021.766398

Association of Systemic Inflammation and Malnutrition With Survival in Nasopharyngeal Carcinoma Undergoing Chemoradiotherapy: Results From a Multicenter Cohort Study

Xin Wang[1,2]*, Ming Yang*[1,2]*, Yizhong Ge*[1,2]*, Meng Tang*[1,2]*, Benqiang Rao*[1,2]*, Yongbing Chen*[1,2]*, Hongxia Xu*[3]*, Minghua Cong*[4]*, Zengqing Guo*[5] *and Hanping Shi*[1,2]*

[1] Departments of Gastrointestinal Surgery and Clinical Nutrition, Beijing Shijitan Hospital, Beijing, China, [2] Department of Oncology, Capital Medical University/Ninth Clinical Medical College, Peking University, Beijing, China, [3] Department of Clinical Nutrition, Daping Hospital, Army Medical University, Chongqing, China, [4] Comprehensive Oncology Department, National Cancer Center/Cancer Hospital, Chinese Academy of Medical Sciences and Peking Union Medical College, Beijing, China, [5] Department of Medical Oncology, Fujian Cancer Hospital, Fujian Medical University Cancer Hospital, Fuzhou, China

OPEN ACCESS

Edited by:
Xiaobiao Zhang,
Fudan University, China

Reviewed by:
Tianwen Gao,
Nanjing Medical University, China
Yongzhen Mo,
Central South University, China

***Correspondence:**
Hanping Shi
shihp@ccmu.edu.cn

Specialty section:
This article was submitted to
Surgical Oncology,
a section of the journal
Frontiers in Oncology

Received: 29 August 2021
Accepted: 06 October 2021
Published: 26 October 2021

Citation:
Wang X, Yang M, Ge Y,
Tang M, Rao B, Chen Y, Xu H,
Cong M, Guo Z and Shi H (2021)
Association of Systemic
Inflammation and Malnutrition
With Survival in Nasopharyngeal
Carcinoma Undergoing
Chemoradiotherapy: Results From
a Multicenter Cohort Study.
Front. Oncol. 11:766398.
doi: 10.3389/fonc.2021.766398

Background: Malnutrition and systemic inflammation are common in patients with nasopharyngeal carcinoma (NPC). The Patient-Generated Subjective Global Assessment (PG-SGA) score and neutrophil-to-lymphocyte ratio (NLR) reflect the integrated nutritional status and inflammatory level of patients with NPC, respectively. We performed this study to identify whether NLR and PG-SGA score are associated with outcome and survival time for patients with NPC undergoing chemoradiotherapy.

Methods: The multicenter cohort study included 1,102 patients with NPC between June 2012 and December 2019. The associations of all-cause mortality with NLR and PG-SGA score were calculated using the Kaplan–Meier method and the log-rank test. We also did a multivariate-adjusted Cox regression analysis to identify the independent significance of different parameters. Restricted cubic spline regression was carried out to evaluate the association between NLR and overall survival (OS). A nomogram was established using the independent prognostic variables. Interaction terms were used to investigate whether there was an interactive association between NLR and PG-SGA.

Results: A total of 923 patients with NPC undergoing chemoradiotherapy were included in this study: 672 (72.8%) were males and 251 (27.2%) were females, with a mean age of 49.3 ± 11.5 years. The Kaplan–Meier curves revealed that patients with malnutrition (PG-SGA score >3) had worse survival than patients who were in the well-nourished group (PG-SGA score ≤3) ($p < 0.0001$). In addition, patients in the high NLR group (NLR ≥ 3) had worse survival than those in the low NLR group (NLR < 3) ($p < 0.0001$). Patients with high PG-SGA and high NLR had the worst survival ($p < 0.0001$). An increase in NLR had an inverted L-shaped dose–response association with all-cause mortality. A nomogram was developed by incorporating domains of NLR and PG-SGA score to accurately predict OS 12–60 months for patients [the C-index for OS prediction of nomogram was 0.75 (95% CI, 0.70–0.80)]. The interaction of PG-SGA with NLR was significant (p = 0.009). Patients with high PG-SGA and high NLR had a nearly 4.5-fold increased risk of death (HR = 4.43, 95% CI = 2.60–7.56) as compared with patients with low PG-SGA and low NLR.

Conclusions: Our study provided clear evidence that high PG-SGA score and high NLR adversely and interactively affects the OS of patients with NPC undergoing chemoradiotherapy.

Keywords: nasopharyngeal carcinoma, PG-SGA, neutrophil-to-lymphocyte ratio (NLR), malnutrition, systemic inflammation, chemoradiotherapy

INTRODUCTION

Nasopharyngeal carcinoma (NPC) is a specific head and neck epithelial malignant tumor with obvious endemic and racial distribution differences, especially in southern China, with the incidence ranging from 20 to 30 per 100,000 (1).

Due to the complex anatomical location, high sensitivity of irradiation, and a locoregional advanced presentation at diagnosis, the primary treatment for non-disseminated NPC is not radical surgery but radiotherapy (RT) alone or concurrent chemoradiotherapy (CCRT), which is recognized as the most effective and reasonable strategy to control local recurrence and prolong survival time (2, 3). However, the therapeutic effect is unsatisfactory (4). More than 20% of the patients with advanced disease still develop local recurrence and distant metastases even after radical RT and systemic chemotherapy (5). Recurrent or metastatic NPC is associated with poor prognosis, with a median survival period of approximately 17 months (6). Therefore, improving the treatment effect and survival time of NPC patients remains challenging.

In clinical practice, malnutrition is one of major problems that can affect the curative effect and prognosis for people with NPC; 35% of NPC patients lose more than 5% of their weight (7). Even for newly diagnosed patients with NPC, through ideal weight percentage and serum albumin level to evaluate the nutritional status, malnutrition has been estimated in 36.5% and 34.6%, respectively (8). RT will cause further aggravation of malnutrition *via* mucositis, reaching a peak in 3 weeks. A clinical observational study reported that 20.19% of patients with NPC under RT were able to lose 10% of their body weight within 2 months (9). Furthermore, side effect, fatigue, anorexia, etc. often lead to malnutrition during the process of chemotherapy for NPC (10).

Malnutrition and weight loss may impair immune function, restrict vitality, reduce resistance to the disease, and decrease wound healing, which lead to complications, treatment-related toxicities, and resistance to cancer treatment (11). In addition, the effectiveness of the chemotherapy and RT will be significantly reduced, if nutritional status of patients becomes so bad (12). The treatments had to be suspended even and terminated early because of intolerance. Therefore, it is not surprising that malnutrition or weight loss during treatments has been found to be significantly associated with poorer survival outcomes and impaired the quality of life (QoL) in NPC. Furthermore, an increase in 20% weight reduction over the course of treatments was significantly associated with toxicity and mortality during RT in NPC (13).

The Patient-Generated Subjective Global Assessment (PG-SGA) was proposed in 1996 and developed by the European Society for Clinical Nutrition and Metabolism (ESPEN), which is a tool that enables evaluation of the nutritional status for patients with cancer (14). This scoring system has two main parts: one questionnaire for the patient with four questions and one questionnaire for the physician. The questionnaire for the patient includes weight change, symptoms, daily diet, and daily activities; the questionnaire for the physician includes diagnosis, physical examinations, metabolic evaluation, and nutrition-related complications. Finally, the grades for nutritional assessment are divided into the following categories: good nutritional status, suspicious malnutrition, moderate malnutrition, and severe malnutrition. A patient with over 3 points would be regarded as relatively malnourished (15). Thus, PG-SGA has been used for guiding nutritional treatment, making clinical decisions, and predicting outcomes in various cancers, including NPC (16).

In recent years, an increasing number of studies have focused on the influence of nutrition and systemic inflammation on the prognosis of patients with cancer (17, 18). Systemic inflammatory response has been shown to be closely associated with weight loss and malnutrition in NPC (4, 9). Neutrophil-to-lymphocyte ratio (NLR), which is calculated based on the absolute neutrophil count divided by the absolute lymphocyte count, is known to be an indicator of both the immune system and systemic inflammation of cancer patients. NLR and other systemic inflammation-related biomarkers [such as prognostic nutritional index (PNI) (19), platelet-to-lymphocyte ratio (PLR) (20), C-reactive protein (CRP) (21)] are commonly used to predict clinical outcomes for patients with various malignancies (17, 18).

The clinical predictive value of a combination of PG-SGA score and NLR has rarely been investigated in patients with NPC undergoing chemoradiotherapy. Therefore, we performed this paper to identify which prognostic factors may help select patients who will benefit from more aggressive treatment and to evaluate the relationship between nutritional status and systemic inflammation in patients with NPC undergoing chemoradiotherapy.

SUBJECTS AND METHODS

Study Design and Participants

The retrospective data were collected from a multicenter, prospective, observational cohort study named the Investigation on Nutrition Status and its Clinical Outcome of Common Cancers (INSCOC) project of China (chictr.org.cn, registration number: ChiCTR1800020329). In the present study, a total of 1,102 patients with NPC were recruited from 40 clinical centers throughout the China from June 2012 to December 2019, who had to meet the following inclusion criteria: 1) aged 18 to 80 years; 2) with pathological diagnosis of NPC; 3) received radical RT, chemotherapy, or both; 4) without liver and kidney dysfunction; and 5) obtained complete baseline clinical information and laboratory data and complete follow-up data.

Data Collection and Variable Definition

Within the first 48 h after hospital admission, demographic and clinicopathological data were collected by trained investigators, including gender, age at diagnosis, body mass index (BMI), smoking status, comorbidities, alcohol consumption, tea consumption, family history of cancer, tumor stage, NLR, and PG-SGA score. The nutritional status of all patients was evaluated using the PG-SGA: a patient with over 3 points would be regarded as relatively malnourished (15); in contrast, less than or equal to 3 points was classified into the well-nourished group. BMI was calculated by body weight in kilograms divided by the height in squared meters (kg/m^2). NLR was used as a continuous variable, and widely accepted values were used to group patients. The optimal cutoff values ("normal" (<3) and "moderate and high" (≥3) inflammation) for NLR were generated according to reference (17). The tumor stage in all patients was confirmed by pathological examination. NPC patients were staged according to the 8th edition of the American Joint Committee on Cancer/Union for International Cancer Control (AJCC/UICC) TNM staging system. The types of chemotherapy or RT included curative, neoadjuvant, adjuvant, maintenance, and palliative types in the study. All patients were regularly followed up *via* outpatient visits or telephone interviews until death, last contact on March 31, 2020. The study was approved by the research ethical committees of all participating institutions and was designed in accordance with the Declaration of Helsinki, and all participants signed the consent before study entry.

Statistical Analysis

Categorical variables were expressed as whole numbers and percentages and were compared by the chi-square test or Fisher's exact test, as appropriate. Quantitative variables were reported as mean ± standard deviation (SD), and differences were analyzed using Student's t-test or the Mann–Whitney U test for groups without a normal distribution. Overall survival (OS) was calculated using the Kaplan–Meier method and the log-rank test, and hazard ratios (HRs) together with 95% CIs were calculated using a univariate Cox regression analysis to investigate the association between potential predictors and mortality. We also did a multivariate-adjusted Cox regression analysis using backward selection to identify the independent significance of different parameters. Restricted cubic spline regression was carried out to evaluate the association between NLR and OS. Based on the results of multivariable analysis, we formulated a nomogram using the "rms" package in R to predict the probability of 12-, 24-, 36-, 48-, and 60-month OS rates for NPC patients after chemoradiotherapy. Harrell's C-index was used to evaluate discernibility ability of the nomogram. The area under the receiver operating characteristic (ROC) curve (AUC) was used to evaluate the predictive accuracy of the 12-, 24-, 36-, and 48-month OS. Interaction terms were used to investigate whether there was an interactive association between NLR and PG-SGA score. All statistical analyses were performed with R software (version 3.6.2, http://www.rproject.org). $p < 0.05$ from the two-sided test was considered statistically significant.

RESULTS

Clinical Characteristics of the Investigated Nasopharyngeal Carcinoma Patients

A total of 923 patients with NPC undergoing chemoradiotherapy were included in this study; the flowchart of screening process is shown in **Figure 1**. One hundred sixty-one patients were excluded due to missing key data or variables in our analysis. A total of 18 cases were lost to follow-up. The follow-up rate was 98.4%. Among the remaining cases, the average follow-up time was 28.3 ± 16.3 months, during which there were 99 deaths. The general characteristics of all participants with NPC undergoing chemoradiotherapy by category of PG-SGA score are shown in **Table 1**. There were 672 (72.8%) males and 251 (27.2%) females, with a mean age of 49.3 ± 11.5 years. Among all NPC patients, the PG-SGA-diagnosed severe malnutrition rate was 16.4% (151 patients, determined by the PG-SGA score >3). The TNM stage and BMI between patients with PG-SGA score >3 and PG-SGA score ≤3 had significant difference ($p < 0.001$).

Risk Factors of All-Cause Mortality for Patients With Nasopharyngeal Carcinoma Undergoing Chemoradiotherapy Were Determined Using Univariate and Multivariate Cox Regression Analyses

The Kaplan–Meier curves revealed that patients with NPC undergoing chemoradiotherapy, with malnutrition (PG-SGA score >3), had worse survival (HR = 1.441, 95% CI = 0.90–2.31, median OS [MOS] = 21.32 months) than patients with NPC who were in the well-nourished group (PG-SGA score ≤3) (MOS = 24.51 months, $p < 0.0001$, **Figure 2A**). In addition, patients in the high NLR group (NLR ≥ 3) had worse survival (HR = 2.36, 95% CI = 1.56–3.56, MOS = 21.16 months) than those in the low NLR group (NLR < 3) (MOS = 24.86 months, $p < 0.0001$, **Figure 2B**). After the study population was further stratified into four subgroups, patients with high PG-SGA (PG-SGA score >3) and

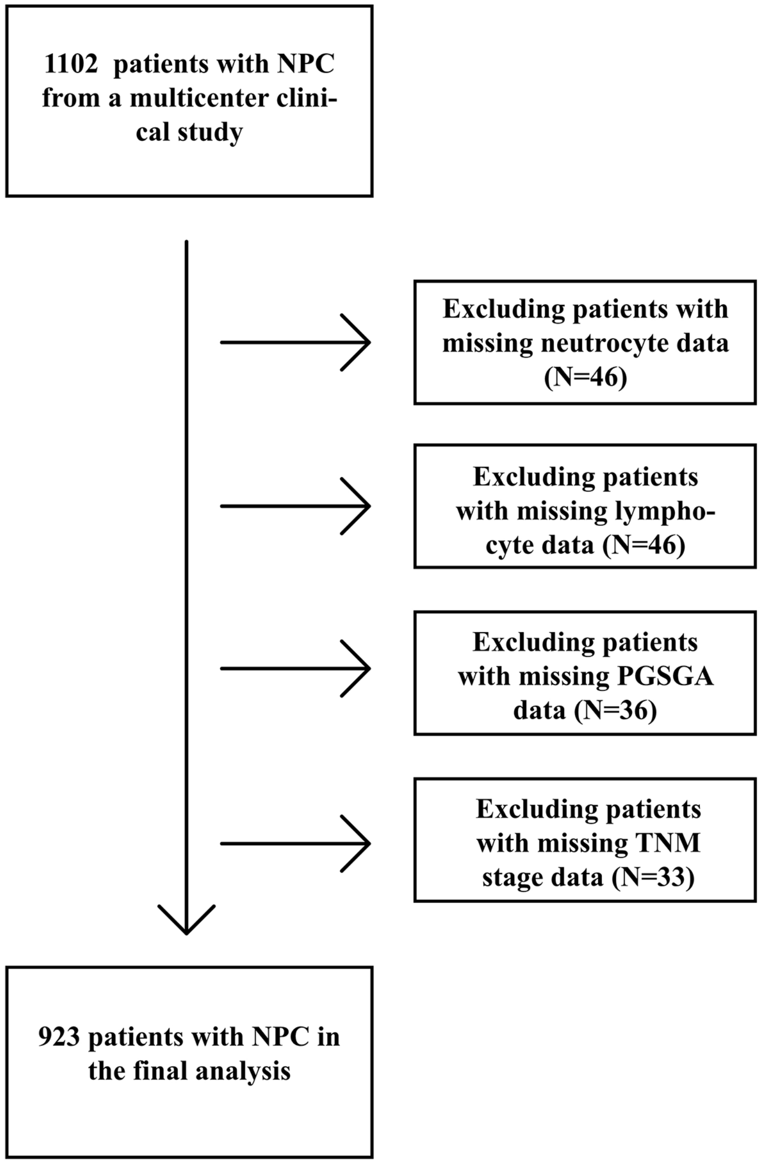

FIGURE 1 | Flowchart of the study design.

high NLR (NLR ≥ 3) had the worst survival (HR = 4.43, 95% CI = 2.60–7.56, p < 0.0001, **Figure 2C**), compared with those in the high PG-SGA and low NLR group, the low PG-SGA and high NLR group, and the low PG-SGA and low NLR group.

We carried out multivariate analyses that included patient age, sex, BMI, alcohol consumption, TNM stage, PG-SGA, and NLR. As shown in **Table 2**, age (HR, 1.040, 95% CI 1.022–1.059; p < 0.001), PG-SGA (HR, 1.070, 95% CI 1.025–1.117; p = 0.002) and NLR (HR, 1.199, 95% CI 1.119–1.285; p < 0.001) were significantly associated with OS. In multivariable Cox proportional hazards models (**Table 3**), high NLR (NLR ≥ 3) was associated with a 135.9% (HR, 2.36; 95% CI, 1.56–3.56) greater risk of death, as compared with those with low NLR (NLR < 3). An increase in 1 score of PG-SGA was associated with a 7% increased risk of death. Additionally, NLR was divided into quartiles; the fourth quartile (≥3) was positively correlated with a worse prognosis (p < 0.001), compared with the first (< 1.61), second (≥1.61, <2.15), and third (≥2.15, <3) quartiles. After the confounding factors were adjusted, HRs of all-cause mortality (HR, 95% CI) were 1.29 (0.63–2.62), 1.38 (0.71–2.70), and 2.90 (1.57–5.34) for the second, third, and fourth quartiles, respectively, showing an increasing trend in the risk of death.

When analyzed as a continuous variable, restricted cubic spline plot showed multivariable-adjusted HRs (95% CI) for NLR, which had an inverted L-shaped dose–response association with the all-cause mortality risk in NPC patients (**Figure 3A**).

TABLE 1 | Demographic and clinical characteristics of patients with NPC undergoing chemoradiotherapy stratified by PG-SGA.

Characteristics	*No. of patients with PG-SGA ≤ 8 (n = 772)*	*No. of patients with PG-SGA > 8 (n = 151)*	*p-Value*
Sex[a] (male)	571 (74.0)	101 (66.9)	0.092
Age in years[b]	49.00 (11.25)	50.77 (12.51)	0.083
BMI[b] (kg/m^2)	23.39 (3.21)	21.54 (3.30)	<0.001
Smoking status[a,c] (yes)	364 (47.2)	79 (52.3)	0.283
Alcohol consumption[a,d] (yes)	179 (23.2)	42 (27.8)	0.265
Tea drinking status[a,e] (yes)	254 (32.9)	38 (25.2)	0.076
Hypertension[a] (yes)	87 (11.3)	13 (8.6)	0.413
Diabetes[a] (yes)	36 (4.7)	8 (5.3)	0.900
Coronary heart disease[a] (yes)	9 (1.2)	1 (0.7)	0.907
Family history of cancer[a] (yes)	120 (15.5)	17 (11.3)	0.219
TNM stage[a]			<0.001
I, II, III	493 (63.9)	72 (47.7)	
IV	279 (36.1)	79 (52.3)	
NLR	5.35 (1.99)	5.21 (0.93)	0.466

NPC, nasopharyngeal carcinoma; PG-SGA, Patient-Generated Subjective Global Assessment; BMI, body mass index; NLR, neutrophil-to-lymphocyte ratio.
[a]Categorical variables are presented as number (percentage).
[b]Continuous variables are presented as mean (standard deviation).
[c]The standard is to smoke more than 20 cigarettes in a lifetime.
[d]The standard is regular drinking in the past year.
[e]The standard is regular drinking tea in the past year.

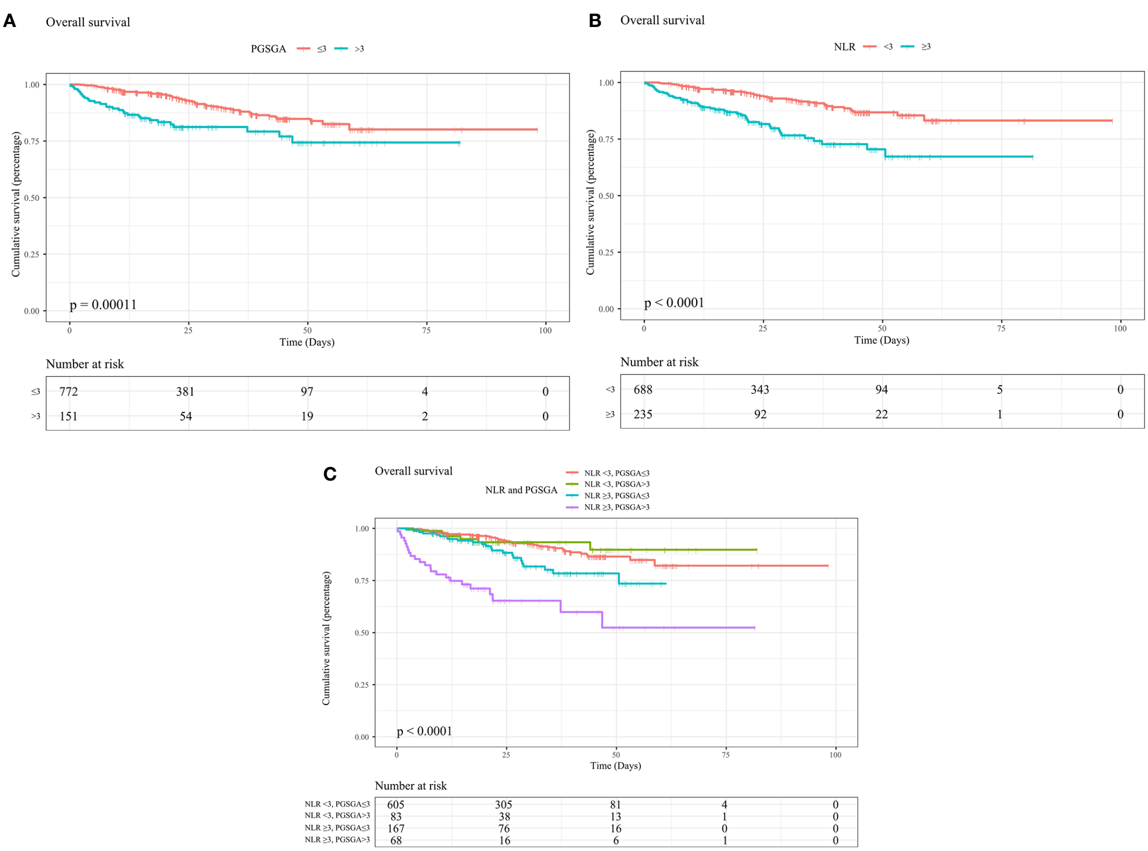

FIGURE 2 | Kaplan–Meier curves show survival rates for patients with NPC undergoing chemoradiotherapy with **(A)** PG-SGA (PG-SGA score >3, ≤3), with **(B)** NLR (NLR ≥ 3, < 3), with **(C)** NLR and PG-SGA (high PG-SGA and high NLR group, high PG-SGA and low NLR group, low PG-SGA and high NLR group, and low PG-SGA and low NLR group). NPC, nasopharyngeal carcinoma; PG-SGA, Patient-Generated Subjective Global Assessment; NLR, neutrophil-to-lymphocyte ratio.

TABLE 2 | Association between clinical variables and OS in patients with NPC undergoing chemoradiotherapy.

Variables	Univariate analysis		Multivariate analysis[a]	
	HR (95% CI)	p-Value	HR (95% CI)	p-Value
Sex	0.546 (0.324, 0.921)	0.023	0.715 (0.409, 1.248)	0.238
Age	1.044 (1.025, 1.062)	<0.001	1.040 (1.022, 1.059)	<0.001
BMI	0.903 (0.848, 0.962)	0.002	0.942 (0.882, 1.006)	0.075
Smoking status[b]	1.342 (0.903, 1.993)	0.145		
Alcohol consumption[c]	1.652 (1.083, 2.518)	0.020	1.491 (0.951, 2.338)	0.082
Tea drinking status[d]	1.098 (0.723, 1.667)	0.662		
Hypertension	1.505 (0.855, 2.649)	0.157		
Diabetes	1.624 (0.753, 3.503)	0.216		
Coronary heart disease	0.965 (0.674, 1.381)	0.845		
Family history of cancer	0.686 (0.375, 1.255)	0.221		
TNM stage				
I, II, III	Reference		Reference	
IV	1.914 (1.289, 2.841)	0.001	1.393 (0.920, 2.110)	0.118
PG-SGA	1.098 (1.061, 1.136)	<0.001	1.070 (1.025, 1.117)	0.002
NLR	1.246 (1.172, 1.325)	<0.001	1.199 (1.119, 1.285)	<0.001

NPC, nasopharyngeal carcinoma; OS, overall survival; HR, hazard ratio; CI, confidence interval; BMI, body mass index; PG-SGA, Patient-Generated Subjective Global Assessment; NLR, neutrophil-to-lymphocyte ratio.

[a]The variables that showed prognostic role in univariate analysis or considered clinically significant were involved in multivariate analysis.

[b]The standard is to smoke more than 20 cigarettes in a lifetime.

[c]The standard is regular drinking in the past year.

[d]The standard is regular drinking tea in the past year.

TABLE 3 | Association between PG-SGA or NLR and OS in patients with NPC undergoing chemoradiotherapy.

Variables	Patients (n)	Crude HR[c] (95% CI)	p-Value	Adjusted HR (95% CI)	p-Value
PG-SGA[a]					
Continuous	923	1.098 (1.061, 1.136)	<0.001	1.070 (1.025, 1.117)	0.002
Categories					
≤3	772	Reference		Reference	
>3	151	2.299 (1.490, 3.547)	<0.001	1.441 (0.899, 2.310)	0.128
NLR[b]					
Continuous	923	1.246 (1.172, 1.325)	<0.001	1.199 (1.119, 1.285)	<0.001
Categories					
<3	688	Reference		Reference	
≥3	235	3.011 (2.027, 4.473)	<0.001	2.359 (1.563, 3.560)	<0.001
Quartiles					
1	228	Reference		Reference	
2	231	1.146 (0.565, 2.326)	0.705	1.286 (0.632, 2.618)	0.488
3	229	1.436 (0.735, 2.808)	0.290	1.380 (0.705, 2.701)	0.348
4	235	3.614 (1.986, 6.575)	<0.001	2.899 (1.574, 5.337)	0.001
PG-SGA and NLR[c]					
Low PG-SGA and low NLR	605	Reference		Reference	
High PG-SGA and low NLR	83	0.874 (0.373, 2.044)	0.755	0.665 (0.280, 1.579)	0.355
Low PG-SGA and high NLR	167	1.951 (1.184, 3.214)	0.009	1.696 (1.022, 2.814)	0.041
High PG-SGA and high NLR	68	6.187 (3.748, 10.211)	<0.001	4.434 (2.602, 7.555)	<0.001

NPC, nasopharyngeal carcinoma; PG-SGA, Patient-Generated Subjective Global Assessment; NLR, neutrophil-to-lymphocyte ratio; OS, overall survival; HR, hazard ratio; CI, confidence interval.

[a]Models were adjusted for sex, age, body mass index, alcohol consumption, TNM stage, and NLR (as a continuous variable).

[b]Models were adjusted for sex, age, body mass index, alcohol consumption, TNM stage, and PG-SGA (as a continuous variable).

[c]Models were adjusted for sex, age, body mass index, alcohol consumption, and TNM stage.

The Nomogram for Predicting the 12–60 Months' Overall Survival Time of Patients With Nasopharyngeal Carcinoma Undergoing Chemoradiotherapy

A nomogram for the 12-, 24-, 36-, 48-, and 60-month OS based on those factors (NLR, PG-SGA, sex, age, BMI, and TNM stage) was developed for predicting OS in patients with NPC undergoing chemoradiotherapy (**Figure 3B**). Scales of the nomogram reflected coefficients from the Cox model converted to a practical 100-point range, and OS was accurately predicted by the nomogram (model) with an AUC of 0.803, 0.759, 0.700, and 0.727 for prediction of mortality in comparison with TNM stage (0.593, 0.603, 0.603, 0.591, respectively) at 12, 24, 36, and 48 months (**Figures 3C** and

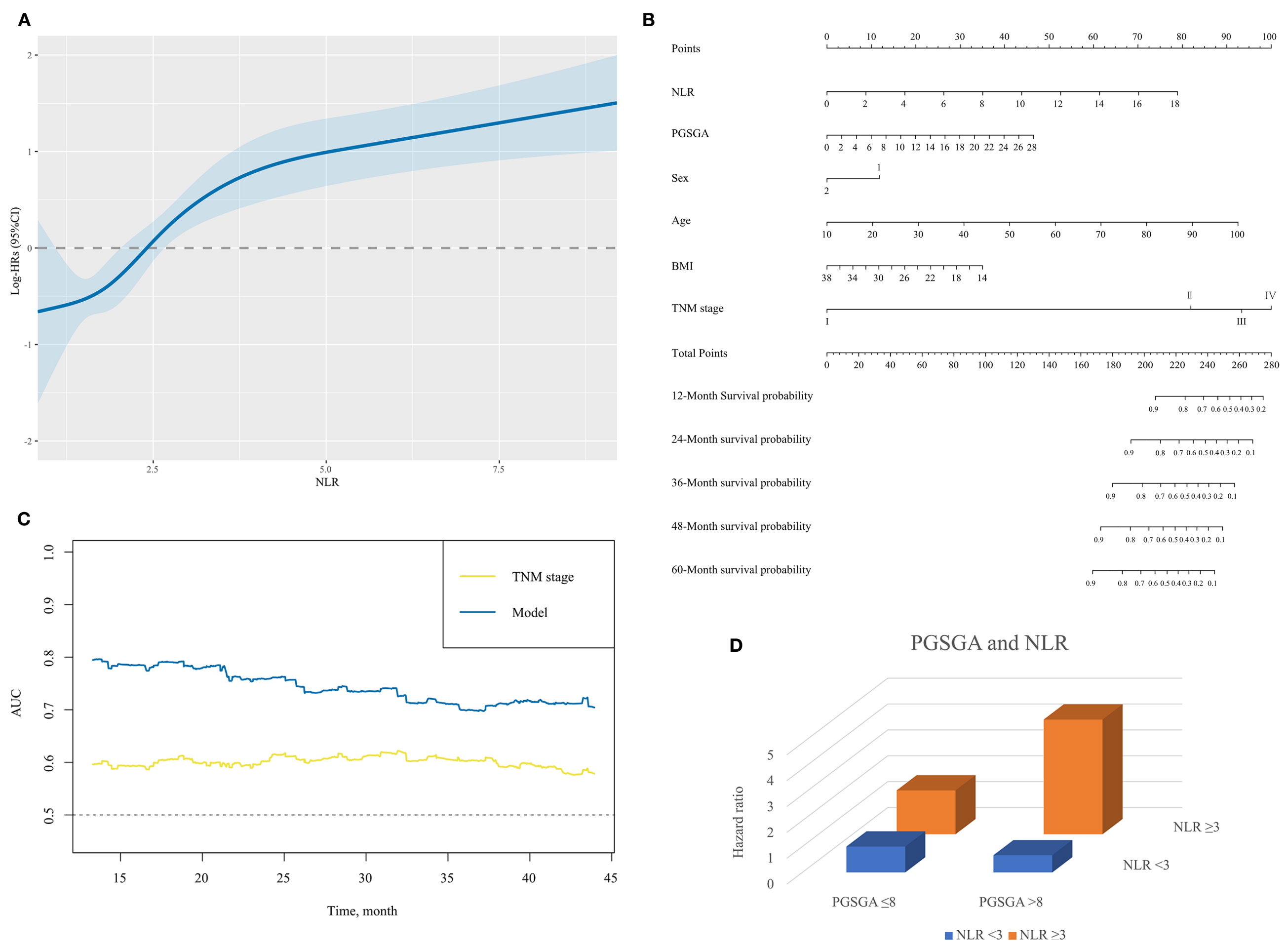

FIGURE 3 | **(A)** The association between NLR (continuous) and hazard ratio of overall survival for patients with NPC undergoing chemoradiotherapy. Splines are adjusted by sex, age, body mass index, alcohol consumption, TNM stage and PG-SGA. **(B)** The nomogram for predicting the 12- to 60-month overall survival time of patients with NPC undergoing chemoradiotherapy. In the nomogram, an individual patient's value is located on each variable axis. Based on the number of points received for each corresponding value, the sum of these numbers is located on the total point axis to determine the likelihood of 12- to 60-month survival in the matched survival axes. **(C)** A summary chart merged the AUC for prediction of survival at 12, 24, 36, or 48 months by nomogram (model) and TNM stage. The predictive capacity of model had a significant improvement as compared with TNM stage. **(D)** The interactive association of NLR and PG-SGA for patients with NPC undergoing chemoradiotherapy, presented by three-dimensional bar diagram. NLR, neutrophil-to-lymphocyte ratio; NPC, nasopharyngeal carcinoma; PG-SGA, Patient-Generated Subjective Global Assessment; AUC, area under the receiver operating characteristic curve.

Supplementary Figure S1). The C-index for OS prediction of nomogram was 0.75 (95% CI, 0.70–0.80), better than that of TNM stage 0.60 (0.54–0.65).

Interactive Association of Exposures With Mortality Between Patient-Generated Subjective Global Assessment and Neutrophil-to-Lymphocyte Ratio

Table 3 and **Figure 3D** illustrate the HR for each condition of exposure combinations compared with the referent: low PG-SGA (PG-SGA score ≤3) and low NLR (NLR < 3) group. The interaction of PG-SGA with NLR was significant (p = 0.009). Patients in NPC with high PG-SGA and high NLR had a nearly 4.5-fold increased risk of death (HR = 4.43, 95% CI = 2.60–7.56) as compared with patients with low PG-SGA and low NLR. PG-SGA and NLR showed synergism with each other.

DISCUSSION

This was a large multicenter study comprising 923 patients with NPC undergoing chemoradiotherapy across several provinces in China, which investigated the relationships between the nutritional status and patients' prognosis through a long-term follow-up. Malnutrition is commonly seen in patients with NPC undergoing chemoradiotherapy (9, 16, 22). Patients with NPC suffer from malnutrition caused by complex factors, including the following: 1) the tumor invades the basis cranii, causing paralysis of the glossopharyngeal nerve, which leads to dysphagia (23). 2) As a consequence of injuries to normal tissues, such as the oral mucosa, taste buds, and salivary glands, radiation-induced oral mucositis and other complications are very common in patients with NPC undergoing RT, causing difficulty in chewing and swallowing (24, 25). 3) The concurrent chemotherapy often cause severe side effects of gastrointestinal tract such as asitia, nausea, and vomiting, which lead to decreased appetite and gastrointestinal dysfunction (26). 4) Patients with NPC also suffer from emotional disorders such as fear, anxiety, and depression, which further impair the patient's ability to eat and digestive function (19, 27). 5) The insufficient nutritional supply or unreasonable ingredients was found in the nursing care of patients with NPC, due to patients' and their relatives' poor nutritional knowledge. However, few data are available regarding the nutritional status of patients with NPC undergoing chemoradiotherapy. This study investigated the nutritional status of patients with NPC who received RT, chemotherapy, or both, on the basis of PG-SGA score and BMI. In addition, an NLR was established to reflect patients' systemic inflammation (28), and the correlation between PG-SGA and NLR on survival time was explored.

Based on our results, we found that PG-SGA score and NLR at admission were associated with poor prognosis of NPC undergoing chemoradiotherapy (**Figures 2A–C** and **Tables 2**, **3**). NLR had an inverted L-shape relationship with mortality risk among patients with NPC undergoing chemoradiotherapy (**Figure 3A**). Furthermore, we established a nomogram model based on domains of NLR, PG-SGA, sex, age, BMI, and tumor stage to predict the OS rate associated with NPC patients undergoing chemoradiotherapy. The nomogram was able to predict an individual's risk of 12-, 24-, 36-, 48-, and 60-month OS rates with relatively good accuracy, especially for predicting the 12-month OS rates (**Figures 3B, C** and **Supplementary Figure S1**). Finally, the co-occurrence of high NLR and high PG-SGA score was associated with a nearly 4.5-fold increased risk of mortality among patients with NPC undergoing chemoradiotherapy (**Table 3** and **Figure 3D**). To sum up, there was a potential synergistic effect of systemic inflammation and severe malnutrition with mortality risks for patients with NPC who received RT, chemotherapy, or both.

In recent years, an increasing number of studies have demonstrated that measures of inflammation and malnutrition are each independently powerful prognostic indicator in patients with cancer (28). A prospective cohort (17) of 2,470 patients with stage I to III CRC revealed that pre-diagnosis inflammation was associated with at-diagnosis sarcopenia. OS was worse in the group with simultaneous existence of sarcopenia and high NLR, which seem to be consistent with our results. In previous studies (18), the level of NLR in patients with cancer cachexia is generally higher than that in patients without cancer cachexia, and the high NLR level was related to poorer survival of cancer patients, indicating that NLR could be used as an independent prognostic factor for patients with cachexia. Wang et al. reported that in patients with NPC, weight loss makes them more vulnerable to recurrent pneumonia. Notably, our results suggest likely synergistic effects between inflammation and malnutrition for patients with NPC undergoing chemoradiotherapy, which explains why nutritional therapy for patients with NPC could be beneficial to reduce systemic inflammation and improve the immunity of patients.

The close connections of nutrition, inflammation, and cancer have been attracting our attentions for many years. Our findings also indicated the effect of chemoradiotherapy on the nutritional status of patients with NPC. In addition to malnutrition, chemoradiotherapy may induce mucositis, tissue damage, and acute toxicities, which may cause systemic inflammatory response (9, 29). Thus, malnutrition and systemic inflammation may have a prognostic role in the process of chemoradiotherapy. Malnutrition expended massive protein, which further disturbs metabolic function, impairs immunity, increases susceptibility to infection, compromises the response to antitumor treatments, and aggravates chemoradiotherapy toxicity, hence severely affecting survival and outcomes (4, 22, 25, 30). Additionally, protein–energy malnutrition may induce a high level of systemic inflammatory factors, such as tumor necrosis factor (TNF)-α and interleukin-6, can facilitate tumor cell proliferation invasion and metastasis, and can enhance malignant properties (31). As a consequence, malnutrition was also an indicator of a systemic inflammatory response. In turn, pro-inflammatory cytokines and tumor factors are involved in high catabolism in the inflammatory state, which consumes a large amount of the patient's skeletal muscle mass and caloric intake (17). This metabolic disorder will eventually lead to continuous weight loss and deterioration of nutritional status, damage to tissue and organ function, increase in the incidence of complications, and decrease in survival time. More importantly, inflammation plays an important role in the occurrence and progression of malignant tumors. Malnutrition, inflammation, and cancer really have become a vicious circle. Therefore, it is particularly important for cancer patients with malnutrition to control systemic inflammatory; and for cancer patients with high levels of inflammation, it is necessary to pay more attention to early nutritional intervention to better improve the prognosis of cancer patients. Interestingly, now that the survival rates of patients with high NLR may potentially benefit from nutritional therapy in our results, some special nutritional support with anti-inflammatory function should be given more to the patients with NPC undergoing chemoradiotherapy, such as ω-3 polyunsaturated fatty acid (ω-3 PUFA)-enriched and β-hydroxy-β-methylbutyrate (HMB)-enriched supplement. ω-3 PUFA has already been widely recognized as one of the anti-inflammatory nutrients (32). HMB, an intermediate metabolite of leucine that exists in human muscle cells, has been shown to inhibit protein degradation, attenuate the decrease in protein synthesis, and improve nutritional status (33). Moreover, one study (34) found that HMB attenuated the inflammatory effect of lipopolysaccharide (LPS), TNF, interferon (IFN), and angiotensin II (ANG II). A randomized trial (35) examined the effects of HMB supplementation on inflammation, protein metabolism, and pulmonary function in patients with chronic obstructive pulmonary disease, requiring mechanical ventilation. After 7 days of intervention, patients who were treated with HMB showed consistent reductions in CRP and in white blood cell counts from baseline, suggesting that HMB plays a positive role in the treatment of chronic inflammation.

To our knowledge, this is one of the meaningful studies on NPC to examine the relationship between malnutrition and biomarkers of systemic inflammation and the only study to examine whether high NLR and high PG-SGA score have a synergetic interaction on the NPC patient's survival risk. The survival difference among the four groups (different combinations of PG-SGA score and NLR) indicates that prolonged survival needs not only a better nutrition status but also low-level systemic inflammation, which is a significant issue that should not be underestimated. Similar to all clinical research, our study was subject to several limitations: first, we could not examine other markers of systemic inflammation, such as PNI (19), PLR (20), and CRP levels (21). Because the related data are so insufficient or inappropriate, we had to stop analyzing them. Second, we did not study whether dynamic NLR could modify the prognostic value. Moreover, other covariates were collected using electronic medical record, questionnaire, or a one-on-one interview; and errors in measurement were inevitable. Finally, different diagnostic and therapeutic levels in the various hospitals might have masked the true associations. Further data are required to confirm these findings and to increase the precision of the effect for these exposures.

CONCLUSIONS

Malnutrition and systemic inflammation are common in patients with NPC. The PG-SGA score and NLR reflect the integrated nutrition status and inflammatory level of NPC patients, respectively. Our study provided clear evidence that high PG-SGA score and high NLR adversely affect the OS of patients with NPC undergoing chemoradiotherapy, suggesting that PG-SGA score and NLR were independent prognostic indicators for patients with NPC undergoing chemoradiotherapy. We also found that PG-SGA and NLR were interactive with each other. The co-occurrence of malnutrition and systemic inflammation at admission identified patients with a nearly 4.5-fold increased risk of mortality as compared with patients with neither condition. Therefore, on the one hand, it is particularly important for cancer patients with malnutrition to control systemic inflammation; on the other hand, for cancer patients with high levels of inflammation, it is necessary to offer nutritional intervention as early as possible to better improve the prognosis of cancer patients. Future studies are required to dynamically explore specific relationships and exact mechanisms between nutrition status and systemic inflammation and could assist to develop better strategies to increase the survival time and QoL of patients with NPC undergoing chemoradiotherapy.

DATA AVAILABILITY STATEMENT

The raw data supporting the conclusions of this article will be made available by the authors, without undue reservation.

ETHICS STATEMENT

Written informed consent was obtained from the individual(s) for the publication of any potentially identifiable images or data included in this article.

AUTHOR CONTRIBUTIONS

HS and XW are responsible for the study design, conceptualization, systematic review, project administration, the decision to publish, and manuscript preparation. MY, YG, and MT helped conduct the statistical analyses. BR and YC revised and edited the manuscript. ZG, HX, and MC provided data support from INSCOC project. All authors contributed to the article and approved the submitted version.

FUNDING

This study was supported by a National Science and Technology Major Project from Ministry of Science and Technology of the People's Republic of China, the National Key Research and Development Program (No: 2017YFC1309200; Title: The key technology of palliative care and nursing for cancer patients).

SUPPLEMENTARY MATERIAL

The Supplementary Material for this article can be found online at: https://www.frontiersin.org/articles/10.3389/fonc.2021.766398/full#supplementary-material

Supplementary Figure 1 | In ROC curve analysis, comparisons of the AUC for prediction of survival at 12- or 24- or 36- or 48- month by nomogram and TNM stage. NPC, Nasopharyngeal carcinoma; PGSGA, Patient-Generated Subjective Global Assessment; NLR, neutrocyte to lymphocyte ratio; HR, hazard ratio; CI, confidence interval; BMI, body mass index; ROC, receiver operator characteristic; AUC, area under curve.

REFERENCES

1. Almomani MH, Zulfiqar H, Nagalli S. Nasopharyngeal Carcinoma (NPC, Lymphoepithelioma). In: *StatPearls*. Treasure Island (FL): StatPearls Publishing (2021).
2. He Q, Huang Y, Wan G, Feng M, Zeng H, Liu M, et al. A Novel Prognostic Marker Based on Risk Stratification With Prognostic Nutritional Index and Age for Nasopharyngeal Carcinoma Patients Who Received Neoadjuvant Chemotherapy. *Biomark Med* (2019) 13:1013–23. doi: 10.2217/bmm-2018-0401
3. Pignon JP, Bourhis J, Domenge C, Designe L. Chemotherapy Added to Locoregional Treatment for Head and Neck Squamous-Cell Carcinoma: Three Meta-Analyses of Updated Individual Data. MACH-NC Collaborative Group. Meta-Analysis of Chemotherapy on Head and Neck Cancer. *Lancet* (2000) 355:949–55. doi: 10.1016/S0140-6736(00)90011-4
4. Tang M, Jia Z, Zhang J. The Prognostic Role of Prognostic Nutritional Index in Nasopharyngeal Carcinoma: A Systematic Review and Meta-Analysis. *Int J Clin Oncol* (2021) 26:66–77. doi: 10.1007/s10147-020-01791-x

5. Lee AW, Lin JC, Ng WT. Current Management of Nasopharyngeal Cancer. *Semin Radiat Oncol* (2012) 22:233–44. doi: 10.1016/j.semradonc.2012.03.008
6. Hsu CL, Chang KP, Lin CY, Chang HK, Wang CH, Lin TL, et al. Plasma Epstein-Barr Virus DNA Concentration and Clearance Rate as Novel Prognostic Factors for Metastatic Nasopharyngeal Carcinoma. *Head Neck* (2012) 34:1064–70. doi: 10.1002/hed.21890
7. Irungu CW, Oburra HO, Ochola B. Prevalence and Predictors of Malnutrition in Nasopharyngeal Carcinoma. *Clin Med Insights Ear Nose Throat* (2015) 8:19–22. doi: 10.4137/CMENT.S12119
8. Li G, Gao J, Liu ZG, Tao YL, Xu BQ, Tu ZW, et al. Influence of Pretreatment Ideal Body Weight Percentile and Albumin on Prognosis of Nasopharyngeal Carcinoma: Long-Term Outcomes of 512 Patients From a Single Institution. *Head Neck* (2014) 36:660–6. doi: 10.1002/hed.23357
9. Hong JS, Wu LH, Su L, Zhang HR, Lv WL, Zhang WJ, et al. Effect of Chemoradiotherapy on Nutrition Status of Patients With Nasopharyngeal Cancer. *Nutr Cancer* (2016) 68:63–9. doi: 10.1080/01635581.2016.1115099
10. Qiu C, Yang N, Tian G, Liu H. Weight Loss During Radiotherapy for Nasopharyngeal Carcinoma: A Prospective Study From Northern China. *Nutr Cancer* (2011) 63:873–9. doi: 10.1080/01635581.2011.582223
11. Larsson M, Hedelin B, Johansson I, Athlin E. Eating Problems and Weight Loss for Patients With Head and Neck Cancer: A Chart Review From Diagnosis Until One Year After Treatment. *Cancer Nurs* (2005) 28:425–35. doi: 10.1097/00002820-200511000-00004
12. Li G, Jiang XY, Qiu B, Shen LJ, Chen C, Xia YF. Vicious Circle of Acute Radiation Toxicities and Weight Loss Predicts Poor Prognosis for Nasopharyngeal Carcinoma Patients Receiving Intensity Modulated Radiotherapy. *J Cancer* (2017) 8:832–8. doi: 10.7150/jca.17458
13. Colasanto JM, Prasad P, Nash MA, Decker RH, Wilson LD. Nutritional Support of Patients Undergoing Radiation Therapy for Head and Neck Cancer. *Oncol (Williston Park)* (2005) 19:371–9. discussion 380-372, 387.
14. Bauer J, Capra S, Ferguson M. Use of the Scored Patient-Generated Subjective Global Assessment (PG-SGA) as a Nutrition Assessment Tool in Patients With Cancer. *Eur J Clin Nutr* (2002) 56:779–85. doi: 10.1038/sj.ejcn.1601412
15. Cao J, Xu H, Li W, Guo Z, Lin Y, Shi Y, et al. Nutritional Assessment and Risk Factors Associated to Malnutrition in Patients With Esophageal Cancer. *Curr Probl Cancer* (2021) 45:100638. doi: 10.1016/j.currproblcancer.2020.100638
16. Ding H, Dou S, Ling Y, Zhu G, Wang Q, Wu Y, et al. Longitudinal Body Composition Changes and the Importance of Fat-Free Mass Index in Locally Advanced Nasopharyngeal Carcinoma Patients Undergoing Concurrent Chemoradiotherapy. *Integr Cancer Ther* (2018) 17:1125–31. doi: 10.1177/1534735418807969
17. Feliciano EMC, Kroenke CH, Meyerhardt JA, Prado CM, Bradshaw PT, Kwan ML, et al. Association of Systemic Inflammation and Sarcopenia With Survival in Nonmetastatic Colorectal Cancer: Results From the C SCANS Study. *JAMA Oncol* (2017) 3:e172319. doi: 10.1001/jamaoncol.2017.2319
18. Zhang Q, Song MM, Zhang X, Ding JS, Ruan GT, Zhang XW, et al. Association of Systemic Inflammation With Survival in Patients With Cancer Cachexia: Results From a Multicentre Cohort Study. *J Cachexia Sarcopenia Muscle* (2021). doi: 10.1002/jcsm.12761
19. Du XJ, Tang LL, Mao YP, Guo R, Sun Y, Lin AH, et al. Value of the Prognostic Nutritional Index and Weight Loss in Predicting Metastasis and Long-Term Mortality in Nasopharyngeal Carcinoma. *J Transl Med* (2015) 13:364. doi: 10.1186/s12967-015-0729-0
20. Yang L, Xia L, Wang Y, Hong S, Chen H, Liang S, et al. Low Prognostic Nutritional Index (PNI) Predicts Unfavorable Distant Metastasis-Free Survival in Nasopharyngeal Carcinoma: A Propensity Score-Matched Analysis. *PloS One* (2016) 11:e0158853. doi: 10.1371/journal.pone.0158853
21. Tang LQ, Hu DP, Chen QY, Zhang L, Lai XP, He Y, et al. Elevated High-Sensitivity C-Reactive Protein Levels Predict Decreased Survival for Nasopharyngeal Carcinoma Patients in the Intensity-Modulated Radiotherapy Era. *PloS One* (2015) 10:e0122965. doi: 10.1371/journal.pone.0122965
22. Miao J, Xiao W, Wang L, Han F, Wu H, Deng X, et al. The Value of the Prognostic Nutritional Index (PNI) in Predicting Outcomes and Guiding the Treatment Strategy of Nasopharyngeal Carcinoma (NPC) Patients Receiving Intensity-Modulated Radiotherapy (IMRT) With or Without Chemotherapy. *J Cancer Res Clin Oncol* (2017) 143:1263–73. doi: 10.1007/s00432-017-2360-3
23. Lengyel E, Baricza K, Somogyi A, Olajos J, Papai Z, Godeny M, et al. Reirradiation of Locally Recurrent Nasopharyngeal Carcinoma. *Strahlenther Onkol* (2003) 179:298–305. doi: 10.1007/s00066-003-1048-6
24. Deng J, He Y, Sun XS, Li JM, Xin MZ, Li WQ, et al. Construction of a Comprehensive Nutritional Index and its Correlation With Quality of Life and Survival in Patients With Nasopharyngeal Carcinoma Undergoing IMRT: A Prospective Study. *Oral Oncol* (2019) 98:62–8. doi: 10.1016/j.oraloncology.2019.09.014
25. Peng H, Chen BB, Tang LL, Chen L, Li WF, Zhang Y, et al. Et Al: Prognostic Value of Nutritional Risk Screening 2002 Scale in Nasopharyngeal Carcinoma: A Large-Scale Cohort Study. *Cancer Sci* (2018) 109:1909–19. doi: 10.1111/cas.13603
26. Pan X, Wang C, Li R, Su L, Zhang M, Cai C, et al. Applicability of the Nutrition Risk Screening 2002 Combined With a Patient-Generated Subjective Global Assessment in Patients With Nasopharyngeal Carcinoma. *Cancer Manag Res* (2020) 12:8221–7. doi: 10.2147/CMAR.S261945
27. McDowell LJ, Rock K, Xu W, Chan B, Waldron J, Lu L, et al. Long-Term Late Toxicity, Quality of Life, and Emotional Distress in Patients With Nasopharyngeal Carcinoma Treated With Intensity Modulated Radiation Therapy. *Int J Radiat Oncol Biol Phys* (2018) 102:340–52. doi: 10.1016/j.ijrobp.2018.05.060
28. Cupp MA, Cariolou M, Tzoulaki I, Aune D, Evangelou E, Berlanga-Taylor AJ. Neutrophil to Lymphocyte Ratio and Cancer Prognosis: An Umbrella Review of Systematic Reviews and Meta-Analyses of Observational Studies. *BMC Med* (2020) 18:360. doi: 10.1186/s12916-020-01817-1
29. Ehrsson YT, Hellstrom PM, Brismar K, Sharp L, Langius-Eklof A, Laurell G. Explorative Study on the Predictive Value of Systematic Inflammatory and Metabolic Markers on Weight Loss in Head and Neck Cancer Patients Undergoing Radiotherapy. *Support Care Cancer* (2010) 18:1385–91. doi: 10.1007/s00520-009-0758-4
30. Hong JS, Hua YJ, Su L, Zhang HR, Lv WL, Chen XY, et al. Modified-Nutrition Index Is a Significant Prognostic Factor for the Overall Survival of the Nasopharyngeal Carcinoma Patients Who Undergo Intensity-Modulated Radiotherapy. *Nutr Cancer* (2017) 69:1011–8. doi: 10.1080/01635581.2017.1359311
31. OuYang PY, Zhang LN, Tang J, Lan XW, Xiao Y, Gao YH, et al. Evaluation of Body Mass Index and Survival of Nasopharyngeal Carcinoma by Propensity-Matched Analysis: An Observational Case-Control Study. *Med (Baltimore)* (2016) 95:e2380. doi: 10.1097/MD.0000000000002380
32. Lavriv DS, Neves PM, Ravasco P. Should Omega-3 Fatty Acids be Used for Adjuvant Treatment of Cancer Cachexia? *Clin Nutr ESPEN* (2018) 25:18–25. doi: 10.1016/j.clnesp.2018.02.006
33. Mirza KA, Pereira SL, Voss AC, Tisdale MJ. Comparison of the Anticatabolic Effects of Leucine and Ca-Beta-Hydroxy-Beta-Methylbutyrate in Experimental Models of Cancer Cachexia. *Nutrition* (2014) 30:807–13. doi: 10.1016/j.nut.2013.11.012
34. Eley HL, Russell ST, Tisdale MJ. Attenuation of Depression of Muscle Protein Synthesis Induced by Lipopolysaccharide, Tumor Necrosis Factor, and Angiotensin II by Beta-Hydroxy-Beta-Methylbutyrate. *Am J Physiol Endocrinol Metab* (2008) 295:E1409–1416. doi: 10.1152/ajpendo.90530.2008
35. Hsieh LC, Chien SL, Huang MS, Tseng HF, Chang CK. Anti-Inflammatory and Anticatabolic Effects of Short-Term Beta-Hydroxy-Beta-Methylbutyrate Supplementation on Chronic Obstructive Pulmonary Disease Patients in Intensive Care Unit. *Asia Pac J Clin Nutr* (2006) 15:544–50. doi: 10.1016/j.appet.2005.10.003

Conflict of Interest: The authors declare that the research was conducted in the absence of any commercial or financial relationships that could be construed as a potential conflict of interest.

frontiers in Oncology

ORIGINAL RESEARCH
published: 05 November 2021
doi: 10.3389/fonc.2021.764946

Dosimetric Comparison of Helical Tomotherapy, Volume-Modulated Arc Therapy, and Fixed-Field Intensity-Modulated Radiation Therapy in Locally Advanced Nasopharyngeal Carcinoma

Shan Lu[1], Huiqi Fan[1], Xueyuan Hu[2], Xin Li[2], Yingying Kuang[1], Deyang Yu[2] and Shanshan Yang[3*]*

[1] Department of Head and Neck Radiotherapy, Harbin Medical University Cancer Hospital, Harbin, China, [2] Department of Radiation Physics, Harbin Medical University Cancer Hospital, Harbin, China, [3] Department of Gynecological Radiotherapy, Harbin Medical University Cancer Hospital, Harbin, China

Edited by:
Weihong Jiang,
Central South University, China

Reviewed by:
Xianjie Jiang,
Central South University, China
Xiaolan Zhu,
Zhenjiang Fourth People's Hospital, China

***Correspondence:**
Deyang Yu
yudeyang@hrbmu.edu.cn
Shanshan Yang
yangshanshan@hrbmu.edu.cn

Specialty section:
This article was submitted to Surgical Oncology, a section of the journal Frontiers in Oncology

Received: 26 August 2021
Accepted: 18 October 2021
Published: 05 November 2021

Citation:
Lu S, Fan H, Hu X, Li X, Kuang Y, Yu D and Yang S (2021) Dosimetric Comparison of Helical Tomotherapy, Volume-Modulated Arc Therapy, and Fixed-Field Intensity-Modulated Radiation Therapy in Locally Advanced Nasopharyngeal Carcinoma. Front. Oncol. 11:764946. doi: 10.3389/fonc.2021.764946

Objective: To compare the dosimetric parameters of different radiotherapy plans [helical tomotherapy (HT), volume-modulated arc therapy (VMAT), and fixed-field intensity-modulated radiation therapy (FF-IMRT)] for locally advanced nasopharyngeal carcinoma (NPC).

Methods: A total of 15 patients with locally advanced NPC were chosen for this retrospective analysis and replanned for HT, VMAT, and FF-IMRT. The prescribed planning target volume (PTV) dose for the primary tumor and metastatic lymph nodes was 70 Gy (2.12 Gy/fraction, delivered over 33 fractions). The prescribed PTV dose for the high-risk subclinical region was 59.4 Gy (1.8 Gy/fraction, delivered over 33 fractions). The dosimetric parameters of the PTV and organs at risk (OARs) and the efficiency of radiation delivery were assessed and compared using the paired-samples t-test.

Results: Compared with VMAT and FF-IMRT plans, HT plans significantly improved the mean conformity index (CI) and homogeneity index (HI). The HT plans reduced the maximum doses delivered to OARs, such as the brainstem, spinal cord, and optic nerves, and significantly reduced the volume delivered to the high-dose region, especially when examining the V_{30} value of the parotid glands. However, VMAT reduced the treatment time and improved the efficiency of radiation delivery compared with HT.

Conclusions: For locally advanced NPC, the results showed that HT and VMAT possessed better target homogeneity and conformity, reducing the dose delivered to OARs compared with conventional FF-IMRT, with HT achieving the best effect. Among the techniques studied, VMAT had the shortest radiation delivery time. The results of this study can provide guidance for the selection of appropriate radiation technologies used to treat patients with locally advanced NPC who are undergoing concurrent chemoradiotherapy.

Keywords: radiotherapy technique, helical tomotherapy (HT), volume-modulated arc therapy (VMAT), fixed-field intensity-modulated radiation therapy (FF-IMRT), nasopharyngeal carcinoma (NPC)

1 INTRODUCTION

Nasopharyngeal carcinoma (NPC) is among the most common head and neck cancer. The incidence of NPC has unique geographical and ethnic distribution patterns, with a high incidence in Asia, particularly in Southeast Asia. According to data from GLOBOCAN 2012, high incidence rates have been identified in several provinces of southeast China (such as Guangdong, Hongkong), Thailand, and the Philippines (1). NPC cases in China represented 48.62% and 50.34% of the incidence and mortality for all cases of Asia in 2012, respectively (2). Approximately 68% of NPC patients suffer from locally advanced disease at the time of diagnosis (3). Due to the complex anatomy and small region for surgery, the primary treatment modality for NPC is radiotherapy. Early-stage NPC can only be treated with radiotherapy. Locally advanced NPC is typically treated with concurrent chemotherapy and radiotherapy (CCRT) (4). However, CCRT can lead to considerable acute and late toxicities in many of the normal structures surrounding the nasopharynx, such as the pharyngeal mucosa, parotid glands, and cranial nerves (5, 6). Therefore, an increasing number of studies have begun to focus on reducing treatment-related side effects in patients with NPC undergoing CCRT.

Modern radiation techniques have evolved alongside the development of radiation equipment and advancements in radiation physics in recent years. Following the conventional three-dimensional conformal radiation therapy (3D-CRT) technique, intensity-modulated radiation therapy (IMRT) can achieve specific dosimetric and clinical objectives through a computer-aided optimization process (7), providing highly conformal dose distributions to the planning target volume (PTV), minimize the dose delivered to organs at risk (OARs) (8, 9), and significantly reduce acute and late toxicity (10, 11). Volume-modulated arc therapy (VMAT) and helical tomotherapy (HT) are gaining increasing attention compared with conventional fixed-field IMRT (FF-IMRT, 5/7/9-field). VMAT uses low monitor units (MUs) and treatment times, varying dose rates, and a dynamic multileaf collimator (MLC) based on a variable-speed rotational treatment paradigm. HT is a new computed tomography (CT)-based rotational IMRT that delivers a highly conformal dose distribution and spares OARs through the use of 51 independent beam directions and 64 pneumatically driven MLC leaves.

However, the high costs of primary equipment and maintenance for HT treatment systems result in increased treatment costs, which limits the use of this modality in clinical practice, especially in lower-income countries. This study aimed to assess three modern IMRT techniques (HT, VMAT, and FF-IMRT) in terms of the dosimetric parameters measured for the PTV and OARs in locally advanced NPC and to determine whether HT has significant dosimetric impacts that might justify the costs associated with this modality.

Abbreviations: NPC, nasopharyngeal carcinoma; HT, helical tomotherapy; VMAT, volume-modulated arc therapy; FF-IMRT, fixed-field intensity-modulated radiation therapy; OARs, organs at risk; CI, conformity index; HI, homogeneity index; CCRT, concurrent chemotherapy and radiotherapy; PTV, planning target volume; MUs, monitor units; MLC, multileaf collimator; AJCC, American Joint Committee on Cancer; RTOG, Radiation Therapy Oncology Group; TMJ, temporomandibular joints; CTV, clinical target volume; DVH, dose–volume histogram; $D_{98\%}$, the dose that received 98% volume of the PTV; D_{max}, the maximum dose; D_{mean}, the mean dose; EGFR, epidermal growth factor receptor; PD-1, programmed cell death 1.

2 MATERIALS AND METHODS

2.1 Patient Characteristics and CT Simulation

A total of 15 patients with Stage III/IVA NPC treated between February 2019 and February 2020 in our hospital were chosen for this research. All patients were staged according to the American Joint Committee on Cancer (AJCC) Manual for Staging of Cancer, 8th edition (12). The selection criterion was biopsy-proven squamous cell carcinoma. The ages of all eligible patients ranged from 39 to 68 years, and the mean and median ages were 56.7 and 60 years, respectively. A total of 10 patients received CCRT, 2 patients received radiotherapy and concurrent weekly targeted therapy with nimotuzumab, and 3 patients received both chemotherapy and targeted therapy with nimotuzumab during radiotherapy. The information for all patients is shown in **Table 1**. Thermoplastic head, neck, and shoulder masks were used to immobilize all patients in a supine position to perform CT simulations with 3-mm slice thickness using a Philips 16-slice Brilliance big bore CT scanner (Philips Medical Systems, Amsterdam, Netherlands) following the administration of intravenous contrast. Scanned images were obtained from the top of the head to the carina for all patients.

2.2 Target and Normal Tissue Volume Definition

All CT images were transferred to the Monaco 5.11 (Elekta AB, Stockholm, Sweden) planning system for contouring. For consistency, all contouring of the target and OARs was performed by the same radiation oncologists who specialized in head and neck radiotherapy. The target volume delineation of the NPC was based on the Radiation Therapy Oncology Group (RTOG) 2009 guidelines (13). The gross tumor volume (GTV_{70}) was defined as the known gross disease of the

TABLE 1 | Clinicopathological characteristics of the patients with nasopharyngeal carcinoma (NPC).

Characteristics	No. of Patients (*N* = 15)
Age(years)	
≤60	9
>60	6
Sex	
Male	13
Female	2
Pathology (SCC*)	
Poorly differentiated	10
Non-keratinizing	5
Clinical stage	
III	10
IVA	5
Concurrent therapy	
Chemotherapy	10
Targeted therapy	2
Chemotherapy + targeted therapy	3

**SCC, squamous cell carcinoma.*

TABLE 2 | The dose–volume constraints of normal tissues in NPC.

Structures	Dose–volume constraints
Brainstem	D_{max} < 54 Gy
Spinal cord	D_{max} < 45 Gy
Optic nerves	D_{max} < 54 Gy or D1 < 60Gy
Optic chiasm	D_{max} < 54 Gy
Lens	D_{max} < 8 Gy
Eyes	D_{max} < 40 Gy
Pituitary	D_{max} < 60 Gy
Mandible	D_{max} < 70 Gy
TMJ	D_{max} < 70 Gy
Brachial plexus	D_{max} < 66 Gy
Oral cavity	V40 < 40%
Parotid gland	V30 < 50%
Temporal lobes	D_{max} < 60 Gy or D1 < 65Gy
Larynx	V45 < 40%
Esophagus	V45 < 40%

nasopharynx. Grossly positive lymph nodes (GTV_{nd}) were defined as any lymph node >1 cm or nodes with necrotic cancer. The clinical target volume for 59.4 Gy ($CTV_{59.4}$) was defined as the region at high risk for microscopic disease, which included all potential routes of spread for primary and nodal diseases. The primary high-risk regions included the entire nasopharynx, anterior one-third of the clivus, skull base, pterygoid fossa, parapharyngeal space, inferior sphenoid sinus, posterior one-fourth of the nasal cavity/maxillary sinuses, inferior soft palate, and retrostyloid space. The common high-risk lymph node regions typically included the bilateral upper deep jugular, retropharyngeal area, and levels II, III, IV, and V lymph nodes. Level IB lymph nodes can be spared in selected patients. The OARs for NPC include the brainstem, spinal cord, optic nerves, optic chiasm, eyes, lens, temporal lobe, parotid glands, pituitary, temporomandibular joints (TMJ), mandible, oral cavity, brachial plexus, esophagus, and larynx. The PTV was defined as the CTV area + 3 mm.

2.3 Treatment Planning and Prescribed Doses

All treatment planning procedures were developed by the same radiation physicist to ensure consistency. The FF-IMRT and VMAT plans were designed using the Monaco planning system version 5.11, and the HT plans were designed in the tomotherapy planning system (Accuray Inc., Madison, USA). The FF-IMRT and VMAT plans were designed to be executed using the Elekta Synergy (Elekta Ltd., Crawley, UK), equipped with 8-MV photon beams, and the MLCi2 (40 pairs of MLC leaves, each with a 1-cm width at the isocenter). The prescribed PTV dose for the primary tumor (PTV_{70}) and metastatic lymph nodes (PTVnd) was 70 Gy (2.12 Gy/fraction, delivered over 33 fractions). The prescribed PTV dose for the high-risk subclinical region was 59.4 Gy (1.8 Gy/fraction, delivered over 33 fractions). The details regarding the dose constraints for normal tissues within the NPC plans are summarized in **Table 2**.

2.3.1 HT Plans

The HT plans were generated using a tomotherapy planning station with a 6-MV X-ray and performed on the Tomo HD (Accuray Inc., Madison, USA). The parameters for beamlet calculation included a field width of 2.5 cm, a pitch value of 0.287, a modulation factor of 3, and a normal dose calculation grid.

2.3.2 VMAT Plans

The VMAT plans were generated in the Monaco 5.11 planning system, and an 8-MV X-ray in a Synergy linear accelerator was used. The VMAT plans were designed using a beam with double 360° arcs, featuring 100 control points per arc. All VMAT plans were designed using the Monte Carlo algorithm in the Monaco 5.11 planning system.

2.3.3 FF-IMRT Plans

The FF-IMRT plans were generated in the Monaco 5.11 planning system, and an 8-MV X-ray in a Synergy linear accelerator was used. Nine evenly distributed coplanar fields with gantry angles of 200°, 240°, 280°, 320°, 0°, 40°, 80°, 120°, and 160° were used, featuring 20 control points in each beam. All FF-IMRT plans were prepared using the Monte Carlo algorithm in the Monaco 5.11 planning system. The optimization functions of the FF-IMRT plans were the same as those in the VMAT plans. The dynamic MLC (DMLC, sliding window) technique was used in the FF-IMRT plans.

2.4 Plan Evaluation Parameters

The data obtained in the dose–volume histogram (DVH) for all plans were analyzed, and plan comparisons focused on the following parameters.

2.4.1 PTV Coverage

The dose that received 98% volume of the PTV ($D_{98\%}$), the dose that received 50% volume of the PTV($D_{50\%}$), the dose received 2% volume of the PTV($D_{2\%}$), the mean dose (D_{mean}), the conformity index (CI), and the homogeneity index (HI) were quantified to evaluate PTV coverage. The CI was used to evaluate the conformity of the prescribed dose distribution:

$$CI = \frac{V_{t,ref}}{V_t} \times \frac{V_{t,ref}}{V_{ref}}$$

where $V_{t,ref}$, V_t, and V_{ref} denote the target volume that received the prescribed dose, the target volume, and the total volume covered by the prescribed dose, respectively. The CI ranges from 0 to 1, with a high CI indicating a high conformal dose delivery to the target. In accordance with The International Commission on Radiation Units and Measurements (ICRU) report No. 83 (14), the HI was calculated using the following formula:

$$HI = \frac{D_{2\%} - D_{98\%}}{D_{50\%}}$$

HI was used to evaluate the homogeneity of the dose distribution. The low HI value indicates good homogeneity of the target volume.

2.4.2 Organs at Risk

For patients with NPC, the following values were determined: the maximum doses (D_{max}) delivered to the brainstem, spinal cord, optic nerves, optic chiasm, lens, eyes, pituitary, mandible, TMJ, and brachial plexus; the mean doses (D_{mean}) delivered to the larynx, oral cavity, and esophagus; the volume that received 30 Gy (V_{30}) and the D_{mean} for the parotid glands; the dose delivered to 1% of the OAR volume (D_1); and the maximum dose (D_{max}) delivered to the temporal lobes.

2.4.3 Treatment Time

The treatment delivery time for each plan was determined and compared.

2.4.4 Data Analysis

All plans were normalized to deliver the prescribed dose to 95% volume of the PTV to allow for comparison across results. The data collected from the DVHs for the PTV and OARs were analyzed using SPSS 19.0 (SPSS, Inc., Chicago, IL, USA). Significant differences were tested using the paired-samples t-test. A $p < 0.05$ was considered significant.

3 RESULTS

3.1 PTV Coverage

The mean PTV_{70}, PTV_{nd}, and $PTV_{59.4}$ values for NPC were 53.6 ± 30.3 cc (11.3–106.5 cc), 41.6 ± 38.9 cc (6.9–107.9 cc), and 674.0 ± 142.4 cc (503.3–874.0 cc), respectively. All HT, VMAT, and FF-IMRT plans were normalized to cover 95% of the PTV with ≥100% of the prescribed dose. The D_{max} constrained in the PTV was <110% of the prescription dose.

The detailed results are shown in **Table 3**. The conformal and homogeneous dose distribution to the PTV target for the HT plans, as assessed using the CI and HI, respectively, were significantly better than those for the VMAT and FF-IMRT plans ($p < 0.001$; **Figure 1**). The HT plans also had the best D_{mean} value ($p < 0.001$), approaching the prescription dose, demonstrating significant advantages over the other two plans. Compared with the conventional FF-IMRT plans, the VMAT plans did not show significant superiority for HI and CI ($p > 0.05$), and only the CI of $PTV_{59.4}$ was better for VMAT compared with FF- IMRT ($p = 0.016$). Typical dose distributions and dose–volume histograms for the three plans are presented in **Figures 2** and **3**.

3.2 OARs

The DVH data for the OARs in NPC are listed in **Table 4**. Our results showed that the D_{max} values for the brainstem, spinal cord, optic nerves, lens, eyes, pituitary, TMJ left, and temporal lobes assessed in HT plans were significantly lower than those in FF-IMRT and VMAT plans ($p \leq 0.01$). HT also resulted in significantly improved dose sparing based on the V_{30} value of the parotid glands, the D_1 of the temporal lobes, and the D_{mean} of the

TABLE 3 | Dosimetric parameters for PTV of three plans.

Parameters	IMRT	VMAT	HT	p*		
				VMAT *vs*. IMRT	HT *vs*. IMRT	HT *vs*. VMAT
PTV70						
D_{mean} (Gy)	72.10 ± 0.49	72.24 ± 0.37	70.63 ± 0.23	0.117	<0.001	<0.001
HI	0.07 ± 0.01	0.07 ± 0.01	0.03 ± 0.01	0.217	<0.001	<0.001
CI	0.75 ± 0.04	0.76 ± 0.03	0.82 ± 0.04	0.086	<0.001	<0.001
PTVnd						
D_{mean} (Gy)	72.11 ± 0.52	72.30 ± 0.25	70.63 ± 0.25	0.409	<0.001	<0.001
HI	0.07 ± 0.02	0.07 ± 0.02	0.03 ± 0.01	0.726	<0.001	<0.001
CI	0.77 ± 0.05	0.78 ± 0.04	0.82 ± 0.04	0.184	<0.001	<0.001
PTV59.4						
D_{mean} (Gy)	62.50 ± 0.60	62.47 ± 0.49	60.85 ± 0.43	0.765	<0.001	<0.001
HI	0.17 ± 0.04	0.17 ± 0.04	0.11 ± 0.01	0.082	<0.001	<0.001
CI	0.65 ± 0.08	0.66 ± 0.08	0.76 ± 0.08	0.016	<0.001	<0.001

**P value was computed by paired t test.*

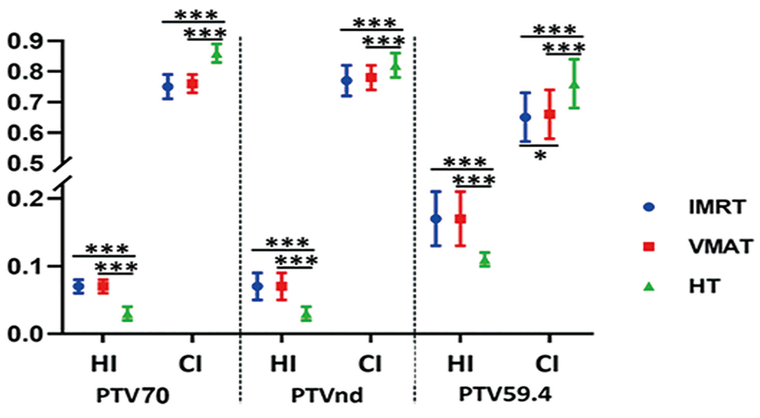

FIGURE 1 | Conformity index (CI) and homogeneity index (HI) for planning target volume (PTV) with intensity-modulated radiation therapy (IMRT; circle), volume-modulated arc therapy (VMAT; square), and helical tomography (HT; triangle). *$p < 0.05$, **$p < 0.01$, ***$p < 0.001$.

larynx, compared with FF-IMRT and VMAT ($p < 0.05$). Compared with FF-IMRT, VMAT significantly decreased the D_{max} of the brainstem, spinal cord, optic nerve, eyes, TMJs, and temporal lobe and decreased the D_{mean} of the larynx and esophagus ($p < 0.05$).

3.3 Treatment Time

The treatment delivery times for the three treatment techniques were determined to study the execution efficiency of the three radiotherapy technologies. The mean treatment delivery times for FF-IMRT, VMAT, and HT were 7.49 ± 0.32, 4.40 ± 0.29,

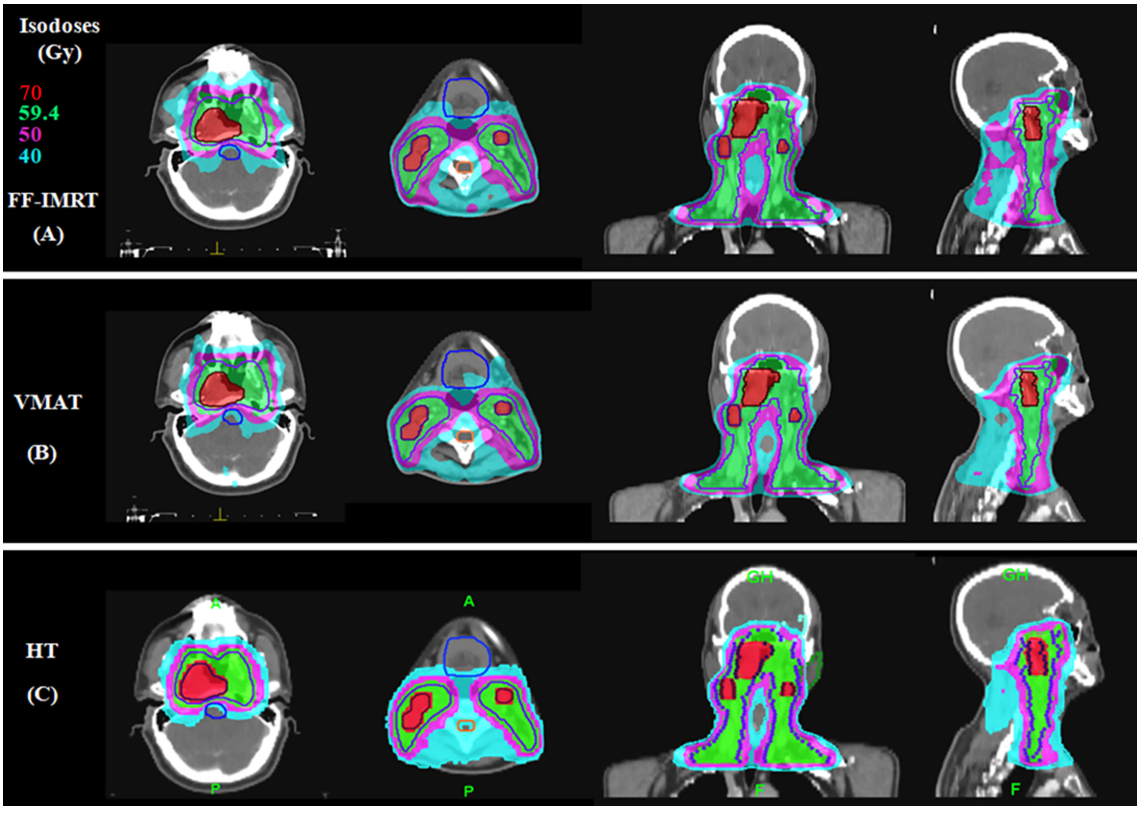

FIGURE 2 | Typical dose distributions for the three plans in locally advanced nasopharyngeal carcinoma (NPC). **(A)** Fixed-field intensity-modulated radiation therapy (FF-IMRT), **(B)** volume-modulated arc therapy (VMAT), and **(C)** helical tomography (HT) plans.

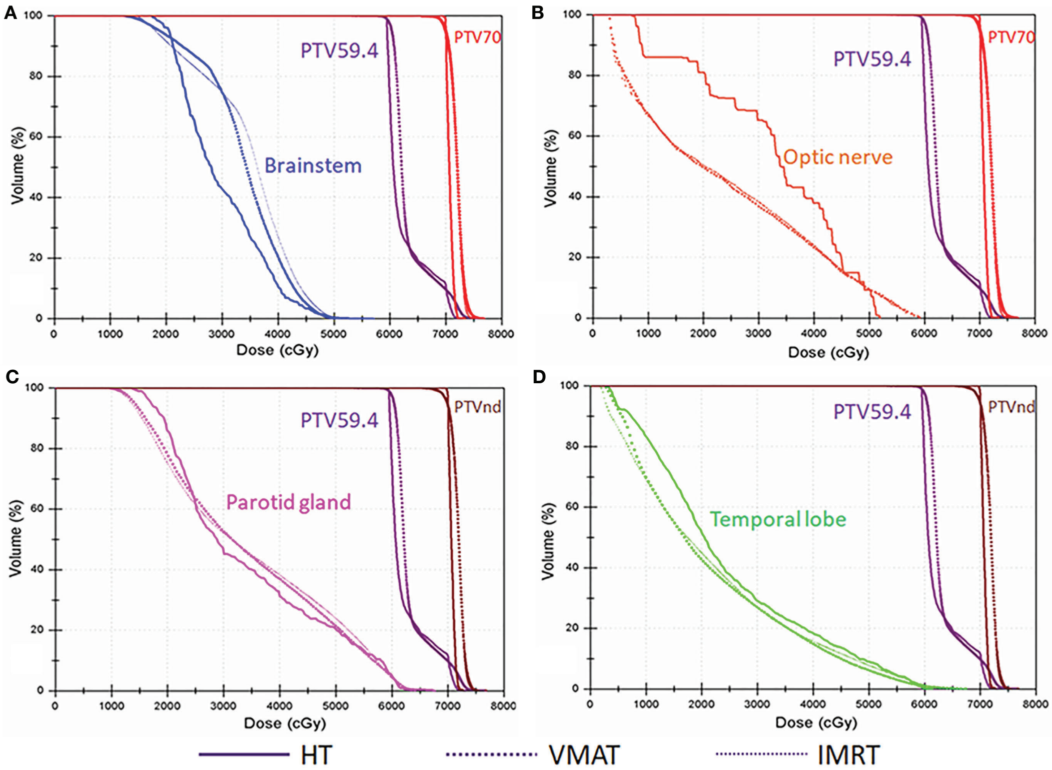

FIGURE 3 | Typical dose–volume histograms for the three plans in locally advanced nasopharyngeal carcinoma (NPC). Dose–volume histograms for planning target volume of 70 Gy (PTV_{70}; red), planning target volume for metastatic lymph nodes (PTV_{nd}; brown), planning target volume of 59.4 Gy ($PTV_{59.4}$; purple), **(A)** the brainstem (blue), **(B)** optic nerve (orange), **(C)** parotid gland (pink), and **(D)** temporal lobe (green).

and 7.59 ± 0.40 min, respectively. Compared with FF-IMRT and HT, VMAT had the highest execution efficiency.

4 DISCUSSION

Cancer is a major public health problem worldwide and is expected to represent the leading cause of death in every country during the twenty-first century. Worldwide, 129,079 newly diagnosed NPC cases and 72,987 NPC-related deaths were reported in 2018 (15). In southeast China, the incidence of NPC is higher than in most other countries. Due to the unique anatomical structure of the nasopharynx and the high sensitivity of NPC to ionizing radiation, radiotherapy is the preferred treatment. With the continued development of radiotherapy technology, local NPC control and survival have significantly improved over the past half-century (16). CCRT is a standard treatment for locally advanced NPC. However, 15.8% of NPC patients experience recurrence within 5 years after radiotherapy, especially among patients with advanced disease (17), indicating that novel treatment approaches remain necessary.

Molecular targeted therapy and immunotherapy represent two new approaches to NPC. Epidermal growth factor receptor (EGFR) is highly expressed in NPC compared with other solid tumors (18). A retrospective analysis showed that an EGFR inhibitor (e.g., nimotuzumab) combined with CCRT was beneficial for treating locally advanced NPC (19). Immunotherapy has become a hotspot for cancer treatment research. Clinical trial data have shown that immune-checkpoint inhibitors, such as those against programmed cell death 1 (PD-1), can be effective in patients with recurrent or metastatic NPC (20, 21). However, the feasibility of concurrent immunotherapy and radiotherapy in locally advanced NPC remains unclear.

For patients with recurrent disease, the primary cause of local recurrence is insufficient irradiation dose delivered to the target area, which is limited by the dose tolerance of the surrounding OARs. Therefore, exploring feasible and optimized radiotherapeutic techniques is critical to achieving highly conformal treatment plans and acquiring good OAR sparing results. A number of constraining organs surround the irradiation area in NPC, and radiotherapy may cause acute or late adverse effects of these structures (e.g., acute mucositis, xerostomia, and temporal lobe neuropathy). Our study aimed to decrease the radiation doses and irradiated volumes of these structures.

CCRT has demonstrated improved survival benefits in locally advanced NPC, but it typically induces acute and late toxicities,

TABLE 4 | Dose–volume histogram comparisons for the main OARs of three plans.

OARs	IMRT	VMAT	HT	p*		
				VMAT *vs.* IMRT	HT *vs.* IMRT	HT *vs.* VMAT
Brainstem						
D_{max} (Gy)	53.77 ± 1.33	53.16 ± 1.26	51.84 ± 1.95	0.006	<0.001	0.002
Spinal cord						
D_{max} (Gy)	43.99 ± 1.03	42.99 ± 1.15	41.34 ± 1.57	0.022	<0.001	<0.001
Optic nerve left						
D_{max} (Gy)	55.46 ± 2.98	54.46 ± 4.13	52.07 ± 3.14	0.040	<0.001	0.002
Optic nerve right						
D_{max} (Gy)	55.05 ± 2.39	55.11 ± 3.13	50.90 ± 3.24	0.881	<0.001	<0.001
Optic chiasm						
D_{max} (Gy)	42.52 ± 11.57	41.88 ± 11.82	42.67 ± 7.26	0.378	0.912	0.600
Lens left						
D_{max} (Gy)	7.43 ± 1.64	7.16 ± 1.94	5.47 ± 0.82	0.346	<0.001	0.001
Lens right						
D_{max} (Gy)	7.69 ± 1.28	7.46 ± 1.36	5.82 ± 0.62	0.502	<0.001	<0.001
Eye left						
D_{max} (Gy)	35.72 ± 4.70	33.06 ± 6.68	28.13 ± 5.25	0.011	<0.001	0.001
Eye right						
D_{max} (Gy)	35.92 ± 3.29	33.62 ± 5.62	26.62 ± 4.59	0.018	<0.001	<0.001
Pituitary						
D_{max} (Gy)	58.22 ± 4.97	58.54 ± 5.35	52.32 ± 6.78	0.375	<0.001	<0.001
Mandible						
D_{max} (Gy)	67.39 ± 3.87	67.76 ± 3.83	66.61 ± 4.20	0.249	0.234	0.095
TMJ left						
D_{max} (Gy)	61.07 ± 2.53	59.16 ± 3.54	57.85 ± 3.42	0.001	<0.001	0.004
TMJ right						
D_{max} (Gy)	60.23 ± 4.88	58.58 ± 5.17	57.10 ± 5.36	0.016	<0.001	0.027
Brachial plexus left						
D_{max} (Gy)	63.93 ± 2.19	64.32 ± 2.18	63.25 ± 3.79	0.132	0.363	0.177
Brachial plexus right						
D_{max} (Gy)	64.20 ± 2.63	64.79 ± 3.00	63.27 ± 4.10	0.074	0.171	0.022
Oral cavity						
D_{mean} (Gy)	38.06 ± 1.48	38.44 ± 1.79	37.68 ± 1.57	0.404	0.356	0.229
Parotid gland left						
D_{mean} (Gy)	33.81 ± 1.34	33.38 ± 1.87	33.64 ± 1.04	0.471	0.683	0.664
V30 (%)	50.58 ± 2.52	49.96 ± 2.70	45.23 ± 1.73	0.537	<0.001	<0.001
Parotid gland right						
D_{mean} (Gy)	34.71 ± 1.08	33.86 ± 1.72	33.87 ± 1.13	0.036	0.048	0.975
V30 (%)	51.15 ± 1.68	50.44 ± 2.06	45.56 ± 2.14	0.359	<0.001	<0.001
Temporal lobe left						
D_{max} (Gy)	65.16 ± 3.94	64.79 ± 3.80	62.09 ± 3.73	0.071	<0.001	<0.001
D1 (Gy)	59.38 ± 1.26	59.13 ± 1.84	58.23 ± 1.28	0.429	0.006	0.028
Temporal lobe right						
D_{max} (Gy)	63.90 ± 1.39	64.08 ± 1.69	60.46 ± 0.77	0.659	<0.001	<0.001
D1 (Gy)	58.87 ± 0.85	59.35 ± 1.05	58.00 ± 1.00	0.080	0.001	<0.001
Larynx						
D_{mean} (Gy)	43.22 ± 1.08	41.99 ± 2.07	39.56 ± 0.98	0.024	<0.001	0.001
Esophagus						
D_{mean} (Gy)	30.41 ± 6.63	28.80 ± 6.58	28.18 ± 5.91	0.007	<0.001	0.371

**p value was computed by paired t test.*

sometimes emerging months or even years after treatment completion (22). A phase II study showed that the addition of an anti-EGFR antibody to radiotherapy enhanced radiotherapy-related acute toxicities to the skin and mucosa (23). Therefore, attention should be paid to side effects related to the treatment and their effects on quality of life among patients with NPC, in addition to the local tumor control rate. As one of the few hospitals in China equipped with several advanced linear accelerators (nine linear accelerators, including Versa HD and HT), our hospital had the unique capacity to perform a dosimetric study of IMRT, VMAT, and HT. Reports comparing the dosimetric parameters of FF-IMRT, VMAT, and HT with regard to the PTV and OARs in NPC are rare. Therefore, this study aimed to estimate which of the three radiotherapy techniques were dosimetrically superior to provide guidance regarding technique selection for patients with locally advanced NPC.

Due to the complex anatomy and various OARs closely positioned to NPC target tissues, radiotherapy for NPC is technically challenging and highly complex. Previous studies have confirmed that the modern IMRT is associated with a significantly steeper dose gradient surrounding the target region compared with conventional 3D-CRT (17, 24). Growing evidence suggests that HT can sculpt radiation doses to fit the complex shapes of tumorous regions, avoiding the delivery of high-dose radiation to OARs through the rapid opening and closing of leaves in a collimator that rotates around the patient (25). Therefore, HT is frequently used to treat various diseases (26–29), including NPC (30). In this study, the results showed that the three IMRT techniques met the clinical demands of NPC therapy but HT presented with a sharp dose gradient associated with optimal HI and CI values. Based on these results, HT is the recommended radiotherapy technique for ensuring local tumor control and improving patient prognosis when treating NPC with radiotherapy.

In addition to improved target conformity and homogeneity, HT demonstrated significantly better performance in sparing the surrounding OARs compared with the other techniques. The nasopharynx is adjacent to several critical organs, such as the brainstem, lens, and optic nerves. To protect critical organs, some parts of the tumor are often underdosed, which may lead to a low local control rate (31). The delivery of high doses of radiation to large volumes of normal tissues typically results in the development of severe adverse effects, such as dysphagia and radiation mucositis, which may interrupt radiation treatment. Therefore, decreasing the dose and volume delivered to normal tissues that surround the targeted radiation regions is crucial. In our study, the results showed that compared with the FF-IMRT and VMAT plans, the HT plans significantly decreased the D_{max} of the brainstem, spinal cord, optic structures, pituitary, TMJ, temporal lobes, and larynx (**Table 4**). Moreover, the HT plans decreased the V_{30} value of the parotid glands compared with the FF-IMRT ($p < 0.001$) and VMAT ($p < 0.001$) plans. Therefore, HT plans may decrease radiotherapeutic adverse effects by reducing the doses and volumes of normal organ irradiation.

The significant advantages of HT plans over FF-IMRT and VMAT plans with regard to PTV coverage and OAR sparing are associated with the following features. First, the linear accelerator used during HT can rotate 360° continuously, with 51 optimized beam angles combined with a continuously moving couch. Second, HT delivers radiation in the form of a helical tomoscan by using constant beam widths of 1, 2.5, and 5 cm. Finally, HT is equipped with a pneumatic binary MLC system with rapid leaf transition times. In addition, the onboard megavoltage CT (MVCT) of HT allows daily setup validation. The margin expanding from the CTV to the PTV can be decreased because setup errors are reduced by daily setup verification, resulting in a reduced dose delivered to OARs. The MVCT can be used to perform adaptive radiotherapy planning, which can eliminate volume variations delivered to the target and OARs between intrafractions.

HT plans also have some drawbacks. Vernat and Pasquier reported that HT increases the normal tissue volume in the low-dose region compared with IMRT and VMAT when applied to oropharyngeal and prostate cancers (32, 33). Xie has reported that the HT plan increased the V_5 and V_{10} values of the lung and heart compared with IMRT and VMAT plans for left-sided breast cancer (34). Therefore, the application of HT in lung and breast cancers remains controversial. In NPC cases, most OARs are serially organized structures, closely related to D_{max}. Thus, our study focused on the D_{max} of most OARs, except for the parotid glands, rather than examining the low-dose volumes. For the parotid glands, the V_{30} and D_{mean} were evaluated according to RTOG guidelines. Our results showed that HT could significantly decrease the V_{30} value of the parotid glands.

Compared with FF-IMRT, VMAT exhibited better OAR sparing abilities. In addition, compared with FF-IMRT and HT, VMAT reduced the treatment time and improved the treatment efficiency while ensuring the treatment effect. Compared with FF-IMRT and HT, VMAT reduced the treatment delivery time by 41.3% and 42%, respectively. Several studies have reported that VMAT achieves higher PTV dose conformity and better OAR sparing abilities with a shorter treatment delivery time than FF-IMRT for various cancers (29, 35, 36). Shortened treatment times may reduce the influence of uncertain factors, including the probability that patients will move and suffer discomfort. Therefore, VMAT is the most appropriate treatment technique for patients who cannot remain in a stable position for long times due to physical or mental discomfort.

Our study had some limitations. First, we only used a nine-field coplanar arrangement for FF-IMRT and a two-arc coplanar beam configuration for VMAT to reduce the complexity of comparisons, as evidence suggests that these two techniques are the best options for obtaining better target coverage with enhanced sparing of the OARs for FF-IMRT and VMAT radiotherapy (37–39). Additionally, the limited sample size in our study may result in insufficient statistical power to identify significance for some of the dosimetric parameters. Therefore, further clinical trials with large sample sizes focusing on the clinical significance of HT in NPC are essential in the future.

5 CONCLUSION

For patients with locally advanced NPC, the HT and VMAT plans showed improvements in target coverage and OAR sparing compared with the FF-IMRT plans. The HT plans achieved optimal conformity and homogeneity for PTV coverage, with optimal OAR sparing. VMAT was associated with reduced treatment time and improved radiation delivery efficiency, which can reduce the patients' discomfort and the probability of movement during treatment. In addition, the treatment costs of VMAT are lower than those of HT. Therefore, our results may provide guidance for technique selection in patients with locally advanced NPC who are undergoing CCRT.

DATA AVAILABILITY STATEMENT

The original contributions presented in the study are included in the article/supplementary material. Further inquiries can be directed to the corresponding authors.

ETHICS STATEMENT

The studies involving human participants were reviewed and approved by the Ethics Committee of Harbin Medical University Cancer Hospital (Harbin, China) was obtained. The patients/participants provided their written informed consent to participate in this study. Written informed consent was obtained from the individual(s) for the publication of any potentially identifiable images or data included in this article.

AUTHOR CONTRIBUTIONS

DY and SY designed the study. SL and HF contoured the targets and OARs. DY, XH, and XL performed the treatment planning design. SL and DY wrote and revised the manuscript. DY and YK collected the data. DY and SY polished the language. All authors contributed to the article and approved the submitted version.

FUNDING

This work was supported by grants from the Haiyan Research fund of Harbin Medical University Cancer Hospital (JJMS2021-27 and JJQN2021-03) and Project of Precise Radiotherapy Spark Program (2019-N-11-11).

ACKNOWLEDGMENTS

The authors thank all the people who participated in this study.

REFERENCES

1. Torre LA, Bray F, Siegel RL, Ferlay J, Lortet-Tieulent J, Jemal A. Global Cancer Statistics, 2012. *CA: Cancer J Clin* (2015) 65(2):87–108. doi: 10.3322/caac.21262
2. Mahdavifar N, Ghoncheh M, Mohammadian-Hafshejani A, Khosravi B, Salehiniya H. Epidemiology and Inequality in the Incidence and Mortality of Nasopharynx Cancer in Asia. *Osong Public Health Res Perspect* (2016) 7 (6):360–72. doi: 10.1016/j.phrp.2016.11.002
3. Mao Y-P, Xie F-Y, Liu L-Z, Sun Y, Li L, Tang L-L, et al. Re-Evaluation of 6th Edition of AJCC Staging System for Nasopharyngeal Carcinoma and Proposed Improvement Based on Magnetic Resonance Imaging. *Int J Radiat Oncol Biol Phys* (2009) 73(5):1326–34. doi: 10.1016/j.ijrobp.2008.07.062
4. Lin J-C, Jan J-S, Hsu C-Y, Liang W-M, Jiang R-S, Wang W-Y. Phase III Study of Concurrent Chemoradiotherapy *Versus* Radiotherapy Alone for Advanced Nasopharyngeal Carcinoma: Positive Effect on Overall and Progression-Free Survival. *J Clin Oncol* (2003) 21(4):631–7. doi: 10.1200/JCO.2003.06.158
5. Toumi N, Kridis WB, Mnejja W, Bouzguenda R, Khanfir A, Ghorbel A, et al. TPF Induction Chemotherapy Followed by Concurrent Chemoradiotherapy for Locally Advanced Nasopharyngeal Carcinoma: Long Term Results of a Tunisian Series. *Cancer/Radiothérapie* (2018) 22(3):216–21. doi: 10.1016/j.canrad.2017.10.005
6. Liao JF, Zhang Q, Du XJ, Lan M, Liu S, Xia YF, et al. Concurrent Chemoradiotherapy With Weekly Docetaxel *Versus* Cisplatin in the Treatment of Locoregionally Advanced Nasopharyngeal Carcinoma: A Propensity Score-Matched Analysis. *Cancer Commun* (2019) 39(1):1–11. doi: 10.1186/s40880-019-0380-x
7. Nguyen K, Cummings D, Lanza VC, Morris K, Wang C, Sutton J, et al. A Dosimetric Comparative Study: Volumetric Modulated Arc Therapy *vs* Intensity-Modulated Radiation Therapy in the Treatment of Nasal Cavity Carcinomas. *Med Dosimetry* (2013) 38(3):225–32. doi: 10.1016/j.meddos.2013.01.006
8. Chung HT, Lee B, Park E, Lu JJ, Xia P. Can All Centers Plan Intensity-Modulated Radiotherapy (IMRT) Effectively? An External Audit of Dosimetric Comparisons Between Three-Dimensional Conformal Radiotherapy and IMRT for Adjuvant Chemoradiation for Gastric Cancer. *Int J Radiat Oncol Biol Phys* (2008) 71(4):1167–74. doi: 10.1016/j.ijrobp.2007.11.040
9. Trip AK, Nijkamp J, van Tinteren H, Cats A, Boot H, Jansen EPM, et al. IMRT Limits Nephrotoxicity After Chemoradiotherapy for Gastric Cancer. *Radiother Oncol* (2015) 114(3):421–6. doi: 10.1016/j.radonc.2015.03.009
10. Portelance L, Chao KC, Grigsby PW, Bennet H, Low D. Intensity-Modulated Radiation Therapy (IMRT) Reduces Small Bowel, Rectum, and Bladder Doses in Patients With Cervical Cancer Receiving Pelvic and Para-Aortic Irradiation. *Int J Radiat Oncol Biol Phys* (2001) 51(1):261–6. doi: 10.1016/S0360-3016(01)01664-9
11. Beriwal S, Gan GN, Heron DE, Selvaraj RN, Kim H, Lalonde R, et al. Early Clinical Outcome With Concurrent Chemotherapy and Extended-Field, Intensity-Modulated Radiotherapy for Cervical Cancer. *Int J Radiat Oncol Biol Phys* (2007) 68(1):166–71. doi: 10.1016/j.ijrobp.2006.12.023
12. Amin MB, Greene FL, Edge SB, Compton CC, Gershenwald JE, Brookland RK, et al. The Eighth Edition AJCC Cancer Staging Manual: Continuing to Build a Bridge From a Population-Based to a More "Personalized" Approach to Cancer Staging. *CA: Cancer J Clin* (2017) 67(2):93–9. doi: 10.3322/caac.21388
13. Lee N, Harris J, Garden AS, Straube W, Glisson B, Xia P, et al. Intensity-Modulated Radiation Therapy With or Without Chemotherapy for Nasopharyngeal Carcinoma: Radiation Therapy Oncology Group Phase II Trial 0225. *J Clin Oncol* (2009) 27(22):3684. doi: 10.1200/JCO.2008.19.9109
14. Grégoire V, Mackie T. State of the Art on Dose Prescription, Reporting and Recording in Intensity-Modulated Radiation Therapy (ICRU Report No. 83). *Cancer/Radiothérapie* (2011) 15(6-7):555–9. doi: 10.1016/j.canrad.2011.04.003
15. Bray F, Ferlay J, Soerjomataram I, Siegel RL, Torre LA, Jemal A. Global Cancer Statistics 2018: GLOBOCAN Estimates of Incidence and Mortality Worldwide for 36 Cancers in 185 Countries. *CA: Cancer J Clin* (2018) 68(6):394–424. doi: 10.3322/caac.21492
16. Ng WT, Lee MC, Hung WM, Choi CW, Lee KC, Chan OS, et al. Clinical Outcomes and Patterns of Failure After Intensity-Modulated Radiotherapy for Nasopharyngeal Carcinoma. *Int J Radiat Oncol Biol Phys* (2011) 79 (2):420–8. doi: 10.1016/j.ijrobp.2009.11.024
17. Mao Y-P, Tang L-L, Chen L, Sun Y, Qi Z-Y, Zhou G-Q, et al. Prognostic Factors and Failure Patterns in Non-Metastatic Nasopharyngeal Carcinoma After Intensity-Modulated Radiotherapy. *Chin J Cancer* (2016) 35(1):1–10. doi: 10.1186/s40880-016-0167-2
18. Chua DT, Nicholls JM, Sham JS, Au GK. Prognostic Value of Epidermal Growth Factor Receptor Expression in Patients With Advanced Stage Nasopharyngeal Carcinoma Treated With Induction Chemotherapy and Radiotherapy. *Int J Radiat Oncol Biol Phys* (2004) 59(1):11–20. doi: 10.1016/j.ijrobp.2003.10.038
19. Liu Z-G, Zhao Y, Tang J, Zhou Y-J, Yang W-J, Qiu Y-F, et al. Nimotuzumab Combined With Concurrent Chemoradiotherapy in Locally Advanced Nasopharyngeal Carcinoma: A Retrospective Analysis. *Oncotarget* (2016) 7 (17):24429. doi: 10.18632/oncotarget.8225
20. Hsu C, Lee S-H, Ejadi S, Even C, Cohen RB, Le Tourneau C, et al. Safety and Antitumor Activity of Pembrolizumab in Patients With Programmed Death-Ligand 1–Positive Nasopharyngeal Carcinoma: Results of the KEYNOTE-028 Study. *J Clin Oncol* (2017) 35(36):4050–6. doi: 10.1200/JCO.2017.73.3675
21. Wang F-H, Wei X-L, Feng J, Li Q, Xu N, Hu X-C, et al. Efficacy, Safety, and Correlative Biomarkers of Toripalimab in Previously Treated Recurrent or

Metastatic Nasopharyngeal Carcinoma: A Phase II Clinical Trial (POLARIS-02). *J Clin Oncol* (2021) 39(7):704–12. doi: 10.1200/JCO.20.02712
22. Chen Y, Sun Y, Liang SB, Zong JF, Li WF, Chen M, et al. Progress Report of a Randomized Trial Comparing Long-Term Survival and Late Toxicity of Concurrent Chemoradiotherapy With Adjuvant Chemotherapy *Versus* Radiotherapy Alone in Patients With Stage III to IVB Nasopharyngeal Carcinoma From Endemic Regions of China. *Cancer* (2013) 119(12):2230–8. doi: 10.1002/cncr.28049
23. Ma B, Kam M, Leung S, Hui E, King A, Chan S, et al. A Phase II Study of Concurrent Cetuximab–Cisplatin and Intensity-Modulated Radiotherapy in Locoregionally Advanced Nasopharyngeal Carcinoma. *Ann Oncol* (2012) 23 (5):1287–92. doi: 10.1093/annonc/mdr401
24. Shen Q, Ma X, Hu W, Chen L, Huang J, Guo Y. Intensity-Modulated Radiotherapy *Versus* Three-Dimensional Conformal Radiotherapy for Stage I-II Natural Killer/T-Cell Lymphoma Nasal Type: Dosimetric and Clinical Results. *Radiat Oncol* (2013) 8(1):1–8. doi: 10.1186/1748-717X-8-152
25. Balog J, Mackie TR, Pearson D, Hui S, Paliwal B, Jeraj R. Benchmarking Beam Alignment for a Clinical Helical Tomotherapy Device. *Med Phys* (2003) 30 (6):1118–27. doi: 10.1118/1.1576395
26. Fiorino C, Dell'Oca I, Pierelli A, Broggi S, De Martin E, Di Muzio N, et al. Significant Improvement in Normal Tissue Sparing and Target Coverage for Head and Neck Cancer by Means of Helical Tomotherapy. *Radiother Oncol* (2006) 78(3):276–82. doi: 10.1016/j.radonc.2006.02.009
27. Duma M, Heinrich C, Schönknecht C, Chizzali B, Mayinger M, Devecka M, et al. Helical TomoTherapy for Locally Advanced or Recurrent Breast Cancer. *Radiat Oncol* (2017) 12(1):1–8. doi: 10.1186/s13014-016-0736-1
28. Lin J-C, Tsai J-T, Chen L-J, Li M-H, Liu W-H. Compared Planning Dosimetry of TOMO, VMAT and IMRT in Rectal Cancer With Different Simulated Positions. *Oncotarget* (2017) 8(26):42020. doi: 10.18632/oncotarget.14923
29. Xu Y, Deng W, Yang S, Li P, Kong Y, Tian Y, et al. Dosimetric Comparison of the Helical Tomotherapy, Volumetric-Modulated Arc Therapy and Fixed-Field Intensity-Modulated Radiotherapy for Stage IIB-IIIB Non-Small Cell Lung Cancer. *Sci Rep* (2017) 7(1):1–9. doi: 10.1038/s41598-017-14629-w
30. Li S, Zhou Q, Shen L-F, Li H, Li Z-Z, Yang Z, et al. Dosimetric Comparisons of Volumetric Modulated Arc Therapy and Tomotherapy for Early T-Stage Nasopharyngeal Carcinoma. *BioMed Res Int* (2018) 2018:1–8. doi: 10.1155/2018/2653497
31. Lee N, Xia P, Quivey JM, Sultanem K, Poon I, Akazawa C, et al. Intensity-Modulated Radiotherapy in the Treatment of Nasopharyngeal Carcinoma: An Update of the UCSF Experience. *Int J Radiat Oncol Biol Phys* (2002) 53(1):12–22. doi: 10.1016/S0360-3016(02)02724-4
32. Vernat SS, Ali D, Puyraveau M, Viard R, Lisbona A, Fenoglietto P, et al. Is IMAT the Ultimate Evolution of Conformal Radiotherapy? Dosimetric Comparison of Helical Tomotherapy and Volumetric Modulated Arc Therapy for Oropharyngeal Cancer in a Planning Study. *Physica Med* (2014) 30(3):280–5. doi: 10.1016/j.ejmp.2013.07.128
33. Pasquier D, Cavillon F, Lacornerie T, Touzeau C, Tresch E, Lartigau E. A Dosimetric Comparison of Tomotherapy and Volumetric Modulated Arc Therapy in the Treatment of High-Risk Prostate Cancer With Pelvic Nodal Radiation Therapy. *Int J Radiat Oncol Biol Phys* (2013) 85(2):549–54. doi: 10.1016/j.ijrobp.2012.03.046
34. Xie Y, Bourgeois D, Guo B, Zhang R. Postmastectomy Radiotherapy for Left-Sided Breast Cancer Patients: Comparison of Advanced Techniques. *Med Dosimetry* (2020) 45(1):34–40. doi: 10.1016/j.meddos.2019.04.005
35. Clivio A, Fogliata A, Franzetti-Pellanda A, Nicolini G, Vanetti E, Wyttenbach R, et al. Volumetric-Modulated Arc Radiotherapy for Carcinomas of the Anal Canal: A Treatment Planning Comparison With Fixed Field IMRT. *Radiother Oncol* (2009) 92(1):118–24. doi: 10.1016/j.radonc.2008.12.020
36. Vanetti E, Clivio A, Nicolini G, Fogliata A, Ghosh-Laskar S, Agarwal JP, et al. Volumetric Modulated Arc Radiotherapy for Carcinomas of the Oro-Pharynx, Hypo-Pharynx and Larynx: A Treatment Planning Comparison With Fixed Field IMRT. *Radiother Oncol* (2009) 92(1):111–7. doi: 10.1016/j.radonc.2008.12.008
37. Pirzkall A, Carol MP, Pickett B, Xia P, Roach IIIM, Verhey LJ. The Effect of Beam Energy and Number of Fields on Photon-Based IMRT for Deep-Seated Targets. *Int J Radiat Oncol Biol Phys* (2002) 53(2):434–42. doi: 10.1016/S0360-3016(02)02750-5
38. Liu R, Buatti JM, Howes TL, Dill J, Modrick JM, Meeks SL. Optimal Number of Beams for Stereotactic Body Radiotherapy of Lung and Liver Lesions. *Int J Radiat Oncol Biol Phys* (2006) 66(3):906–12. doi: 10.1016/j.ijrobp.2006.05.014
39. Verbakel WF, Cuijpers JP, Hoffmans D, Bieker M, Slotman BJ, Senan S. Volumetric Intensity-Modulated Arc Therapy *vs*. Conventional IMRT in Head-and-Neck Cancer: A Comparative Planning and Dosimetric Study. *Int J Radiat Oncol Biol Phys* (2009) 74(1):252–9. doi: 10.1016/j.ijrobp.2008.12.033

Conflict of Interest: The authors declare that the research was conducted in the absence of any commercial or financial relationships that could be construed as a potential conflict of interest.

frontiers in Oncology

ORIGINAL RESEARCH
published: 03 January 2022
doi: 10.3389/fonc.2021.780551

Endoscopic Endonasal Intraconal Approach for Orbital Tumor Resection: Case Series and Systematic Review

Xin Zhang[1,2,3,4,5†], Wei Hua[1,2,3,4,5,6†], Kai Quan[1,2,3,4,5], Guo Yu[1,2,3,4,5], Zunguo Du[7], Zixiao Yang[1,2,3,4,5], Xiaowen Wang[1,2,3,4,5], Jianping Song[1,2,3,4,5], Liang Chen[1,2,3,4,5] and Wei Zhu[1,2,3,4,5*]

[1] Department of Neurosurgery, Huashan Hospital, Shanghai Medical College, Fudan University, Shanghai, China, [2] National Center for Neurological Disorders, Shanghai, China, [3] Shanghai Key Laboratory of Brain Function and Restoration and Neural Regeneration, Shanghai, China, [4] Neurosurgical Institute of Fudan University, Shanghai, China, [5] Shanghai Clinical Medical Center of Neurosurgery, Shanghai, China, [6] Research Unit of New Technologies of Micro-Endoscopy Combination in Skull Base Surgery (2018RU008), Chinese Academy of Medical Science, Shanghai, China, [7] Department of Pathology, Huashan Hospital, Fudan University, Shanghai, China

OPEN ACCESS

Edited by:
Xiaobiao Zhang,
Fudan University, China

Reviewed by:
Weiping Liu,
Fourth Military Medical University, China
Qing Wang,
Nanjing Medical University, China

***Correspondence:**
Wei Zhu
drzhuwei@fudan.edu.cn

†These authors have contributed equally to this work and share first authorship

Specialty section:
This article was submitted to Surgical Oncology, a section of the journal Frontiers in Oncology

Received: 21 September 2021
Accepted: 06 December 2021
Published: 03 January 2022

Citation:
Zhang X, Hua W, Quan K, Yu G, Du Z, Yang Z, Wang X, Song J, Chen L and Zhu W (2022) Endoscopic Endonasal Intraconal Approach for Orbital Tumor Resection: Case Series and Systematic Review. Front. Oncol. 11:780551. doi: 10.3389/fonc.2021.780551

Intraorbital tumor could be approached by numerous surgical methods. The neuroendoscopic endonasal approach could provide a feasible corridor for indicated tumors. Herein we present a series of 6 consecutive intraorbital tumors from April 2018 to October 2020, which received endonasal endoscopic resection. Cadaveric dissection was performed for the intraconal approach, and the literature was also reviewed. Five tumors were located intraconally, while one extraconally. The pathology revealed 1 angioleiomyoma, 1 cavernous hemangioma, 1 pilocytic astrocytoma, 1 meningioma, and 2 schwannomas. Five of the six achieved gross total resection, including 3 tumors with lateral extension beyond the optic nerve. Preoperative visual deterioration was observed in 4 of the 6 patients, and all got improvement postoperatively. Transient oculomotor nerve palsy was presented in one patient postoperatively. No cerebrospinal fluid leakage, enophthalmos, or strabismus was observed. The median follow-up time is 27 months (11~41 months). At the 6-month follow-up, the visual acuity remained unchanged compared with that at discharge. Proptosis was resolved in 2 of the 3 patients; diplopia was improved in one patient. In conclusion, endoscopic endonasal intraconal approach could be suitable for selected pathological conditions, and for both medial or beyond medial extraconal and intraconal orbital tumors.

Keywords: orbital tumor, intraconal, nasal-cranial base tumor, neuroendoscope, endonasal approach

1 INTRODUCTION

The intraorbital tumor is a variety of conditions commonly seen by neurosurgeons. The most common symptoms are exophthalmos and visual deterioration (1). The surgery is challenging for both neurosurgeons and ophthalmologists because of the deep-seated position and adherence with the cranial nerves. A variety of surgical approaches have been used in the management of the tumors involving the orbit. External approaches to the orbit have been well established, including transconjunctival, transcutaneous, and transcranial approaches (2, 3). External orbitotomies are usually performed with or without osteotomy. Norris et al. applied the endoscope to remove orbital foreign bodies and treat fistula through transconjunctival or external approaches in 1981 (3). An orbit-zygomatic approach could be applied for large tumors involving the lateral orbit or for the exposure of the optic canal.

The endoscopic endonasal approach could provide a minimally invasive corridor to the skull base, extending from the cribriform plate to C2. The lateral skull base tumor involving the orbit and the pterygopalatine fossa could also be approached *via* an endoscopic endonasal approach, pioneered by Kassam AB et al. (4, 5). Herman first described the endoscopic endonasal approach for the removal of an orbital cavernoma in 1999 (6). The endoscopic endonasal approach could provide an alternative corridor for the intraorbital lesions. Several studies demonstrated that this approach was suitable for the inferomedial orbital tumors, especially soft benign extraconal tumors (2, 5, 7). Ma et al. reported 23 intraorbital cavernous hemangiomas (CHs) transnasally resected with endoscopy in a single institution (8). Paluzzi summarized an algorithm of "round-the-clock" surgical access to the orbit, in order to guide surgeons to choose the most appropriate approach (9).

Herein, we present a consecutive cohort of 6 intraorbital tumors with different pathologies in our center to illustrate our opinion on choosing the best approach. The clinical features, surgical outcomes, and technical advantages are presented, and related literature is reviewed.

2 PATIENTS AND METHODS

2.1 Patient Population

A retrospective study of 6 consecutive cases of intraorbital tumors from April 2018 to October 2020 was conducted, all of which were surgically resected *via* a purely endonasal endoscopic approach in the Department of Neurosurgery, Huashan Hospital, Fudan University. Medical records and radiological images were reviewed. Surgical approaches, complications, cranial nerve outcomes, and follow-up were analyzed. All the patients were fully informed with written consent after approval by the Huashan Hospital Institutional Review Board.

2.2 Anatomic Study

We performed an anatomic study in the laboratory. The endoscopic endonasal intraconal approach was applied on two cadaveric heads. Intraorbital neurovascular structures from the endonasal view were dissected and exposed.

2.3 Surgical Technique

The patient was placed in the supine position with the head slightly rotated toward right and the chin tilted toward the surgeon. Magnetic resonance image (MRI)- guided neuronavigation was applied during the operation. Abdominal incision was prepped for later skull base reconstruction in case of cerebrospinal fluid (CSF) leakage. A four-hand bi-nostril technique was applied with a 0° or 30° endoscope (Karl Storz, Germany), and the ipsilateral middle turbinate was resected to expand the surgical corridor. After removal of the lamina papyracea, the periorbita was exposed. The optic canal bony decompression was performed for intraconal tumor. The intraconal surgical corridor was created between the medial and inferior rectus muscles. After removal of the tumor, the medial orbital wall was reconstructed with Gelfoam and bone fragment and fixed with BioGlue. A nasoseptal flap was harvested in circumstance of grade 2 or grade 3 CSF leakage (10).

2.4 Postoperative Examination and Follow-up

After the surgery, prophylactic antibiotics were prescribed for 48 h, and the lumbar drainage was applied under the circumstance of intraoperative CSF leakage. The visual acuity and visual field were examined by the ophthalmologists and neurosurgeons postoperatively, and the head MRI was performed before discharge for most cases. The patients were scheduled with a follow-up MRI 3 months after the surgery. Surgical complications were identified through the operative reports and postoperative clinic notes.

2.5 Literature Search

A literature search was completed in September 2021 using the PubMed database. We used a search strategy for ("transnasal" or "transsphenoid*" or "endonasal") AND ("endoscop*") AND (orbital disease [MeSH Terms]) AND ("tumor*" OR "hemangioma*" OR "schwannoma*" OR "meningioma*" OR "glioma"). Non-English articles were excluded.

2.6 Statistical Analysis

Statistical analyses were performed using SPSS (version 20). All statistical methods were two-tailed test, and a p value of < 0.05 was considered significant.

3 RESULTS

3.1 Clinical Features

The demographics and clinical features of the six patients are shown in **Table 1**. The mean age of the four patients is 37 years, including five female and one male. Unilateral visual loss is presented in four patients, with the worst of no light perception. Proptosis is presented in three patients and diplopia in one patient (**Table 1**).

The median maximal diameter of the tumor is 27.9 mm (range, 20.0–47.8 mm). The pathology includes 1 angioleiomyoma, 1 cavernous hemangioma, 1 meningioma, 1 pilocytic astrocytoma, and 2 schwannomas. Regarding the tumor location, four are intraconal and two are extraconal. Four of the six tumors invaded lateral to the optic nerve, and the other two tumors confined inferiomedially. Three of the four tumors with lateral occupation were intraconally located.

TABLE 1 | Characteristics of the demographics and surgical outcomes.

No.	Age (years), sex	Side	Symptoms	Pre-op CN deficits	Location/relationship with CN II	Pathology	EOR	Post-op CN palsy	Adjuvant therapy	Follow-up
1	8, F	Rt	Heterotropia	II (NLP)	Intraconal/Md, Ltl	Pilocytic astrocytoma	GTR	II unchanged	None	No recurrence
2	41, M	Lt	Proptosis	/	Intraconal/Md, Ltl	Schwannoma	GTR	Transient III palsy, proptosis resolved	None	No recurrence
3	46, F	Rt	Proptosis, diplopia	VI	Extraconal/Md	Angioleiomyoma	GTR	Proptosis and VI palsy resolved	None	CR
4	43, F	Rt	Visual loss, proptosis	II	Intraconal/Md, Ltl	Meningioma	PR	II and proptosis unchanged	None	SD
5	34, F	Rt	Visual loss	II	Intraconal/Md	Schwannoma	GTR	II unchanged	None	No recurrence
6	47, F	Lt	Visual loss	II	Extraconal/Ltl	Hemangioma	GTR	II unchanged	None	No recurrence

EOR, extent of resection; F, female; M, male; Rt, right; Lt, left; NLP, no light perception; Md, medial; Ltl, lateral; GTR, gross total resection; PR, partial resection; CR, complete remission; SD, stable.

The age prevalence of intraorbital lesions is unremarkable according to previous reviews (11). The patients usually present with proptosis, visual impairment, local pain, and diplopia (1). The most seen pathologies of intraorbital tumors are slow-growing benign tumors, such as hemangioma, schwannoma, optic nerve sheath meningioma (ONSM) and osteomas.

3.2 Adequate Opening and Optic Decompression Could Be Achieved *via* the Endonasal Intraconal Approach

In this consecutive cohort, all 6 cases received middle turbinectomy to expand the corridor to the medial orbit. Four patients with intraconal tumor received optic canal bony decompression. Surgical technique and steps are shown in **Figures 1A–C** (see *Patients and Methods*). Intraoperative CSF leakage occurred in one patient with pilocytic astrocytoma. Five of the six cases achieved gross total resection, including three tumors with lateral invasion to the optic nerve. Only one case with intraconal meningioma got partial resection and optic canal bony decompression, considering extreme adherence with the optic nerve and copious bleeding. Previous literature on surgical resection of intraorbital tumors is reviewed in **Table 2**.

We performed orbital dissection of the endoscopic endonasal intraconal approach on two cadaveric heads. After removing the lamina papyracea and the medial wall of the orbit, we created the corridor between the medial and inferior rectus muscles. The optic nerve, oculomotor nerve to the medial rectus muscle, and branches of the ophthalmic artery could be exposed well from this approach (**Figure 1D**).

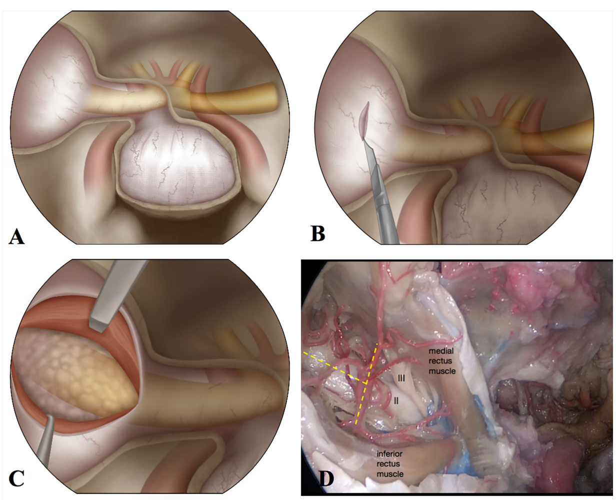

FIGURE 1 | The illustration of surgical steps and anatomic dissection of the orbit from an endoscopic endonasal view. **(A)** After opening the sella floor, lamina papyracea, and optic canal, right orbit is exposed. **(B)** The periorbita is cut open with a blade. **(C)** Retracting the medial rectus muscle and inferior rectus muscle to expose the intraconal lesion. **(D)** The anatomic dissection of the orbit from the endoscopic endonasal approach. The optic nerve, oculomotor nerve, and branches of ophthalmic artery are exposed.

3.3 Surgical Outcome

Pre- and postoperative neurological functions of the six patients are shown in **Table 1**. Cranial nerve (CN) II impairment in patients 1, 4, 5, and 6 remained stable postoperatively, without newly developed visual impairment. Transient CN III palsy was presented in patient 2 postoperatively, which was resolved at the 6-month follow-up. Preoperative CN VI palsy of patient 3 was resolved 6 months after the surgery. Two of the 3 patients with proptosis recovered postoperatively. No patient complained of CSF leakage postoperatively. No enophthalmos or strabismus was observed after tumor resection.

3.4 Long-Term Outcome

By September 2021, the median follow-up time is 27 months (11~41 months). At the 6-month follow-up, the visual acuity remained unchanged compared with that at discharge. Proptosis was resolved in 3 patients; diplopia was improved in patient 3. No patient received chemotherapy or radiotherapy after the surgery.

3.5 Case Illustration

Two cases are illustrated below, and the other four cases are shown in the **Supplementary Materials**.

TABLE 2 | Literature review of the intraorbital tumors using purely endoscopic transnasal approach.

Year/author	Cases	Location	Approach	Outcome
2004, Tsirbas	3	Orbital apex	Combined transnasal and transconjunctival	NA
2010, McKinney	6	Intraconal	Transnasal	67% GTR
2012, Castelnuovo	16	Intraconal medially located	Transnasal	8 GTR extra-intraconal/6 biopsy intraconal, diplopia
2013, Muscatello	3	Inferio-medial orbit	2 transnasal, 1 external	All GTR
2014, Chhabra	5	Medial orbital		4 GTR, 1 STR, transient diplopia, enophthalmos
2014, Healy DY	1	Intraconal	Transnasal	GTR
2014, Karligkiotis A	3	Extraconal involving medial orbital wall	Transnasal	Resolution of ophthalmological symptoms
2015, Arai Y	4	Extraconal or intraconal/medial or lateral	2 transnasal/2 staged surgery (craniotomic/transantral)	2 cases endo biopsy first then transfer to craniotomy/transantral
2015, Shin M	15	Aggressive tumor involving the orbit	Transnasal	12/15 GTR
2016, Shafi F	1	Intraconal orbital apex	Transnasal	Biopsy
2016, Chen YB	11	Optic canal	Transnasal	All GTR, visual all improved
2017, Sun MT	2	Medial orbital apex	Transnasal	GTR
2018, Montano N	70	Orbital	Craniotomic/transnasal/trans eyelid	28 ONSM, 14 CH, 6 schwannoma
2019, Castelnuovo	2	Intraconal, inferomedial	Transnasal	GTR, complete resolution of symptoms
2019, Ma JY	23	7 extraconal, 16 intraconal	Transnasal	16 of 23 GTR

GTR, gross total resection; NA, not available; ONSM, optic nerve sheath meningioma; STR, subtotal resection.

3.5.1 Case 1

An 8-year-old girl presented with heterotropia of the right eye for 1 year, and aggravated visual loss for 2 months. Neurologically, she was alert, with normal visual acuity on the left and no light perception on the right, right pupil diameter 5 mm, direct light reflex (-), indirect light reflex (+), right eye proptosis and right papilledema, otherwise intact. Preoperative computed tomography (CT) scan revealed right intra-orbital lesion, with both medial and lateral invasion to the optic nerve and right optic canal enlargement. MRI indicated that the tumor was iso-intense in T1- and T2-weighed images, homogenously enhanced on gadolinium, with a length of 27 mm on its largest axis. Right intra-orbital glioma or schwannoma was suspected preoperatively. A purely endoscopic tumor resection *via* the trans-nasal trans-orbital approach was performed. During the surgery, the medial orbital wall was removed, the tumor was resected between the interspace of the medial and inferior rectus muscles. The tumor originated from the optic nerve (see **Supplementary Video 1**). Postoperative CT and MRI scan showed total resection of the tumor. The pathology confirmed the diagnosis of pilocytic astrocytoma. The patient recovered well postoperatively and received continuous lumber drainage for 1 week (**Figure 2**).

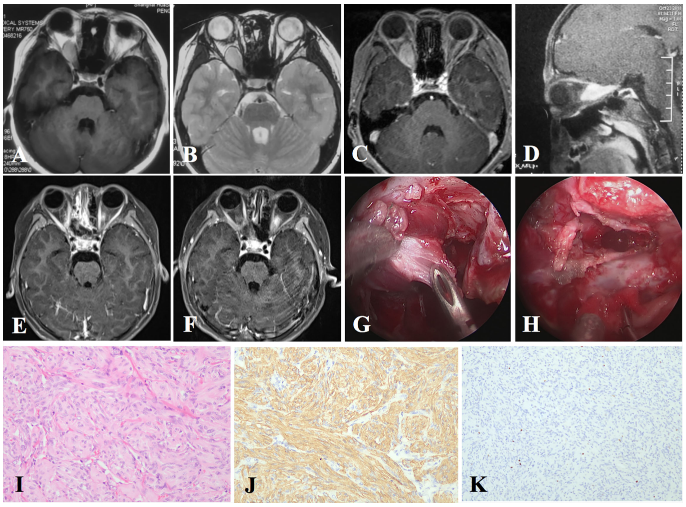

FIGURE 2 | The radiological images, intraoperative pictures, and pathological staining of Case 1. **(A–D)** Preoperative MRI indicates an intraconal lesion with both medial and lateral extension to the optic nerve. **(E)** Postoperative MRI shows total resection of the tumor. **(F)** Six-month follow-up MRI shows no recurrence. **(G)** Intraoperatively, the intraconal tumor is found to be tenacious. **(H)** The tumor is totally resected. **(I)** Hematoxylin–eosin (H&E) staining shows the optic nerve completely replaced by neoplastic spindle cells with a nested pattern in microscope (original magnification ×200). **(J)** Tumor cells are positive for glial fibrillary acidic protein (GFAP) in immunochemistry (original magnification ×200). **(K)** Ki-67 index is relatively low (original magnification ×100).

3.5.2 Case 2

A 41-year-old male complained of left eye proptosis for 6 months. Physical examination showed visual acuity 20/20 on the left, and 20/25 on the right; left eye proptosis and left corneal reflex decreased. MRI showed left intraorbital tumor with both medial and lateral extension to the optic nerve. Endoscopic endonasal tumor resection was performed, and the intraconal tumor was resected through the corridor between inferior and medial rectus muscles. The tumor originated from the branch of the oculomotor nerve, and total resection was achieved. The pathology indicated schwannoma. Postoperatively, the patient had left transient oculomotor nerve palsy, which was resolved at the 6-month follow-up (**Figure 3**).

4 DISCUSSION

Intraorbital tumor is a variety of conditions that may need surgical resection. However, the surgical approach to the orbit is still controversial. External approaches and transcranial approaches have been used in the resection of intraorbital tumors, especially for those located superior or anterior to the orbit. However, the endoscopic endonasal approach provides a corridor for minimal invasive surgery of the skull base tumor, which has been developed over the last decade.

The key anatomic landmark between intraconal and extraconal orbital tumors is the position relative to the boundaries of the extraocular muscles (5). In previous reports, the extraconal tumor can be easily approached by the endonasal corridor. However, the intraconal tumors located in the superior and lateral aspect of the orbit are more difficult to be approached by this technique. McKinney and his colleagues stated that the benign soft-tissue tumors in the medial-inferior quadrant of the orbit were the most feasible for the endoscopic endonasal approach. They advocated the rule of avoiding crossing the optic nerve (5). As for the intraconal lesions, some surgeons stated that the surgical indication and approaches should be carefully considered with a wider opening of the periorbital window, and gross total resection was more difficult to achieve compared to extraconal lesions *via* this approach (7, 8). Montano summarized 70 cases of intraorbital tumors who underwent tumor resection; they recommended the endoscopic endonasal approach for primary orbital tumors located in the medial or inferior orbital walls without extra-orbital extension, the trans-eyelid approach for tumors in the upper and upper-lateral quadrants extraconally located, and the fronto-orbital approach for intraconally located tumors involving more than one quadrant (2). Rassi et al. advocated a novel CHEER staging system for evaluating the surgical approaches of intraorbital CH (12).

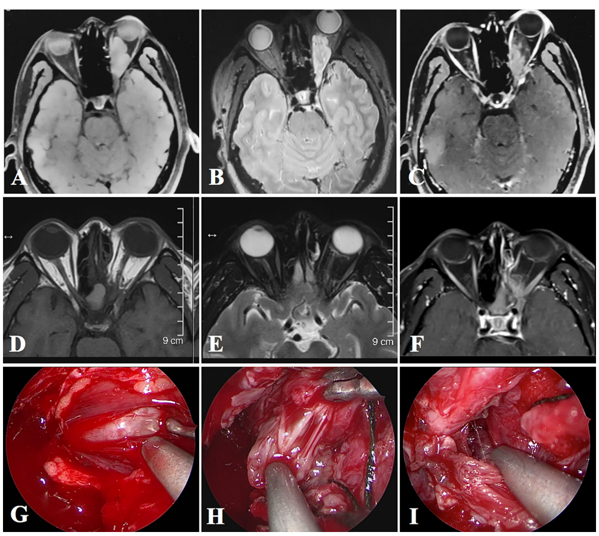

FIGURE 3 | Images of Case 2. **(A–C)** Preoperative MRI shows an intraconal lesion in the left orbit, with both medial and lateral extension. **(D–F)** Six-month follow-up MRI shows no recurrence of the tumor. **(G)** Exposure of the intraconal tumor. **(H)** The carrier nerve of the tumor. **(I)** Inspection after total resection of the tumor.

Some surgeons summarized a 360° "round-the-clock" surgical access to the orbit (9, 13), and they suggested the endoscopic endonasal approach for lesions at the mid or posterior orbit or orbital apex from 1 to 7 o'clock. In our case series, four of the six tumors occupied the lateral quadrants to the optic nerve, three of which were intraconal tumors. Only one case with meningioma was partially resected because of the fibrous tumor and extreme adherence with the optic nerve. The other three tumors with lateral invasion achieved gross total resection, including one pilocytic astrocytoma, one schwannoma, and one hemangioma. Postoperatively neurological deficits were unremarkable. From our perspective, the orbital tumor with lateral extension to the optic nerve is not a contraindication for the endoscopic endonasal approach.

Regarding the outcome, preservation of the cranial nerve is the top priority for the surgery of intraorbital tumor. Cranial nerves should be monitored during the surgery (14). Optic damages are often caused by direct damage, inappropriate traction, or vascular supply impairment during the dissection. Neuro-navigation is recommended during this approach (15). In our cohort, 3 of the 4 patients with intraconal lesions presented with preoperative optic neuropathy, without improvement after the surgery. Moreover, the other patient with intraconal schwannoma developed transient CN III palsy postoperatively. This result indicates that intraconal lesions are more vulnerable for cranial nerve impairment during the surgery.

It is believed that removal of the lamina papyracea or even the medial wall of the orbit does not cause eyeball disposition. However, removal of the periorbita or additional fat dissection may result in orbital fat herniation that can lead to permanent or transient diplopia, enophthalmos, and strabismus (8). Some surgeons suggested reconstruction of the medial orbital wall with bone and nasoseptal flap in case of large defect (16, 17). It was reported to use a thick silastic sheet in the nasal cavity to prevent orbital content herniation then remove 4 weeks after the surgery (18).

Still, there are some limitations of this approach. A preoperative evaluation of the accessibility of the medial and lateral borders of the tumor should be performed. Potential malignancy of the lesion should also be considered because the endoscopic endonasal tumor resection could lead to incomplete resection (19). This approach would be challenging for fibrous tumors with lateral extension to the optic nerve. In such cases, other approaches or staged surgeries should be considered. Adjuvant therapy should also be recommended as an alternative treatment.

In conclusion, the endoscopic endonasal approach is applicable for selected intraorbital tumors both medially and laterally located. The pathology of the lesion and adhesion to adjacent neurovascular structures should also be considered to determine the most appropriate approach.

DATA AVAILABILITY STATEMENT

The raw data supporting the conclusions of this article will be made available by the authors, without undue reservation.

ETHICS STATEMENT

The studies involving human participants were reviewed and approved by the Huashan Hospital Institutional Review Board. Written informed consent to participate in this study was provided by the participants' legal guardian/next of kin.

AUTHOR CONTRIBUTIONS

Study conception and design: WZ and WH. Acquisition of data and follow-up: XZ. Surgical participation: XZ, WH, KQ, GY, ZY, XW, JP, LC, and WZ. Pathological confirmation: ZD. Drafting of manuscript: XZ and WH. Critical revision: all authors. XZ and WH contributed equally to this study and shared the first authorship. All authors contributed to the article and approved the submitted version.

FUNDING

This study was supported and granted by the CAMS Innovation Fund for Medical Sciences (CIFMS, 2019-I2M-5-008).

SUPPLEMENTARY MATERIAL

The Supplementary Material for this article can be found online at: https://www.frontiersin.org/articles/10.3389/fonc.2021.780551/full#supplementary-material

REFERENCES

1. Castelnuovo P, Dallan I, Locatelli D, Battaglia P, Farneti P, Tomazic PV, et al. Endoscopic Transnasal Intraorbital Surgery: Our Experience With 16 Cases. *Eur Arch Otorhinolaryngol* (2012) 269(8):1929–35. doi: 10.1007/s00405-011-1917-z
2. Montano N, Lauretti L, D'Alessandris QG, Rigante M, Pignotti F, Olivi A, et al. Orbital Tumors: Report of 70 Surgically Treated Cases. *World Neurosurg* (2018) 119:e449–e58. doi: 10.1016/j.wneu.2018.07.181
3. Norris JL, Cleasby GW. Endoscopic Orbital Surgery. *Am J Ophthalmol* (1981) 91(2):249–52. doi: 10.1001/archopht.1981.03930020274014
4. Scholtz HJ. Present Results of Treatment of Malignant Tumors of the Internal Nose and Paranasal Sinuses. *Dtsch Gesundheitsw* (1964) 19:152–62. CONTD.
5. McKinney KA, Snyderman CH, Carrau RL, Germanwala AV, Prevedello DM, Stefko ST, et al. Seeing the Light: Endoscopic Endonasal Intraconal Orbital Tumor Surgery. *Otolaryngol Head Neck Surg* (2010) 143(5):699–701. doi: 10.1016/j.otohns.2010.07.010
6. Herman P, Lot G, Silhouette B, Marianowski R, Portier F, Wassef M, et al. Transnasal Endoscopic Removal of an Orbital Cavernoma. *Ann Otol Rhinol Laryngol* (1999) 108(2):147–50. doi: 10.1177/000348949910800208
7. Shin M, Kondo K, Hanakita S, Suzukawa K, Kin T, Shojima M, et al. Endoscopic Transnasal Approach for Resection of Locally Aggressive Tumors in the Orbit. *J Neurosurg* (2015) 123(3):748–59. doi: 10.3171/2014.11.JNS141921
8. Ma J, Zhou B, Qian H, Huang Z, Jitong S. Transnasal Endoscopic Resection of Orbital Cavernous Hemangiomas: Our Experience With 23 Cases. *Int Forum Allergy Rhinol* (2019) 9(11):1374–80. doi: 10.1002/alr.22383
9. Paluzzi A, Gardner PA, Fernandez-Miranda JC, Tormenti MJ, Stefko ST, Snyderman CH, et al. "Round-the-Clock" Surgical Access to the Orbit. *J Neurol Surg B Skull Base* (2015) 76(1):12–24. doi: 10.1055/s-0033-1360580
10. Esposito F, Dusick JR, Fatemi N, Kelly DF. Graded Repair of Cranial Base Defects and Cerebrospinal Fluid Leaks in Transsphenoidal Surgery. *Oper Neurosurg (Hagerstown)* (2007) 60(4 Suppl 2):295–303. doi: 10.1227/01.NEU.0000255354.64077.66
11. Dubal PM, Svider PF, Denis D, Folbe AJ, Eloy JA. Short-Term Outcomes of Purely Endoscopic Endonasal Resection of Orbital Tumors: A Systematic Review. *Int Forum Allergy Rhinol* (2014) 4(12):1008–15. doi: 10.1002/alr.21402
12. El Rassi E, Adappa ND, Battaglia P, Castelnuovo P, Dallan I, Freitag SK, et al. Development of the International Orbital Cavernous Hemangioma Exclusively Endonasal Resection (CHEER) Staging System. *Int Forum Allergy Rhinol* (2019) 9(7):804–12. doi: 10.1002/alr.22316
13. Caballero-Garcia J, Aparicio-Garcia C, Linares-Benavides YJ, Lopez-Sanchez M, Abreu-Perdomo FA, Huanca-Amaru J. Minimally Invasive 360-Degree Approach to Intraconal Orbital Tumors. *Am J Ophthalmol* (2021) 224:301–9. doi: 10.1016/j.ajo.2020.07.035
14. Chen Y, Tu Y, Chen B, Shi J, Yu B, Wu W. Endoscopic Transnasal Removal of Cavernous Hemangiomas of the Optic Canal. *Am J Ophthalmol* (2017) 173:1–6. doi: 10.1016/j.ajo.2016.09.022
15. Hodaj I, Kutlay M, Gonul E, Solmaz I, Tehli O, Temiz C, et al. The Use of Neuronavigation and Intraoperative Imaging Systems in the Surgical Treatment of Orbital Tumors. *Turk Neurosurg* (2014) 24(4):549–57. doi: 10.5137/1019-5149.JTN.9605-13.1
16. Melder K, Zwagerman N, Gardner PA, Wang EW. Endoscopic Endonasal Approach for Intra- and Extraconal Orbital Pathologies. *J Neurol Surg B Skull Base* (2020) 81(4):442–9. doi: 10.1055/s-0040-1713940
17. Banks C, Husain Q, Bleier BS. Endoscopic Endonasal Intraconal Orbit Surgery. *World J Otorhinolaryngol Head Neck Surg* (2020) 6(2):100–5. doi: 10.1016/j.wjorl.2019.07.001
18. Karligkiotis A, Appiani MC, Verillaud B, Herman P. How to Prevent Diplopia in Endoscopic Transnasal Resection of Tumors Involving the

Medial Orbital Wall. *Laryngoscope* (2014) 124(9):2017–20. doi: 10.1002/lary.24657

19. Arai Y, Kawahara N, Yokoyama T, Oridate N. Endoscopic Transnasal Approach for Orbital Tumors: A Report of Four Cases. *Auris Nasus Larynx* (2016) 43(3):353–8. doi: 10.1016/j.anl.2015.10.009

Conflict of Interest: The authors declare that the research was conducted in the absence of any commercial or financial relationships that could be construed as a potential conflict of interest.

The handling editor declared a shared parent affiliation with the authors at time of review.

Publisher's Note: All claims expressed in this article are solely those of the authors and do not necessarily represent those of their affiliated organizations, or those of the publisher, the editors and the reviewers. Any product that may be evaluated in this article, or claim that may be made by its manufacturer, is not guaranteed or endorsed by the publisher.

frontiers in Surgery

ORIGINAL RESEARCH
published: 01 February 2022
doi: 10.3389/fsurg.2021.799405

Check for updates

Olfactory Neuroblastoma: Surgical Treatment Experience of 42 Cases

Xiao Cai [1,2,3,4], Zhouying Peng [1,2,3,4], Hua Zhang [1,2,3,4], Ruohao Fan [1,2,3,4], Yan Fang [1,2,3,4] and Zhihai Xie [1,2,3,4*]

[1] Department of Otolaryngology-Head and Neck Surgery, Xiangya Hospital, Central South University, Changsha, China, [2] Otolaryngology Major Disease Research Key Laboratory of Hunan Province, Changsha, China, [3] National Clinical Research Center for Geriatric Disorders, Xiangya Hospital, Central South University, Changsha, China, [4] Anatomy Laboratory of Division of Nose and Cranial Base, Clinical Anatomy Center of Xiangya Hospital, Central South University, Changsha, China

Objective: Our purpose was to estimate the safety and effectiveness of the endoscopic endonasal approach (EEA) in olfactory neuroblastoma (ONB) and determine whether preservation of the dura and olfactory bulb could be considered in selected patients.

Methods: We retrospectively reviewed patients diagnosed with ONBs between July 2010 and June 2021 at our institution, and collected data on demographic, disease stage, surgical approach, overall survival (OS), disease-free survival (DFS), and postoperative complications.

Results: The study sample included 42 patients (8 treated for recurrence and 34 initial cases), 28 of which were men and 14 were women with a median age of 47.19 years. The mean duration from the beginning of treatment and follow-up time was 8.91 and 51 months, respectively. Among the 42 patients, 32 had unilateral lesions, and the rest had bilateral lesions. Patient symptoms were predominantly nasal, and four patients presented without any symptoms. The modified Kadish staging was A in three patients, B in 14 patients, C in 17 patients, and D in 8 patients. According to the preoperative examinations, five patients had cervical lymph node metastasis, and no patients had distant metastases. EEA was used in 38 patients, cranioendoscopic approach in 3, and open craniofacial approach in 1. The 5-year OS and DFS rates were 89.1 and 79.2%, respectively. The 2-year OS and DFS rates were both 89.1%. The overall surgical complication incidence was 9.52% (one cerebrospinal fluid rhinorrhea, one cervical hematoma, and two epileptic seizures).

Conclusion: The present results support the importance of earlier treatment for advanced ONB and the fact that it is safe and efficacious to treat ONBs *via* EEA. The preservation of the dura can be considered for select patients—specifically those without skull base involvement and who underwent postoperative comprehensive therapy.

Keywords: olfactory neuroblastoma, endoscopic endonasal surgery, skull base surgery, survival rate, prognosis

Edited by:
Xiaobiao Zhang,
Fudan University, China

Reviewed by:
A. B. Zulkiflee,
University Malaya Medical Centre, Malaysia
Jianfeng Liu,
China-Japan Friendship Hospital, China

****Correspondence:***
Zhihai Xie
xiedoctor@csu.edu.cn

Specialty section:
This article was submitted to Surgical Oncology, a section of the journal Frontiers in Surgery

Received: *21 October 2021*
Accepted: *29 December 2021*
Published: *01 February 2022*

Citation:
Cai X, Peng Z, Zhang H, Fan R, Fang Y and Xie Z (2022) Olfactory Neuroblastoma: Surgical Treatment Experience of 42 Cases. Front. Surg. 8:799405. doi: 10.3389/fsurg.2021.799405

INTRODUCTION

Olfactory neuroblastoma is an extremely rare malignant tumor of the nasal cavity that arises from the olfactory neuroepithelium. It accounts for 3–6% of the nasal cavity and nasal sinus malignancies; although, as contemporary histologic techniques are likely to increase detection, it is difficult to determine the true incidence (1). Although olfactory neuroblastoma (ONB) is an uncommon disease, a portion of its characteristics has been identified. Its incidence does not differ significantly according to gender distribution. It affects a wide range of age groups, but most commonly occurs between 50 and 60 years of age. The tumor can involve peripheral parts such as the paranasal sinuses, cribriform plate, and orbits (2). The most common site of metastasis is the cervical lymph nodes (10–33% of patients), with relatively few distant metastases. Kadish et al. developed the most referenced staging system. This system divides tumors into three groups: group A tumors are limited to the nasal cavity, group B tumors involve the nasal cavity and paranasal sinuses, and group C tumors extend beyond the nasal cavity and paranasal sinuses (3). The modification of this staging system by Morita et al. established group D for tumors with regional (neck lymph nodes) or distant metastases (4).

The standard treatment for ONB is a comprehensive therapy that includes surgical resection and postoperative radiotherapy. En-block resection *via* craniofacial approach (CFA) has been the gold standard surgical modality for ONB previously (5). However, the treatment modalities have changed. Based on remarkable progress in technology, endoscopic endonasal approaches (EEAs) have gained acceptance and become an alternative standard for the surgical treatment of ONB (1, 6–9).

Our purpose was to estimate the safety and effectiveness of EEA as an ONB surgical treatment standard. We also strove to determine whether preservation of the dura and olfactory bulb could be considered in select patients without skull base involvement and if outcomes were similar to those who underwent resection of the dura and olfactory bulbs.

TABLE 1 | The clinical and demographic data of the patients.

	Number of patients	Percentage (%)
Sex		
Males	28	66.67
Females	14	33.33
Age		
>45 years	27	64.29
≤45 years	15	35.71
Initial cases	34	80.95
Unilateral lesion	32	76.19%
Symptom		
Epistaxis	21	
Nasal obstruction	20	
Hyposmia or anosmia	5	
Headache	5	
Ocular symptoms	5	
Pain of nose	3	
No symptom	4	
Kadish		
A	3	7.14
B	14	33.33
C	17	40.48
D	8	19.05
NLN* metastasis (before the treatment)	5	11.9

NLN, neck lymph node.

MATERIALS AND METHODS

Patient Characteristics

The study included all patients with ONB who underwent surgery between July 2010 and June 2021 at our institution. Each case was diagnosed *via* histopathological examination. Seven patients who had been treated for recurrence were identified among 42 patients with ONB. Each patient underwent a preoperative endoscopy, a sino-nasal CT scan, MRI, and a CT scan or X-ray of the chest. Tumor staging was based on the Kadish staging system, which was initially based on imaging data and then corrected after surgery based on histological data. All patients underwent surgery by the same surgeon.

Surgical Technique

There are three surgical methods for treating ONB: EEA, CFA, and the cranioendoscopic approach. The first step is tumor resection of the nasal cavity and sinuses. It is vital to identify the attachment of the tumor origin and resection of the sino-nasal component. The lamina papyracea, cribriform plate, fovea ethmoidalis, planum sphenoidale, dura, brain, olfactory bulbs, and tracts were resected depending on the extent of tumor involvement. The skull base is reconstructed in multiple layers, including the fascia lata of the thigh or mucosa flap, when available.

Statistical Methods

We studied epidemiological data, treatment options, histologic outcomes, postoperative complications, disease-related or other outcomes, and the course of the disease. Descriptive statistics for scaled values and frequencies of study patients within the categories for each of the parameters of interest were enumerated. OS and DFS rates were determined using the Kaplan-Meier method. The statistical significance of differences between the actuarial curves was evaluated using the log-rank test. Follow-up time was defined as the time from the end date of treatment for the original disease to first recurrence, death, or last contact. For all tests, the significance was set at $p < 0.05$. Statistical tests were performed with the assistance of the Statistical Product and Service Solutions (SPSS) Statistics 24 statistical software application (International Business Machines Corporation, USA).

RESULTS

Patients

The clinical and demographic data of the patients are summarized in **Table 1**. The study sample included 8 patients

TABLE 2 | Treatment modality.

	Number of patients	Percentage (%)
Surgery methods		
EEA*	38	90.48
Cranioendoscopic approach	3	7.14
CFA**	1	2.38
Resection including dura, part of brain, and olfactory bulbs, and tracts	31	73.81
Surgery only	14	33.33
Comprehensive therapy* **	28	66.67

*EEA, endoscopic endonasal approach; **CFA, open craniofacial approach.
***Comprehensive therapy, Surgery and radiotherapy or chemotherapy or both.

TABLE 3 | Treatment strategies used for each resection range.

Group	A*	B*
Total	11	31
Kadish		
A	1	2
B	7	7
C	1	16
D	2	8
Comprehensive therapy	100%	54.84%
Hymans		
1–2	3	17
3–4	3	8
Surgery methods		
EEA	100%	87.10%

*A, Resection without dura, part of the brain, and olfactory bulbs, and tracts; B, Resection including dura, part of the brain, and olfactory bulbs, and tracts.

who had been treated for recurrence (19.05%) and 34 initial cases (80.95%). Included in this study were 28 males (66.67%) and 14 females (33.33%). The average age at presentation was 47.19 years (range = 16–79 years). The mean duration from the beginning of treatment and follow-up time was 8.91 months (range = 5 days—72 months) and 51 months (range = 2–127 months), respectively. Among the 42 patients, 32 (76.19%) had only unilateral lesions and the remainder (23.81%) had bilateral lesions. The order of symptom sequence was epistaxis (n = 21), nasal obstruction (n = 20), hyposmia or anosmia (n = 5), headache (n = 5), ocular symptoms (n = 5), and pain in the nose (n = 3). There were four patients without any symptoms. The modified Kadish staging was A in 3 patients (7.14%), B in 14 patients (33.33%), C in 17 patients (40.48%), and D in 8 patients (19.05%). Five patients (11.90%) had cervical lymph node metastasis, while no patients had distant metastasis at presentation according to the preoperative examination.

Operative Findings and Additional Treatment

All patients underwent surgery with curative intent. The treatment modalities are shown in **Table 2**. There were 38 patients who used EEA (90.48%), 3 used the cranioendoscopic approach (7.14%), and 1 used CFA (2.38%). Of the 42 patients, 31 (73.81%) underwent resection including the dura, part of the brain, olfactory bulbs, and tracts (**Table 3**). We decided the resection range according to the preoperative images (preoperative endoscopy, a skull-base HRCT scan, MRI) and intraoperative observation which could help us to estimate that if there were skull base involvement. Some patients without skull base involvement estimated by the preoperative images and intraoperative observation also underwent resection including the dura, part of the brain, olfactory bulbs, and tracts, for example, the patient No. 27 (**Supplementary Figure 1**). Postoperative radiotherapy was performed in 27 patients (64.29%), of whom 14 (51.85%) underwent chemotherapy at the same time. Postoperative radiotherapy was not performed in 15

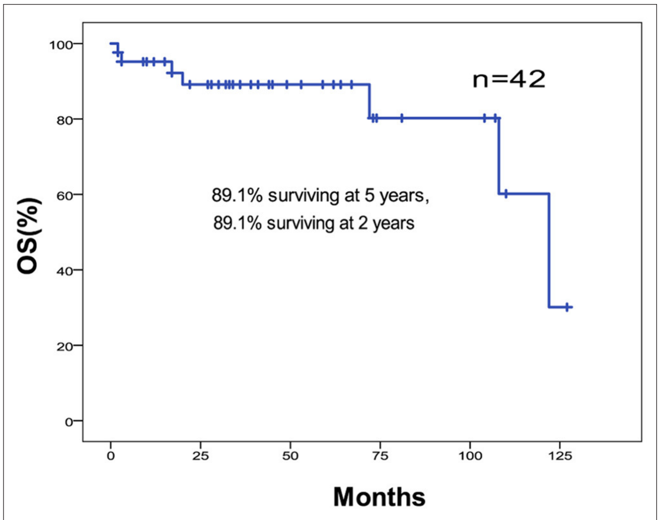

FIGURE 1 | Kaplan-Meier graph of OS of 42 cases of ONB.

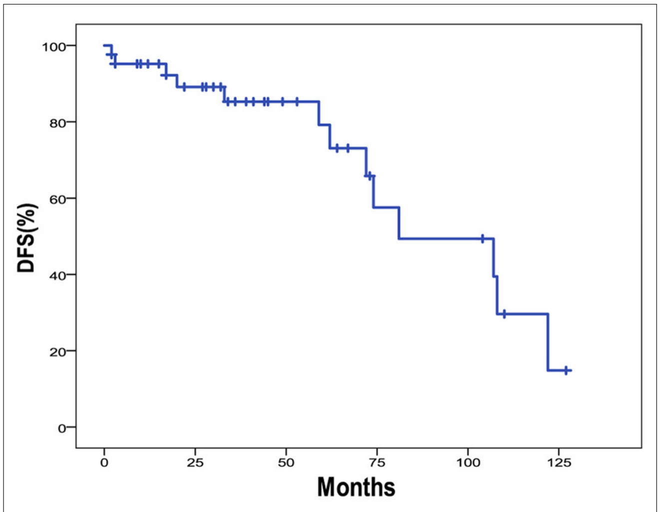

FIGURE 2 | Kaplan-Meier graph of DFS of 42 cases of ONB.

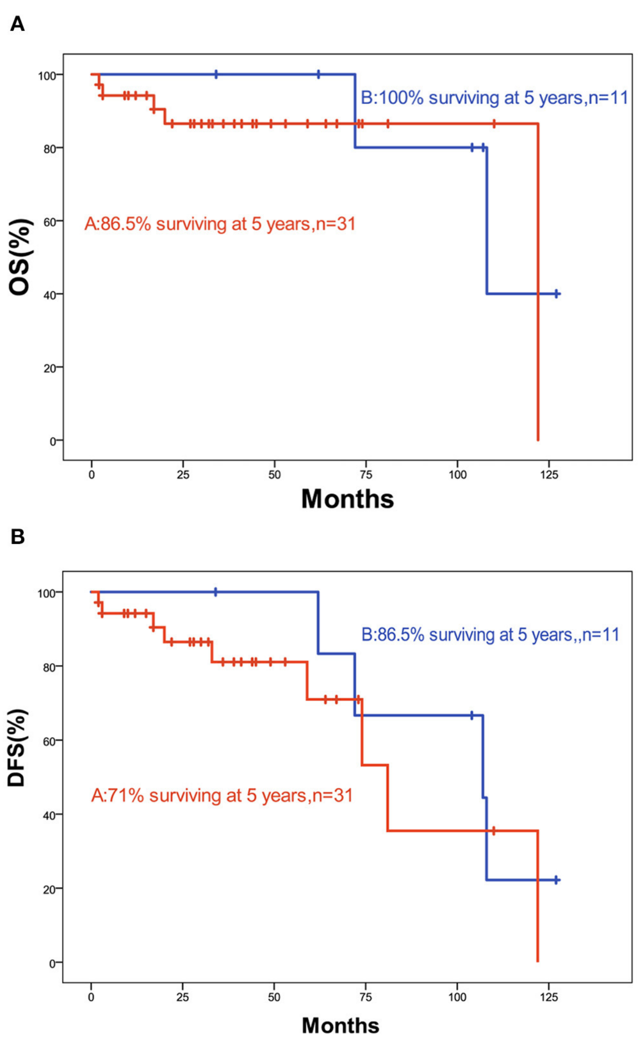

FIGURE 3 | (A) Kaplan-Meier graph of OS according to resection; **(B)** Kaplan-Meier graph of DFS according to resection (a, including dura, part of the brain, and olfactory bulbs, and tracts; b, not).

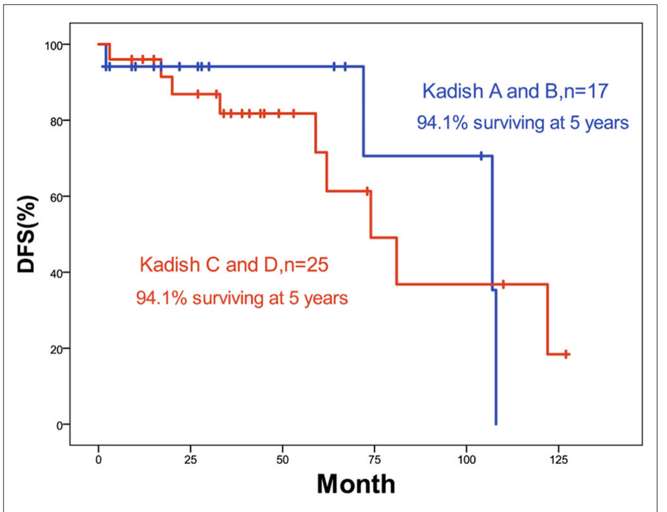

FIGURE 4 | Kaplan-Meier graph of DFS according to Kadish stage.

patients (35.71%), but one of them underwent chemotherapy (6.67%). All symptoms were relieved after the surgery.

Oncological Outcomes

The 5-year OS and DFS rates were 89.1 and 79.2%, respectively. The 2-year OS and DFS rates were 89.1% (**Figures 1**, **2**). The incidence of local and regional recurrence was 11.9% (5 of 42), and the average recurrence time was 51.6 months (range = 11–102 months). Three patients (7.14%) had cervical lymph node metastasis, while 5 patients (11.9%) had distant metastasis. The 5-year cumulative OS and DFS in patients treated with resection of the dura, part of the brain, and olfactory bulbs, and tracts was 86.5 and 71% compared to 100 and 100% for those who were not by Kaplan Meier (**Figure 3**). There was no significant difference in DFS between patients who underwent open and endoscopic surgery ($p = 0.44$). The DFS of patients was separately assessed according to the modified Kadish stage of tumors ("A and B" or "C and D"). Although the 5-year DFS of patients with more advanced tumors (71.5%) was lower than that of patients with early-stage tumors (94.1%), the differences were not statistically significant ($p = 0.7$) (**Figure 4**).

Complications

The overall surgical complication incidence was 9.52% (4 of 42). One patient had cerebrospinal fluid rhinorrhea, and one had a cervical hematoma. Both patients underwent another surgery. Two patients had epileptic seizures.

Representative Case

A 41-year-old man with persistent nasal obstruction had a left nasal mass (**Figure 5**). The patient underwent an EEA for tumor resection. Dural resection was performed, and the brain appeared uninvolved. Radiotherapy and chemotherapy were administered postoperatively. No postoperative complications were observed. The patient remained disease-free 29 months postoperatively.

DISCUSSION

The Kadish staging system was established in 1976 with three grades (A, B, and C) based on the extent of the primary tumor. This was modified to include a new grade (D) for patients with lymph nodes or distant metastases. However, the prognostic value of the Kadish staging system was not constant. Several studies have found that the early Kadish stages (A or B) have favorable survival rates (2, 10, 11) whereas having not (12, 13). In our study, the 5-year DFS of patients with higher grades (C, D) was lower than that of patients with lower grades (A, B). The differences were not statistically significant. All 3 patients who had neck lymph node metastasis after the therapy had the highest grades (C, D) at first, and only 1 of 5 patients who had distant metastasis after therapy had the lower grade (B) at first.

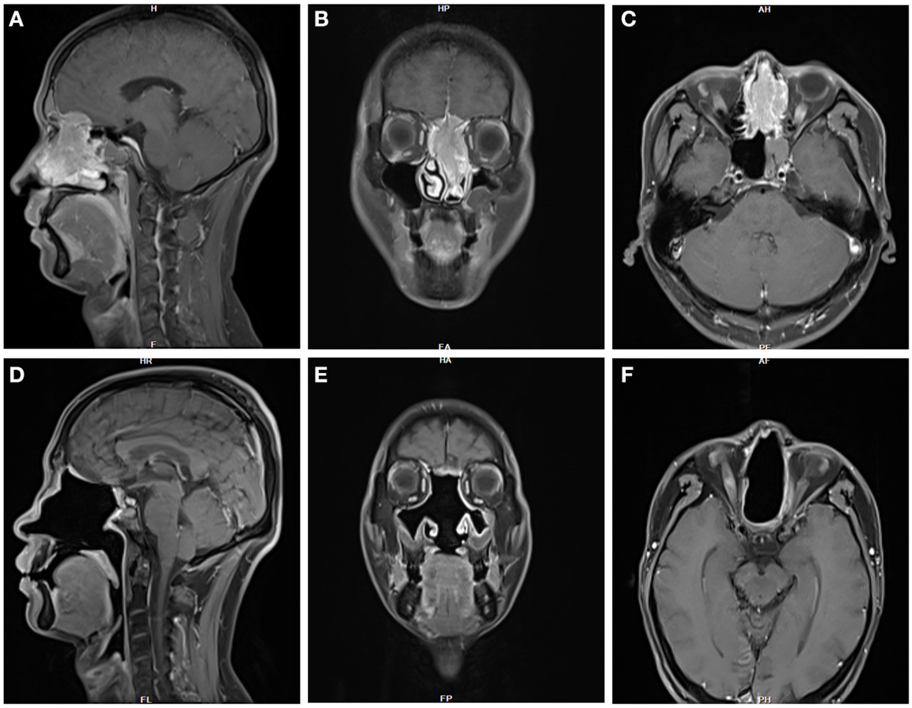

FIGURE 5 | (A–C) MRI imaging in this 41-year-old male patient with persistent nasal obstruction revealed a large, left nasal mass. **(D–F)** The patient remained disease-free 29 months postoperatively.

These findings emphasize the importance of earlier treatment of advanced ONB.

The gold standard treatment for sino-nasal tumors since it was first described by Ketcham et al. (14) was open craniofacial resection and radiotherapy. Recently, EEA has been accepted as a common surgical method as an alternative to CFA. Previous reports have indicated that endoscopic resection can replace traditional craniofacial resection in select patients with ONBs (1, 6–9). Rimmer et al. reviewed 95 patients with ONB for a mean follow-up of 89 months, who were treated with endoscopic or craniofacial resection and reported no significant difference in outcomes between endoscopic and craniofacial resection (2). A recent meta-analysis of 609 patients with ONBs concluded that endoscopic resection has a comparable control rate to craniofacial resection (10). In our study, there was no significant difference in the 5-year DFS between endoscopic and craniofacial resection. Functional preservation and fewer complications should be noted as advantages of EEA in comparison to traditional CFA. There was only one patient who had a cervical hematoma and one of two patients in our study, who had epileptic seizures after surgery, underwent CFA. Of the possible post-operative complications, CSF leak is the most relevant and was found in ∼10% of cases in previous studies (2, 15–17). In the present study, only one CSF leak was observed, suggesting the safety of our surgical modality. However, long-term observational studies are required to validate this finding, particularly for local recurrence.

Although postoperative radiotherapy is standard, there are some exceptions like the small tumors with good prognosis and extensive surgical resection both visually and histologically (including some ONBs) (18). We advised all the patients to go to the oncology department and ask for comprehensive therapy like radiation therapy. And the oncologists evaluated if the patients need and are able to endure comprehensive therapy according to our surgery and patients' physical condition. In our study, comprehensive therapy was not performed in 14 patients.

Traditionally, resection of the cribriform, dura, part of the brain, olfactory bulbs, and tracts, regardless of tumor stage, has been the standard for all ONB treatments. This is due to two reasons. First, the gold standard treatment for sino-nasal tumors is open craniofacial resection. The development of endoscopic surgery allows for resection of the intranasal tumor and cribriform plate bone while avoiding unnecessary resection of the dura and olfactory bulb, and it is now the treatment for select sino-nasal tumors. Second, the theory that the origin of the tumor is the olfactory neuroepithelium in the superior nasal vault and cribriform is widely held, and many surgeries are considered incomplete unless the dura and olfactory apparatus are resected. The olfactory neuroepithelium is also dispersed throughout the superior turbinate, middle turbinate, nasal cavity, and numerous reports of ectopic origins of ONB have been reported in recent studies (19, 20). Besides the low rates of complications, there was no difference in survival in our study in patients treated with or without resection of the dura and olfactory bulb, suggesting that without skull base involvement, the morbidity of dural resection could have been avoided in selected patients. In our study, we decided the resection range according to the preoperative images (preoperative endoscopy, a sino-nasal CT scan, MRI) and intraoperative observation to estimate the presence of skull base involvement. All patients in whom no resection of the dura and olfactory bulb(s) was performed had no skull base involvement, and they underwent postoperative comprehensive therapy (radiotherapy, chemotherapy, or both).

Long-term observation is critical to determine the oncological outcomes of ONBs. The mean follow-up period in the present study was 51 months, which is not sufficient to evaluate the effect of the intervention on prognosis. Rimmer et al. reported that after an average of 49 months, local and regional recurrence occurred (2) and Nalavenkata et al. reported an average of 60 months (21). Therefore, continuous and careful observation is necessary for our study.

CONCLUSION

The present results support the importance of earlier treatment of advanced ONB and the thesis that it is safe and efficacious to treat ONBs *via* EEA. The present results also suggested that preservation of the dura may be considered in select patients without skull base involvement and who were able to undergo postoperative comprehensive therapy. This should be reassessed following long-term observations of oncologic outcomes in our series.

DATA AVAILABILITY STATEMENT

The original contributions presented in the study are included in the article/**Supplementary Materials**, further inquiries can be directed to the corresponding author.

ETHICS STATEMENT

The study was reviewed and approved by The Medical Ethics Committee of Xiangya Hospital of Central South University. Ethical review and approval was not required for the study on human participants, in accordance with the local legislation and institutional requirements.

AUTHOR CONTRIBUTIONS

ZX, HZ, and RF contributed to conception and design of the study. HZ, RF, and YF organized the database. XC performed the statistical analysis and wrote the first draft of the manuscript. ZP and ZX wrote sections of the manuscript. All authors contributed to manuscript revision, read, and approved the submitted version.

SUPPLEMENTARY MATERIAL

The Supplementary Material for this article can be found online at: https://www.frontiersin.org/articles/10.3389/fsurg.2021.799405/full#supplementary-material

Supplementary Figure 1 | All the pictures were from patient No. 27. **(A)** HES ×5: Pathological picture of the olfactory bulbs. And the olfactory bulbs were not involved. **(B)** HES ×20: Pathological picture of the olfactory bulbs. **(C)** HES ×5: Pathological picture of tumor tissues. **(D)** The tumor cells were positive for Ki-67.

REFERENCES

1. Klironomos G, Gonen L, Au K, Monteiro E, Mansouri A, Turel MK, et al. Endoscopic management of Esthesioneuroblastoma: our experience and review of the literature. *J Clin Neurosci.* (2018) 58:117–23. doi: 10.1016/j.jocn.2018.09.011
2. Rimmer J, Lund VJ, Beale T, Wei WI, Howard D. Olfactory neuroblastoma: a 35-year experience and suggested follow-up protocol. *Laryngoscope.* (2014) 124:1542–9. doi: 10.1002/lary.24562
3. Kadish S, Goodman M, Wang CC. Olfactory neuroblastoma. A clinical analysis of 17 cases. *Cancer.* (1976) 37:1571–6. doi: 10.1002/1097-0142(197603)37:3<1571::AID-CNCR2820370347>3.0.CO;2-L
4. Morita A, Ebersold MJ, Olsen KD, Foote RL, Lewis JE, Quast LM. Esthesioneuroblastoma: prognosis and management. *Neurosurgery.* (1993) 32:706–14; discussion: 714–5. doi: 10.1097/00006123-199305000-00002
5. Dulguerov P, Allal AS, Calcaterra TC. Esthesioneuroblastoma: a meta-analysis and review. *Lancet Oncol.* (2001) 2:683–90. doi: 10.1016/S1470-2045(01)00558-7
6. Nakagawa T, Kodama S, Kobayashi M, Sanuki T, Tanaka S, Hanai N, et al. Endoscopic endonasal management of esthesioneuroblastoma: a retrospective multicenter study. *Auris Nasus Larynx.* (2018) 45:281–5. doi: 10.1016/j.anl.2017.05.001
7. Casiano RR, Numa WA, Falquez AM. Endoscopic resection of esthesioneuroblastoma. *Am J Rhinol.* (2001) 15:271–9. doi: 10.1177/194589240101500410
8. de Gabory L, Verillaud B, Rumeau C, Herman P, Jankowski R, Michel J, et al. Multicenter assessment of exclusive endoscopic endonasal approach for the treatment of 53 olfactory neuroblastomas. *Head Neck.* (2018) 40:1000–7. doi: 10.1002/hed.25064
9. Ramakrishnan VR, Orlandi RR, Citardi MJ, Smith TL, Fried MP, Kingdom TT. The use of image-guided surgery in endoscopic sinus surgery: an evidence-based review with recommendations. *Int Forum Allergy Rhinol.* (2013) 3:236–41. doi: 10.1002/alr.21094
10. Fu TS, Monteiro E, Muhanna N, Goldstein DP, de Almeida JR. Comparison of outcomes for open versus endoscopic approaches for olfactory neuroblastoma: a systematic review and individual participant data meta-analysis. *Head Neck.* (2016) 38(Suppl. 1):E2306–16. doi: 10.1002/hed.24233
11. Modesto A, Blanchard P, Tao YG, Rives M, Janot F, Serrano E, et al. Multimodal treatment and long-term outcome of patients with esthesioneuroblastoma. *Oral Oncol.* (2013) 49:830–4. doi: 10.1016/j.oraloncology.2013.04.013
12. Patel SG, Singh B, Stambuk HE, Carlson D, Bridger PG, Cantu G, et al. Craniofacial surgery for esthesioneuroblastoma: report of an international collaborative study. *J Neurol Surg B Skull Base.* (2012) 73:208–20. doi: 10.1055/s-0032-1311754
13. Malouf GG, Casiraghi O, Deutsch E, Guigay J, Temam S, Bourhis J. Low- and high-grade esthesioneuroblastomas display a distinct natural history and outcome. *Eur J Cancer.* (2013) 49:1324–34. doi: 10.1016/j.ejca.2012.12.008

14. Ketcham AS, Wilkins RH, Vanburen JM, Smith RR. A combined intracranial facial approach to the paranasal sinuses. *Am J Surg*. (1963) 106:698–703. doi: 10.1016/0002-9610(63)90387-8
15. Hanna E, DeMonte F, Ibrahim S, Roberts D, Levine N, Kupferman M. Endoscopic resection of sinonasal cancers with and without craniotomy: oncologic results. *Arch Otolaryngol Head Neck Surg*. (2009) 135:1219–24. doi: 10.1001/archoto.2009.173
16. Lund VJ, Wei WI. Endoscopic surgery for malignant sinonasal tumours: an eighteen year experience. *Rhinology*. (2015) 53:204–11. doi: 10.4193/Rhino14.318
17. Nicolai P, Battaglia P, Bignami M, Bolzoni VA, Delu G, Khrais T, et al. Endoscopic surgery for malignant tumors of the sinonasal tract and adjacent skull base: a 10-year experience. *Am J Rhinol*. (2008) 22:308–16. doi: 10.2500/ajr.2008.22.3170
18. *Réseau d'Expertise Français sur les Cancers ORL Rares [Recommandations pour la Pratique Clinique - Tumeurs malignes primitives des fosses nasales et des sinus]*. Available online at: http://refcor.org/files/81/G1-sinus-recommandations.pdf (accessed December 17, 2021).
19. Pinna FR, Ctenas B, Weber R, Saldiva PH, Voegels RL. Olfactory neuroepithelium in the superior and middle turbinates: which is the optimal biopsy site? *Int Arch Otorhinolaryngol*. (2013) 17:131–8. doi: 10.7162/S1809-97772013000200004
20. Storan MJ, Key B, Septal organ of Gruneberg is part of the olfactory system. *J Comp Neurol*. (2006) 494:834–44. doi: 10.1002/cne.20858
21. Nalavenkata SB, Sacks R, Adappa ND, Palmer JN, Purkey MT, Feldman MD, et al. Olfactory neuroblastoma: fate of the neck–a long-term multicenter retrospective study. *Otolaryngol Head Neck Surg*. (2016) 154:383–9. doi: 10.1177/0194599815620173

Conflict of Interest: The authors declare that the research was conducted in the absence of any commercial or financial relationships that could be construed as a potential conflict of interest.

Publisher's Note: All claims expressed in this article are solely those of the authors and do not necessarily represent those of their affiliated organizations, or those of the publisher, the editors and the reviewers. Any product that may be evaluated in this article, or claim that may be made by its manufacturer, is not guaranteed or endorsed by the publisher.

frontiers in Oncology

ORIGINAL RESEARCH
published: 08 February 2022
doi: 10.3389/fonc.2022.778704

Check for updates

A Modified Microscopic-Endoscopic Bilateral Transseptal Approach for Pituitary Adenomas: Comparisons of Nasal Outcome and Quality of Life Using the Microscopic Transnasal Approach

Junjie Zhong[1,2,3,4,5†], *Yanfang Gu*[1,2,3,4,5†], *Jie Zheng*[1,2,3,4,5], *Bojie Yang*[1,2,3,4,5], *Zengxin Qi*[1,2,3,4,5], *Tianwen Li*[1,2,3,4,5], *Chao Shen*[1,2,3,4,5,6*] and *Zhifeng Shi*[1,2,3,4,5,6*]

[1] Department of Neurosurgery, Huashan Hospital, Shanghai Medical College, Fudan University, Shanghai, China, [2] Neurosurgical Institute of Fudan University, Shanghai, China, [3] Shanghai Clinical Medical Center of Neurosurgery, Shanghai, China, [4] Shanghai Key Laboratory of Brain Function Restoration and Neural Regeneration, Shanghai, China, [5] National Center for Neurological Disorders, Shanghai, China, [6] Research Units of New Technologies of Micro-Endoscopy Combination in Skull Base Surgery (2018RU008), Chinese Academy of Medical Sciences, Shanghai, China

Objectives: In this study, we introduced a novel modified microscopic-endoscopic bilateral transseptal approach for pituitary adenoma resection to minimize surgery-related nasal injury. We also retrospectively compared comprehensive nasal outcomes and quality of life between the microscopic transnasal approaches.

Methods: Patients with pituitary adenomas who underwent modified microscopic-endoscopic bilateral transseptal or microscopic transnasal approaches were assessed for olfactory function and quality of life using the Sniffin' Sticks test, the Sino-Nasal Outcome Test-22 (SNOT-22), the SF-36, the anterior skull base (ASK) nasal inventory, and the subjective visual analog scale (VAS) before and 1 and 3 months after surgery. A nasal endoscopy procedure was also performed to evaluate structure abnormalities at 1 and 3 months after surgery.

Results: Fifty-eight patients who underwent either modified microscopic-endoscopic bilateral transseptal (35 patients) or microscopic transnasal (23 patients) surgery were consecutively enrolled. Patients who underwent either transnasal approach experienced similar surgical complications, except for intraoperative cerebrospinal fluid leakage (43.5% vs 14.3% for modified microscopic-endoscopic bilateral transseptal or microscopic transnasal approach, respectively; p = 0.013). Patients who underwent the two approaches fully recovered according to the SF-36, SNOT-22, VAS, and Sniffin' Sticks surveys, but not ASK scores, 3 months post-operatively. There was no significant difference in nasal endoscopy outcome at 3 months follow-up between the two approaches.

OPEN ACCESS

Edited by:
Xiaobiao Zhang,
Fudan University, China

Reviewed by:
Marco Artico,
Sapienza University of Rome, Italy
Zhenlin Wang,
Xuanwu Hospital, Capital Medical University, China

***Correspondence:**
Chao Shen
170385140@qq.com
Zhifeng Shi
shizhifeng@fudan.edu.cn

[†]These authors have contributed equally to this work

Specialty section:
This article was submitted to Surgical Oncology,
a section of the journal Frontiers in Oncology

Received: 17 September 2021
Accepted: 18 January 2022
Published: 08 February 2022

Citation:
Zhong J, Gu Y, Zheng J, Yang B, Qi Z, Li T, Shen C and Shi Z (2022) A Modified Microscopic-Endoscopic Bilateral Transseptal Approach for Pituitary Adenomas: Comparisons of Nasal Outcome and Quality of Life Using the Microscopic Transnasal Approach.
Front. Oncol. 12:778704.
doi: 10.3389/fonc.2022.778704

Conclusions: The modified microscopic-endoscopic bilateral transseptal approach showed largely similar nasal mucosa protective outcomes to those of the microscopic transnasal approach for pituitary adenoma surgery. After pituitary adenoma resection using the modified approach, patients' postoperative olfactory function, nasal structure, and quality of life can be restored to preoperative status within 3 months.

Keywords: olfaction, smell, anterior skull base, pituitary, endoscopic skull base, trans-transseptal, trans-sphenoid

1 INTRODUCTION

Surgical approaches in the sellar region have evolved during the past century. In the 1897, Davide Giordano, a Venetian anatomist and surgeon, proposed a transglabellar approach to the pituitary involving resection of the nose and frontal sinus, followed by removal of the ethmoid bone, allowing wide access to the sphenoid sinus and sella (1). Hermann Schloffer was greatly inspired and extensive researched on the surgical methods of the pituitary gland, and reported the first successful removal of a pituitary tumor *via* a superior transsphenoidal approach in 1907. Combing previous investigations, Harvey Cushing, in 1910 to 1925, treated 231 pituitary tumors *via* the trans-sphenoidal route with a mortality rate of 5.6% in the preantibiotic era (2). Since the 1990s, endoscopic endonasal techniques have been integrated into sellar surgery because of developments in endoscopic concepts of nasal surgery and improvements in endoscopic equipment (3). As fully endoscopic trans-sphenoidal approach has been widely applied, great credit should be given to Edward Laws for having studied the technique and the pituitary adenoma in all its aspects, with a personal series of >6000 cases treated transsphenoidally. The endoscope provides a panoramic view of the suprasellar and parasellar compartments, especially with the use of an angled endoscope. This enhanced visualization has enabled improvements in the extent of resection and reductions in hospital stay duration and operative complications compared with those following the traditional microscopic transnasal transsphenoidal approach (4–7). However, nasal complications following full endoscopic approaches remain controversial. Several studies have reported that endoscopic surgery offers similar or perhaps more advantages over microscopic approaches for the protection of olfactory function (8–11), whereas other studies have reported the endoscopic approach changes the postoperative nasal anatomical structure and may result in headache, nasosinusitis, rhinorrhea, nasal incrustation, anosmia, and disturbance of ventilation (12–18). Theoretically, a binostril four-hand operation endoscopic surgery requires the removal of more nasal structures to make more room for endoscopic instruments. Therefore, maintaining postoperative nasal structure and function during binostril microscopic surgery is not as easy as during uninostril microscopic surgery. It has been reported that compared with the endoscopic approach, microscopic pituitary surgery provides better early postoperative sinonasal quality of life (QoL) and comparable olfactory outcomes (19). However, numerous modified endoscopic transnasal approaches have been developed to further protect the postoperative integrity of nasal function, such as the single-nostril transseptal transsphenoidal approach (20), the bilateral modified nasoseptal rescue flaps approach (21), the bilateral transseptal approach (with the help of a nasal speculum) (22), and the binostril approach (one side transseptal with the other side transnasal) (23). All approaches have shown good postoperative olfactory function and sinonasal QoL; however, few have been compared with typical uninostril transnasal microscopic approaches. Therefore, in this paper, we introduced a new modified microscopic-endoscopic bilateral transseptal approach without the use of a speculum and compared postoperative sinonasal QoL, QoL, olfactory function, and nasal structure integrity outcomes with those of the traditional microscopic trans-nasal approach for pituitary adenoma resection.

2 MATERIALS AND METHODS

2.1 Patient Population and Study Design

We retrospectively reviewed all patients who underwent pituitary tumor resection using the modified microscopic-endoscopic bilateral transseptal approach (transseptal approach) and the microscopic transnasal approach (microscopic approach) by the same surgeon (B.Y.) at Huashan hospital between March 2019 and January 2021. The study was approved by the Institutional Ethics Committee of Huashan hospital Fudan University.

Patients (aged 18–65 years) underwent nasal endoscopy and magnetic resonance image (MRI) of the head before surgery, and those with a history of previous sinonasal surgery or nasal abnormalities were excluded. Patient diagnosed with neurodegenerative disease, which might cause olfactory disorder, were excluded. Patient demographics, tumor dimensions, length of hospital stay, surgical approach, outcomes, complications, and pathologic diagnosis (according to the World Health Organization classification) were collected. The goal of the surgery (gross total resection or subtotal/partial resection) was established preoperatively and determined by neuroradiologists according to the MRI obtained postoperatively as part of routine care.

2.2 Quality of Life, Olfactory Function, and Nasal Outcome Assessments

QoL was evaluated using the 36-item short-form health survey (SF-36). Olfactory function was assessed by the Sniffin' Sticks test (Burghardt, Wedel, Germany) and the Visual Analogue Scale (VAS) according to the manufacturer's protocols (24, 25). The Sniffin' Sticks test has been confirmed to be suitable to be applied to a Chinese population (26). Examinations were performed by an independent person who was not involved in the surgical procedure. We only assessed binostril olfaction because some patients felt discomfort during the full test. The TDI score was calculated as the sum of odor threshold (OT), discrimination (OD), and identification (OI) scores. Because olfactory function varies by sex and age, the 10th percentile is routinely used to define the lower limit of normosmia in different age groups. A total TDI score (i.e., OT, OD, and OI) of ≤ 15 indicated that the patient was functionally anosmic. In cases whose TDI score was above the 10th percentile for their age group, the patient was considered normosmic, otherwise, hyposmia was considered. Nasal QoL and outcome were assessed subjectively *via* the 22-item Sino-Nasal Outcome Test (SNOT-22) (27) and the Anterior Skull Base Nasal Inventory-12 (ASK Nasal-12) (28). All tests and surveys were conducted before and 1 and 3 months after surgery. At postoperative follow-up, we examined patients using a nasal endoscope in the outpatient clinic of the otorhinolaryngology department and recorded nasal structural abnormalities, which included nasal septum perforation, nasal scabs, nasal congestion, nasal ostium obstruction, hypertrophy of the nasal turbinate, and deviated nasal septum.

2.3 Surgical Technique

All surgical procedures were performed by a senior neurosurgeon (B.Y.) with over 5 years' experience in both microscopic and endoscopic transnasal pituitary surgery. Only endoscopic tumor resection requires two neurosurgeons, whereas other procedures can be completed by one neurosurgeon. Neuro-navigation was routinely used in tumor recurrent cases or those with other complicated conditions.

2.3.1 Microscopic Transnasal Approach

After administration of general anesthesia, the patient was elevated by 15° using an operative pillow. The patient's head was then fixed in a head holder with 10°–20° rotation towards the operator. A standard microscopic uninostril transseptal technique was performed during the surgery. After binostril preparation and draping, a hemitransfixion incision was made in the right nasal septal mucosa. Then, a subperiosteal dissection was performed between the septal bone and mucosa with a nasal speculum to expose the anterior wall of the sphenoidal sinus. We opened the sphenoidal sinus widely and resected the sphenoidal spectrum and sinus mucosa to reach the sellar floor. An X-shaped incision was used to incise the dura, and the tumor was resected using various angled curettes, pituitary rongeurs, and suction. Following the resection of the tumor and hemostasis, we carefully inspected the sellar cavity and used multilayer techniques to reconstruct the sellar floor, which included fat (if necessary), Dural Graft Matrix (DuraGen, INTEGRA, USA), artificial dura (Aesceulap, USA), and a Porcine Fibrin Sealant Kit (BeiXiu, China). Finally, we inspected the whole surgical cavity, repositioned the right septal mucosa flap, and inserted two nasal tamponades (MEROCEL, Medtronic, USA) into each nasal cavity.

2.3.2 Modified Microscopic-Endoscopic Bilateral Transseptal Approach

2.3.2.1 Microscopic Phase

Most procedures of this phase were the same as those of the microscopic transnasal approach. We removed the bony sphenoidal sinus under microscopy as much as possible to reach the same exposure extent as that of the endoscopic surgery to avoid the limitation of maneuverability of endoscopic instruments. After adequate removal of the bony sphenoidal sinus, spectrum, and sellar floor, we made another hemitransfixion incision in the left septal mucosa. Subperiosteal dissection was performed to complete the binostril septal surgical trajectory. Each septal mucosa flap was pulled laterally by one suture fixed to the surgical drapes to maintain the binostril septal entrance.

2.3.2.2 Endoscopic Phase

The bilateral septal mucosa flaps were infiltrated by two gauze strips with lidocaine-containing epinephrine (1:100,000) solution for vasoconstriction. Each gauze strip was placed between the posterior nasal septum and septal mucosa flap on the bony surface, inferior to the anterior sphenoidal wall, to maintain the surgical trajectory.

After using a hydrogen peroxide cotton sponge to sterilize the surgical working field, the binostril endoscopic technique was performed for tumor resection (**Figure 1**). After resection and hemostasis of the sellar cavity, a multilayer technique was used to reconstruct the sellar floor. We then repositioned the two nostril septal flaps, inspected the two nasal cavities, and inserted two nasal tamponades.

2.4 Statistical Analysis

Data were analyzed using standard software (jamovi) with Student's t-test, Wilcoxon-signed rank test, and paired t-tests. Statistical significance was set at $p < 0.05$.

3 RESULTS

3.1 Patient Characteristics

Fifty-eight patients were enrolled in this study. Thirty-five patients underwent the microscopic approach, and 23 underwent the transseptal approach. There were no significant differences in age, sex, length of hospital stay, or Knosp grade between the two approach groups (**Table 1**). However, the tumor volume of the transseptal group was significantly larger compared with that of the microscopic group (10.5 ± 16.3cm vs 2.90 ± 4.36cm; $p = 0.011$). In the microscopic group, gross total resection (GTR) of the tumor was achieved in 30/35 patients, and GTR of the tumor was achieved in 20/23 patients who underwent the transseptal approach. GTR was not significantly different between the two groups. **Figure 2** shows the representative preoperative and postoperative magnetic resonance images of the two groups.

3.2 Quality of Life Scales

QoL and SF-36 scale scores before and 1 and 3 months after surgery are provided in **Table 2**. Although preoperative bodily pain (BP) and general health perception (GH) subdomain scores were lower in the transseptal group than in the microscopic group, there were no significant differences in the SF-36 score in either group at 1 or 3 months postoperatively. In the microscopic group, Physical (PF) and physical role (PR) functioning subdomain scores showed significant decreases 1 month

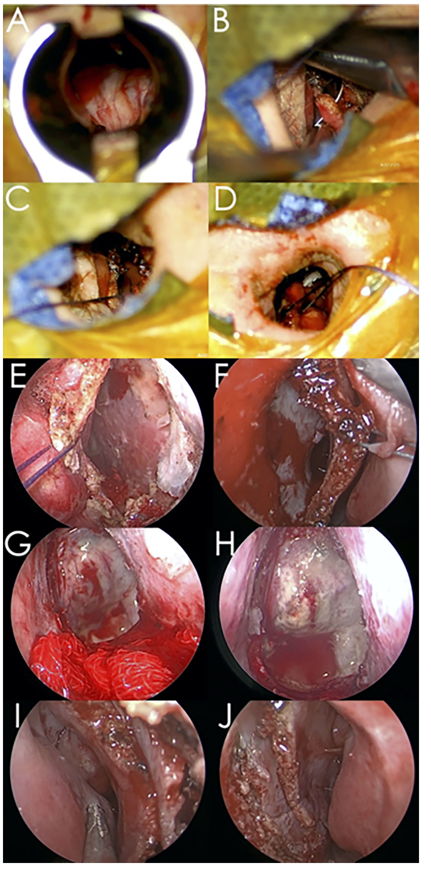

FIGURE 1 | Representative surgical procedure images involved in the modified microscopic-endoscopic bilateral transseptal transsphenoidal approach. **(A)** Removal of the bony sellar floor using the uninostril microscopic technique. **(B)** Make a tagging suture on the left septal mucosa. **(C)** Suture between the left septal mucosa flap and the surgical drapes. **(D)** Suture between the right septal mucosa flap and surgical drapes. **(E)** Endoscopic view of the right nostril entrance. **(F)** Endoscopic view of the left nostril entrance. **(G)** Two epinephrine gauze strips were placed between the septal mucosa flaps to maintain the surgical corridor. **(H)** Endoscopic view of the seller floor and internal part of the olfactory cleft area mucosa. **(I)** Inspection of the right nasal cavity and repositioning of the septal mucosa flap. **(J)** Inspection of the left nasal cavity after final inspection. Asterisk: internal part of the olfactory cleft area mucosa.

TABLE 1 | Patient demographics.

Variable	Microscopic (n = 35)	Transseptal (n = 23)	*P* Value
Age in yrs	37.8 ± 10.9	41.7 ± 10.4	0.180
Sex			0.200
Male	16	7	
Female	19	16	
Length of stay in days	4.49 ± 1.69	5.09 ± 1.38	0.160
Functional adenomas	24	17	0.311
GH-secreting	3	3	0.584
luteinizing hormone/follicle stimulating hormone secreting	4	4	0.519
Prolactinoma	9	5	0.729
Adrenocorticotropic hormone secreting	3	2	0.987
Plurihormonal	5	3	0.893
Tumor vol in cm^3	2.90 ± 4.36	10.53 ± 16.34	**0.011**
Knosp grade			
1-2	12	8	0.970
3-4	23	15	
Gross total resection	30	20	0.893

Values represent mean ± standard deviation.
Bold values: statistically significant.

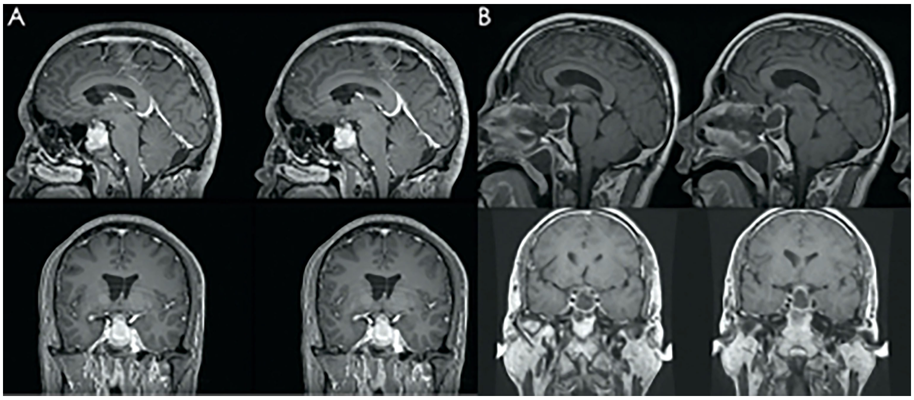

FIGURE 2 | Representative image of preoperative magnetic resonance imaging (MRI) **(A)** and postoperative MRI follow-up **(B)**. The MRI shows gross total resection of the tumor.

TABLE 2 | SF-36.

	Preoperative			PO 1 Month			PO 3 Months		
	Microscopic	Transseptal	*p* Value	Microscopic	Transseptal	*p* Value	Microscopic	Transseptal	*p* Value
Physical functioning	92.7 ± 13.8	93.4 ± 6.97	0.828	84.8 ± 17.3	83.4 ± 15.6	0.767	87.8 ± 18.5	90 ± 9.03	0.627
Physical role functioning	74.3 ± 37.6	84.1 ± 37.4	0.341	39.3 ± 37.5	35.2 ± 32.4	0.689	77.5 ± 36.2	67.5 ± 37.3	0.395
Bodily pain	85.5 ± 16.8	76.7 ± 14.0	**0.047**	80.8 ± 13.6	78.2 ± 14.1	0.511	88.4 ± 16.0	83.5 ± 14.5	0.311
General health perceptions	69.3 ± 17.9	57.1 ± 18.3	**0.017**	70.8 ± 16.3	70.0 ± 17.1	0.856	73.3 ± 17.7	65.9 ± 19.7	0.216
Vitality	71.7 ± 17.4	71.6 ± 15.6	0.978	73.9 ± 13.9	68.6 ± 19.5	0.268	76.5 ± 12.3	70.5 ± 15.2	0.178
Social role functioning	94.6 ± 18.8	88.9 ± 23.1	0.310	90.6 ± 21.9	86.4 ± 25	0.524	99.4 ± 16	88.8 ± 25.9	0.127
Emotional role functioning	64.8 ± 44.2	66.7 ± 37.1	0.867	69 ± 41.5	65.2 ± 41.8	0.744	86.7 ± 27.4	76.7 ± 30.8	0.284
Mental health	73.6 ± 16.3	69.8 ± 16.4	0.398	77.7 ± 16.6	70.5 ± 19.8	0.206	75.2 ± 17.4	75 ± 13.4	0.968
Reported Health Transition	41.4 ± 17.1	46.6 ± 20.8	0.312	51.8 ± 26.3	52.3 ± 24.3	0.947	50 ± 26.9	62.5 ± 25	0.136
Total	124 ± 15.6	120 ± 12.2	0.361	122 ± 13.4	118 ± 16.2	0.365	127 ± 11.7	123 ± 12.9	0.332

Values represent mean± standard deviation.
Bold values: statistically significant.

postoperatively ($p = 0.005$ and $p < 0.001$, Wilcoxon-signed rank test) and full recovery 3 months postoperatively from preoperative scores ($p = 0.178$ and $p = 0.906$, respectively, Wilcoxon-signed rank test). However, other subdomains did not significantly change 1 or 3 months postoperatively. In the transseptal group, the PF and PR subdomain scores significantly decreased at 1 month postoperation ($p = 0.004$, $p = 0.002$, respectively, Wilcoxon-signed rank test). However, only the PR score fully recovered 3 months postoperatively from preoperative scores ($p = 0.105$, Wilcoxon-signed rank test), whereas the PF subdomain score did not ($p = 0.019$, Wilcoxon-signed rank test). The GH subdomain score significantly improved at both 1 and 3 months postoperatively.

3.3 Sino-Nasal Quality of Life Scales

No statistically significant difference in total SNOT-22 scores between the two groups was observed before surgery (**Table 3**). The transseptal group showed significantly lower total SNOT-22 scores than the microscopic group at 1 month postoperatively ($p = 0.011$); however, no significant difference was observed at 3 months postoperatively. Both groups showed a significant increase in SNOT-22 score from preoperation to 1 month postoperatively (microscopic group: 13.7 ± 3.11, $p < 0.001$; transseptal group: 11.3 ± 2.89, $p < 0.001$) and recovered by 3 months postoperatively (microscopic group: 2.06 ± 1.29; $p = 0.174$, transseptal group: 1.5 ± 0.76; $p = 0.687$).

Both groups showed a significant change in ASK score at 1-month follow-up from preoperation ($p < 0.001$) but did not recover by 3 months postoperatively ($p < 0.001$; **Table 4**). Furthermore, the transseptal group showed lower ASK scores than those of the microscopic group 3 months postoperatively ($p = 0.025$).

3.4 Olfactory Functions

Subjective olfactory function based on VAS score showed a marked decrease 1 month after surgery (microscopic group: 7.17 ± 1.76 vs 9.43 ± 1.40, $p = 0.002$; transseptal group: 6.50 ± 1.77 vs 9.88 ± 0.342, $p = 0.001$) in both groups (**Table 5**). Only the microscopic group fully recovered olfactory function to preoperative scores at 3 months postoperative follow-up (microscopic group: 8.93 ± 0.832 vs 9.43 ± 1.40, $p = 0.092$; transseptal group: 8.91 ± 0.970 vs 9.88 ± 0.342, $p = 0.003$). No significance difference in VAS score was found between the two groups in preoperatively ($p = 0.22$) or at 1-month ($p = 0.29$) or 3-months follow-up ($p = 0.95$).

TABLE 3 | SNOT-22.

	Microscopic (n = 35)	Transseptal (n = 23)	*P* Value
Pre-operation	1.43 ± 1.07	1.39 ± 1.16	0.892
PO 1 month	13.7 ± 3.11	11.3 ± 2.89	**0.011**
PO 3 months	2.06 ± 1.29	1.5 ± 0.76	0.112

Values represent mean± standard deviation.
Bold values: statistically significant.

TABLE 4 | Anterior skull base nasal inventory survey.

	Microscopic (n = 35)	Transseptal (n = 23)	*P* Value
Pre-operation	2.21 ± 1.04	1.96 ± 0.976	0.366
PO 1 month	11.4 ± 4.26	10.5 ± 5.41	0.523
PO 3 months	9.26 ± 4.71	6.29 ± 3.30	**0.025**

Values represent mean± standard deviation.
Bold values: statistically significant.

TABLE 5 | Olfactory function based on VAS.

	Preoperative			PO 1 Month			PO 3 Months		
	Microscopic	Transseptal	*p* Value	Microscopic	Transseptal	*p* Value	Microscopic	Transseptal	*p* Value
VAS	9.43 ± 1.40	9.88 ± 0.342	0.222	7.17 ± 1.76	6.50 ± 1.77	0.291	8.93 ± 0.832	8.91 ± 0.970	0.951

Values represent mean± standard deviation.

According to the Sniffin' Sticks test, in the microscopic group, five cases (14%) were defined as hyposmic 1 month after surgery, and two cases (6%) were defined as hyposmic 3 months after surgery (**Table 6**). In contrast, one case (4%) was defined as hyposmic 1 and 3 months after surgery in the transseptal group. No anosmic patients were found in either the microscopic or transseptal group. No significant difference was observed for total TDI scores among preoperative and 1 and 3 months postoperative scores in either group (**Table 7**). Similarly, OT, OD, and OI scores showed no significant differences among time points in either group.

3.5 Post-Operative Nasal Endoscopy Outcomes

All patients were followed up using nasal endoscopy in the outpatient department at 1 and 3 months postoperatively. No significant differences were observed for the following outcomes: nasal septum perforation, nasal scabs, nasal congestion, nasal ostium obstruction, hypertrophy of the nasal turbinate, or deviated nasal septum between the two groups (**Table 8** and **Figure 3**).

3.6 Complications

No carotid artery injury, intracerebral hemorrhage, epistaxis, meningitis, or visual worsening occurred in either group (**Table 9**). Postoperative nasal hemorrhage and unplanned second surgery rates were not significantly differently distributed between the two approaches. We observed a significantly higher incidence of intraoperative cerebrospinal fluid (CSF) leakage in the transseptal group than in the microscopic group (p = 0.013). Complication results are summarized in **Table 8**.

4 DISCUSSION

The transnasal endoscopic route for pituitary surgery has been a favorable access route that has numerous advantages over microscopic surgery for large invasive cases. However, some studies have reported a negative impact on short-term olfaction and nasal QoL. A recent meta-analysis revealed a similar result on postoperative olfaction outcomes, although heterogeneity across the included studies was high ($I^2 > 95\%$, p

TABLE 6 | Olfactory function based on the Sniffin' Sticks test.

	PO 1 Month			PO 3 Months		
	Microscopic	Transseptal	*p* Value	Microscopic	Transseptal	*p* Value
Normal	30	22	0.498	33	22	0.818
Hyposmics	5	1	0.224	2	1	0.818
Anosmics	0	0	NA	0	0	NA

NA, Not applicable.

TABLE 7 | TDI scores of the Sniffin' Sticks test.

	Preoperative			PO 1 Month			PO 3 Months		
	Microscopic	Transseptal	*p* Value	Microscopic	Transseptal	*p* Value	Microscopic	Transseptal	*p* Value
OT	8.96 ± 3.16	8.64 ± 3.39	0.759	8.79 ± 2.36	8.97 ± 3.33	0.845	9.20 ± 1.90	9.51 ± 2.97	0.692
OD	13.0 ± 1.72	11.8 ± 2.88	0.111	12.5 ± 2.61	11.1 ± 3.77	0.167	12.4 ± 2.24	12.2 ± 2.96	0.769
OI	12.0 ± 1.68	12.1 ± 2.36	0.930	11.9 ± 1.68	11.5 ± 2.83	0.595	12.0 ± 1.02	11.9 ± 2.11	0.829
TDI	34.1 ± 4.16	32.5 ± 5.94	0.318	33.2 ± 4.47	31.7 ± 8.49	0.470	33.6 ± 3.39	33.5 ± 6.35	0.916

TABLE 8 | Nasal endoscopy outcomes.

Symptom	PO 1 Month			PO 3 Months		
	Microscopic	Transseptal	p Value	Microscopic	Transseptal	*p* Value
Nasal septum perforation	4	4	0.519	2	2	0.661
Nasal scabs	12	8	0.969	2	1	0.837
Nasal congestion	12	6	0.509	6	4	0.980
Nasal ostium obstruction	8	6	0.779	0	1	0.213
Hypertrophy of nasal turbinate	8	7	0.519	6	5	0.662
Deviated nasal septum	8	5	0.920	2	4	0.153

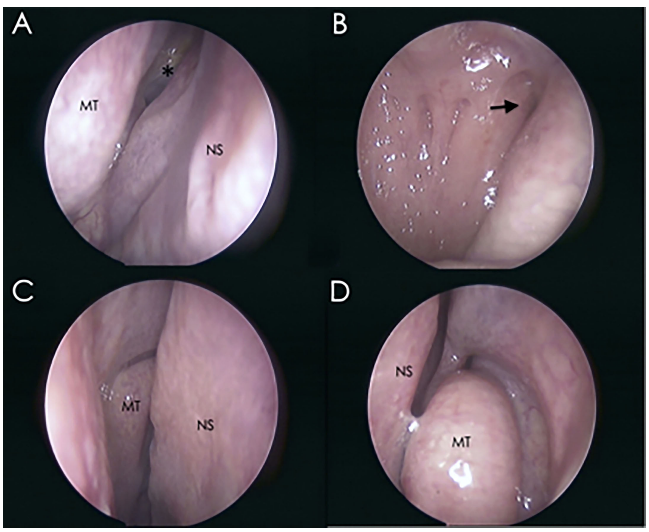

FIGURE 3 | Representative nasal endoscopic images of outpatients at 1-month follow-up after the operation. Images show the integrity of the nasal structure. **(A)** Endoscopic view of the sphenoid ostium from the right nostril. **(B)** View of the nasopharynx. **(C)** Endoscopic view from the right nostril. **(D)** Endoscopic view from the left nostril. Asterisk, sphenoid ostium; arrow, pharyngeal recess; MT, middle turbinate; NS, nasal septum.

TABLE 9 | Complications.

Variable	Microscopic (n=35)	Transseptal (n=23)	*P* Value
Carotid artery injury	0	0	>0.99
Intracerebral hemorrhage	0	0	>0.99
Epistaxis	0	0	>0.99
Meningitis	0	0	>0.99
Visual worsening	0	0	>0.99
Intraoperative CSF leakage	5	10	**0.013**
Postoperative CSF leakage	1	1	0.761
Postoperative nasal hemorrhage	2	1	0.818
Unplanned 2nd surgery	2	1	0.818

Bold values, statistically significant.

<.01), which suggested significant variation in the included studies (9).

The purpose of this study was to introduce a novel modified microscopic-endoscopic bilateral transseptal approach and compare sinonasal QoL, olfactory function, and nasal endoscopy outcomes with those of the traditional microscopic approach. We hypothesized that this modified approach would be associated with similar nasal outcomes because it theoretically allows the preservation of almost all nasal mucosa and nasal structures.

4.1 Characteristics of the Modified Microscopic-Endoscopic Bilateral Transseptal Approach

The advantages of the modified microscopic-endoscopic bilateral transseptal approach are:

1. Bilateral nasalseptal mucosa flaps can be protected and left intact after the operation.
2. All surgical procedures can be performed by one person before tumor resection.
3. Surgical exposure is similar to that of the standard binostril endoscopic approach.
4. All surgical instruments are limited to the corridor between the two nasalseptal mucosa flaps, which makes it easier to achieve aseptic status. When intraoperative CSF leakage occurs, it is important to maintain an aseptic status to avoid severe central nervous system infection.
5. Final inspection of the surgical field after tumor resection can be performed quickly and easily. The frequency of electrocoagulation hemostasis is much lower than that of the standard endoscopic approach.
6. Each nasalseptal mucosa flap is theoretically large enough to be used as a pedicled nasal mucosal flap to reconstruct the skull base in larger extensive surgery.
7. The resected nasalseptal bone can be inserted and repositioned between the bilateral nasalseptal mucosa flaps.

The disadvantages and limitations of the modified microscopic-endoscopic bilateral transseptal approach are:

1. In cases of narrow nasal space, more attention needs to be paid to the dissection of the whole nasalseptal mucosa flap to minimize surgery-related injury.
2. Lateral exposure is limited by the narrow anterior wall of the sphenoidal sinus and bilateral superior turbinate.
3. Because bilateral mucosa linear incision is near the nasal vestibule, postoperative acute bleeding must be prevented.
4. In recurrent cases, the dissection of the bilateral nasalseptal mucosa flap is difficult.

We recommend the following surgical technique tips:

1. Bilateral hemitransfixion incisions on the septal mucosa should not be the same depth in case of postoperative nasal septal perforation.
2. Infiltration of the epinephrine solution should be performed after the dissection of the bilateral septal mucosa flaps. Because the mucosa flap will be vasoconstricted and thinner, it will be vulnerable to becoming lacerated during the subperiosteal dissection of the septal flap.
3. The anterior sphenoidal wall should be removed as much as possible under microscopy by one neurosurgeon.

According to our experiences on the modified microscopic-endoscopic bilateral transseptal approach, it might be not appropriate for those who need nasal mucosa flap to repair CSF leakage. Thus, further studies are required to optimize this approach. Another limitation of this approach is re-transnasal surgery, because the septal mucosa flap is easier to be broken during dissection. The standard endoscopic approach would be more appropriate for recurrent pituitary adenomas.

4.2 Clinical Outcomes

In this study, the transseptal approach was demonstrated to be an effective and safe transsphenoidal approach for pituitary adenoma resection. Although the tumors were significantly larger in the transseptal group, the same surgical effect was achieved in terms of GTR rate and surgery-related complications, which included artery injury, intracerebral hemorrhage, meningitis, visual worsening, postoperative CSF leakage, and epistaxis. In the transseptal group, we observed a higher incidence of intraoperative CSF leak due to aggressive resection of the larger tumor using endoscopic instruments. However, the incidence of postoperative CSF leak during the transseptal approach was not significantly higher than that during the microscopic approach, which demonstrated that the intraoperative repair of CSF rhinorrhea under the transseptal approach is reliable.

4.3 Quality of Life

The SF-36 test to evaluate the postoperative QoL of patients showed that of the eight subdomains, the PF and PR subdomain scores decreased at 1-month follow-up in both groups; however, full recovery at 3 months postoperatively was only achieved in the microscopic group, which indicated that the microscopic approach could enable patients to be physically ready for regular work and activities in 3 months. In contrast, the transseptal approach may require more than 3 months to achieve full recovery of PF function; although postoperative GH significantly improved following surgery, which was not observed in the microscopic group. This may be attributed to the larger tumor volume and higher incidence of CSF leak in the transseptal group. Because of the larger tumor size, the transseptal group patients experienced more complaints and clinical syndromes than did the microscopic group. Thus, preoperative GH subdomain scores were much lower in the transseptal group than in the microscopic group. After tumor resection, both groups' complaints and clinical syndromes significantly improved, which resulted in a significant difference in the GH subdomain score. During preoperative instructions of the surgery, patients in both groups were routinely informed of the size of the pituitary tumor and the possible complications during surgery. As a result, the transseptal group had a larger tumor size and higher occurrence of intraoperative CSF leak. Although the repair of the sellar floor was successful, we still strongly recommended patients who had intraoperative CSF leak to remain home to rest and avoid any heavy work or strenuous exercise following discharge. Such preoperative instruction and postoperative education may have influenced the PF subdomain scores at the 3-month follow-up. These patients likely required more time to convince themselves that they are of sufficient health and ready to return to work.

4.4 Nasal Outcome

Postoperative endoscopic inspection revealed no differences between the two groups for nasal septum perforation, nasal scabs, nasal congestion, nasal ostium obstruction, hypertrophy of the nasal turbinate, or deviated nasal septum. Three months after the operation, the nasal structure of most patients returned to the preoperative level (**Table 7**).

At 1 month postsurgery, patients in both groups showed significantly higher SNOT-22 and ASK scores. However, the scores of the transseptal group were significantly lower than those of the microscopic group, which was not expected. At 3 months postoperatively, SNOT-22, but not ASK, scores had fully recovered in both groups, and neither SNOT-22 nor ASK scores were significantly different between the two groups. This demonstrated that surgery-related nasal QoL decreased 1 month postoperatively, and more than 3 months were needed to achieve full recovery of nasal QoL. The transseptal approach was slightly better than the microscopic approach in the early stage of recovery.

The subjective olfactory VAS test showed that the scores of both groups significantly decreased 1 month after surgery, but full recovery after 3 months was achieved in only the microscopic group. However, the semi-objective olfactory test results did not change preoperatively to 1 month after surgery in either group, and no differences were found between groups at 1- or 3-months follow-ups. These contradicted results between the subjective olfactory VAS test and the semi-objective Sniffin' Sticks test are intersesting. This suggests that subjective evaluations, such as the VAS test, may not provide an accurate assessment of olfactory function due to patients' subjective scoring. Thus, the Sniffin' Sticks test, a validated psychophysical tool allowing detailed, semi-objective evaluation of a patient's olfactory performance, is recommended for accurate evaluations.

Taken together, our results indicated that the transseptal approach enables the preservation of nasal QoL, olfactory function, and nasal structure to the levels achieved by the microscopic approach. Olfactory dysfunction, which often presents as hyposmia or anosmia, and a decrease in nasal QoL leads to a profound decrease in QoL and mental health and an increase in depression. A pituitary adenoma is a benign lesion that can be controlled or cured long-term by total or partial removal of the tumor. Thus, neurosurgeons should consider preservation of QoL as one of the primary objectives of surgery. However, a paradigm shift in recent decades has placed greater importance on patients' functional outcomes, which has prompted investigations on olfactory function and nasal QoL after transsphenoidal surgery for pituitary adenoma. We modified a previously implemented transseptal approach to achieve not only the same protection of nasal mucosa as that of microscopic surgery but also the same surgical effects as endoscopic pituitary adenoma surgery. Moreover, we compared this modified transseptal approach with the microscopic transnasal approach in terms of olfactory outcomes, nasal QoL, QoL, and postoperative nasal structure. The overall outcome of this new modified approach was largely positive, as expected.

4.5 Limitations

Several limitations of this study should be considered. Although the sample size met the criteria of the power calculation, preoperative SF-36 scores for BP and GH components were poorer in the transseptal group compared with those of the microscopic group. Furthermore, patients in the transseptal group had larger pituitary tumor volumes compared with those of the transnasal group. A larger sample size may allow further comparisons with standard transnasal endoscopic approaches or even extended skull base surgery. Moreover, a longer follow-up period will enable additional and longer-term characterization of changes in olfactory outcomes. Future large-scale prospective or randomized controlled trials are needed to verify these findings.

5 CONCLUSIONS

The modified microscopic-endoscopic bilateral transseptal approach provides similar postoperative nasal QoL, olfactory function, nasal structure, and QoL as does the microscopic approach. Olfactory function recovered to preoperative levels 1 month after surgery following either approach. Full recovery of nasal and general QoL requires at least 3 months. The transseptal approach resulted in similar olfactory outcomes as those achieved using the uninostril microscopic approach but without any loss of endoscopic surgical vision, combined with the advantages of both the microscopic and endoscopic approaches. This modified approach has the potential to become the optimal endoscopic approach for pituitary adenoma surgery.

DATA AVAILABILITY STATEMENT

The raw data supporting the conclusions of this article will be made available by the authors, without undue reservation.

ETHICS STATEMENT

The studies involving human participants were reviewed and approved by The Institutional Ethics Committee of Huashan hospital Fudan University. The patients/participants provided their written informed consent to participate in this study. Written informed consent was obtained from the individual(s) for the publication of any potentially identifiable images or data included in this article.

AUTHOR CONTRIBUTIONS

CS and BY conceived of the presented idea. JJZ developed the theoretical formalism, performed the anlytic calculations. YG and JJZ performed the surverys. BY supervised the project.

All authors discussed the results and contributed to the final verion of the manuscript.

FUNDING

This work was supported by grants (82001140) from The National Nature Science Foundation and Shanghai Municipal Government, and also supported by CAMS Innovation Fund for Medical Sciences (CIFMS, 2019-I2M-5-008).

ACKNOWLEDGMENTS

The authors thank Prof. Wenhong Yan for his assistance in conducting the nasal endoscopy assessment.

REFERENCES

1. Artico M, Pastore FS, Fraioli B, Giuffrè R. The Contribution of Davide Giordano (1864-1954) to Pituitary Surgery: The Transglabellar-Nasal Approach. *Neurosurgery* (1998) 42(4):909–11; discussion 911-2. doi: 10.1097/00006123-199804000-00121
2. Cushing H. Notes Upon a Series of Two Thousand Verified Cases With Surgical-Mortality Percentages Pertaining Thereto. *Am J Surg* (1932) 16:348. doi: 10.1016/S0002-9610(32)90942-8
3. Jankowski R, Auque J, Simon C, Marchal JC, Hepner H, Wayoff M. Endoscopic Pituitary Tumor Surgery. *Laryngoscope* (1992) 102(2):198–202. doi: 10.1288/00005537-199202000-00016
4. Castano-Leon AM, Paredes I, Munarriz PM, Jimenez-Roldan L, Hilario A, Calatayud M, et al. Endoscopic Transnasal Trans-Sphenoidal Approach for Pituitary Adenomas: A Comparison to the Microscopic Approach Cohort by Propensity Score Analysis. *Neurosurgery* (2020) 86(3):348–56. doi: 10.1093/neuros/nyz201
5. Akbari H, Malek M, Ghorbani M, Ramak Hashemi SM, Khamseh ME, Zare Mehrjardi A, et al. Clinical Outcomes of Endoscopic Versus Microscopic Trans-Sphenoidal Surgery for Large Pituitary Adenoma. *Br J Neurosurg* (2018) 32(2):206–9. doi: 10.1080/02688697.2018.1429569
6. Goudakos JK, Markou KD, Georgalas C. Endoscopic Versus Microscopic Trans-Sphenoidal Pituitary Surgery: A Systematic Review and Meta-Analysis. *Clin Otolaryngol* (2011) 36(3):212–20. doi: 10.1111/j.1749-4486.2011.02331.x
7. Chen CJ, Ironside N, Pomeraniec IJ, Chivukula S, Buell TJ, Ding D, et al. Microsurgical Versus Endoscopic Transsphenoidal Resection for Acromegaly: A Systematic Review of Outcomes and Complications. *Acta Neurochir (Wien)* (2017) 159(11):2193–207. doi: 10.1007/s00701-017-3318-6
8. Kahilogullari G, Beton S, Al-Beyati ES, Kantarcioglu O, Bozkurt M, Kantarcioglu E, et al. Olfactory Functions After Transsphenoidal Pituitary Surgery: Endoscopic Versus Microscopic Approach. *Laryngoscope* (2013) 123 (9):2112–9. doi: 10.1002/lary.24037
9. Thiensri T, Limpoka A, Burusapat C. Analysis of Factors Associated With Temporal Hollowing After Pterional Craniotomy. *Indian J Plast Surg* (2020) 53(1):71–82. doi: 10.1055/s-0040-1709953
10. Ammirati M, Wei L, Ciric I. Short-Term Outcome of Endoscopic Versus Microscopic Pituitary Adenoma Surgery: A Systematic Review and Meta-Analysis. *J Neurol Neurosurg Psychiatry* (2013) 84(8):843–9. doi: 10.1136/jnnp-2012-303194
11. Yin LX, Low CM, Puccinelli CL, O'Brien EK, Stokken JK, Van Abel KM, et al. Olfactory Outcomes After Endoscopic Skull Base Surgery: A Systematic Review and Meta-Analysis. *Laryngoscope* (2019) 129(9):1998–2007. doi: 10.1002/lary.28003
12. Batra PS, Citardi MJ, Lanza DC. Isolated Sphenoid Sinusitis After Transsphenoidal Hypophysectomy. *Am J Rhinol* (2005) 19(2):185–9. doi: 10.1177/194589240501900212
13. Zada G, Kelly DF, Cohan P, Wang C, Swerdloff R. Endonasal Transsphenoidal Approach for Pituitary Adenomas and Other Sellar Lesions: An Assessment of Efficacy, Safety, and Patient Impressions. *J Neurosurg* (2003) 98(2):350–8. doi: 10.3171/jns.2003.98.2.0350
14. Dusick JR, Esposito F, Mattozo CA, Chaloner C, McArthur DL, Kelly DF. Endonasal Transsphenoidal Surgery: The Patient's Perspective-Survey Results From 259 Patients. *Surg Neurol* (2006) 65(4):332–41, discussion 341-2. doi: 10.1016/j.surneu.2005.12.010
15. Charalampaki P, Ayyad A, Kockro RA, Perneczky A. Surgical Complications After Endoscopic Transsphenoidal Pituitary Surgery. *J Clin Neurosci* (2009) 16(6):786–9. doi: 10.1016/j.jocn.2008.09.002
16. Sowerby LJ, Gross M, Broad R, Wright ED. Olfactory and Sinonasal Outcomes in Endoscopic Transsphenoidal Skull-Base Surgery. *Int Forum Allergy Rhinol* (2013) 3(3):217–20. doi: 10.1002/alr.21103
17. Rotenberg BW, Saunders S, Duggal N. Olfactory Outcomes After Endoscopic Transsphenoidal Pituitary Surgery. *Laryngoscope* (2011) 121(8):1611–3. doi: 10.1002/lary.21890
18. Tam S, Duggal N, Rotenberg BW. Olfactory Outcomes Following Endoscopic Pituitary Surgery With or Without Septal Flap Reconstruction: A Randomized Controlled Trial. *Int Forum Allergy Rhinol* (2013) 3(1):62–5. doi: 10.1002/alr.21069
19. Hong SD, Nam DH, Seol HJ, Choi NY, Kim HY, Chung SK, et al. Endoscopic Binostril Versus Transnasal Transseptal Microscopic Pituitary Surgery: Sinonasal Quality of Life and Olfactory Function. *Am J Rhinol Allergy* (2015) 29(3):221–5. doi: 10.2500/ajra.2015.29.4165
20. Kawabata T, Takeuchi K, Nagata Y, Ishikawa T, Choo J, Sato Y, et al. Preservation of Olfactory Function Following Endoscopic Single-Nostril Transseptal Transsphenoidal Surgery. *World Neurosurg* (2019) 132:e665–9. doi: 10.1016/j.wneu.2019.08.051
21. Kim BY, Shin JH, Kang SG, Kim SW, Hong YK, Jeun SS, et al. Bilateral Modified Nasoseptal "Rescue" Flaps in the Endoscopic Endonasal Transsphenoidal Approach. *Laryngoscope* (2013) 123(11):2605–9. doi: 10.1002/lary.24098
22. Al-Baldawi IA. Bi-Nostril Transseptal Endoscopic Approach to the Sphenoidal Gate. A New Technique. *Acta Neurochir (Wien)* (2017) 159 (7):1247–52. doi: 10.1007/s00701-017-3193-1
23. Hong SD, Nam DH, Kong DS, Kim HY, Chung SK, Dhong HJ. Endoscopic Modified Transseptal Transsphenoidal Approach for Maximal Preservation of Sinonasal Quality of Life and Olfaction. *World Neurosurg* (2016) 87:162–9. doi: 10.1016/j.wneu.2015.12.050
24. Hummel T, Sekinger B, Wolf SR, Pauli E, Kobal G. 'Sniffin' Sticks': Olfactory Performance Assessed by the Combined Testing of Odor Identification, Odor Discrimination and Olfactory Threshold. *Chem Senses* (1997) 22 (1):39–52. doi: 10.1093/chemse/22.1.39
25. Hummel T, Kobal G, Gudziol H, Mackay-Sim A. Normative Data for the "Sniffin' Sticks" Including Tests of Odor Identification, Odor Discrimination, and Olfactory Thresholds: An Upgrade Based on a Group of More Than 3,000 Subjects. *Eur Arch Otorhinolaryngol* (2007) 264(3):237–43. doi: 10.1007/s00405-006-0173-0
26. Yang L, Wei YX, Ren YY, Yu D, Sun YX, Yang BB. Clinical Application of Sniffin' Sticks Olfactory Psychophysical Measurements. *Zhonghua Er Bi Yan Hou Tou Jing Wai Ke Za Zhi* (2013) 48(9):741–5. doi: 10.3760/cma.j.issn.1673-0860.2013.09.009
27. Morley AD, Sharp HR. A Review of Sinonasal Outcome Scoring Systems - Which is Best? *Clin Otolaryngol* (2006) 31(2):103–9. doi: 10.1111/j.1749-4486.2006.01155.x
28. Little AS, Jahnke H, Nakaji P, Milligan J, Chapple K, White WL. The Anterior Skull Base Nasal Inventory (ASK Nasal Inventory): A Clinical Tool for Evaluating Rhinological Outcomes After Endonasal Surgery for Pituitary and Cranial Base Lesions. *Pituitary* (2012) 15(4):513–7. doi: 10.1007/s11102-011-0358-4

Conflict of Interest: The authors declare that the research was conducted in the absence of any commercial or financial relationships that could be construed as a potential conflict of interest.

The handling editor declared a shared parent affiliation with the authors at time of review.

Publisher's Note: All claims expressed in this article are solely those of the authors and do not necessarily represent those of their affiliated organizations, or those of the publisher, the editors and the reviewers. Any product that may be evaluated in this article, or claim that may be made by its manufacturer, is not guaranteed or endorsed by the publisher.

Advantages of publishing in Frontiers

OPEN ACCESS
Articles are free to read for greatest visibility and readership

FAST PUBLICATION
Around 90 days from submission to decision

HIGH QUALITY PEER-REVIEW
Rigorous, collaborative, and constructive peer-review

TRANSPARENT PEER-REVIEW
Editors and reviewers acknowledged by name on published articles

Frontiers
Avenue du Tribunal-Fédéral 34
1005 Lausanne | Switzerland

Visit us: www.frontiersin.org
Contact us: frontiersin.org/about/contact

REPRODUCIBILITY OF RESEARCH
Support open data and methods to enhance research reproducibility

DIGITAL PUBLISHING
Articles designed for optimal readership across devices

FOLLOW US
@frontiersin

IMPACT METRICS
Advanced article metrics track visibility across digital media

EXTENSIVE PROMOTION
Marketing and promotion of impactful research

LOOP RESEARCH NETWORK
Our network increases your article's readership